DOCTOR OF PHILOSOPHY

Analysis of mitotic and post-mitotic functions of Spindly in Drosophila melanogaster

Clemente, Giuliana

Award date:
2015

University of Dundee

Cell and Developmental Biology Department

College of Life Sciences

Analysis of mitotic and post-mitotic functions of Spindly in *Drosophila melanogaster*

Giuliana Clemente

A thesis submitted for the degree of
Doctor of Philosophy
University of Dundee
September 2015

Declaration

I declare that the following thesis is based on the results of investigations conducted by myself, and that this thesis is of my own composition. Work other than my own is clearly indicated in the text by reference to the relevant researchers or to their publications. This dissertation has not in whole, or in part, been previously submitted for a higher degree.

Giuliana Clemente

I certify that Giuliana Clemente has spent the equivalent of at least nine terms in research work at the College of Life Sciences, University of Dundee, and that she has fulfilled the conditions of the Ordinance General No. 14 of the University of Dundee and is qualified to submit the accompanying thesis in application for the degree of Doctor of Philosophy.

Dr. Arno Müller

List of abbreviations

°C	Degree Celsius
AEF	After egg fertilisation
Amp	Ampicillin
APC	Anaphase promoting complex
AP-MS	Affinity-purification Mass Spectrometry
Asp	Abnormal Spindle Protein
ATP	Adenosine-5'-triphosphate
BSA	Bovine Serum Albumin
BUB	Budding uninhibited by benzimidazole
C. elegans	*Caenorhabditis elegans*
C/EBP	CCAAT-enhancer binding protein
CaM	Calmodulin
CAN	Acetonitrile
CCAN	Constitutive Centromere-associated Network
Cdc-20	Cell-division cycle protein-20
Cdk	Cyclin-dependent kinase
CENP-A	Centromere Protein A
CENP-C	Centromere Protein C
CENP-E	Centromere-associated protein E
CH	Calponin Homology
Chr.	Chromosome
CON	Contaminants
Con-A	Concanavalin-A
CPC	Chromosome Passenger Complex
C-terminal	Carboxy-terminal
CZ	Cortical zone
Da	Dalton
DABCO	1,4- Diazabicycle [2,2,2] octan
DAPI	4',6-diamidino-2-phenylindole
dH2O	Distilled water
Dm Spindly	Drosophila Spindly
DN	Dominant-negative
DNA	Deoxyribonucleic acid
dsRNA	double-stranded RNA
DTT	Dithiothreitol
E.coli	*Escherichia coli*
EcR	Ecdysone Receptor
EDTA	Ethylenediamine tetraacetic acid
EGF	Epidermal growth factor
EGFR	Epidermal growth factor receptor
ER	Endoplasmatic Reticulum
FAK	Focal adhesion kinase
FDR	False-discovery rate
FOG	Friend-of-GATA
g	gram (weight) or gravity (centrifugation)
GCM	Glial-cell-missing

GFP	Green fluorescent protein
GSC	Germline Stem Cell
GSCs	Germline stem cells
GST	Glutathione S-Transferase
GTP	Guanosine-5'-triphosphate
h	hour(s)
H_3	Histone protein 3
HRP	Horseradish peroxidase
hSpindly	human Spindly
IAA	Iodoacetamide
IgG	Immunoglobulin G
INCENP	Inner Centromere Protein
IP	Immuno-precipitation
IPTG	isopropyl β-D-l thyogalactopyranoside
JAK	Janus kinase
JNK	Jun-N terminal kinase
Kan	Kanamycin
kDa	Kilodalton
K-fibers	Kinetochore fibers
KMN	KNL1, Mis12, and Ndc80
KNL-1	Kinetochore null protein 1
LCEs	Long cellular extensions
Lis-1	Lissencephaly-1
Lz	Lozenge
m	Milli
M	Molar
Mad	Mitotic Arrest Deficient
MAP	Microtubule associated protein
MBP	Maltose Binding Protein
MCAK	Mitotic centromere-associated kinesin
min	minute
Mol	Mole
Mps1	Monopolar spindle 1 kinase
mRNA	messenger RNA
MS	Mass-spectrometry
MS-MS	Tandem Mass-spectrometry
MTOC	Microtubule Organizing Centre
MZ	Medullar zone
n	Nano
NAPDH	Nicotinamide adenine dinucleotide phosphate
nc	Nurse cells
Ndc80	Nuclear division cycle 80
NOX	NAPDH oxidase
N-terminal	Amino-terminal
Nud-E	Nuclear distribution-E
O	Oocyte
OD	Optical Density
OTE	Off-target effect
PAGE	PolyAcrylamide Gel Electrophoresis

PBS	Phosphate buffered saline
PBT	Phosphate buffered saline- Tween-20
PCC	Pearson's Correlation Coefficient
PCR	Polymerase chain reaction
PDGF	Platelet-derived growth factor
PEP	Posterior Error Probability
pH	Potential of Hydrogen
PI3K	Phosphoinositide 3-kinase
PP-1	Protein Phosphatase-1
PP-2	Protein Phosphatase-2
PPIs	Protein-prootein interactions
PSC	Posterior signalling centre
PTEN	Phosphatase and tensin homolog
PTGS	Post-translational gene silencing
PVDF	Polyvinylidene fluoride
Pvf	PDGF/VEGF-related factor
PVR	PDGF/VEGF receptor
Pxn	Peroxidasin
Rack1	Receptor of activated C kinase
RNA	RiboNucleic Acid
RNAi	RNA-interference
rpm	Revolutions per minute
RT	Room temperature
RZZ	Rod–Zw10–Zwilch
SAC	Spindle Assembly Checkpoint
SDS	Sodium Dodecyl Sulfate
SDS-PAGE	Sodium dodecyl sulphate polyacrylamide gel electrophoresis
sec	second
shRNA	short-hairpin RNA
Slbo	slow border cell
Srp	Serpent
SSCs	Somatic stem cells
STAT	Signal transducer and activator of transcription
TAI	Taiman
TFA	Trifluoroacetic acid
TRIP	Transgenic RNAi Project
Tris	Tris (hydroxymethyl) aminomethane
UAS	Upstream Activating Sequence
Upd	Unpaired
Ush	U-shaped
USP	Ultraspiracle
UV	ultraviolet
V	Volts
VEGF	Vascular endothelial growth factor
VNC	Ventral nerve cord
µ	Micro

Summary

The gene *spindly* encodes for a coiled-coil containing protein required for the successful completion of mitosis and yet undefined activity in the control of cytoskeleton remodelling in post-mitotic cells. This research project aims to elucidate the requirement for *Drosophila* Spindly in both scenarios, mitosis and interphase. To address this question, loss- and gain-of-function experiments were performed to screen the effects of both downregulation and overexpression of Spindly, in a variety of cellular and developmental backgrounds. *Drosophila* is an elegible system for this analysis since it is highly genetically tractable and provides a well-characterised model for cell migration and cell division.

We found that loss of Spindly disrupts normal embryonic development resulting in a deregulation of cytoskeletal components as well as an alteration of centrosome biology. A proteomic approach based on affinity-purified mass spectrometry experiments was undertaken to identify novel binding partners for Spindly and narrow down the molecular pathway(s) in which Spindly activity may be required during develpment. MS data support its potential interaction with known regulators of centrosome biology and mitotic spindle activity, corroborating our phenotypic observations.

Similarly, the overexpression of a GFP-tagged version of the protein affects embryonic development. Increased levels of Spindly above the wild-type threshold resulted in reduced embryo survival and in altered egg morphology, pointing to a potential function for this factor in egg elongation.

To investigate the role of Spindly in post-mitotic cells and to unravel additional, uncharacterised function(s) of this protein during interphase, cells were examined for abnormalities in cell migration upon either Spindly depletion or overexpression. Downregulation of Spindly causes border cells to move sooner or faster through the egg chamber. Conversely, upregulation delays the migration of these cells towards the oocyte and in addition causes severe morphological alterations of the cluster.

In summary, Spindly has a major role in the control of cell division, mainly via co-ordination of cytoskeleton components during mitosis. Additionally, this study shows for the first time a role for Spindly in post-mitotic cells, namely border cell migration. This system therefore provides a basis for functional dissection of Spindly function in cell migration.

Contents

Figures and Tables

Figures

Tables

Chapter I: Introduction

Chapter I: Introduction

Introduction

1. Overview

This research project has been developed over a period of three years with the purpose of gaining a better understanding of the activity of Spindly in regulating mitosis as well as cytoskeleton remodelling in interphase cells. The fruit fly *Drosophila melanogaster* has been chosen as the experimental model as it provides excellent genetic tools to explore a broad range of developmental and cellular processes.

In the context of this PhD thesis loss-of-function as well as gain-of-function experiments were performed with the aim of screening the effects of downregulation and overexpression of Spindly in a variety of cellular and developmental processes. Particularly, we evaluated the contribution of Spindly to embryo development as well as to cell migration. The introduction of this thesis describes the developmental events that take place in a normal situation while the results discuss how these processes are altered by manipulating Spindly. The results are presented in three parts. Part I describes the developmental effects of altered Spindly expression on embryo viability. In Part II, the requirement of Spindly for the regulation of cell migration is investigated in two experimental models: border cells and embryonic haemocytes. Part III details the identification of potential binding partners of Spindly.

1.1. Overview on the cell cycle and the M phase

The cell cycle is a complex and co-ordinated sequence of events that regulates cell growth and culminates with the generation of two genetically identical daughter cells by the process of cell division. The cell cycle is divided into two main phases: interphase and mitosis. During interphase the cell prepares for mitosis through three phases: a G phase 1 (Gap 1), an S phase (Synthesis) and a G phase 2 (Gap 2). During mitosis, the duplicated chromosomes are segregated into two daughter nuclei and the cell is physically divided into two daughter cells in a process known as cytokinesis (Figure 1-1).

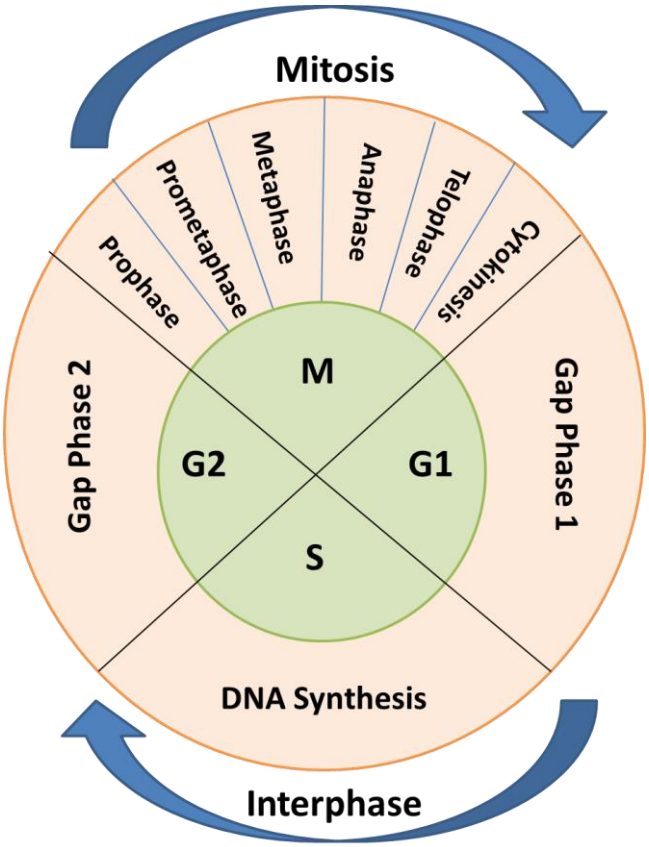

Figure 1- 1: Phases of the cell cycle. The cell cycle consists of two major phases: Interphase and Mitosis. During Interphase, cells proceed through three stages, Gap-1, Synthesis and Gap-2, during which they prepare for the following Mitosis. The M phase is composed of two tightly interconnected processes, mitosis and cytokinesis, during which the duplicated chromosomes are divided into two distinct sets and are segregated to generate two identical cells.

The progression through the different phases of the cell cycle is tightly controlled by regulatory machinery, called checkpoints that constantly monitor cell growth and genome integrity. Furthermore, cells are guided along the cell cycle by the sequential activation of heterodimeric complexes made up of a regulatory subunit, the cyclin, and a catalytic subunit, the cyclin-dependent protein kinase (Cdk). While the checkpoints monitor cell cycle progression safeguarding the accurate completion of each phase before transition into the next one, the oscillatory expression of cyclin subunits and the sequential activation of Cdk-cyclin complexes confer unidirectionality to the process. Indeed, whereas Cdks are constitutively expressed, cyclins undergo repeated cycles of synthesis and degradation and the oscillation in their levels is crucial for the timely assembly and activation of different cyclin-Cdk complexes, driving the correct progression along the cell cycle.

Of all the four phases of the cell cycle, mitosis is the most dynamic as cells are subjected to substantial changes in chromosome and cytoskeleton rearrangements which contribute to the preservation of genomic integrity during cell proliferation. Therefore, mitosis is the most delicate phase of the cell cycle and errors in this process lead to severe alterations in chromosome number, a condition known as aneuploidy (Holland and Cleveland 2009).

Similarly to interphase, mitosis is divided into sub-phases known as prophase, pro-metaphase, metaphase, anaphase, telophase and cytokinesis (Figure 1-1).

During prophase, the duplicated genomic material becomes packed into mitotic chromosomes. These structures consist of two identical sister chromatids bound together at the primary restriction, or centromere. At beginning of pro-metaphase, the duplicated centrosomes migrate to opposite ends of the cell and nucleate a functional

mitotic spindle by polymerisation of microtubule fibres. As soon as the assembly of the mitotic spindle is completed, microtubules emanated from opposite poles are engaged in finding and capturing the sister kinetochores, specialised multi-protein structures assembled at the centromere of each sister chromatid. At metaphase, chromosomes that have been stably bound to the kinetochore fibres are forced to move towards the spindle equator, or metaphase plate, and to orient the sister kinetochores towards the opposite poles of the spindle, a configuration known as bi-orientation. The cohesion between the sister chromatids resists the pulling forces of microtubules upon bi-orientation, generating inter-kinetochore tension. Sister kinetochore tension is critical for sensing bi-orientation and allows chromosome segregation to proceed. Loss of cohesion between sister chromatids allows their translocation along the microtubules towards opposite spindle poles in anaphase. Once segregated, chromosomes decondense during telophase and a contractile actin-myosin ring, the cleavage furrow, assembles to divide the cell into two during cytokinesis.

Although many of the molecular events governing mitosis have been extensively studied and characterised, many aspects of this important cellular process are still poorly defined and need to be elucidated. This introduction reviews the mechanisms that control the activity of the spindle in capturing the mitotic chromosomes as well as the signalling pathways responsible for correct bi-orientation. In this context, the relevance of novel mitotic proteins in the control of these aspects of mitotic progression will be discussed, focusing in particular on Spindly and its crucial activity in coupling chromosome alignment to inactivation of the mitotic checkpoint

A second section describes the importance of *Drosophila melanogaster* as versatile model organism for biomedical research.

1.2 Functional structures in mitosis: Mitotic Spindle and Kinetochore

1.2.1 Function and Regulation of the Mitotic Spindle

Segregation of chromosomes in mitosis relies on the activity of a bipolar microtubule-based machinery, the mitotic spindle that assembles dynamically at pro-metaphase consuming the energy derived from the hydrolysis of GTP molecules.

The microtubules emanate from the opposite poles of the spindle and are oriented with the dynamic plus-ends facing the duplicated chromosomes and the minus-ends tethered at the spindle poles. Three populations of microtubules have been identified (Torsten Wittmann 2001). The first class attaches the chromosomes at the level of the kinetochore and is responsible for chromosome alignment and segregation. These microtubules are named kinetochore microtubules or K-fibres. The second class includes the so-called interpolar microtubules; they assemble at each pole and overlap at the spindle equator where they are cross-linked together to provide stability to the structure. Finally, a third class of microtubules extends away from the pole and is involved in the process of spindle positioning. These microtubules are known as astral microtubules.

The assembly and the function of the mitotic spindle rely on the activity of microtubule-dependent molecular motors, belonging to two distinct families of ATP-dependent proteins: Kinesins and Dyneins. These factors regulate the activity of the spindle performing three main functions: they bridge and slide anti-parallel microtubules, they move molecules across the surface of the microtubules and they combine microtubule dynamics with chromosome movements in mitosis (David J. Sharp 2000).

The family of kinesins plays a crucial role in spindle biogenesis based on the ability of this class of motors to cross-link microtubules fibres into bundles. Early in prophase, microtubules originated from each pair of centrioles contact each other forming overlapping interactions favoured by kinesin proteins, such as Eg5 and Kif15. These motors form tetrameric structures characterised by a central rod-like domain ending with motor heads at each extremity. The motor domains at each end contact antiparallel microtubules bridging them together and sliding them across one another. Therefore, walking towards the microtubule plus-ends, kinesin motors may generate outward forces responsible for centrosome separation and assembly of a bipolar spindle. This idea is reinforced by experimental data showing that inhibition of Kinesin activity results in loss of pole separation and therefore generation of monopolar spindles (Tanenbaum and Medema 2010).

However, the activity of motors on the spindle needs to be carefully balanced to maintain spindle integrity and stability. Specifically, Kinesin activity is counteracted by the motor protein Dynein that, moving towards the minus-ends, produces inwards forces that prevent the spindle from collapsing (van Heesbeen, Tanenbaum et al. 2014). Dynein motors are also found at the cortex where it has been suggested they bridge the astral microtubules to the plasma membrane contributing to spindle anchoring and positioning during mitosis (Kotak, Busso et al. 2012). In *Drosophila* early embryos, this activity of dynein at the cortex is shown to contribute to KLP61F kinesin-dependent centrosome separation and spindle elongation during prometaphase-metaphase (David J. Sharp 2000).

Microtubules motors also guarantee the coordinated movements of chromosomes and their proper positioning on the spindle. Specifically, the kinesin CENP-E and the dynein

motor localise to the kinetochores and are responsible for chromosome congression (Kenneth W. Wood 1997) and chromosome segregation (Raaijmakers and Medema 2014) during mitosis, respectively.

Additionally, CENP-E is thought to maintain kinetochores stably bound to the depolymerising plus-ends of microtubules, thereby coupling chromosome movement in anaphase to microtubule dynamics (Vivian A. Lombillo 1995). In this regard, the ability of CENP-E to tether kinetochores to the microtubule plus-ends is combined with the activity of the centromere protein MCAK in destabilising microtubules (Todd Maney 1998). The current model suggests that the kinesin MCAK promotes the depolymerisation of the K-fibres generating the driving force that promotes chromosome movement in anaphase. CENP-E, binding the plus-ends, provides the physical link between kinetochores and microtubules. CENP-E therefore couples microtubule shortening with chromosome polewards movement.

1.2.2 The dynamic platform of the kinetochore

For chromosome segregation to occur, the mitotic spindle needs to unequivocally recognise on each sister chromatid a specialised multi-protein complex, the kinetochore. This platform is the unique site of attachment for kinetochore microtubules and it also recruits regulators of the mitotic progression that monitor the state of kinetochore-microtubule interactions.

The kinetochore assembles on mitotic and meiotic chromosomes at the centromere, a specialised region of DNA that marks the site of assembly of a functional kinetochore. The centromere is specified during S phase by incorporating a H3 histone variant, the Centromeric Protein A (CENP-A), that orchestrates the assembly of an inner

kinetochore plate by associating tightly with sixteen additional CENP proteins (Cheeseman and Desai 2008). This protein network co-localises stably with CENP-A throughout the cell cycle and it is named Constitutive Centromere-associated Network (CCAN). In *Drosophila* as well as *C elegans* the network is extremely simplified being composed of only two proteins, CENP-A and CENP-C. However, regardless of the model organism examined, the CCAN is fundamental for kinetochore assembly and therefore chromosome segregation. The CCAN ensures that the platform for anchoring the spindle microtubules will be built in a single and highly specialised region of the chromosome, the centromere (Figure 1-2).

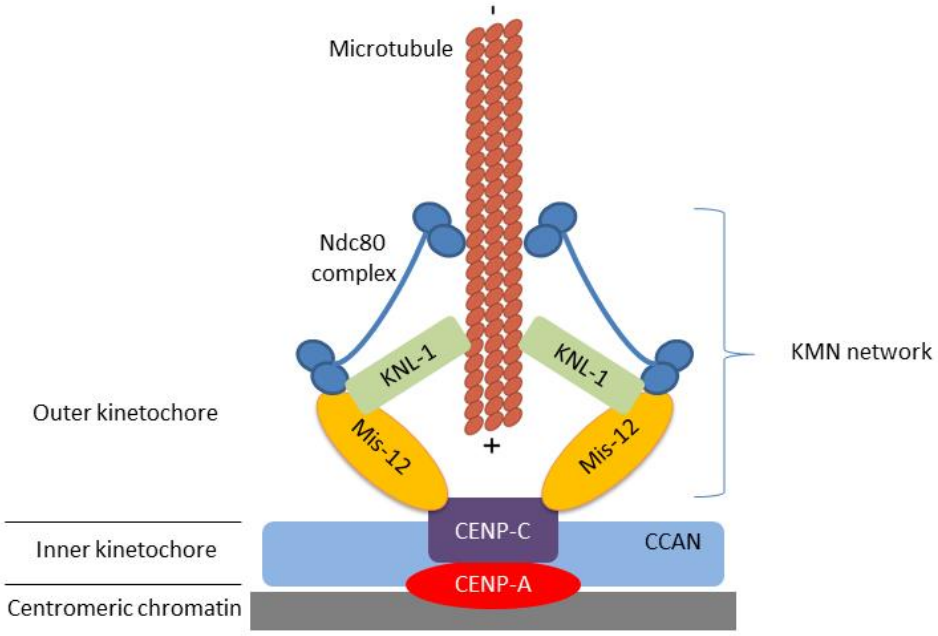

Figure 1- 2: **Organisation of the outer kinetochore plate.** The constitutive cemtromere-associated network (CCAN, light blue) associates with the centromere protein-A (CENP-A, in red) throughout the cell cycle. During mitosis, the CCAN subunit CENP-C (in purple) recruit the so-called KMN network. This complex consists of Mis-12 (in orange), KNL-1 (in green), responsible for the kinetochore localisation of mitotic checkpoint players (see Figure 1-4) and Ndc80 (in dark blue) that provides the primary microtubule-binding interface at the kinetochore.

As soon as the cell enters mitosis, the inner kinetochore dynamically recruits a set of proteins to form the outer kinetochore plate. Localisation of Mis-12 at the centromere

is fundamental to this process. Mis-12 in fact binds to the Kinetochore null protein 1 (KNL-1) and to the Ndc-80 complex building a protein complex, the KMN network, which performs many key activities in mitosis (Figure 1-2).

KNL-1 is a scaffold protein involved in the interaction of kinetochore components and mitotic players, controlling the state of microtubule-kinetochore attachments and therefore progression through mitosis. Depletion of KNL-1 results in a null-kinetochore phenotype (herein its name) and causes severe segregation defects.

NDC-80 is a complex of four proteins (Spc24, Spc25, Nuf2 and Ndc-80) and it represents the microtubule-binding interface at the kinetochore. These proteins are characterised by Calponin Homology (CH) domains that interact electrostatically with the microtubule surface. Additionally the N-terminal unstructured tail of Ndc-80 is reported to be fundamental for establishing microtubule attachment (Ciferri, Pasqualato et al. 2008). The binding of NDC-80 to microtubules is cooperative meaning that the presence of multiple complexes increases the affinity of kinetochore for the K-fibres. Additionally, the interaction is highly regulated and its stability depends upon Aurora B kinase-dependent phosphorylation of the KMN network (Welburn, Vleugel et al. 2010).

Aurora B is part of a complex, the Chromosome Passenger complex (CPC) that includes Survivin, Borealin and Inner Centromere Protein (INCENP). The CPC localises to the centromere during pro-metaphase (Vader, Maia et al. 2008). The CPC is responsible for kinetochore-microtubule turnover, particularly for the correction of erroneous kinetochore-microtubule binding. The current model predicts that Aurora B activity results in inhibition of Ndc-80 microtubule-binding ability, setting the kinetochore back to a microtubule-free state prone to interact with newly forming microtubules.

The KMN network is therefore a fundamental core component of the kinetochore being able to combine structural activities with regulatory functions. Indeed of its three components, KNL-1 acts as a recruitment platform for additional structural kinetochore components as well as for regulators of mitotic progression whereas the Ndc-80 complex mediates the interaction with the K-fibres. The KMN network is therefore the structural module at the kinetochore where establishment of stable kinetochore-microtubule interactions and cell cycle control mechanisms are integrated to promote mitotic exit.

1.3 The Spindle Assembly Checkpoint

Faithful chromosome segregation in mitosis is fundamental for maintaining genome stability and cell viability. The physical separation of the duplicated chromosomes is accomplished by anchoring the sister chromatids to opposite poles of the mitotic spindle, a configuration known as amphitelic or bi-oriented attachment. The establishment of such conformation is a challenging task for cells as it often results in incorrect binding of sister kinetochores to the spindle fibres. Therefore, cells have circumvented this issue by developing two surveillance mechanisms that act in parallel during mitosis to ensure bi-orientation of chromosomes on the metaphase plate.

The first mechanism involves the detection of improper attachments and the turnover of unstable kinetochore-microtubule interactions, limiting the rate of segregation defects. Concomitantly, cells arrest the progression in mitosis gaining time to successfully align chromosomes before anaphase onset. This second mechanism responsible for the cell cycle arrest is known as the Spindle Assembly Checkpoint (SAC). Solving the molecular mechanism underlying SAC activation and activity has been an

enduring scientific goal. The next section describes the main discoveries in the field focusing on the mechanisms that regulate the functional state of the mitotic checkpoint.

1.3.1 Molecular mechanism of SAC activation

The first evidence for the existence of a mitotic checkpoint came from genetic screens in budding yeast for mutants that failed to arrest in response to microtubule depolymerising agents (M. Andrew Hoyt 1991, Rong Li 1991). These screens identified two sets of genes encoding for well-described players of the SAC at kinetochores: the Budding uninhibited by benzimidazole genes, *BUB1*, *BUB2* and *BUB3*, and the Mitotic arrested-deficient genes *MAD1*, *MAD2* and *MAD3*.

Two evolutionary conserved protein kinases, Aurora B and Monopolar Spindle 1 (Mps1), orchestrate the hierarchical assembly of these proteins on kinetochores activating a series of reversible events that converge on the assembly of a mitotic checkpoint complex (MCC). MCC is the cytosolic effector of the SAC being responsible for the inhibition of the E3 ubiquitin ligase Anaphase Promoting Complex/Cyclosome (APC/C). The APC/C ligase targets mitotic substrates for proteasome-dependent degradation and couples chromosome bi-orientation with progression into anaphase and mitotic exit. The activation of the ubiquitination activity relies on the interaction with mitotic co-activators: Cell-division cycle protein-20 (Cdc-20) and Cdh-1. These activators sequentially bind to APC/C regulating the specificity of the ligase for its substrates. At the metaphase-to-anaphase transition the enzyme is preferentially in a complex with Cdc-20 and shows increased binding affinity for Securin and Cyclin B. The mitotic checkpoint complex delays the degradation of these substrates by sequestering

Cdc-20 and preventing its binding to the APC ligase until all chromosomes have reached bi-orientation on the metaphase plate.

The presence of a single unattached kinetochore triggers a phosphorylation cascade that amplifies the wait-anaphase signal, resulting in the step-wise assembly of a functional MCC and the prompt inhibition of APC/C. Aurora B is one of the kinases involved in the process and its activity impacts on the functional state of the checkpoint in two main ways. Firstly, Aurora B is the master regulator of the error-correction mechanism that releases the improper attachments and generates free-kinetochores, signalling the cell to keep the checkpoint in an active state. Secondly, the kinase is responsible for the transactivation of MpsI and its binding to Ndc80, regulating directly the activation of the SAC (Saurin, van der Waal et al. 2011). In fact, phosphorylation of MpsI acts as a molecular switch for checkpoint activation as it mediates the recruitment of SAC proteins to kinetochores by promoting the phosphorylation of an evolutionary conserved substrate, KNL-1 (Figure 1-3).

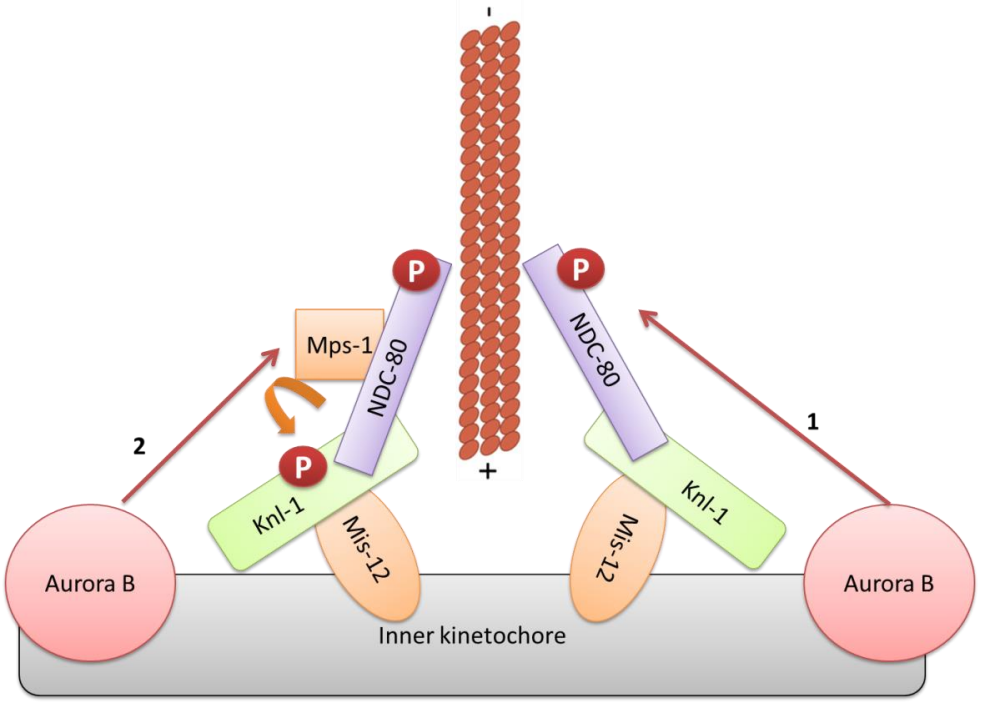

Figure 1- 3: Model of Aurora B and Mps-1 activity during mitosis. Improper kinetochore-microtubule attachments generate a phosphorylation cascade that results in the assembly of a functional MCC and generation of the wait-anaphase signal. Aurora B and Mps-1 are the protein kinases involved in this process. Aurora B is responsible for the phosphorylation of the NDC-80 complex (red arrow, 1) and release of the microubule plus-ends. Moreover, Aurora B trans-activates Mps-1 allowing its binding to NDC-80 (red arrow, 2). MpsI acts as a molecular switch for checkpoint activation: the kinase phosphorylates Knl-1 on its MELT domains and therefore mediates the recruitment of SAC proteins to kinetochores.

KNL-1 has indeed emerged as both a structural component of the kinetochore as well as a docking platform for signalling molecules, catalysing the assembly of the MCC in a step-wise manner (Ghongane, Kapanidou et al. 2014). This protein is characterised by a variety of functional motifs: the RSVF-SILIC N-terminal motifs that regulate the stability of the kinetochore-microtubule interactions, the N-terminal and central MELT motifs and the C-terminal RWD domain.

Structural analysis has revealed that the C-terminal region of KNL-1 mediates binding to other kinetochore proteins such as Mis-12, Hec-1 and Zwint. This latter interaction is indispensable for the Aurora B-dependent localisation of another component of the outer kinetochore plate, the RZZ complex (Kasuboski, Bader et al. 2011). These data

point to a crucial function for KNL-1 in orchestrating the dynamic assembly of the outermost plate of the kinetochore.

The N-terminal and central MELT motifs on KNL-1 are recognised and phosphorylated by MpsI and are essential for the localisation of Bub and Mad proteins at the kinetochore (Figure 1-4). The binding of Bub3 to the phosphorylated MELT domains triggers the recruitment of Bub1 and BubR1 and this is the limiting step in the activation of the SAC (London, Ceto et al. 2012, Shepperd, Meadows et al. 2012, Moyle, Kim et al. 2014). Indeed, recent studies point at Bub1 as the main factor for Mad-1 localisation to the kinetochore and confirm the importance of MpsI-dependent phosphorylation in the process. Interfering with Mad-1/Bub1 interaction by knocking down Bub1 or mutating the Bub1-binding site on Mad-1 completely abolishes Mad-1 kinetochore localisation (London and Biggins 2014, Moyle, Kim et al. 2014). Additionally, stable binding of Bub1 to the kinetochore in a phospho-deficient KNL-1 mutant background is sufficient to recruit Mad-1 and activate the checkpoint. All together these data confirm the requirement of both, the phosphorylation event and Bub1, for the controlled localisation of Mad-1 at the kinetochore (London and Biggins 2014). Moreover, these results imply that Bub3 is only required for the initial localisation of SAC components at kinetochores but does not have any additional functions in the activation of the SAC cascade. Despite these observations, the mechanism of Mad-1 localisation is still controversial and the protein requires additional receptors to bind stably at the kinetochore. Recently, a linear Bub1-RZZ-Mad1 pathway has been suggested, in which Bub1 and RZZ cooperate to achieve the successful binding of Mad-1 at kinetochore (Zhang, Lischetti et al. 2015).

The final step of this cascade is the recruitment to the kinetochore and activation of Mad-2 through binding with Mad-1 (Figure1-4). Mad-2 shuttles between two conformational states: a cytosolic inactive form, known as Open Mad-2 (O-Mad-2), and a close active form, known as C-Mad-2. Binding of Mad-2 to Mad-1 triggers the conversion of O-Mad-2 into the active C-Mad-2 conformation and generates a Mad1-Mad2 template that recruits additional O-Mad-2 from the cytosol. This mechanism generates a large amount of C-Mad-2 molecules free to bind Cdc-20 at high affinity and to assemble a functional MCC complex for the inhibition of APC (De Antoni, Pearson et al. 2005, Nezi, Rancati et al. 2006, Tipton, Ji et al. 2013). Indeed, the binding of Mad-2 to Cdc-20 induces a conformational change on the APC/C coactivator, releasing an autoinhibitory interaction between N-terminal and C-terminal domains and making accessible a previously masked BubR1 binding site. In other words, the interaction with Mad-2 primes Cdc-20 for the binding with BubR1, leading to the final inhibition of the APC/C E3 ligase (Han, Holland et al. 2013). Therefore the kinetochore constitutes a niche where SAC proteins concentrate and are forced to interact, forming the MCC complex.

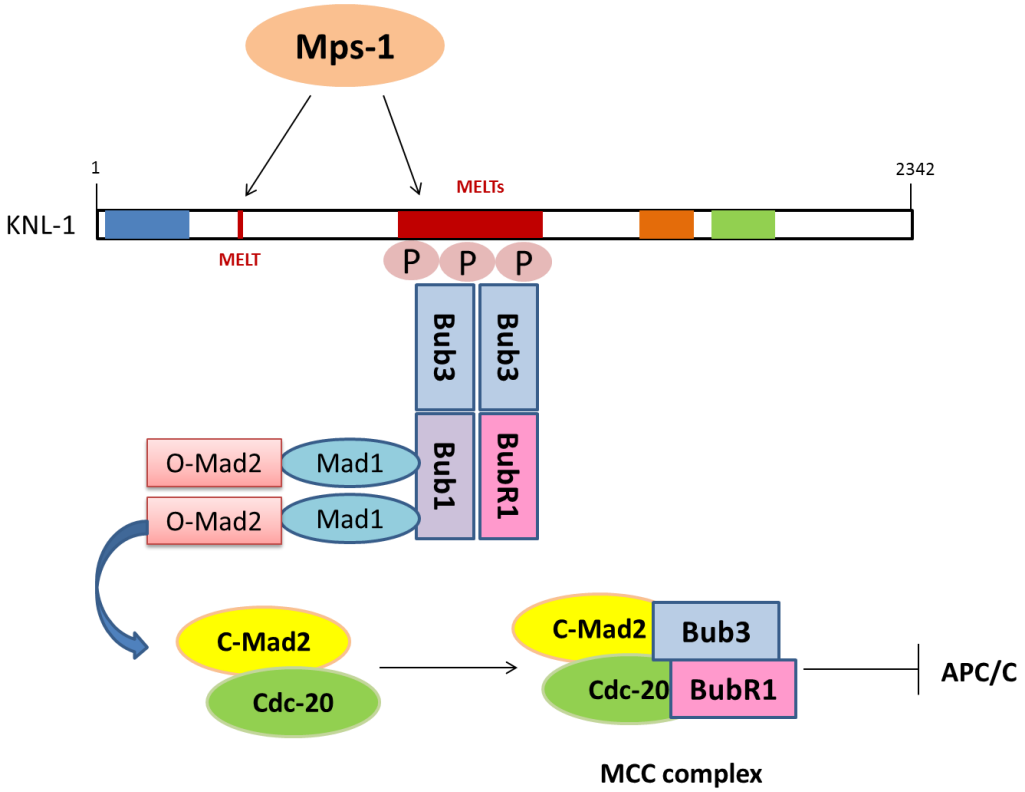

Figure 1- 4: Summary of the recruitment cascade of SAC component to unattached kinetochores. The assembly of a functional mitotic checkpoint complex is a step-wise process. The kinetochore protein KNL-1 becomes the recruitment platform on which the MCC assembles upon Mps-1-dependent phosphorylation of the MELT repeats. The phosphorylation event results in the recruitment of Bub3/Bub1 and Bub3/BubR1 heterodimers at the kinetochore. The next step consists in the localisation of Mad-1/Mad-2 heterodimers through a Mad-1-Bub1 interaction. The Binding of Mad-2 to kinetochore triggers its conversion from the inactive O-Mad-2 to the active C-Mad-2, able to bind Cdc-20 and assemble a functional MCC, inhibiting the E3 ubiquitin ligase APC/C.

1.3.2 Mechanisms of SAC Inactivation

The bipolar attachment of chromosomes to the mitotic spindle is achieved when all the duplicated chromosomes are attached to microtubules originating from the opposing poles of the mitotic spindle. The main function of the SAC is to guarantee the faithful segregation of chromosomes, monitoring the establishment of proper kinetochore-microtubule interaction and allowing cells to proceed into anaphase only when bi-orientation is achieved. Even if considerable progress has been made in defining the details of SAC activation and in uncovering the mechanism(s) that propagate(s) this signal, how chromosome attachment is coupled to SAC inactivation and anaphase onset is still unclear and poorly characterised.

1.3.2.1 Current models of mitotic checkpoint inactivation

Current research in the field of mitosis focuses on understanding how the APC/C-dependent inhibition of anaphase onset is released once all sister chromatids have achieved bipolar attachment to the mitotic spindle. Several mechanisms are activated simultaneously to ensure the rapid inactivation of the SAC and progression into anaphase. Firstly, key players of the checkpoint, such as Mad1 and Mad2, need to be removed from the outer surface of the kinetochore, thereby preventing the propagation of the anaphase-inhibitory signal. Secondly, residual MCC complexes that persist in the cytoplasm need to disassemble in order to free Cdc-20 and allow binding to APC/C. Finally, the regulation of the phospho-equilibrium at the kinetochore plays an important role in regulating the on-off state of the mitotic checkpoint.

1.3.2.1.1 Motor protein-based mechanism of SAC inactivation: kinetochore stripping

The composition of the outer kinetochore plate changes drastically upon the establishment of stable microtubule attachments both in terms of number and types of proteins that constitute it. Indeed a subset of proteins, including also SAC components, is actively removed from kinetochores prior to progression into anaphase, highlighting the fundamental requirement of this process for inhibiting the SAC. In support of this idea, the overexpression of a Mad-1 construct that constitutively binds to kinetochores prolongs the mitotic arrest, greatly delaying the exit from mitosis (Maldonado and Kapoor 2011). The process of kinetochore stripping is dependent on the kinetochore activity of the minus-end-directed motor dynein (Howell, McEwen et al. 2001, Griffis, Stuurman et al. 2007, Mische, He et al. 2008).

Dynein localises at three distinct sub-cellular locations during mitosis: cell cortex, spindle poles and the kinetochore. This diverse distribution of dynein at the G_2/M transition reflects the variety of processes that require the presence of this motor during mitosis. Cytoplasmic dynein is implicated in many mitotic functions, including focusing of the spindle and organisation of the spindle apparatus, spindle rotation and positioning, anaphase chromosome movement and stabilisation of the kinetochore fibres (Yang, Tulu et al. 2007). Given the multiple functions of dynein during mitosis, the kinetochore specific role(s) of the motor have been quite difficult to assess.

The localisation of the motor at kinetochores is mediated by the RZZ complex (Rough Deal (Rod), ZW10 and Zwilch) and it is regulated by Plk1-dependent phosphorylation of the dynein light chain (Whyte, Bader et al. 2008, Bader, Kasuboski et al. 2011). The RZZ complex influences dynein recruitment to the kinetochore directly, by mediating its

interaction with p50/dynamitin subunit of the dynactin complex and with the dynein intermediate chain, as well as indirectly via a novel mitotic factor named Spindly (Griffis, Stuurman et al. 2007, Gassmann, Essex et al. 2008, Chan, Fava et al. 2009, Gassmann, Holland et al. 2010)

Selective depletion of dynein from kinetochores can be achieved by disassembling the RZZ complex and this strategy has provided a powerful means to establish the activity of the motor at kinetochores and to understand its contribution to chromosome alignment as well as SAC regulation without affecting dynein activity at other mitotic loci (Daniel A. Starr, Thomas S. Hays et al. 1998, Kops, Kim et al. 2005).

Depletion of ZW10 abrogates dynein recruitment to kinetochores, causes delay in chromosome congression and increases the number of lagging chromosomes at anaphase (Buffin, Emre et al. 2007). Moreover, failure in localising dynein at kinetochores results in a strong and prolonged mitotic block and abnormal accumulation of Mad-2 at kinetochores (Edward Wojcik 2001, Howell, McEwen et al. 2001). These data support a double activity for kinetochore dynein in mitosis, implicating the motor protein in both, formation of stable kinetochore-microtubule interactions early in mitosis and inhibition of the mitotic checkpoint upon bi-orientation. These two activities are independent from its other mitotic functions because inhibition of the motor at pro-metaphase does not compromise the formation of a bipolar spindle nor the congression of chromosomes to the metaphase plate (Howell, McEwen et al. 2001).

Although these two functions for dynein at the kinetochore have been individually characterised, it is unclear how they are coordinated to ensure mitotic exit. A possible

solution comes from the characterisation of Spindly as a kinetochore-specific regulator of dynein.

1.3.2.1.2 Spindly activity in linking chromosome alignment with SAC inactivation

Spindly was discovered in 2007 by performing a genome-wide RNAi screen in *Drosophila* S2 cells for proteins whose depletion was able to block progression through mitosis and alter cell morphology in interphase (Griffis, Stuurman et al. 2007). Spindly protein has a predicted rod-like structure and contains 780-amino acids forming four N-terminal coiled-coil domains, a short sequence twenty-one amino acid long named Spindly box, and four positively-charged Carboxy-terminal (C-terminal) repeats. Additionally, sequence analysis revealed the presence of a potential Mad-2 binding site at the C-terminus (Figure1-5) (Griffis, Stuurman et al. 2007).

Since the initial discovery of the *Drosophila* homologue, Spindly has been identified also in human (hSpindly/CCDC99, 605 residues) and in *C. elegans* (SPDL-1, 479 residues). The orthologues show substantial difference in size and a low level of sequence homology that is restricted to the short N-terminal motif lying between the coiled-coil domains (Figure 1-5).

Figure 1- 5: Domain composition of Drosophila Spindly. The diagram illustrates the main domains identified: four coiled-coil domains (orange) separated by the highly conserved Spindly box (purple) and a series of positively charged domains towards the C-terminus (blue). A potential binding-site for Mad-2 is present at the C-terminus (red box).

In all the species studied, Spindly is positioned in a linear pathway for the hierarchical recruitment of dynein to kinetochores, physically bridging the motor protein and the RZZ complex. The localisation of Spindly at the outer kinetochore plate depends on the RZZ complex and evidence for a weak, direct interaction between the two have been reported in human and worms (Gassmann, Essex et al. 2008, Barisic, Sohm et al. 2010). Moreover, recent studies have clarified a fundamental role for post-translational modifications in regulating the subcellular localisation of the human homologue, revealing that farnesylation of the C-terminal domain is indispensable to enhance the ability of hSpindly to bind to kinetochores (Holland, Reis et al. 2015, Moudgil, Westcott et al. 2015). Once bound to the RZZ complex, this elongated protein stretches out from the kinetochore acting as a recruitment platform for the dynein motor (Varma, Wan et al. 2013).

Depletion of Spindly by RNAi has major consequences. Firstly, cells arrest in metaphase accumulating high levels of SAC components at kinetochores. Secondly severe chromosome alignment defects were observed (Griffis, Stuurman et al. 2007, Gassmann, Essex et al. 2008, Gassmann, Holland et al. 2010). Unexpectedly, co-depletion of the RZZ complex alleviates the Spindly-RNAi phenotype, allowing cells to progress through mitosis with minor chromosome alignment defects and a low rate of mis-segregation (Gassmann, Essex et al. 2008).

Therefore, in mitotic cells Spindly is proposed to contribute to the establishment of stable and mature kinetochore-microtubule attachments in a dynein-dependent manner (Gassmann, Essex et al. 2008). The protein emerges as a crucial coordinator between two important kinetochore modules, RZZ and dynein, establishing itself as bridge link between the achievement of bi-orientation and control of cell cycle

progression. However, the molecular basis of the dynamic interplay between these three components remains to be elucidated.

1.3.2.1.3 Requirement of Spindly during meiosis

Similar to mitosis, faithful segregation of the genetic material is required also during meiosis as any error in these events leads to infertility and birth defects. Currently, the regulation of SAC activity during germ cell meiosis is a field of intense research and the mechanisms that ensure the dynamic control of kinetochore-microtubule interaction as well as spindle stability start to be elucidated (Sun and Kim 2012).

The localisation and activity of Spindly has been extensively characterised during mitosis. However, given the important role of this factor in the control of somatic cell division, it is reasonable to hypothesise an equally crucial function during meiosis. Localisation and activity of Spindly have been studied during mouse female meiosis (Qing-Hua Zhang 2010). The protein localises mainly to kinetochores and shows partial relocalisation to the spindle poles in oocytes at stage MI and MII. While overexpression of the protein does not cause profound changes in SAC activity and progression through meiosis, downregulation arrests oocytes at stage MI. The majority of the oocytes fail to extrude the first polar body, show defects in chromosome alignment to the metaphase plate and display abnormal mitotic spindle morphology. Therefore, mSpindly is required for inactivation of the mitotic checkpoint, spindle formation and regulation of kinetochore-microtubule attachments, suggesting that Spindly performs similar activities in mitosis and meiosis (Qing-Hua Zhang 2010).

In *Drosophila* the requirement of Spindly during meiosis has not been elucidated yet. Recent reports suggest that the fine regulation of the phosphorylation status of

Spindly as well as other proteins is required to accomplish the egg-to-embryo transition, in a process known as egg activation (Krauchunas, Horner et al. 2012, Amber R. Krauchunas 2013). The biological relevance of this dephosphorylation event at the onset of egg activation has not been clarified. The nucleus of a mature oocyte in Drosophila is arrested in metaphase I of the meiotic cycle (Horner and Wolfner 2008). At egg activation this arrest needs to be released and cell cycle has to resume. Given the role of Spindly in the regulation of metaphase-to-anaphase transition, it is likely that dephosphorylation of Spindly favours the transition into anaphase and completion of meiosis but this hypothesis needs to be carefully tested.

1.3.2.1.4 Potential function(s) for Spindly in post-mitotic cells

Unlike its homologues, *Drosophila* Spindly has been proposed to regulate interphase cell morphology. In S2 cells, Spindly is found at the plus-ends of microtubules with the plus-end binding protein EB-1 and when overexpressed it decorates the entire length of microtubules, suggesting this protein has the ability of binding the microtubule network. Additionally, the protein shows localisation at cell protrusions (Griffis, Stuurman et al. 2007).

Knockdown of the protein results in a typical interphase phenotype: Spindly-RNAi indeed affects the formation of actin-based lamellopodia and favours the appearance of long microtubule projections (Figure 1-6) (Griffis, Stuurman et al. 2007).

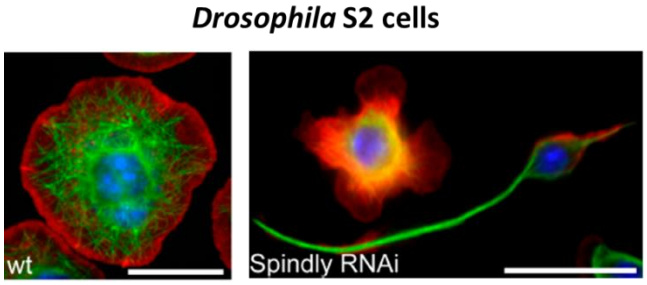

Figure 1- 6: Effect of the knockdown of Spindly on cell morphology. *Drosophila* S2 cells adopt a typical spread cell morphology when plated on Concanavalin-A (Con-A) (wt). Down-regulation of Spindly by RNAi (Spindly RNAi) profoundly alters cell shape, causing defects in actin lamellae and the appearance of long projection enriched in microtubules. Nuclei are in blue, actin in red and tubulin in green. Image was adopted from (Griffis, Stuurman et al. 2007).

Overall, these data reason in favour of a potential requirement for Spindly in influencing the dynamic behaviour of F-actin and the microtubule cytoskeleton via yet unknown mechanism(s) during interphase.

1.3.2.1.5 Mechanism(s) of MCC disassembly

The dissociation of the SAC proteins Mad-2, Bub-3 and BubR-1 from the MCC complex is another key event that helps extinguish the anaphase-inhibitory signal. The mechanism(s) of MCC disassembly and consequent SAC inactivation remain(s) poorly understood. Several recent studies have focussed on the contribution of $p31^{COMET}$ to this process. $p31^{COMET}$ antagonises the activity of the SAC acting as a positive regulator of the metaphase-to-anaphase transition (Westhorpe, Tighe et al. 2011). This protein was initially identified as a Mad-2 interactor (Toshiyuki Habu 2002); subsequent *in vitro* studies showed that the binding of $p31^{COMET}$ to Mad-2 inhibits the recruitment of other O-Mad-2 molecules and their conversion into the active C-Mad-2 form. This observation led to the postulation of the “capping” model according to which $p31^{COMET}$ binds to Mad-1/Mad-2 heterodimers at kinetochores preventing the propagation of the wait-anaphase signal.

Later studies advanced our understanding about $p31^{COMET}$ activity, raising the possibility of a different but still intriguing mechanism of p31-dependent inactivation of the mitotic checkpoint. According to this alternative model, $p31^{COMET}$ binds to the MCC by interacting with Mad-2 and promotes the ATP-dependent dissociation of Mad-2 and BubR-1 from Cdc-20 (Teichner, Eytan et al. 2011).

In addition to $p31^{COMET}$ other factors have a role in MCC disassembly. APC15, a small subunit of the APC E3 ligase, is required for Cdc-20 auto-ubiquitination and degradation, facilitating rapid MCC dissociation. This discovery implicated that cycles of synthesis and APC-mediated degradation of Cdc-20 occur during mitosis, favouring the dynamic assembly and disassembly of MCC and guaranteeing a quick and reversible inactivation of the mitotic checkpoint (Foster and Morgan 2012, Uzunova, Dye et al. 2012).

1.3.2.1.6 Contribution of protein phosphatases to silencing the SAC

Given the importance of phosphorylation events in catalysing the recruitment of SAC components to kinetochores, dephosphorylation of mitotic substrates can be equally crucial in reversing the on-state of the checkpoint. The families of Protein Phosphatase 1 and 2 (PP-1 and PP-2) are central components of a phospho-regulatory mechanism that tunes the phosphorylation levels of mitotic substrates according to the functional state of kinetochore-microtubule interactions. Particularly, PP-1 has been shown to localise at kinetochores by interacting with KNL where it counteracts the activity of Aurora B kinase stabilising microtubules attachments (Liu, Vleugel et al. 2010). This implies that when chromosomes are not bi-oriented and the kinetochores are not under tension, Aurora B phosphorylates its mitotic substrates, including Hec-1 and

KNL-1, depolymerising microtubules and inhibiting PP-1 recruitment. Conversely, the tension applied on kinetochores once bi-orientation is achieved, reduces the activity of the kinase and increases that of PP-1, resulting in stabilisation of kinetochore-microtubule attachments and SAC silencing (Liu, Vleugel et al. 2010).

With a similar mechanism to PP-1, PP2A-B56 promotes SAC inactivation by balancing the phosphorylation activity of Mps-1 on KNL-1. Mps-1 phosphorylates KNL-1 on its MELT repeats and this phosphorylation event is indispensable for the recruitment of Bub-1, Bub-3 and BubR-1 at kinetochores and therefore the initiation of the wait-anaphase signal (Fig. 1-3). Upon stable microtubule attachments, the activity of Mps-1 declines and the phospho-residue on KNL-1 is removed thanks to the upregulated activity of PP2A, resulting in loss of SAC components from kinetochores (Espert, Uluocak et al. 2014). Overall, these findings highlight a remarkable mechanism by which the tension across the sister chromatids regulates and balances the activity of kinases and phosphatases at kinetochores, modulating the level of mitotic checkpoint activation. Aurora B localises at the centromere therefore the ability to phosphorylate its targets at the kinetochore decreases with the distance. When sister chromatids are under tension the sister kinetochores are subjected to a stretch that separates the kinase from its substrates, downregulating the SAC. Concomitantly the increased activity of protein phosphatases generates a positive feedback loop that triggers exit from mitosis.

1.4 The relevance of *Drosophila melanogaster* as model organism

Drosophila melanogaster has been adopted as a model organism for biomedical research for over hundred years. They are beneficial for many reasons including their rapid development, the ability to produce a large number of offspring and the high evolutionary conservation with humans. The genetics of fruit-fly development is well established and an unrivalled set of methods are available to successfully manipulate the fly genome, making *Drosophila* a popular system to advance our understanding in several biological areas, including embryonic development, behaviour and aging. Additionally, the remarkable conservation between human and *Drosophila* genes has given the possibility of easily determining the biological effects of gene deletion, overexpression or mutations in functional domains, simplifying the aim of establishing their requirement in humans and developing new treatments. *Drosophila* is therefore a very elegant and versatile model to uncover the genetic pathways controlling various developmental and cellular processes, including regulation of cell cycle progression and control of the mitotic checkpoint.

In the context of this PhD thesis, we aim to define how and to what extent the mitotic and post-mitotic activity of Spindly contributes to embryo development. Specifically, we aim to clarify whether the activities of Spindly in controlling the functional state of the mitotic checkpoint and in regulating cytoskeleton dynamics coordinate the numerous developmetal and morphological events that take place during embryogenesis.

Therefore, the next session of the introduction will describe the early stages of Drosophila embryogenesis focusing on the mechanisms that couple the execution of rapid nuclear divisions to cytoskeleton remodelling.

1.4.1 Development of *Drosophila melanogaster*

Drosophila is a holometabolic insect meaning that it undergoes complete metamorphosis during its life cycle (Figure 1-7). Its life cycle takes approximately 10 days at 25°C and it consists of three stages before emerging as an adult: egg/embryo, larva and pupa.

The development from embryonic stage to larva lasts 24 hours. Larvae are the worm-like stage of the early *Drosophila* life cycle, which lasts over a period of 4 days and it consists of three developmental stages, known as instars. The third instar larva then moves to a dried surface and it forms a shell in which it morphs into the adult fly in a process known as pupation. Metamorphosis requires an additional 4-5 days to be completed and at the end of this period an adult fly is formed.

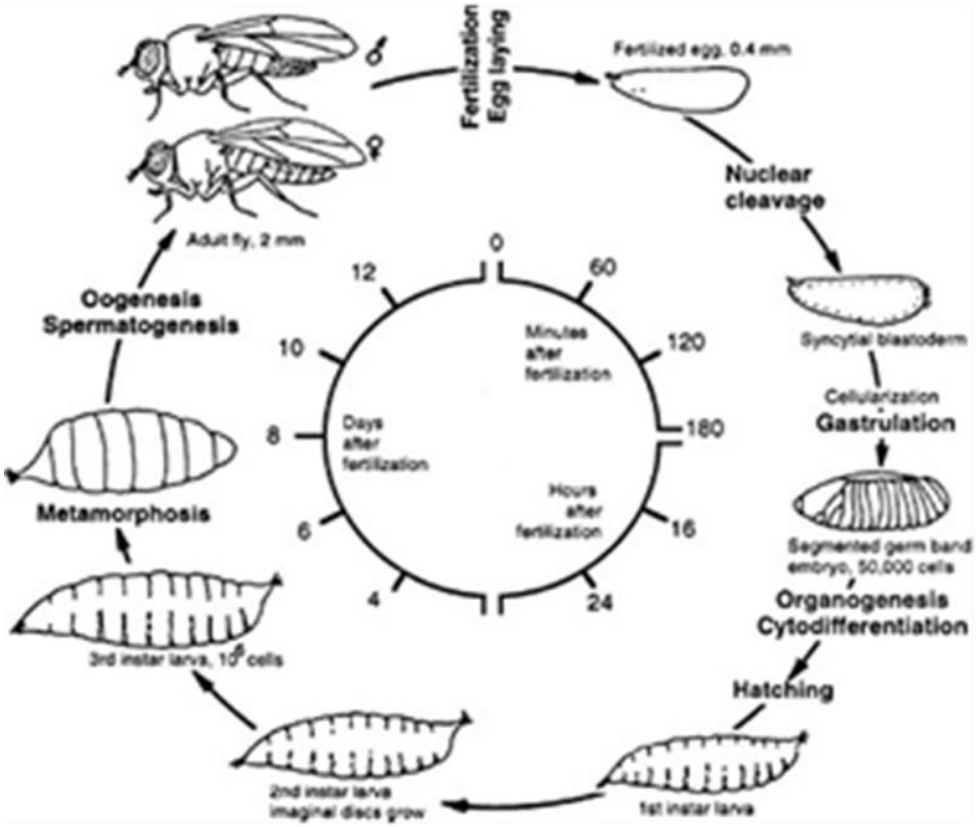

Figure 1- 7: Life cycle of *Drosophila melanogaster*. *Drosophila melanogaster* exhibits a complete metamorphosis. The life cycle of a fruit-fly consists of complex developmental stages, highly different between each other: egg, a larval form, which comprises three instars, a pupal stage and a flying adult Image was adopted from Wolpert et al., 1998.

1.4.2 Early development of the *Drosophila* embryo

Embryonic development in *Drosophila* can be subdivided into 17 stages on the basis of the most prominent development changes taking place (Campos-Ortega, J.A., Hartenstein, 1985). The first 180 min of embryo development are characterised by a series of rapid, synchronous cleavages of the zygotic nucleus. Indeed, shortly after egg fertilisation and fusion of the male and female pronuclei, the zygotic nucleus undergoes 13 cycles of divisions not accompanied by cytokinesis, resulting in a syncytium of 6000 nuclei that will be packed into individual cells during a process of membrane invagination known as cellularisation (Figure 1-8).

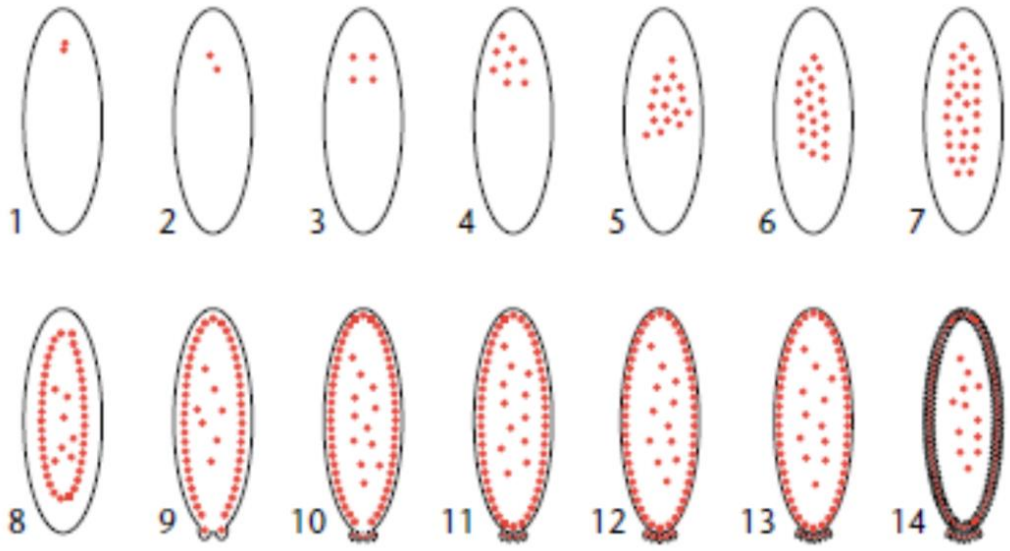

Figure 1- 8: Nuclear division and migration during early stages of *Drosophila* embryogenesis. After the fusion of the two pronuclei, the zygotic nucleus starts dividing rapidly for 13 cycles in a common cytoplasm. The first rounds of division occur in the interior of the embryos in an ellipsoid. From the interphase of cycle 8, the nuclei undergo cortical migration and they position underneath the plasma membrane. Few yolk nuclei are left behind. The cortical nuclei undergo four additional divisions before cellularisation takes place. Image was adopted from (Uyen Tram 2002)**.**

The first 7 cycles take place in the interior of the embryo and result in a total of 128 nuclei distributed in an ellipsoid in the centre of the embryo. An actin-myosin-based process known as axial expansion achieves the even distribution of nuclei throughout the surface of the embryo. During the first three syncytial divisions, the nuclei cluster together at the anterior third of the embryo. From cycle 4, the process of axial expansion causes the nuclei to equally spread along the anterior-posterior axis of the embryo, (Jayne Baker 1993). Axial expansion is driven by the dynamic contraction of the actin-myosin cytoskeleton and it is temporally coordinated with progression through mitosis. Indeed, cortical recruitment of Myosin II takes place at the end of telophase resulting in a wave of myosin-dependent contraction and therefore in cytoplasmic streaming that distributes the nuclei along the length of the embryo.

Myosin II disperses at the beginning of mitosis before another round of nuclear division occurs (Royou, Sullivan et al. 2002). Axial expansion continues until the interphase of cycle 8.

By the end of mitotic cycle 8, nuclei undergo cortical migration. Most of the nuclei leave their position in the ellipsoid and move synchronously towards the periphery, reaching the cortex by the interphase of cycle 10. A *Drosophila* embryo at this stage of embryonic development is named the syncytial blastoderm. Cortical migration is accompanied by the formation of a microtubule-network that links the migrating nuclei between each other and with the yolk nuclei. Cortical migration is therefore suggested to rely on the sliding of antiparallel microtubules apart from each other (Jayne Baker 1993). Approximately 26 nuclei don't participate in the cortical migration and they are left behind constituting a small group of yolk nuclei in the interior. The yolk nuclei divide three additional times and eventually become polyploid.

The first nuclei that populate the posterior end of the cortex are packed into individual cells and form a cluster of specialised cells, the pole cells, which represent the precursors of the germline.

The cortical nuclei of the syncytial blastoderm continue to divide synchronously for 4 additional cycles (cycle 10-13). During each of these final cortical divisions the actin and microtubule cytoskeleton undergo profound rearrangements (Timothy L. Karr 1986). In early embryos, prior to cortical migration, actin and tubulin cytoskeleton form a dense array 3-4 μm in depth underneath the plasma membrane. When the rounds of cortical divisions begin, the actin cytoskeleton organises caps above each nucleus that reaches the surface, positioning themselves between the plasma membrane and the apical pair of sister centrosomes. As soon as the cell cycle

progresses from interphase to prophase, the sister centrosomes start moving apart, to reach equatorial opposing positions, and the actin invaginates laterally, forming an hexagonal pseudo-furrow that surrounds the developing mitotic spindle. During metaphase, the furrow invaginates further reaching a maximum depth of 8 µm. The mitotic furrow provides anchoring for the mitotic spindle and serves as a physical barrier to keep neighbouring spindles apart. By the end of the telophase the furrow has regressed, centrosomes have completed their cycle of duplication and have moved apically and the actin caps reform above each nucleus (Figure 1-9).

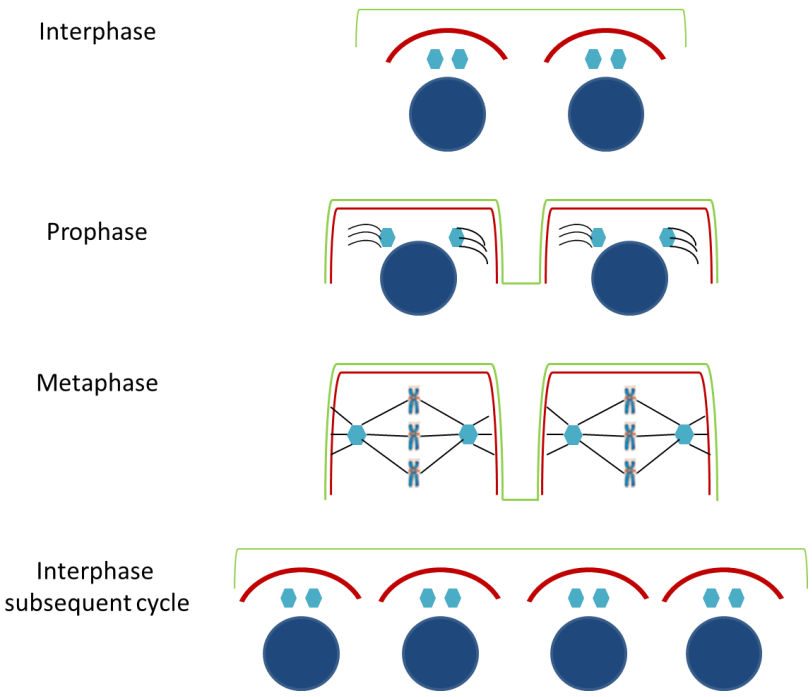

Figure 1- 9: Cytoskeleton rearrangement during syncytial division 10-13. During interphase, the actin cytoskeleton organises a cap (in red) above each individual cortical nucleus (in dark blue) between the apical centrosomes (in light blue) and the plasma membrane (in green). When the nuclei enter the prophase, the actin cap invaginates, forming the so-called pseudocleavage furrow. In metaphase the furrow invaginates more to a depth of 8 µm, surrounding each spindle. At the end of telophase the furrow retracts and the nuclei return to be again evenly distributed underneath the plasma membrane.

The interphase of cycle 14 is characterised by the formation of somatic cells during a remarkable process that consists of the extension of membrane furrows in between the syncytial blastoderm nuclei. This process, known as cellularisation, requires the extensive growth of the plasma membrane via insertion of intracellular membrane vesicles (Thomas Lecuit 2000), the subsequent inwards movement of the membrane between nuclei at the cortex and establishment of epithelial polarity with the formation of baso-lateral and apical junctional complexes.

Shortly after cellularisation, the gradual and coordinated movements of cells typical of gastrulation take place, resulting in the formation of germ layers.

1.4.3 *Drosophila* as a model system to study cell migration

The concerted movement of groups of cells is a fascinating and complex feature of multicellular organisms. During development, cell migration controls many aspects of organogenesis and tissue homeostasis but it also represents a key event in many pathological conditions, including birth defects, inflammatory diseases and tumour metastasis. The observation of cultured cells migrating on flat substrates *in vitro* has provided us with a good understanding of many aspects of this process, including the dynamics of the actin cytoskeleton and the regulation of cell-substrate interaction. However, cell motility *in vivo* requires a higher level of spatial and temporal control. Indeed, once they acquire an invasive potential, cells must coordinate their movement with the other developmental events in space and time.

The accuracy of genetic screening and the amenability for live imaging have made the use of *Drosophila* an excellent *in vivo* system to decipher the pathways that dictate when, where and how cells move. *Drosophila* offers various models of cell migration

enabling us to address the mechanisms of motility in the context of a wide range of processes such as epithelial-to-mesenchymal transition, angiogenesis, inflammation and wound healing. Particularly, haemocyte migration to an epithelial wound during mid-embryogenesis and border cell migration during oogenesis are the most widely analysed systems to ascertain the basic requirement for cell migration during development.

In a way to establish whether the ability of Spindly in controlling the dynamic organisation of cytoskeleton components is restricted to mitosis, we aim to study the requirement of this protein for a cytoskeleton-based process such as cell migration. Therefore our goal is to analyse how Spindly misexpression could affect the motile properties of the aforementioned model systems, border cells and haemocytes.

The following section gives an overview of the key events that take place during *Drosophila* oogenesis and egg-chamber development, focusing on border cell cluster specification and the mechanisms regulating its migration. Additionally, the origin of immunity in flies and the main aspects of haemocyte biology are discussed.

1.4.3.1 Drosophila oogenesis and egg-chamber development

The *Drosophila* female reproductive apparatus consists of a pair of ovaries each of which is composed of 15-20 ovarioles. The ovariole is a tubular structure in which oocytes form and complete development in a protected environment known as the egg chamber. A single ovariole is a linear array of six to seven egg chambers at increasing stages of development with the most mature one facing the oviduct (Figure 1-10 A and B) (Ogienko, Fedorova et al. 2007).

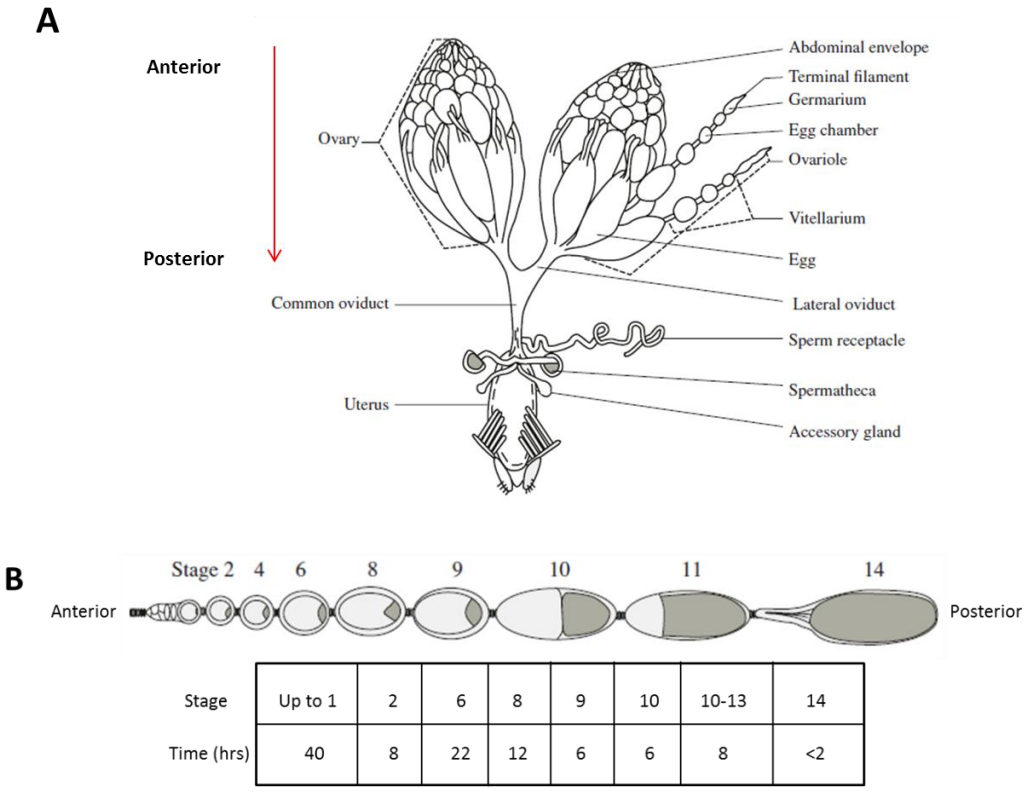

Stage	Up to 1	2	6	8	9	10	10-13	14
Time (hrs)	40	8	22	12	6	6	8	<2

Figure 1- 10: *Drosophila* female reproductive apparatus. A) The reproductive apparatus of an adult female fly consists of a pair of ovary, each made up of 16-20 ovarioles. Mature eggs ready for fertilisation are located at the innermost end, facing the oviduct. Eggs are fertilised in the uterus. B) Representation of a wild-type ovariole. The germarium is located at the anteriormost end of the structure. Egg chambers at increasing stages of maturation are organised in a linear array. A timeline of the developmental stages of an egg chamber is reported. Pictures are modified from (Ogienko, Fedorova et al. 2007).

The most anterior portion of the ovariole consists of the germarium. Two distinct populations of stem cells resides in this structure: germline stem cells (GSCs) and somatic stem cells (SCSs) (Horne-Badovinac and Bilder 2005). These two populations are located into two distinct structural regions of the germarium and they give rise to germline and somatic cells respectively.

The germarium can be divided into four functional regions along the anterior-posterior axis (Figure 1-11).

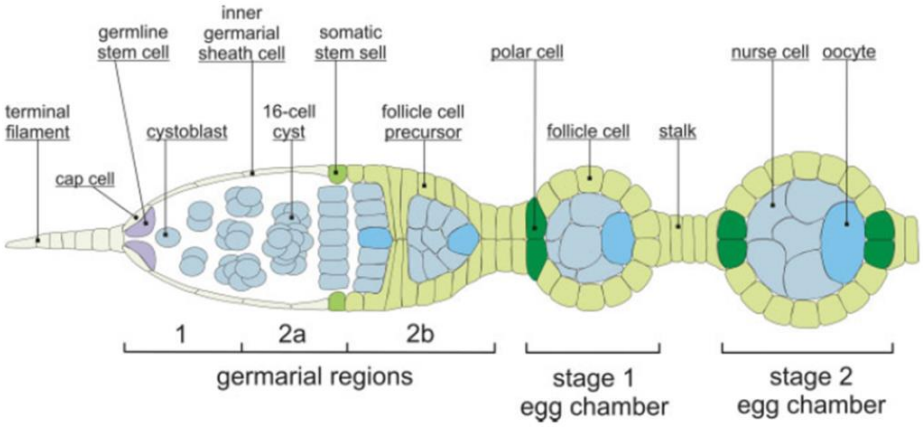

Figure 1- 11: Schematic representation of the germarium and of the earliest events during *Drosophila* oogenesis. The schematic shows the basic events that lead to the formation of the egg chamber, the unit of *Drosophila* oogenesis. In region 1 of the germarium the cystoblast divides repeatedly to form a 16-cell cyst. In region 2B epithelial follicle cells form a mono-layered epithelium completely surrounding the cyst. The other follicle cell precursors differentiate into stalk cells and polar cells. The egg chamber leaves the germarium and continues its development in the vitellarium where it undergoes 14 stages of growth. Picture was adopted from (Horne-Badovinac and Bilder 2005).

In region 1 of the germarium, a GSC divides asymmetrically, producing a new stem cell and a cystoblast. The cystoblast will undergo four additional rounds of mitotic divisions with incomplete cytokinesis producing the cyst. Therefore, the cyst is a syncytium of 16 cells interconnected by cytoplasmic bridges, which will later form the ring canals. Of these 16 cells, only one will differentiate into the oocyte while the other 15 will undergo several cycles of endoreplication and differentiate into nurse cells, the function of which is to supply the oocyte with proteins and mRNAs.

In region 2A and 2B of the germarium the cyst undergoes two major rearrangements. Firstly, the microtubule network becomes polarised with the minus-ends directed towards the oocyte. As a consequence, this cell becomes the target of microtubule-based transport of oocyte-specific proteins, such as BIC-D and ORB, as well as mRNA molecules including *orb* and *osk* (Huynh and St Johnston 2004, Roth and Lynch 2009). Secondly, SSCs located at the boundary between region 2A and 2B divide and

differentiate to produce follicle cells that surround the cyst in a process known as encapsulation, generating the basic structure of the egg-chamber.

Follicle cells can be divided into three subtypes: epithelial follicle cells surrounding the cyst, 4-6 interfollicular cells, also known as stalk cells and two pairs of polar cells. While stalk cells have the function of keeping apart adjacent egg chambers one another, polar cells perform two key functions. Firstly, this subpopulation of follicle cells is responsible for the early establishment of the anterior-posterior polarity inducing the oocyte to localise posteriorly inside the cyst. Secondly, they secrete a paracrine-signalling molecule that induces the differentiation of neighbouring follicle cells into stalk cells, border cells and centripetal cells.

The third region of the germarium contains a single egg chamber at stage 1 of development (Figure 1-11). This egg chamber is ready to pinch-off and to enter the vitellarium, where it further grows into a mature egg ready to be fertilised. The development of the egg chamber has been divided into 14 stages and the entire process is estimated to last 3 days (Figure 1-10 B).

1.4.3.2. Development of the egg chamber in the vitellarium

Further development of the egg chamber in the vitellarium includes complex morphological changes to the follicular epithelium and growth of the oocyte.

Follicle cells actively divide until stage 6 of egg-chamber development reaching the number of 650 and they organise a cuboidal epithelium surrounding the egg chamber. Subsequently, these cells exit mitosis in favour of endoreplication cycles, starting a period of post-mitotic cell growth that lasts until stage 10 (Figure 1-12 B). The mitosis-to-endocycle switch is important because contributes to the production of material required for the deposition of the eggshell at later stages of oogenesis. From stage 7 onwards, dramatic morphological changes can be described. The majority of follicle cells migrate posteriorly, acquire a cylindrical shape and form a columnar epithelium around the oocyte. A group of 8 to 10 cells delaminate from the epithelium and migrate independently towards the oocyte. This cluster, known as the border cell cluster, contributes to the formation of the micropyle, the site of sperm entry. 50 follicle cells remain anteriorly, flatten and stretch forming a squamous epithelium overlaying the nurse cells. Follicle cells undergo apoptosis at the end of egg-chamber development (Figure 1-12 A) (Horne-Badovinac and Bilder 2005).

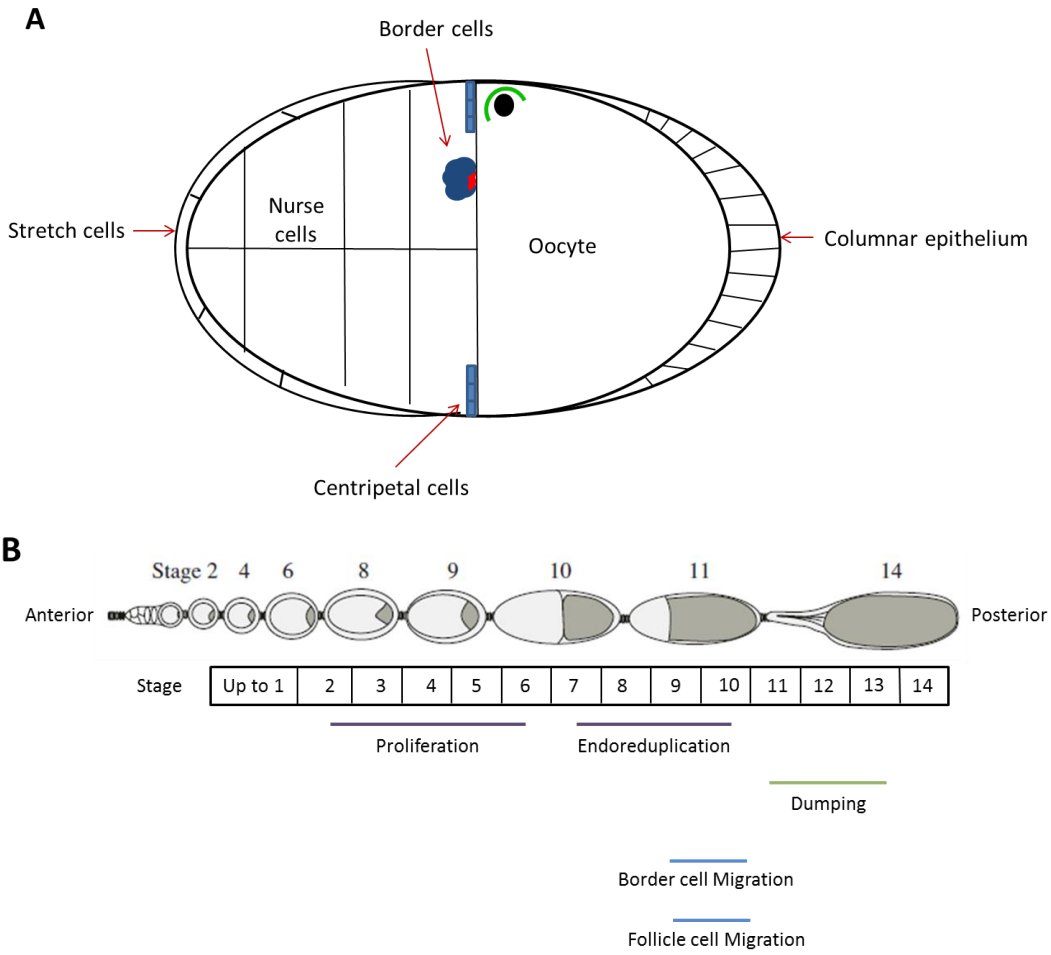

Figure 1- 12: Rearrangement of the follicular epithelium during later stages of egg-chamber development. A) Types of follicular cells in an early stage-10 egg chamber. Until stage 6, follicular cells are uniform in shape and size. From stage 7 onwards, profound morphological changes occur and three distinct subpopulations are discernible at stage 10 of development: anterior stretch cells, forming a squamous epithelium around the nurse cells, epithelial follicle cells, overlying the oocyte, and border cells, located at the nurse cells-oocyte boundary. The anterior-dorsal positions of the oocyte and the dorsal determinant Gurken (in green) are depicted. B) Timeline of the main critical morphological rearrangement of the follicular epithelium. Picture in B was modified from (Horne-Badovinac and Bilder 2005, Ogienko, Fedorova et al. 2007).

While these complex rearrangements are taking place, the oocyte nucleus moves anteriorly into the dorsal quadrant and the microtubule cytoskeleton gets repolarised (Huynh and St Johnston 2004, Roth and Lynch 2009). Microtubules are assembled from the lateral and anterior cortex and orient their plus-ends towards the centre of the oocyte. As a consequence, microtubule-dependent transport segregates mRNA to

specific locations. For example *osk* mRNA localises at the posterior cortex in a kinesin-dependent manner, while dynein transports *bcd* mRNA to an anterior location (Jens Januschke, Julia A. Kaltschmidt et al. 2002). Migration of the oocyte nucleus to an anterior-dorsal location is an important event for the establishment of the dorso-ventral (D/V) axis of the future embryo (Roth 2003). The proper positioning of the nucleus is indeed essential for the localisation of *gurken* mRNA to the future dorsal side and therefore for the D/V patterning of the follicular epithelium (Figure 1-12 A).

Lastly, another important event of oocyte growth is the transport of the cytoplasmic content of the nurse cells into the oocyte. This process occurs in two steps. Initially, the active movement of proteins and mRNAs molecules is highly selective and slow. This selective transport takes place during the first three days of egg-chamber development and includes Bic-D, Orb and Cup proteins, *bcd*, *osk* and *Bic-D* mRNAs and organelles. Later on, after stage 10 of egg-chamber development, fast and non-selective transport of the nurse cells cytoplasmic content takes place, in a process known as dumping (Figure 1-12 B). This process is completed within 30 minutes and terminates with the production of a mature egg. The dumping requires the assembly of a robust actin-myosin network in the nurse cells as well as proper maturation of the ring canals, the cytoplasmic bridges interconnecting nurse cells between each other and with the oocyte.

Defective dumping due to mutations that affect the actin cytoskeleton or structural abnormalities in the ring canals results in the so-called dumpless phenotype and the production of small rounded eggs (Horacio M. Frydman 2001, Jack Bateman and Vactor 2001, Groen, Spracklen et al. 2012, Sally Horne-Badovinac 2012).

Some of the processes described in this section, including positioning of the oocyte nucleus to an antero-dorsal position, the process of dumping and border cell migration, have been analysed in this study following Spindly misexpression and have been proved to be altered.

1.4.3.3 Border cell migration during *Drosophila* oogenesis

1.4.3.3.1 Specification of the border cell cluster

The border cell cluster is specified during stage 8 of oocyte development in the follicular epithelium surrounding the egg chamber. At this stage of oogenesis, the anterior polar cells secret a paracrine cytokine ligand inducing the neighbouring companions to form a cluster, delaminate from the epithelium and migrate as a coherent group towards the oocyte. The cluster navigates between the nurse cells with an average speed of 0.5 μm/min and over a distance of 150 μm. Migration proceed over a period of 5-6 hours and it is completed by stage 10 of oogenesis once that cells have reached the border between the nurse cells and oocyte (hence their name) (Prasad and Montell 2007).

The border cell cluster is composed of 8 to 10 cells, with two polar cells residing in the centre and 6 to 8 border cells surrounding them. Polar cells are not motile and they are passively carried to the final destination by the rest of the cluster. However, these cells perform key functions in inducing border cell fate and in keeping the cluster motile. Polar cells produce and secrete the cytokine-like molecule Unpaired. The ligand binds to the receptor Domeless and activates the JAK/STAT pathway in the neighbouring follicle cells resulting in border cell fate specification (Silver D. L. 2001, Simone Beccari 2002). Cells that express high levels of STAT will transcribe many genes among which

slow border cell (*slbo*) encoding for a transcription factor of the CCAAT-enhancer-binding-protein (C/EBP) family (Denise J. Montell 1992). This transcriptional circuit upregulates many essential downstream targets, including *jing,* a Zinc-finger transcription factor (Yuru Liu 2001), *shotgun* encoding *Drosophila* E-cadherin (Borghese, Fletcher et al. 2006) and *Fak*, codifying for the Focal Adhesion Kinase (Jianwu Bai 2000). STAT activity is not only required for commitment into a border cell fate. It has been shown that inactivation of the JAK/STAT pathway in a migrating cluster causes border cells to arrest before reaching the oocyte, indicating that these cells need a constant permissive signal to complete migration (Figure 1-13) (Silver, Geisbrecht et al. 2005).

The ligand Unpaired is constantly produced in polar cells from the earliest stages of oogenesis, as soon as the egg chamber emerges from the germarium (Jennifer R. McGregor 2002); however the cluster only starts moving at stage 9. This observation raises the problem of identifying an additional signal that controls the timing of border cells specification and synchronises their movement with the other developmental rearrangements taking place at that stage of oogenesis. The steroid hormone ecdysone is known to regulate the timing of many aspects of egg-chamber development (Michael Buszczak and Segraves 1999). In this specific context, it has been shown that injection of the steroid hormone causes precocious movement of the border cell cluster, suggesting a role for the ecdysone-signalling pathway in setting the right timing for migration. The production of the steroid hormone reaches the highest levels at stage 9 of egg-chamber development and coincides with the beginning of border cell migration (Figure 1-13).

The molecular details of the ecdysone response have been partially elucidated. Expression of the ecdysone receptor (EcR) makes border cells responsive to the high concentration of the hormone. The activated receptor translocates into the nucleus where it binds to Ultraspiracle (Usp) (Bonnie L. Hall 1998) and the co-activator Taiman (Tai) (Jianwu Bai 2000) to form a functional transcription factor that switches on the expression of migration-related target genes.

Nevertheless, what is important to understand is how spatial and temporal cues are integrated to promote invasiveness. The protein Abrupt is having such a role in border cells. Abrupt is enriched in the cells of the anterior follicular epithelium where it down-regulates ecdysone signalling by sequestering the co-activator Tai and preventing its binding to the EcR/Usp heterodimer (Jang, Chang et al. 2009). However, activation of the JAK/STAT pathway results in the reduction of Abrupt protein levels in border cells and the generation of a positive feedback loop that enhances the ecdysone response (Figure 1-13).

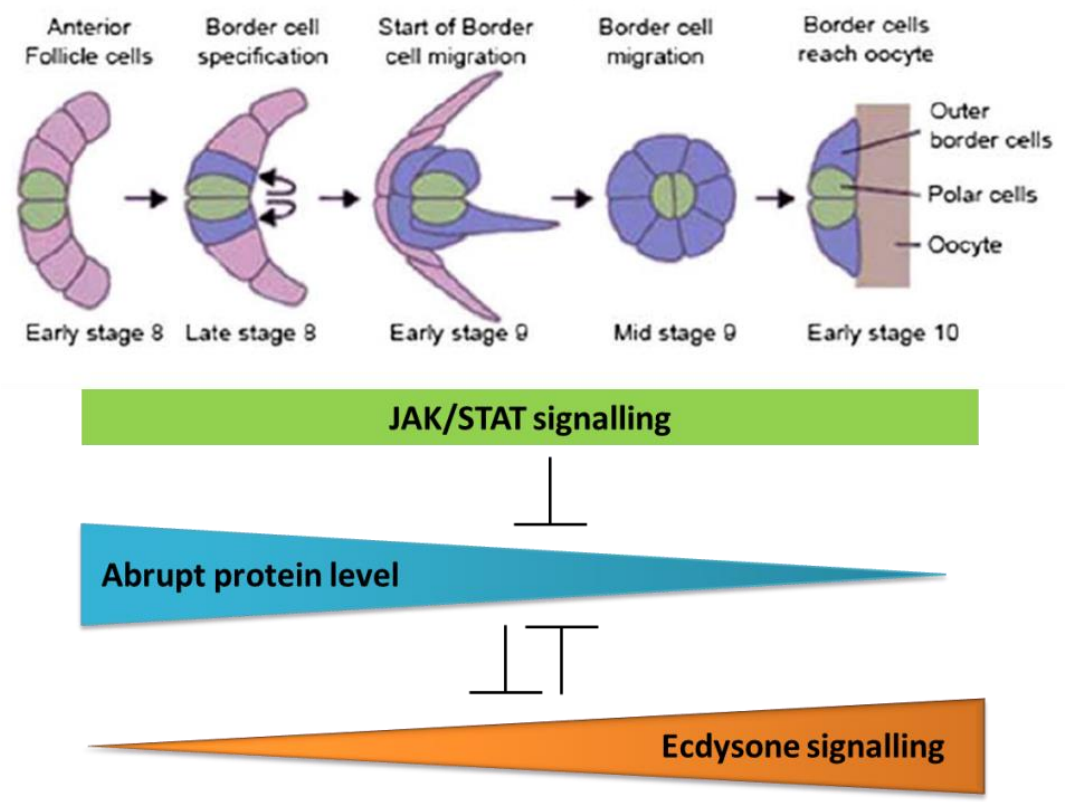

Figure 1- 13: Signalling pathways controlling border cells specification and timing of migration. Anterior polar cells release the paracrine signalling molecule Unpaired and activate the JAK/STAT signalling pathway in the neighbouring follicle cells, committing them to a border cell fate. Migration of the cluster starts only at stage 9 of oogenesis in response to increased levels of the steroid hormone ecdysone. At the molecular level, the removal of Abrupt is important for setting the right timing of border cell cluster migration. Efficient downregulation of Abrupt requires the combined activity of JAK/STAT and ecdysone signalling pathways. Image was adopted from (Belles X 2014).

1.4.3.3.2 Regulation of border cell cluster motility and guidance

In their migration along the anterior-posterior axis, border cells always polarise their movement towards the oocyte, navigating down the centre of the egg-chamber without deviating from their main track. The oocyte indeed secretes a chemoattractant, probably generating a gradient that gives directionality to the movement of the cluster (Jocelyn A. McDonald 2003). This chemoattractant is the PDGF/VEGF-related factor 1 (Pvf-1) (Figure 1-14). Uniform overexpression of Pvf-1 in

the egg chamber disrupts any graded distribution of the chemoattractant, resulting in the loss of guidance cues and therefore a significant delay in the migration (Peter Duchek 2001). Border cells are able to respond to the Pvf-1 ligand because they express on their surface the PDGF/VEGF tyrosine kinase receptor PVR. The small GTPase Rac is one of the downstream signalling targets of PVR and its activation results in the generation of actin-rich protrusions (Peter Duchek 2001). The high concentration of the PVR receptor and consequently the preferred activation of Rac at the front of the cluster confer front-back polarity to the cluster and ensure polarised movement along the anterior-posterior axis.

Interestingly, interfering with PVR activity by expressing a dominant-negative form of the receptor (DN-PVR) results in a surprisingly mild defect with only 30% of the mutant egg chambers showing an incomplete migration phenotype (McDonald, Pinheiro et al. 2006). Therefore an additional chemoattractant signal must influence border cell migration. It has been shown that the EGF pathway acts redundantly to PVR in mediating migration towards the oocyte and simultaneous inhibition of both signalling pathways is necessary to fully inhibit migration (McDonald, Pinheiro et al. 2006). However, EGFR becomes indispensable during the second and last phase of migration towards the oocyte, guiding the cluster dorsally in response to the ligand Gurken (Figure 1-14) (Peter Duchek 2001).

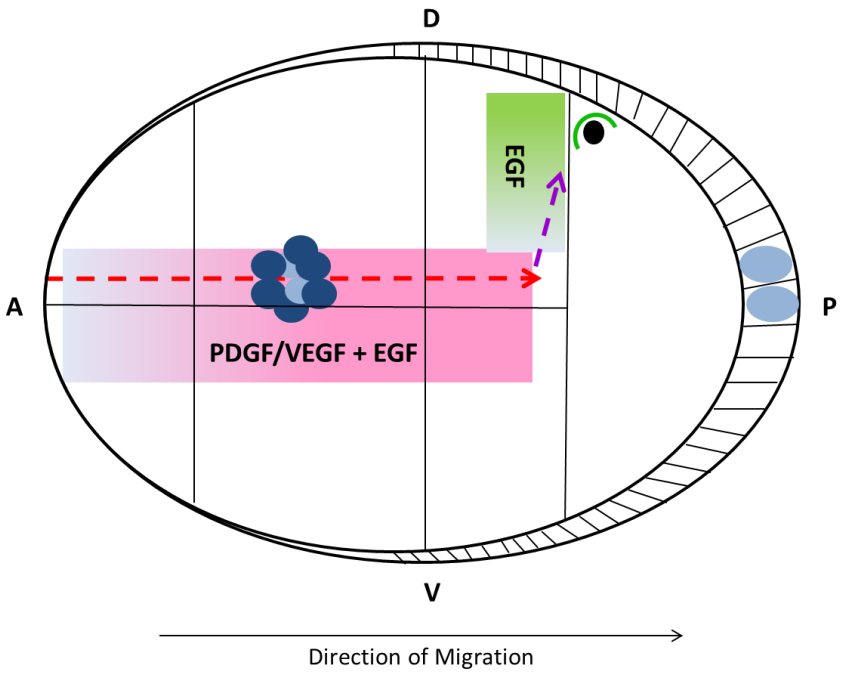

Figure 1- 14: Contribution of PDGF/VEGF and EGF signalling pathways in guiding border cell migration. To correctly navigate toward the oocyte, border cells need to read guidance cues and respond accordingly. A combined gradient of PDGF/VEGF and EGF growth factors (pink box) guide the cluster along the anterior-posterior axis to the oocyte (dashed red line). EGF signalling only regulates movement of border cells to a dorsal location. The ligand Gurken (in green) is highly concentrated in an anterior-dorsal position around the oocyte nucleus (black filled-in circle). This peculiar localisation allows the generation of a gradient (green box) that regulates the second and last part of the migration (purple dashed line). Polar cells are in light blue, border cells in dark blue.

1.4.3.3.3 Regulation of cell adhesion during collective migration

Border cells move as a compact group down the centre of the egg chamber towards the oocyte. An important point to address is the relevance of cell adhesion in the system and to understand how border cells maintain relatively stable cell-cell contacts and at the same time adhere to their substrate, the nurse cells, generating traction. The perfect balance between cohesion and traction is achieved by tightly regulating the expression level of E-cadherin.

E-cadherin is a homophilic cell-cell adhesion molecule and its expression levels in border cells are controlled in a *slbo*-dependent manner (Paulina Niewiadomska 1999). The distribution of the protein inside the cluster has been characterised. E-cadherin concentrates at the interface between polar cells and border cells as well as at the border cell-border cell boundary, ensuring that these cells will migrate as a compact aggregate. Also, E-cadherin is expressed at the nurse cells-border cells interface and the motility of the cluster is compromised when the adhesion molecule is downregulated in either one of the two cell types, meaning that the dynamic regulation of the adhesion provides enough traction to ensure forward movement (Paulina Niewiadomska 1999). Myosin VI is required to stabilise E-cadherin-mediated adhesions. The motor protein is able to physically bind E-cadherin/Armadillo complexes at the membrane and reduction in its levels results in downregulation of these two adhesion molecules, causing severe migration defects (Geisbrecht and Montell 2002).

Reduced expression of E-cadherin negatively affects the initial recruitment of cells in the cluster and therefore its formation, and impairs cell movement. However it does

not affect cell-cell association once the cluster is formed. Therefore other molecules may be required to maintain cluster cohesion.

The asymmetric distribution of well-known polarity regulators, such as Par-6, Par-3/Bazooka and α-PKC, is essential for maintaining stable cell-cell contacts inside the cluster. The dynamic localisation of these proteins throughout migration has been accurately described. At early stage 9, Par-6 and Par-3 accumulate at the leading edge of the cluster. As soon as delamination takes place, these proteins get redistributed and accumulate preferentially at the apical surface, at the junction between adjacent border cells (Pinheiro and Montell 2004). RNA interference (RNAi) experiments proved that the establishment of the apical/basal polarity at the onset of migration is fundamental for controlling invasiveness and motility (Pinheiro and Montell 2004). Loss of either Par-6 or Par-3 compromises cluster integrity and morphology, resulting in severe migration defects. Indeed, as a consequence of the reduced cohesion, the cluster appears abnormally elongated and disorganised; individual border cells detach from the main group and extend long protrusions that sometimes are necessary to keep the contact with the more distal cells. Additionally, the localisation of a variety of membrane proteins is affected. Particularly, even distribution of E-cadherin at the membrane, accumulation of E-cadherin and β–integrin in the cytoplasm and aggregation of PVR receptor at the surface were described (Pinheiro and Montell 2004). Even though there is a basic understanding of how border cells adhere to one another and how the cohesion is maintained, little is known about the signalling pathway(s) controlling cluster integrity. Recently, it has been reported that reduced JNK activity causes loss of Par-3/Baz from the apical surface as well as significant reduction of E-cadherin at the cell membrane, leading to the dissociation of cells from

the cluster (Llense and Martin-Blanco 2008). The dissociated cells acquire mesenchymal characteristics: they emanate long extensions (LCEs) enriched in β-integrin receptor and they acquire the ability to move as single entities (Llense and Martin-Blanco 2008).

All together these observations suggest that as in other biological contexts the maintenance of cell polarity in migrating border cells is a key requirement for sorting proteins and for keeping them confined in distinct functional domains. Specifically, in the contest of border cell migration, this mechanism helps the cluster in establishing a front-back polarity, with a leading edge able of making dynamic contacts with the underlying substratum while keeping the ability to move as a coherent group.

1.4.4 *Drosophila* immune system as a model to study cell adhesion and cell migration

1.4.4.1 *Drosophila* haematopoietic system: cell types, their functions and origin

Drosophila melanogaster contains a subset of specialised macrophage-like cells, the haemocytes, representing the cellular components of the innate immune system of insects. The great similarity with its vertebrate counterpart makes the *Drosophila* immune system a valuable tool to genetically define the signalling pathways regulating innate immunity and haematopoiesis and to identify those transcription factors crucial for regulating proliferation, differentiation and lineage commitment. Also the imaging amenability of the system makes haemocytes an attractive model to study cell migration and the processes of chemotaxis and inflammation. Therefore, it is not surprising that over the past 20 years the *Drosophila* immune system has been successfully used to clarify the genetic and molecular regulation of these processes, providing insights into the basics of many human dysfunctions.

In flies only three types of mature blood cells have been described: plasmatocytes, crystal cells and lamellocytes (Holz, Bossinger et al. 2003, Tim Lebestky 2003, Bataille, Auge et al. 2005). Plasmatocytes constitute 95% of the haemocyte population and they conduct a wide range of activities in embryos, larvae and adults. Phagocytosis represents their primary function; during embryos development as well as larval stages these cells engulf and remove apoptotic cells and debris. They are also responsible for the production and deposition of a huge amount of extra-cellular matrix components, including Peroxidasin (Pxn) and Laminin. These two activities are extremely important for sculpting various tissues and organ. *pvr* mutant embryos, in which plasmatocytes migration is dramatically impaired, show severe defects in ventral nerve cord (VNC) condensation due to a lack of cell debris engulfment as well as of cellular-matrix deposition (Sears 2003). Plasmatocytes also contributes to humoral immunity by producing and secreting antimicrobial peptides, such as Cecropin A1 and Diptericin (Kavanagh and Reeves 2004).

Crystal cells represent the remaining 5% of the haemocytes population and they are responsible for a highly important immune reaction known as melanisation. Melanisation causes resistance to infection and host damage based on the production of reactive oxygen species during the synthesis of melanin (Kavanagh and Reeves 2004).

The third sub-population of haemocytes, the lamellocytes, can be found only during larval stages. These cells are not present in healthy larvae but they differentiate upon infestation by invaders too big to be phagocytosed by plasmatocytes, such as wasp eggs.

Like in vertebrates, haematopoiesis in *Drosophila* takes place in two phases. The first round occurs during stage 5 of embryo development in the procephalic mesoderm and results in the generation of a fixed number of haemocyte precursors, the pro-haemocytes, all expressing the GATA transcription factor Serpent (Srp) (Holz, Bossinger et al. 2003, Tim Lebestky 2003). Upon stage 12, pro-haemocytes differentiate into 700 plasmatocytes that migrate from the site of origin to populate the entire embryo, and 30 crystal cells, that stay anteriorly in proximity of the proventriculus, a foregut-associated organ that acts as a valve regulating the passage of food into the midgut. Haemocytes maturation is accompanied by the expression of transcription factors that govern lineage commitment. Specifically, plasmatocytes differentiation requires the expression of Glial-cells-missing (GCM) and Glial-cells-missing 2 (GCM 2) as well as the Friend-of-GATA (FOG) homolog U-shaped (Ush) that it has been shown to antagonise crystal cells differentiation. On the other hand, the Runt-domain protein Lozenge (Lz) is fundamental for the commitment of the precursors to crystal cells fate (Bataille, Auge et al. 2005).

How differentiation of lamellocytes is triggered is still a matter of debate. However, recent studies show that the transcription factors Hemese (Kurucz, Zettervall et al. 2003), Collier (Crozatier 2004

) and Yantar (Sinenko, Kim et al. 2004) are involved in the differentiation of this cell type.

The second round of haematopoiesis occurs during larval stage in a specialised organ known as lymph-gland (Figure 1-15) (Jung, Evans et al. 2005).

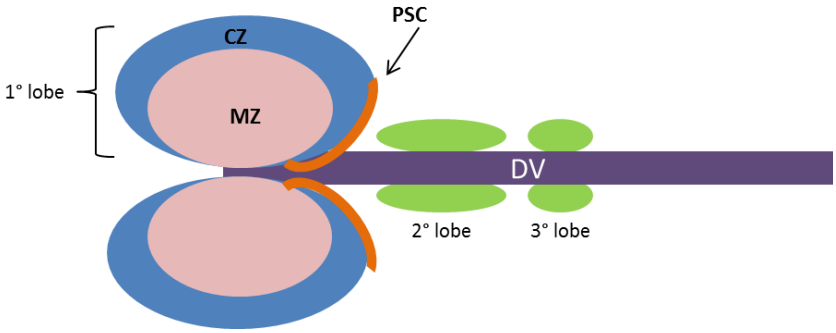

Figure 1- 15: Schematic representation of a third instar lymph gland. *Drosophila* lymph gland is made up of 7 pairs of lobes positioned bilaterally to the dorsal vessel (DV). The primary lobe is the biggest and is structured in three areas: a medullary zone (MZ) where pre-haemocytes reside, a cortical zone (CZ) containing mature haemocytes, and the posterior signalling centre (PSC). The other pairs of lobes are smaller and inactive. Haemocytes production and differentiation in these additional structures occurs only upon severe infestations.

The lymph gland forms during embryogenesis from the cardiogenic mesoderm and increases in size by cell division during the first and second instars larva stages. By the third instar, the lymph gland is composed of two to seven pairs of lobes positioned bilaterally to the dorsal vessel. The first pair of lobes is the biggest and sustains the production and differentiation of haemocytes, whereas the secondary lobes get activated only upon severe infestations, when a robust immune response is needed. The primary lobes can be divided into three main regions: the inner medullary zone, the cortical area and the posterior signalling centre (PSC). The medullary zone and the cortex are the area of haemocytes production and differentiation whereas the PSC plays a key role in controlling the balance between pro-haemocyte production and their differentiation (Jung, Evans et al. 2005). Even though haemocytes follow a stereotyped program of proliferation and differentiation in the lymph gland, under normal conditions they are not released into circulation before the onset of metamorphosis. Therefore, circulating haemocytes in larva stages have embryonic origin.

1.4.4.2 Mechanisms of Haemocytes migration

1.4.4.2.1 Haemocytes developmental migration during embryogenesis

By the end of stage 12 of development the haemocytes produced in the procephalic region start to migrate along developmentally established routes to populate the entire embryo (Ulrich Tepass 1994).

The first haemocytes leaving the head move dorsally and infiltrate the germ band, which at this stage is juxtaposed to the head. Germ band retraction brings this population of cells posteriorly. This process generates two sub-sets of cells, one anterior-dorsal and one posterior, which start migrating towards each other along the ventral nerve cord until they meet in the middle. At the same time, cells keep migrating along four invariant pathways: between the ventral epidermis and the ventral nerve cord, between the ventral surface of the ventral nerve cord and the mesoderm, along the dorsal vessel and along the gut primordium (Figure 1-16 A) (Ulrich Tepass 1994). The embryo is evenly populated with haemocytes by the end of stage 14.

Haemocyte migration along the ventral side of the ventral nerve cord is the best characterised: indeed haemocytes are lying ventrally underneath the epithelium and therefore they are easy to image. In vivo time-lapse imaging has revealed that haemocytes from the anterior and posterior ends migrate slowly towards each other and by the end of stage 14 they are occupying the entire length of the ventral midline. Directly afterwards, these cells migrate out from the midline at a considerably higher speed to occupy more lateral position, forming two additional parallel lines flanking the VNC (Figure 1-16 B) (Wood, Faria et al. 2006).

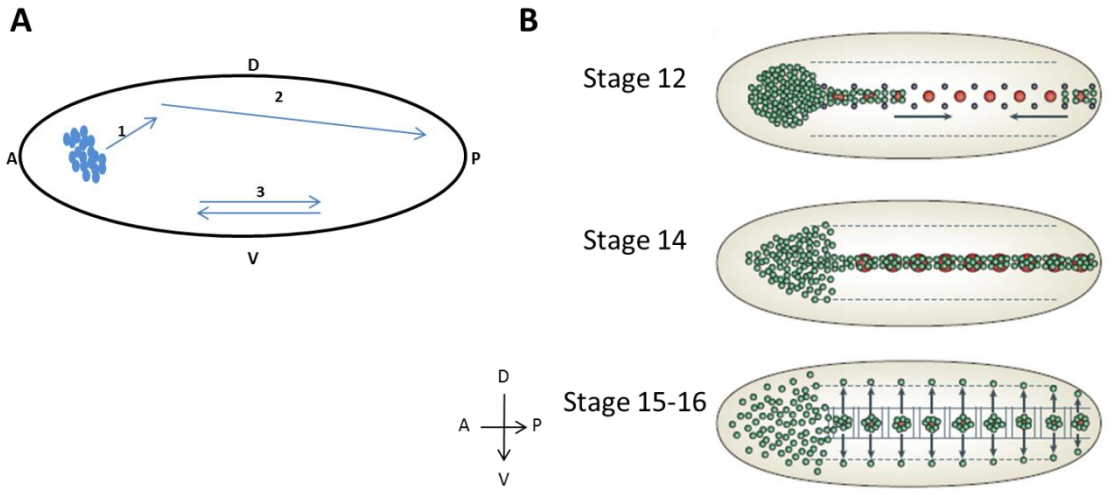

Figure 1- 16: Summary of the routes that haemocytes travel during their dispersal migration. *Drosophila* haemocytes (in light blue) originate in the procephalic mesoderm and at stage 12 of development they start migrating across established routes to populate the entire embryo. Firstly these cells migrate dorsally to infiltrate the germband (arrow 1). The process of germband retraction brings this subpopulation posteriorly (arrow 2). These two initial movement result in the generation of two populations, one anterior and one posterior, that start moving ventrally towards each other along the nerve cord (arrow 3). B) Ventral view of haemocyte migration along the nerve cord. At stage 12, the anterior and posterior population of haemocytes migrate ventrally toward each other along until they completely cover the entire length of the midline. From stage 15, haemocytes move laterally to form to additional subpopulations of cells flanking the nerve cord. The image was adopted from (Wood and Jacinto 2007).

During embryogenesis haemocyte dispersal is regulated upon signalling between the chemoattractant ligands Pvf-2 and Pvf-3 and the PVR receptor. Haemocytes express the PVR receptor and previous studies had shown that its primary function is to mediate cell survival (Bruckner, Kockel et al. 2004). *pvr* mutants lack of normal haemocytes migration and show accumulation of apoptotic cells in the cephalic region (Sears 2003). The survival defects can be rescued by expression of the pan-caspase inhibitor p35 (Bruckner, Kockel et al. 2004). However, the rescued haemocytes are still unable to migrate posteriorly (Wood, Faria et al. 2006). These data, along with the observation that ectopic expression of Pvf-2 and Pvf-3 in different tissues disturbs

embryonic haemocytes migration during development (Nam K. Cho 2002), suggest that PDGF/VEGF ligands in *Drosophila* embryos function also as chemoattractants.

Pvf-2 and Pvf-3 are expressed in temporally and spatially different domains during embryo development and work redundantly to guide haemocytes along the established routes (Wood, Faria et al. 2006).

1.4.4.2.2 Haemocyte migration towards a wound

Once their developmental dispersion is completed by late stage 14, haemocytes become responsive to tissue damage and rapidly deviate from their developmental routes to reach the wounded epithelium in a process similar to vertebrate inflammation (Moreira 2010).

Live-imaging microscopy has allowed the description of haemocyte recruitment to epithelial wounds at great detail (Figure 1-17). The damaged tissue generates a chemotactic gradient that attracts haemocytes, which in turn will polarise their movement accordingly. Haemocytes recruitment to the site of damage is independent of Pvr-Pvf signalling and the molecular basis of the process has been recently characterised. The current model suggests that cells at the site of damage release calcium from their cytoplasmic storage and calcium spreads like a wave up to 40 µm away from the wound edge. The release of calcium results in the local activation of the NAPDH oxidase (NOX) DUOX enzyme, leading to the production of oxygen peroxide (H_2O_2) and stimulating an inflammatory response (Moreira, Stramer et al. 2010, Razzell, Evans et al. 2013). H_2O_2 is a well-established wound attractant signal: it has been indeed shown that impairing the production of H_2O_2 via inhibition of the DUOX

enzyme drastically impair the haemocytes ability of reaching to the wound (Moreira, Stramer et al. 2010).

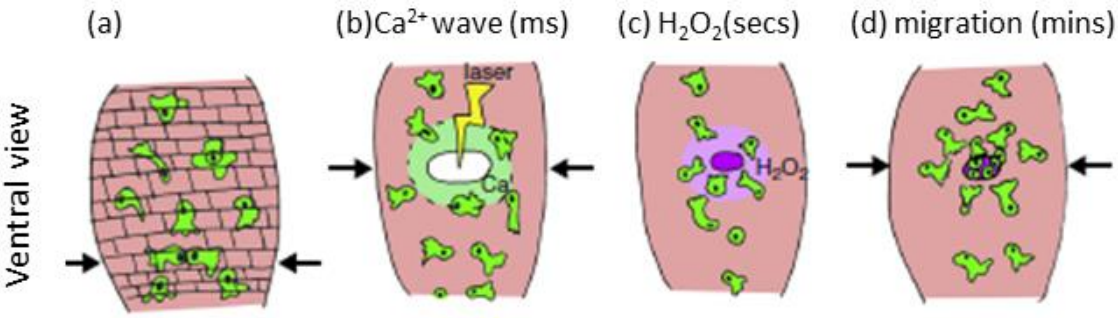

Figure 1- 17: Mechanism of haemocyte recruitment to the site of a wound. Laser-wounding of the epidermis (in pink) activates a rapid immune response for healing the tissue. At the molecular level, the presence of a wound in the epithelium causes a local increase in the concentration of intracellular calcium that like a wave spreads over a distance of 40 µm from the site of the damaged tissue. Subsequently, calcium activates the production of H_2O_2 which attracts haemocytes (in green) to the wound, allowing re-epithelisation. Image was adopted from (Evans and Wood 2014).

Wounding triggers a very rapid response and results in the recruitment of approximately 8 cells within an hour from up to 40 µm from the wound edge. These cells surround the wound and engulf cellular debris and apoptotic bodies; eventually they slowly disperse away (Stramer, Wood et al. 2005). The polarised movement towards the wound requires the activation of PI3K at the leading edge of the migrating cells and mutations in the enzyme prevent haemocytes from detecting a wound up to 1 hour post-wounding. PTEN activity is also upregulated at the rear in order to maintain the gradient of PIP_3 required to maintain cytoskeleton polarisation towards the wound (Wood, Faria et al. 2006). The Rho-family of small GTPase, including Rho, Rac and Cdc42, are all required to regulate actin cytoskeleton remodelling and lamellopodia and filopodia formation (Stramer, Wood et al. 2005). Finally, it is not surprising that microtubules and microtubule-regulating proteins play an important role in this migration. A recent work elegantly shows that haemocytes polymerise a

bundle of microtubules in the direction of the migration and this helps in maintaining polarisation of the movement. Both, overexpression of Spastin, a microtubule-severing protein, or a mutation in Orbit, a microtubule-associated protein (MAP) required for microtubule stability, strongly reduce haemocytes migration towards a wound (Stramer, Moreira et al. 2010).

1.5 Aim of the Study

This study aims to explore the contribution of Spindly to the developmental processes described above using a combination of biochemical and genetic methods, seeking to better understand the activity of this protein in mitosis as its functions in post-mitotic cells.

Drosophila Spindly has been shown to be required for successful completion of mitosis (Griffis, Stuurman et al. 2007). However the lack of structural information and its poorly defined protein interactions limit our understanding of this protein activity during cell division, raising the question of how Spindly localises at kinetochores, how it influences the architecture of the outer kinetochore plate and finally what interaction(s) this protein establishes during mitosis. To address these questions we aim to perform a loss-of-function study based on RNA silencing technique, testing to what extent the downregulation of Spindly affects *Drosophila* embryo development and establishing whether this provides a favourable background where to perform structure-function analysis for the identification of the structural domains that contribute to Spindly activity.

In the work of Griffis et al. (Griffis, Stuurman et al. 2007), Spindly was one of the few genes whose depletion resulted not only in mitotic defects but also in altered cell

morphology in interphase. This discovery raises the question whether this factor controls cytoskeleton remodelling not only during mitosis but also in post-mitotic cells. A further aim of the work is therefore to unravel additional, uncharacterised function(s) of Spindly during interphase, testing whether cells will exhibit cytoskeletal defects and abnormalities in cell migration upon its depletion.

Finally, to clarify the contribution of Spindly in embryonic development, we aim to define a comprehensive network of Spindly interactions identifying potential binding partners for Spindly. In this regard, we seek to develop an affinity-purification method that combined with proteomic analysis will be an invaluable tool to define the signalling and developmental pathways that require the activity of Spindly.

Chapter II: Materials and Methods

Chapter 2 : Materials and Methods

2.1 Materials

2.1.1. Chemicals

The chemicals used in this work were purchased from the companies Bio-Rad, Fermentas, Fluka, GE Healthcare/Amersham, Invitrogen, New England Biolabs, Roche, or Sigma-Aldrich unless stated otherwise.

2.1.2 Oligonucleotides

Oligonucleotides used in this thesis were synthesised by the company Eurofins MWG Operon (United Kingdom, http://www.eurofins.co.uk/).

A complete list of the oligonucleotides is reported in Table 2-1.

Table 2- 1: List of forward, reverse and sequencing primers used in this study

Purpose	Name	Sequence (5'-->3')
Cloning of spindly cDNA in pLou3 vector	spindly full EcoRI_fwd	ggcacgaattcatgtacaaaaacttggaccttgacac
	spindly full XhoI_rev	ctcgagtcatttcataattggtttacgag
	spindly N-terminal XhoI_rev	ctcgagtcaagttttgagttccgcctcc
	spindly C-terminal EcoRI_ for	gaattcatggcattgccccgcattgtcagtgtag
Site directed mutagenesis of wild-type *spindly*	spindly_Rescue_Forward	caagatgccgtggacattaagacggagttggaagctccagaattaattcc
	spindly_Rescue_Reverse	cttaatgtccacggcatcttgctgttccaagtttaagtcgatttctcg
	spindly_Mad2 Mutant_Forward	cgggaatctactgtgagctctcgtaaaccaattatgaaatga
	spindly_Mad2 Mutant_Reverse	agagctcacagtagattcccgtatgatgtttggcttcttaattg
Cloning of Mad-2 in pGEX-6P1 vector	mad-2 EcoRI_fwd	gaattcatgtcaactgcccaggcga
	mad-2 XhoI_rev	ctcgagttaagtgctcatcttgtagttgac
Cloning of GFP-Spindly Rescue cDNA in pUASp K10 vector	eGFP_KpnI_fwd	atcttaggtaccatggtgagcaagggcgaggagctgttc
	spindly full_Stop_BamHI_rev	gtccgaggatcctcatttcataattggtttacgagagctcacaac
spindly sequencing	spindly seq 397-376	gctCatttgacctggaggcgga
	spindly seq 458-477	aaaagctggccgagtatgag
	spindly seq 868-889	cacattcttttgcagtgcggaca
	spindly seq 1293-1313	tcgttttcaagcccatgcagg
	spindly seq_shRNA	gtatccgaaagcaaggcttg
	spindly seq 2113-2133	aaaaccgcagcgcaaaggaac

2.1.3 Cloning Vectors

K10 UASP - expression vector for transgenesis (Koch et al., 2009), 9 kb, AmpR

pGEX-6-P-1 (GE Healthcare), 4.9 kb, AmpR

pLou3 vector (Professor Ron Hay, University of Dundee), 6.7 kb, AmpR

2.1.4 Antibodies

The primary and secondary antibodies used for Western blotting (WB), Immunofluorescence (IF) and Immuno-precipitation experiments (IP) are listed in Table 2-2.

Table 2- 2: List of primary and secondary antibodies used for immunofluorescence staining (IF), Western blotting (WB) and Immunoprecipitation (IP).

Antibody	Species	Application	Company
Centrosomine	rabbit	IF: 1:250	Jordan Raff
Cyclin B	mouse	WB: 1:50	DSHB F1F4
GST (B-14)	mouse	WB: 1:2000	St Cruz (# sc-138)
Mad-2	rabbit	WB: 1:1000 ; IP: 1:500	Claudio Sunkel
MBP	mouse	WB: 1:10000	New England Biolabs (#E8032S)
Spindly	rabbit	WB: 1:2000 ; IP: 1:1000	this work
α actin	rabbit	WB: 1:3000	Sigma (#A2066)
α tubulin	mouse	WB: 1:2000	DSHB 12G10
β tubulin	mouse	IF: 1:50	DSHB E7
anti-mouse HRP IgG	goat	1:2000	Roche
anti-rabbit HRP IgG	goat	1:5000	Thermo Scientific (#31460)
anti-rabbit Alexa 647	goat	1:250	Invitrogen (#A27040)
anti-mouse Alexa 488	goat	1:250	Invitrogen (#A11001)
anti-mouse Cy3	donkey	1:250	Stratech (#715-167-003-JIR)

2.1.5 Drosophila stocks

The Drosophila stocks used in this thesis are listed inTable 2-3. These stocks were either obtained from the stock collection in Bloomington, from other Drosophila labs, or created in this work.

Table 2- 3: Fly stocks

Strain/genotype	Description	Reference
wild type		Müller stock collection
w^{1118}	white eyes	Bloomington #5905
nos >Gal4 VP16	express Gal4 under the control of *nanos* promoter; 2nd chr.	Ulrike Gaul
w; *mat-betatubulin_VP16[67]* /CyO[twi::lacZ] ; TM6/MKRS	express Gal4 under the control of *maternal tubulin 67c* promoter; 2nd chr.	Müller stock collection
w[1118]; *slbo* >Gal4 /CyO	express Gal4 under the control of *slow border cells* promoter; 2nd chr.	Denise Montell
srp [hemo]>Gal4 , *UAS* >GFP	express Gal4 under the control of serpent promoter; 2nd chr.	Mike Williams
y[1] sc[*] v[1]; P{y[+t7.7] v[+t1.8]=TRiP.HMS01283}attP2	Express dsRNA for RNAi of Spindly under *UAS* control (TRIP project); 3rd chr.	Bloomington #34933
y[1] sc[*] v[1]; P{y[+t7.7] v[+t1.8]=TRiP.HM05274}attP2	Express dsRNA for RNAi of Spindly under *UAS* control (TRIP project); 3rd chr.	Bloomington #36104
w; p*UAS* p>GFP-Spindly/TM6	Express a GFP-tagged variant of Spindly under *UASp* control; 3rd chr.(68A4)	this work
w[1118]; If/CyO; MKRS/TM6B[Tb1]	balancer line of the2nd and the 3rd chr.	Müller stock collection
w[*]; TM3, Sb[1] Ser[1]/TM6B, Tb[1]	balancer line of the 3rd chr.	Müller stock collection

2.1.6 Instruments

UV Spectrophotometer: Biophotometer eppendorf (#AG 22331) for measuring optical density (OD) and determining DNA concentration

Centrifuge 5424 (Eppendorf)

Master Cycler Gradient (Eppendorf) for PCR- 53 -

Consort EV202 Electrophoresis Power Supply (Consort)

Transilluminator VMR, Genostar/ VideoGraphic Printer (Sonic)

Orbital shaker, Forma Scientific

Olympus BX61 Microscope / Aquisition and Shutter Hubs (Improvision) / Orca ER

Digital Camera (Hamamatsu)

Leica Confocal SP8

LTQ Orbitrap Velos Pro and LTQ Orbitrap XL (Thermo Scientific) for MS-MS of protein samples.

2.1.7 Software

A Plasmid Editor (APE) (M.W. Davis, University of Utah) for DNA sequence analysis.

Volocity (Perkin Elmer) for image acquisition and visualisation.

ImageJ (Abramoff et al., 2004) for image analysis. ImageJ plugins: Manual tracking, Chemotaxis and Migration Tool.

Photoshop CS5 (Adobe) for enhancing contrast of images and image analysis

MaxQuant (Cox and Mann 2008) for large-scale analysis of MS and MS-MS data.

2.2 Methods

2.2.1 Polymerase Chain Reaction (PCR)

For molecular cloning, DNA fragments were amplified from plasmid DNA or genomic DNA by PCR. A standard reaction was carried out in a final volume of 25-50 µl. Each reaction mixture contained 1x reaction buffer, 100 ng template DNA, 1mM total dNTP, 1 µM of forward and reverse primers and 2.5U of DNA Polymerase (Phusion Hot Start II, Thermo Scientific, #473855). Standard reactions were carried out according to manifacture instruction. Annealing temperature and extension time were adjusted according to the needs of each individual reaction. The cycling parameters of a standard reaction are reported in Table 2-4.

Table 2- 4: Standard PCR cycling parameters.

	Temperature	Duration
Initial Denaturation	95°C	2 min
Denaturation	95°C	30 s-1 min
Annealing	55-60°C	30 s
Extension	72°C	1 min/Kb
Cycles: Repeat from step 2, 30 times		
Final extension	72°C	10 min

2.2.2 Site-directed mutagenesis

Mutagenesis PCR is a molecular biology method to introduce targeted mutations in a DNA construct by designing primers that are not fully complementary with the template DNA. Cycling parameters adopted for the site-directed mutagenesis are reported in Table 2-5.

Table 2- 5: Cycling parameters of a typical site directed mutagenesis PCR.

	Temperature	Duration
Initial Denaturation	95°C	3 min
Denaturation	95°C	30 s
Annealing	52-54°C	30 s
Extension	72°C	10 min
Cycles: Repeat from step 2, 5 times		
Denaturation	95°C	30 s
Annealing	54-60°C	30 s
Extension	72°C	10 min
Cycles: Repeat from step 2, 20 times		
Final extension	72°C	10 min

Following PCR, 2 µl of the reaction were run on a gel to verify the efficiency of the amplification. The remaining volume was incubated at 37°C for 1-2 hours with the restriction enzyme DpnI, which digests specifically the original methylated template.

2.2.3 Standard method to culture E. coli

E. coli strains were grown in Luria-Bertani (LB) medium at 37°C. For selective growth Ampicillin was added at a final concentration of 100 µg/ml. Alternatively, Kanamycin was used at a concentration of 50 µg/ml. Solid medium for LB plates contained 2 % agar.

LB medium composition: 1 % Trypton, 0.5 % yeast extract, 1 % NaCl.

2.2.4 Isolation of plasmid DNA from E. coli

For molecular cloning, sequencing and transformation of flies, plasmid DNA was purified using the Spin Miniprep kit (QIAprep; #27106) or QIAGEN Midiprep kit (Qiagen; #12143) according to the amount of plasmid DNA needed. The preparation was performed following the manufacturer's instructions.

E. coli cells transformed with the desired plasmid DNA were cultured overnight in 3ml of LB medium containing the appropriate antibiotic selection. Cells were sedimented by centrifugation (5000 rpm, 2 min) and the pellet was used for Miniprep. Altenatively, 1 ml of the pre-culture was inoculated overnight in 100-150 ml of LB medium and incubated overnight at 37°C. The culture was centrifuged and the cells were used for Midiprep.

2.2.5 DNA restriction

For diagnostic digestion, 1 µg of DNA was digested with 1Unit of restriction enzymes in a final volume of 20 µl for 2 hours at 37°C. For cloning purpose, a minimum amount of 5 µg of DNA was digested with restriction enzymes in a final volume of 100 µl. Restriction enzymes used in this work were purchased either from Roche or NEB.

2.2.6 Agarose gel electrophoresis

For analysis of restriction products or PCR amplification products DNA samples were mixed with 6X DNA Loading Buffer and loaded on a 1% agarose gel prepared in 1x TAE Buffer to which 5 µl of Gel Red, Nucleic Acid Stain (Biotium; #41003) were added. A standard 1 Kb Ladder (Gene ruler 1kb Plus; Thermo Scientific #SM1331) was loaded to determine the size of the DNA bands. DNA bands were detected with UV light (λ = 254 nm).

Solutions
Loading Buffer (Thermos Scientific #R0611): 10 mM Tris-HCl (pH 7.6), 0.03% bromophenol blue, 0.03% xylene cyanol FF, 60% glycerol, 60 mM EDTA.
TAE Buffer: 40 mM Tris-Acetate, 20 mM NaAcetate, 2 mM EDTA, pH 8.3.

2.2.7 Isolation of DNA from an agarose gel

DNA fragments derived from PCR reactions or restriction digestions were separated on an agarose gel. The bands of interest were excised from the gel with a scalpel and placed into an eppendorf tube. DNA fragments were recovered from the gel using the Wizard SV Gel and PCR Clean-Up System (Promega; # A9281) according to the manufacturers' protocol.

2.2.8 Ligation of DNA fragments

Linearised DNA fragments were ligated in a reaction volume of 20 µl containing 5 units T4-DNA-Ligase (Thermo Sceintific, #EL0011) and 1 to 10 µg/ml DNA at RT for 1 hour or at 16°C overnight. Before performing ligation, the vector was dephosphorylated at RT for 1h using 1 Unit of alkaline phosphatase (FastAP Fermentas, #EF0651). The molar Vector/Insert DNA ratio used was between 1:6 and 1:10. The correct amounts of vector and insert DNA were calculated using the formula shown in **Error! Reference ource not found.**. The ligation reaction was used to transform chemically competent E. coli cells.

Table 2- 6: Formula used to calculate the optimal vector-insert ratio for ligation reaction.

$$\text{ng insert} = \frac{\text{ng}_{\text{vector}} \times \text{kb}_{\text{insert}} \times \text{5-10 excess}}{\text{kb}_{\text{vector}}}$$

2.2.9 Transformation of DNA into chemically competent E.coli

Chemically competent E.coli cells stored at -80°C were thawed on ice. 50 µl of bacteria were transformed with 2-10 µl of plasmid DNA and incubated on ice for 30 min. The cells were heat-shocked transferring the vials in a water bath for 40 sec at 42°C. Cells were allowed to recover on ice for 5 min. 250 µl of pre-warmed LB medium were added and cells were incubated at 37°C for 30-60 min, while shaking. The mixture was plated on LB agar plates containing an appropriate antibiotic for selection and plates were incubated overnight at 37°C. Colonies were isolated from the plates and used to grow 3 ml pre-culture or for large-scale purification of the vector.

2.2.10 Colony PCR

As a fast and efficient readout of the cloning reaction, colony PCR was performed. A minimum number of 5 colonies for each cloning reaction were screened. Colonies were picked with a pipette tip. The tip was used to quickly stir 50 µl of dH2O and then transferred in 50 µl of LB medium. 50 µl of dH2O containing the bacteria were boiled for 5 min and 1 µl of the sample was added as DNA template to a PCR mix previously prepared as described in 2.2.1. For the colonies that resulted to be positive, 50 µl of LB medium were inoculated in 3 ml of LB medium and cultured overnight at 37°C. The following day, the DNA plasmid was purified and sent to sequence.

2.2.11 Estimation of DNA concentration

DNA concentration after PCR reactions, gel band extraction or plasmid DNA isolation was estimated using a spectrophotometer. 2µl of DNA sample were mixes with 98µl of dH2O. Absorbance of light (λ=260nm) was measured and DNA concentration values were given in µg/ml. 100 µl of dH20 were used as blank measurement.

2.2.12 DNA sequencing

DNA sequencing was performed by the DNA Sequencing Services (College of Life Sciences, University of Dundee). 600 ng of plasmid DNA per sequencing reaction were provided and 10 µl of 3.2µM primer solution was sent. To sequence a PCR product 2-40 ng of DNA per reaction were sent, depending on size of the product.

Protein Biochemical Methods

2.2.13 Extraction of proteins from embryos

Embryos were collected in apple juice agar plates and washed in water. Sodium-Hypochlorite (NaHCl) was added to remove the chorion. Embryos were extensively washed in Triton-Salt solution, transferred in eppendorf tubes and snap frozen in liquid nitrogen. For protein extraction, embryos were lysed in RIPA buffer containing a mixture of protease inhibitors (Mini-complete EDTA free –Roche, 1 tablet/10 ml), using a plastic pestle. The grinded tissue was incubated on ice for 30 min. Subsequently, the sample was centrifuged at 13000 rpm for 30 min at 4°C to remove debris. The protein extract was either stored at -80°C or immediately used for further analysis.

Solutions
RIPA Buffer: 50 mM Tris-HCL pH 8.0, 150 mM NaCl, 1 % NP-40, 0.5 % Sodiumdeoxycholate, 0.1 % SDS.

2.2.14 Protein estimation using Bradford Assay

1 µl of protein extract was diluted in water to a final volume of 20 µl. 780 µl of Bradford reagent (Comassie Protein Assay Reagent_Thermo Scientific Pierce) were added and the sample was transferred into UV cuvette. Absorbance value was read at 600 nm using a photometer (Biophotometer, Eppendorf_Hamburg). The absorbance value was compared with those ones obtained preparing a standard curve with Bovine Standard Albumin (BSA) dilutions of known concentration (1mg/ml, 0.75mg/ml, 0.5mg/ml, 0.25mg/ml, 0.125mg/ml).

2.2.15 SDS-PAGE and Western Blotting

10 µg of proteins were heat-denatured and resolved onto a Tris-HCl poly-acrylamide gel in Running Buffer. As a molecular weight marker 5 µl of Page Ruler pre-stained protein ladder (Thermo Scientific; # 26619) were loaded. The gel was run at 150 V for 90 min. Proteins were then transferred at 100V for 120 min to a nitrocellulose membrane and blocked for 60 min at RT with 10% powdered milk in TBT. The membrane was then incubated with primary antibody diluted in 5% powdered milk in TBT. Equal protein loading was confirmed by detection of the housekeeping protein α-tubulin. Incubation with primary antibodies was performed overnight at 4°C.

After extensive washes, the membrane was incubated with HRP-conjugates species-specific secondary antibody for 60 min at room.

Solutions
Running Buffer: 25 mM Tris, 200 mM glycine and 0.1%SDS.
Transfer Buffer: 480 mM Tris, 390 mM glycine, 0.1% SDS and 10% methanol
1X PBT: 1X PBS + 0.1%Tween-20
Blocking solution: TBT + 10% milk

2.2.16 Affinity-purification Mass Spectrometry (AP-MS) analysis

Immunoprecipitation experiment

0-7-hour-old embryos were collected in apple juice plates, washed with water and incubated in NaHCl to remove the chorion. Successively, embryos were resuspended in lysis buffer containing 10U/ml of Benzonase (Novagen; # 71206-3) and ground using a plastic pestle. Lysate was passed through a 21G needle and incubated with 2000 Kunizt Units of pre-activated DNase I. DNase I was previously reconstituted in 500 µl of PBS

containing 2 mM MgCl2. Incubation with DNaseI was carried out as follows: 5 min at 37°C, 5 min at RT, 10 min at 4°C. All the incubation steps were performed on a rocking platform. Samples were cleared of embryos debris by centrifugation (15 min, 5000g, 4°C). Subsequently, the supernatants were filtered through 2 layers of Miracloth (Calbiochem, #475855). Samples were incubated with 5 µl of primary antibody for 1 hour at 4°C, rotating. Normal rabbit IgG were used as negative control. Thereafter, 10 µl of Dynabeads Protein A (Life Technology; # 10001D) were added and incubation was performed for at least 3 additional hours at 4°C, rotating. Protein-antibody complexes were washed 3 times for 15 min at 4°C with an appropriate volume of lysis buffer. Subsequently, beads were transferred into microtubes and samples were placed on a magnetic stand. Beads were washed quickly two additional times: one with lysis buffer and one with 1x PBS. Elution of the protein complexes from beads was carried out twice at RT for 10 min with 600 µl of Ammonium hydroxide (NH4OH), whilst rotating. The eluted samples were transferred into a vacuum centrifuge (SpeedVac, Eppendorf) and were concentrated to 100 µl. 500 µl of ultrapure water were added to each sample and they were concentrated to 100 µl. The procedure was repeated three times and helped to remove the excess of NH4OH. After the final wash, 900 µl of cold acetone were added and samples were incubated at -20°C overnight. The following day, proteins were precipitated by ultracentrifugation (21000g, 10 min, 4°C). The supernatant was carefully removed and the precipitate was dried. Samples were processed for Mass Spectrometry analysis (see below). Along the experiment steps, aliquots of each sample were collected, resuspended in 20 µl of 2x sample buffer and separated on SDS-PAGE for Western blotting.

Solutions

Lysis Buffer: 50 mM Tris pH7.5, 150 mM NaCl, 1 mM EGTA, 1 mM EDTA, 0.3 % CHAPS, 270 mM Sucrose, 1 mM Sodium Orthovanadtae, 10 mM Sodium Glycerophosphate (Sigma; #G9422-10G), 10 mM Sodium Pyrophosphate (Sigma; #221368-100G), 50 mM SodiumFluoride, 0.1% betamercaptoethanol, 10 mM Iodoacetamide (Sigma, #I1149-5G), Protease inhibitors (1 tablet/ 50 ml).

In solution digestion of lyophilised proteins

Lyophilysed pellets were resuspended with 50 mM Ammonium bicarbonate (NH_4HCO_3). To the mixture 45mM DTT were added and samples were incubated at 50°C while shaking for 15 min. Samples were cooled at RT and 100 mM of Iodoacetamide (IAA) diluted in 25 mM NH_4HCO_3 were added. Samples were shaded from light and incubated at RT for 15 min. The protein mixture was incubated with trypsin peptidase reconstituted in 50 mM NH_4HCO_3 (pH 8.0). Incubation was performed overnight at 37°C to achieve complete digestion. Trypsin was added to the sample in a 1:100 enzyme:protein ratio.

Purification of peptides with C18 columns

Digested protein samples were cleaned up using a C18 “Ziptip” column. The procedure helps in removing the excess of salts and polymers from the samples. C18 columns were activated washing them with 20 µl of a Acetonitrile (ACN): trifluoroacetic acid (TFA) solution (50% ACN:0.1% TFA). The excess of 50% ACN:0.1% TFA was washed off using 0.1% TFA and columns were loaded with 60 µl of the sample each time, while the flow-through was kept. The unbound waste was washed away using 20 µl of 0.1% TFA and bound peptides were eluted in a clean microtube with 40 µl of 50% ACN:0.1% TFA. The elution step was repeated twice for a final volume of 80 µl. Finally, samples were dried in a vacuum centrifuge system at 60°C to a final volume of 10 µl.

Mass-spectrometry and proteomic analysis:

All MS analysis was performed by the FingerPrints Proteomics Facility (University of Dundee). MS-MS data were analysed using MaxQuant (Cox and Mann 2008).

Peptide samples were run on an Ultimate 3000 RSLCnano system (Thermo Scientific) coupled to a LTQ OrbiTrap Velos Pro (Thermo Scientific). Chromatographic separation was performed on an Easy-Spray PepMap RSLC C18 column (75 µM x 50 cm) (Thermo Scientific) using a gradient of 2-40% Buffer A: Buffer B ratio over 156 min with a flow rate of 0.3 µl/min. Mass spectrometry analysis was performed via a 'top 15' method in which a survey scan was followed by MS/MS of the fifteen most abundant precursor ions. An initial precursor scan is performed to identify the most abundant peptide precursor ion within a preselected m/z range. The selection of the peptide ions take also into account other criteria such as peak intensity and charge state. Normally, the most intense peaks (meaning the most abundant) in the scan survey are subsequently isolated and chosen to undergo fragmentation and collision. Fragmented ions are finally scanned out the mass analyser.

Survey scans were acquired in the Orbitrap with a m/z range 335-1800, an automatic gain control (AGC) target of 1 × 106 charges, a maximum fill time of 500 ms, and a resolution of 60,000. Collision induced dissociation (CID) was performed in the linear ion trap (AGC target: 5000 charges) with a normalised collision energy of 35%.

MS-MS data were analysed using MaxQuant 1.5.1.2.8, using a Uniprot Drosophila Database to identify peptides. In addition to peptide identification and generation of quantitative data, the software allows the identification of any modifications to peptides, including carbamidomethylation, oxidation, phosphorylation and acetylation.

Solutions
Buffer A: 0.1% formic acid
Buffer B: 80% acetonitrile in 0.08% formic acid

2.2.17 In vitro Binding Assay using recombinant proteins

A series of Spindly constructs and a wild-type Mad-2 construct were expressed as Maltose Binding Protein (MBP) fusion proteins or Glutathione S-Transferase (GST) fusion protein respectively in E. coli strain BL21. Expression and purification of the recombinant proteins were carried out as described in 2.2.18.

The purified proteins were dialysed and stored in binding buffer. 10 µg of GST-Mad-2 fusion protein or 10 µg of GST control were mixed with 10 µg of each Spindly construct and the volume was brought up to 1ml with binding buffer. Incubation was carried out overnight at 4°C on a rocking platform. After this period of incubation, 20 µl of glutathione beads (Glutathione Sepharose 4B, GE Healthcare; # 17-0756-01) were added and rotation was resumed for 2 additional hours at 4°C. Beads were recovered by centrifugation at 1000 rpm for 1 min and washed 3 times in binding buffer. Once the last wash was removed, 20 µl of 2x sample buffer were added to each sample and proteins were boiled for 5 min. Protein samples were run on a SDS-PAGE and the suspected interaction revealed by Western Blotting.

Solutions
Binding Buffer: 50mMTris, 5mM MgCl2; 250mM NaCl; 0.01%TritonX-100_pH8.0

2.2.18 Expression of recombinant proteins in E. coli and purification protocol

BL21 cells carrying the constructs of interest were grown overnight at 37°C in a small volume of LB containing antibiotic for selection. The following day, 1 ml was poured into 500-1000 ml of Terrific Broth (TB) medium and incubated at 37°C while shaking. To determine the amount of bacteria within the culture, optical density at λ= 600 (OD600) was measured using a spectrophotometer. 1 ml of uninoculated media was used for a blank measurement. When OD600 reached a value 0.6-0.8, isopropyl β-D-l thyogalactopyranoside (IPTG) was added to a final concentration of 1 mM for 3 hours at 37°C to induce protein expression. Alternatively, the culture was cooled on ice before adding IPTG and the expression of the recombinant protein was induced overnight at 16°C. Protein induction efficiency was checked by running non-induced and induced samples on a SDS-PAGE gel and staining gels with Coomassie Blue. Cells were spun down and lysed in lysis buffer. Lysis was carried out on ice with a sonicator (5x 30 sec pulse, 30 sec rest in between). Lysates were incubated 1 hour at 4°C following addition of 1% Triton-X 100. Lysates were cleared of the debris by centrifugation 5000 rpm for 5 min at 4°C. The supernatant were carefully recovered and placed in fresh tubes. Proteins were purified adding either Ni-NTA agarose beads (Qiagen; #30210) or glutathione sepharose beads (GE Healthcare, #17-0756-01) for a minimal period of 1 hour at 4°C. After the incubation, beads were washed three times in lysis buffer (15 min at 4°C, each wash) and elution of the bound protein was achieved with 1 ml of elution buffer. During the purification, fractions were collected and run on a SDS-PAGE gel that was subsequently Coomassie Blue stained. The purified proteins were dialysed in dialysis tubing overnight at 4°C in the buffer of choice (Fisher Scientific; #BID-010-040-B; 14000MWCO).

Solutions
TB medium: 1.2% Tryptone, 2.4% Yeast extract, 0.4% Glycerol, 17 mM KH2PO4, 72 mM K2HPO4
Lysis Buffer: 50 mM Tris pH 8, 250 mM NaCl, protease inhibitors
Elution Buffer (for GST-tagged constructs): 10mM Glutathione, 150mM Tris-HCl, pH8.0
Elution Buffer (for 6X-His-tagged constructs): 250 mM Imidazole, 50 mM Tris pH 8.0, 250 mM NaCl.

Affinity purification of anti-Spindly antibody

A portion of the Drosophila spindly gene codifying for the C-terminal half of the protein (amino acids 451-780) was cloned in the pET28a vector. The construct was a kind gift of Dr E. Griffis, University of Dundee (Griffis, Stuurman et al. 2007). The vector was used to transfrom BL21 competent cells. The recombinant 6xHis-tagged C-terminal fragment of Spindly (antigen) was expressed and purified as described in 2.2.18. Affinity-purification of the antibody was achieved using a Cyanobromide (CnBr) Sepharose resin (CnBr-activated Sepharose 4 Fast Flow, Pharmacia Biotech, # 17-0981-01). In principle, the cyanogen bromide coupled to the sepharose support reacts with the primary amines to immobilise the desired protein to the beads. The procedure to purify the antibody was completed in three days as described below.

Day 1: Coupling of ligands to beads

The appropriate amount of dried CnBr resin was weighed (350 mg of sepharose for 5-10 mg of purified protein) and dissolved in 50 ml of cold 1 mM HCl. The solution was transferred into a 15 ml tube and the resin was allowed to settle. The HCl solution was removed and the gel was washed 5 times with 15 ml of 1 mM HCl. Washes were carried out at 4°C on rotator for 15 min. Afterwards, the CnBr gel was washed three times with 15 ml of ice-cold coupling buffer for 5 min at 4°C. At the end of the last washing step, the resin was pelletted by centrifugation and the supernatant was

removed. The antigen was diluted in cold coupling buffer to a concentration of 1mg/ml and added to the resin. The sample was incubated overnight at 4°C on rotator to couple the protein to the CnBr sepharose beads.

Day 2: Washing of Beads

The sample was spun and the beads were washed twice 10 min at 4°C with 10 ml of coupling buffer. The pellet was washed by incubating 3 hours at 4°C with 15 ml of 0.1M Tris HCl, pH 8.0, while rotating. Subsequently, beads were washed with 15 ml of Elution Buffer followed by a wash with 15 ml of wash buffer. This last step was repeated twice. The resin was stored in wash buffer at 4°C, overnight.

Solutions Day 1 and 2
Coupling Buffer: 0.1 M $NaHCO_3$, 0.5 M NaCl. Adjust pH to 8.0. (make fresh each time)
Elution Buffer: 100 mM Glycine, pH 2.5
Wash Buffer: 0.1 M Tris, 0.5 NaCl. Adjust pH to 8.0.

Day 3: Affinity purification from CnBr resin

The resin was collected and blocked with 15 ml of blocking buffer at RT on rotator for 1 hour. The gel was spun down and the supernatant gently removed. A rabbit serum (kindly provided by Dr E. Griffis) was diluted 1:5 in serum dilution buffer and added to the resin. Sample was incubated at RT for 2 hours on rotator. After this incubation step, beads were washed with 15 ml of wash buffer and transferred to a column. The bound antibody was eluted in 10 ml of elution buffer. Specifically, 1 ml aliquots were collected into eppendorf tubes previously prepared with 1/10 volume of 1 M Tris, pH 8.0. The column was washed with 10 ml of wash buffer and stored at 4°C. Affinity purified antibody was concentrated using a concentrator (VIVASPIN 20, 10000 MWCO; # VS2002) to a volume of 500 µl. Specificity of the antibody was tested by Western

blotting (Figure 2-1) and Immunofluorescence analysis. For Western blotting the antibody was tested at a range of concentration from 1:200 to 1:10000. In Immunofluorescence the antibody was tested in a range of concentration from 1:100 to 1:4000.

Solutions Day 3
Coupling Buffer: 0.1 M NaHCO3, 0.5 M NaCl. Adjust pH to 8.0. (make fresh each time)
Blocking Buffer: 1% BSA, 50 mM Tris, 250 mM NaCl. Adjust pH to 8.0.
Serum Dilution Buffer: 0.1M Tris, 250 mM NaCl. Adjust pH to 8.0.
Elution Buffer: 100 mM Glycine, pH 2.5
Wash Buffer: 0.1 M Tris, 0.5 NaCl. Adjust pH to 8.0.

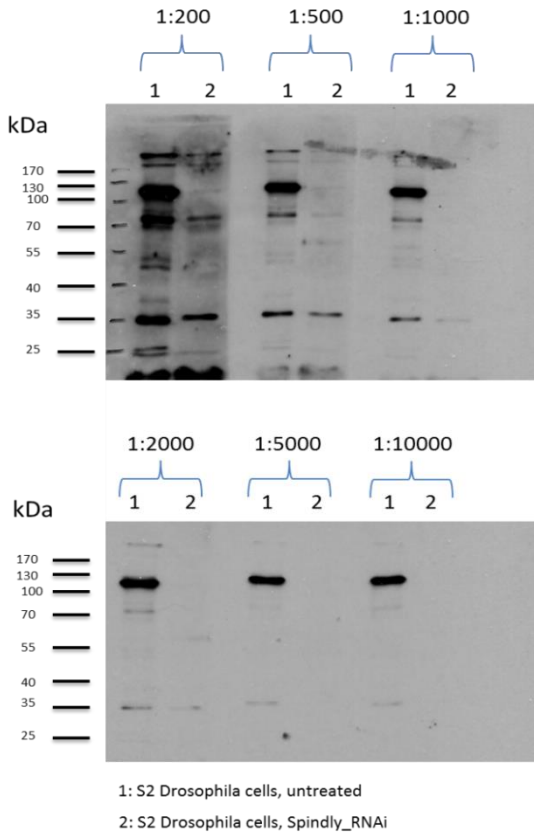

Figure 2- 1: **Specificity of affinity-purified Spindly antibody used in this study.** Western blot analysis was performed to test the specificity of the affinity-purified antibody. 10 µg of protein lysate from untreated S2 Drosophila cells or from S2 cells in which the expression levels of Spindly were reduced by treating with dsRNA were loaded on adjacent lanes (1 and 2 respectively). Proteins were run on a SDS-PAGE and transferred into nitrocellulose membranes. Membranes were probed with the Spindly antibody, used at the dilutions indicated in pictures. A standard protein molecular weight marker is included and numbers in kDa are shown on the left. The calculated molecular weight for wild-type full-length Spindly is 100 kDa; the apparent molecular weight is 120 kDa.

Genetic methods

2.2.19 Drosophila culture and crosses

Flies were maintained in bottles and vials containing standard medium. Flies of the desire genotypes were collected twice daily by anesthetising them on CO2 emitting pads. Female virgins were selected based on a light body colour, body shape and the presence of the meconium.

To set up crosses, male and female flies were mated in vials or bottles containing dried yeast powder to stimulate egg laying. Crosses were tipped into fresh vials every 3 days. Flies of the F1 generation were anesthetised on CO2 emitting pads and selected under the dissection microscope for the desired genotype. These flies were put into cups placed on agar plates containing apple juice and fresh yeast for egg collection or used for subsequent crosses. Crosses were kept at 25°C unless otherwise stated.

Solutions
Standard food medium: 134.4g yeast, 569.6g cornmeal, 76g soya flour, 40g agar, 360g mal extract, 320g molasses, 36ml propionic acid, 12 g nipagen, 7.9L water.
Apple juice agar: 27g agar, 12.5g sucrose, 15ml of 10% nipagen, 250ml apple juice and water.

2.2.20 Hatching rate determination

Flies were placed on yeasted apple juice plates overnight at different temperature (RT, 18°C, 23°C and 25°C). The laid eggs were counted immediately for a total of 100. After 48 hours, the remaining embryos that did not hatch were counted and the hatching rate was determined by the calculating the percentage of hatched versus non-hatched embryos.

2.2.21 UAS/Gal4 System

Adopted from yeast, the Gal4/UAS system is extensively used in Drosophila to spatially and temporarily control the ectopic expression of a transgene (Andrea H. Brand 1993). In this bipartite system the two components are maintained separated into two parental fly lines. The first line, known as driver/activator line, expresses the transcription factor Gal4. The effector/responder line has the transgene of interest under the control of the Upstream Activating Sequence (UAS)-containing promoter. The binding of Gal4 protein to the regulatory elements UAS induces the expression of the transgene (Figure 2-2).

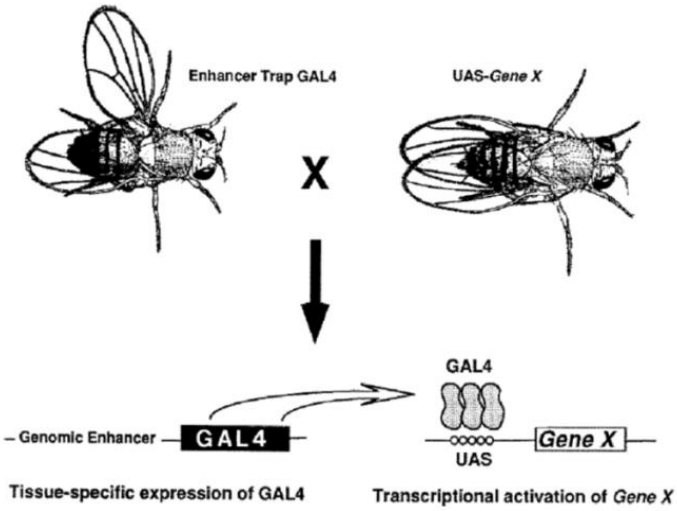

Figure 2- 2: **The Gal4/UAS expression system.** The driver line expresses Gal4 under the control of any promoter. The effector line carries the transgene of interest under the control of the UAS elements. When flies from the two lines are mated together, progeny carrying both constructs is generated. Image was adopted from (Andrea H. Brand 1993).

2.2.22 Balancer Chromosomes

Balancer chromosomes are a powerful tool in Drosophila genetics. These chromosomes have two main features: they have inversion breakpoints, functioning therefore as crossover suppressor, and they carry lethal recessive mutations.

By suppressing crossing over, balancer chromosomes allow to stably maintain a mutation in heterozygosity. Moreover, a balancer chromosome contains dominant markers allowing to track these chromosomes along complex crossing schemes.

2.2.23 Germline transformation, Outcrossing and Balancing

To generate transgenic fly lines a transformation vector is injected into the germline of Drosophila embryos. The company Rainbow Transgenic Flies, Inc performed the injection procedure. (Newbury Park, CA 91320 USA; rainbowgene.com). The attP-attB recombination system is used to ensure genome engineering in Drosophila. Adopted from bacteriophage, this system relies on the activity of the large serine integrase PhiC31 that mediates sequence-directed recombination between two attachment sites, called attP and attB (Amy C. Groth 2004). As a product of the reaction, the PhiC31 integrase generates two different sites, attL and attR, between which recombination cannot occur. Therefore, the reaction is unidirectional. Drosphila fly lines with attP docking site at specific genomic loci have been generated in 2007 by Johannes Bischof (Bischof, Maeda et al. 2007).

In this study a fly line with attP site at the genomic location 68A4 on the third chromosome has been used to integrate a transformation vector carrying an attB site. To identify flies carrying the transgene of interest integrated into the genome, these have been crossed to w^{1118} flies and the next generation has been screened for flies with red eyes. This phenotypic characteristic is indeed the sign of successful integration of the transgene into the genome. Positive flies were eventually crossed to balancer stocks to generate stable lines.

Histological methods

2.2.24 Embryos fixation and antibody staining

Flies were put in egg-laying cups on top of apple juice agar plate. Embryos were collected for immunofluorescence analysis every three hours.

Embryos were washed in water and NaHCl was added to remove the chorion. Embryos were then resuspended in PEM Buffer containing 1 µM taxol (Tocris). 1:1 volumes of heptane were added and, after a quick shake, 1 ml of 20% formaldehyde. Shaking was resumed for 10 min at 350 rpm. Formaldehyde was removed and replaced with methanol. Shaking was resumed for 10 min at 350 rpm. This procedure helps in removing the vitelline envelope.

Alternatively, embryos were resuspended in 5 ml of 4% formaldehyde in PBS mixed with a 1:1 volume of heptane and fixation was performed for 20 min at RT, while rotating. Subsequently, the fixing solution was removed and 5 ml of methanol were added and embryos vigorously shacked to remove the vitelline envelope. Finally, embryos were transferred into Eppendorf tubes and washed with methanol twice. After this step, embryos were either stored at 20°C or processed for immunofluorescence.

2.2.25 Immunofluorescence staining

For fluorescent staining embryos were washed 3 times for 15 min in PBT and incubated in a blocking solution for 1 hour at room temperature. Primary antibodies were diluted in blocking solution and embryos were incubated overnight at 4°C, under constant agitation. On the next day, samples were incubated with secondary antibodies coupled with fluorescent markers for 1 hour at RT. After 3 washes of 15 min each in PBT, DNA

was stained with DAPI (1:1000, Sigma Aldrich; #D9542-1mg) for 10 min. After few final washes in PBT, embryos were embedded in Mowiol /DABCO (Sigma Aldrich) and mounted on glass slides. A coverslip was gently added and secure in place using nail varnish. Microscopy was performed using an Olympus BX-61, TRF fluorescence microscope or a confocal laser-scanning microscope (Leica TCS SP8). Images were processed using Volocity (Improvision, Perkin Elmer) and Adobe Photoshop.

2.2.26 Ovaries preparation, fixation and staining

Female flies were killed by crushing the thorax with tweezers. Ovaries were isolated and fixed in cold 4% Formaldehyde for 15 min. After this period of incubation, the ovaries were washed in PBT and incubated for 2 hours in PBTx solution supplemented with 5% Foetal Calf Serum (FCS). Samples were incubated overnight at 4°C in a solution of PBT containing primary antibodies. F-actin staining was achieved by adding a fluorochrome-conjugated phalloidin (Phalloidin-Alexa594, Invitrogen #A12381) in 1:50 dilution. The day after, samples were washed 3 times in PBT for 15 min and incubated with secondary antibodies for 1 hour at RT, on rocking platform. Nuclei were stained with DAPI for 10 min (1:1000 dilution). After extensive washes, the ovaries were embedded in Mowiol /DABCO (Sigma Aldrich) and mounted on coverslips. Microscopy was performed using an Olympus BX-61, TRF fluorescence microscope or a confocal laser-scanning microscope (Leica TCS SP8). Images were processed using Volocity (Improvision, Perkin Elmer) and Adobe Photoshop.

Solutions
PEM Buffer: 0.1 M Pipes; 1 mM MgCl2; 1 mM EGTA pH 6.9
10X PBS: 1.3M NaCl, 0.07M Na2HPO4, 0.03M NaH2PO4, ad 1L H2O, autoclave (adjust pH to 7.4)
1X PBT: 1X PBS + 0.1%Tween-20
Blocking Solution: 1X PBT + 10% Donkey Serum
Blocking Solution: 1XPBS+ 0.5% Triton-X 100+ 5% FCS

Mowiol: 24g glycerol (Sigma Aldrich #G-6279), 9.6g Mowiol 4-88 (Fluka-Sigma Aldrich, #81381), 48ml 0.2M Tris Buffer pH 8.5, 24 ml water.

2.2.27 Cuticle preparation

An overnight egg laying collection was taken and aged for another 24 hours at 25°C to allow completion of embryonic development. Hatched larvae were removed from the apple juice agar plate. The remaining embryos were collected and dechorionated in sodium hypochlorite. After extensive washes with a solution of PBS/0.1% Triton-X 100, embryos were mounted on slides with Hoyer's mounting medium containing a 1:1 volume of Lactic Acid. Samples were incubated overnight at 65°C and the coverslips were fixed afterwards with nail polish on the slide and imaged using the Olympus BX-61, TRF microscope system.

Live samples

2.2.28 Mounting of embryos for live imaging

Flies were placed in laying cages and left to acclimatise for a period of 2 days during which the apple juice agar plates were changed daily. After this period, plates were changed late in the afternoon and overnight embryo collection was processed the following morning for the experiment. Laying cages were kept constantly at 25°C. Embryos were collected in a mesh by gently dislocating them with a paintbrush in a small volume of distilled water. Embryos were dechorionated by submerging the mesh in undiluted commercial bleach for 1 min. Embryos were rinsed with distilled water to remove the excess of bleach and kept in distilled water to prevent them from dehydrating. Prior mounting, slides were prepared as follows. A strip of double-sided

sticky tape (Scotch) was placed along the length of a glass slide (Fisher). 22x22mm glass coverslips were attached at both ends, leaving space for the embryos in the centre. Embryos of the required stage were selected under the dissection microscope and transferred to the center of the slide. Embryos were orientated ventral side up using a tungsten needle. Each embryo was covered by a small drop of Voltalef oil (VWR International) using a tungsten needle. Finally a coverslip was carefully laid on top of the side bridges using forceps and secured in place using nail varnish.

2.2.29 Wounding and time-lapse imaging

Stage 15 live embryos expressing GFP were dechorinated and mounted ventral side up on glass slides as described. The epithelium of the embryo between the ventral midline and lateral lines of hemocytes was wounded using a micropoint nitrogen ablation laser (Andor). Images were captured using a Leica DMI6000B Ultraview Vox spinning-disk system (Perkin Elmer) with a 40x oil objective. Haemocytes were imaged at 30 sec intervals for a total of 60 mins on Spinning Disc microscope.

2.2.30 Image processing and analysis

Time-lapse movies acquired on the Leica DMI6000B Ultraview Vox spinning-disk system (Perkin Elmer) were processed using Image J (NIH). The spinning disk files were exported from Velocity (Perkin Elmer) as TIFF files and z-projected in Image J. To analyse migratory velocity, the centre of the haemocytes cell body was tracked using the Image J plugin ‘manual tracking’. Haemocyte migration was tracked every 3 minutes post-wounding over a period of 60 minutes. 5 cells for each movie were analysed.

Culture of Drosophila S2 cells

2.2.31 Culturing Drosophila Schneider 2 cells

Drosophila S2 cells were derived from embryos at late stage of embryonic development (SCHNEIDER 1972). These cells exhibit mesodermal characteristics and their profile of gene expression suggests that they are derived from haemocytes.

For routine culture, S2 cells were grown at 25°C without CO2 in 25-cm2 or 75-cm2 tissue culture flasks (CellStar, Greiner bio-one; #690160; #658170). Cells grew in a loose, semi-adherent monolayer and they were passed every 3 or 4 days at a 1:2 to 1:5 dilution. Cells were cultured in Schneider's Drosophila medium (Life Technologies #21720-024) supplemented with 10% Foetal Bovine Serum (FBS) (Life Technologies #10270106), 1% L-Glutamine (Life Technologies #25030-024), 1% Penicillin/Streptomycin (Pen/step) solution (Life Technologies, #15140-122).

For colchicine treatment, cells were grown in 75 cm2 flasks at 25°C (a minimal number of 3 flasks for each condition tested). Colchicine (5µg/ml, Calbiochem, #CAS 64-86-8) was added to a confluent culture and cells were incubated for an additional period of 12 hours. The following day, the medium was removed and cells were harvested.

2.2.32 Lysis of Drosophila S2 cells

S2 cells were harvested and centrifuged for 5 min at 1000 rpm. Culture medium was removed and cells were washed twice in PBS. Cells were pelleted by centrifuging the samples at 1000 rpm for 5 min and PBS was removed. S2 cells were lysed by pipetting them up and down in an appropriate volume of cold lysis buffer supplemented with

protease inhibitors and were incubated on ice for 30 min. Samples were centrifuged at 14.000 rpm at 4°C for 30 min and the supernatant was transferred into a new eppendorf tube. Protein concentration was determined as described in 2.2.14. Protein lysate was either stored at -80°C or immediately used for downstream applications.

2.2.33 Co-immunoprecipitation (Co-IP) experiment

S2 cells were washed extensively with 1x PBS and lysed in 1 ml of lysis buffer. 500 µg of protein extract were used for immune-precipitation experiments in a final volume of 200 µl. An input sample of 20 µl was taken as control. Protein lysate was mixed in a 1:1 volume with Buffer D and samples were incubated with primary antibody overnight at 4°C on a rocking platform. The day after, 20 µl of Sepharose-A agarose beads (Protein A Sepharose, GE Healthcare #17-5280-01) were added and incubation was carried out for 2 additional hours at 4°C, on a rotor. Beads were recovered by centrifugation at 1000 rpm for 1 min. Beads were washed once with 1x PBS. Immunocomplexes were eluted from beads by boiling the samples for 5 min after addition of 20 µl of 2X loading buffer. The detection of potential binding partners was performed by separation via SDS-PAGE and Western Blotting. The Lysis Buffer used for the co-IP experiments was that one optimised for the immunoprecipitation of the human homologue (Dr E. Griffis, confidential communication).

Solutions
Lysis Buffer: 50 mM Tris pH7.5, 150 mM NaCl, 1 mM EGTA, 1 mM EDTA, 0.3 % CHAPS, 270 mM Sucrose, 1 mM Sodium Orthovanadtae, 10 mM Sodium Glycerophosphate, 50 mM SodiumFluoride, 0.1% betamercaptoethanol, 100mM NEM, Protease inhibitors (1 tablet/ 50 ml).
Buffer D: 20mM Hepes pH 7.9, 0.5 mM DTT, 20% Glycerol, protease inhibitors (1 tablet/10 ml)

Chapter III: Results Part I

Requirement of Spindly for cell division

Chapter 3 Result Part I: Requirement of Spindly for cell division

3. Introduction to chapter III

Post-transcriptional gene silencing (PTGS) mediated by double-stranded RNA (dsRNA) is an effective method to reduce gene expression. The technique was first characterised in *C. elegans* where it was discovered that the injection of dsRNA into embryos was extremely efficient in manipulating gene expression (Fire, Xu et al. 1998). The method was proved to be highly applicable to other genetically tractable organisms including *Drosophila*, establishing the RNA Interference (RNAi) technology as an important method for high-throughput reverse genetics. The efficacy and penetrance of this tool in flies was first demonstrated using cell-based assays. In particular, Clemens *et al.* demonstrated that by downregulating the expression of known proteins of the insulin signalling cascade they were able to reproduce the effects of known mutations (Clemens, Worby *et al.* 2000). Subsequently, the application of the technique *in vivo* provided immediate insights into the biological relevance of uncharacterised genes by loss-of-function analysis. Specifically, by placing short hairpin RNA (shRNA) under the control of an Upstream Activating Sequence (UAS)-containing promoter, gene knockdown could be easily achieved by genetic crossing (Andrea H. Brand 1993). The wide variety of available Gal4 drivers allowed to conditionally control the levels of transcriptional activity by inducing gene knockdown in specific tissues and at a specific developmental stage. Furthermore, the inducible RNAi system allows the modulation of transcriptional activity by several means. Drivers that express different levels of Gal4 with a similar spatiotemporal pattern provided the possibility of studying the effects of a variable knockdown efficiency in the same

tissues. Moreover, the knockdown efficiency could be influenced by variating other factors such as temperature. Indeed, the UAS/Gal4 binary system is temperature-sensitive with a low activity at 18°C and a high activity at 25°C in *Drosophila*. Therefore, variations in the temperature modulate the strength of the system, providing a good way to control target gene knockdown. Specifically, higher temperature positively regulates the Gal4 activity enhancing the knockdown effects.

Currently, several collections of transgenic *Drosophila* RNAi strains are available to perform *in vivo* RNAi experiments. Of these, the transgenic RNAi Project (TRIP) is the most recently developed collection (http://www.flyrnai.org/TRiP). The major advantage of this collection is that the integration of the shRNA transgene is controlled by phiC31-mediated approach using a family of so-called VALIUM vectors that were developed for their ability of inducing optimal somatic and germline RNAi effects (Ni, Markstein et al. 2008, Ni, Liu et al. 2009). Additionally, a series of genomic insertion sites were screened and only those sites that showed the highest level of Gal4-driven expression of the transgene as well as the lowest basal level in the absence of Gal4 induction were selected for the integration procedure (Michele Markstein 2008).

Therefore, the improvement of the approach and the development of genome-wide RNAi resources have revolutionised the field of reverse genetics screens and have allowed the investigation of cell- and tissue-specific functions of still uncharacterised genes.

3.1 Loss-of-function genetics of *spindly* locus

In the present study the Gal4/UAS system was adopted to drive the tissue-specific expression of a shRNA construct directed against *spindly* mRNA. The application of this strategy was necessary to get insights into the biological function(s) of *spindly* since there are no mutant alleles available for the *Drosophila* gene CG15415, encoding Spindly. Two maternal Gal4 lines were used to eliminate the contribution of the maternal gene to embryo development and explore the function(s) of this uncharacterised factor in the context of *Drosophila* embryogenesis.

Shortly after fertilisation, a *Drosophila* embryo undergoes thirteen fast, synchronous mitotic divisions in a common cytoplasm without intervening cytokinesis. These mitotic cell cycles only consist of M and S phases depending on maternally provided regulators including Cyclin and CDK1 and do not require zygotic gene transcription. For these reasons *Drosophila* is a well-suited organism to study the dynamics of mitotic spindle assembly and activity.

Immunostaining of wild-type early embryos showed that this machinery was properly arranged within individual mitotic domains in the syncytial embryo. In these embryos, nuclei were homogenously distributed along the surface and kinetochore microtubules, nucleated from the opposite poles of the spindle, helped chromosomes to congress and align to the metaphase plate (Figure 3-1).

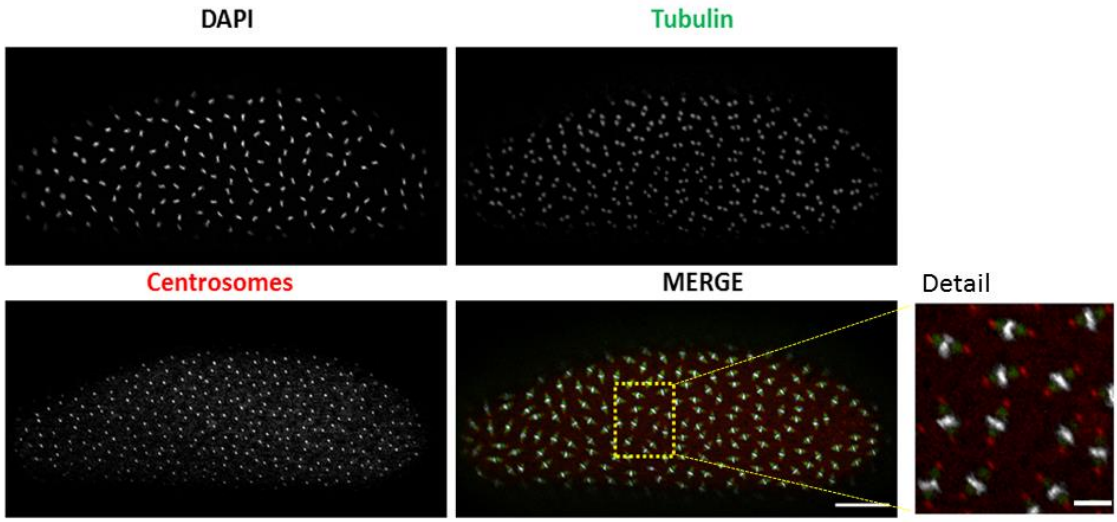

Figure 3- 1: Organisation of mitotic domains in a wild-type syncytial blastoderm embryo. In a wild-type *Drosophila* embryo, nuclei in the syncytium are evenly distributed through the surface of the embryo and divide synchronously during the first 13 cycles. At metaphase, chromosomes align to the cell equator and are stably bound to the fibres of a bipolar mitotic spindle. Detail shows the organisation of adjacent mitotic domains. Nuclei are stained with DAPI (grey), tubulin is in green and centrosomes in red. Scale bar represents 50 µm; scale bar of the detail represents 10 µm.

Given its requirement for cell division in tissue culture cells, we assumed that Spindly also functions in cell divisions in the context of a living organism.

To investigate whether Spindly controls mitotic progression through the syncytial divisions, the shRNA transgene targeting *spindly* mRNA was expressed during oogenesis using either the *nanos*>Gal4 or the maternal *alpha tubulin 67c*>Gal4 driver lines, for which a differential pattern of expression has been reported (Figure 3-2). Indeed, the gene *nanos* is highly expressed in the dividing cystoblast, within the germarium (Lehmann 1998) while the maternal α-tubulin 67C is expressed in egg chambers at stage 2 of development onwards (Matthews, Miller et al. 1989) (Figure 3-2).

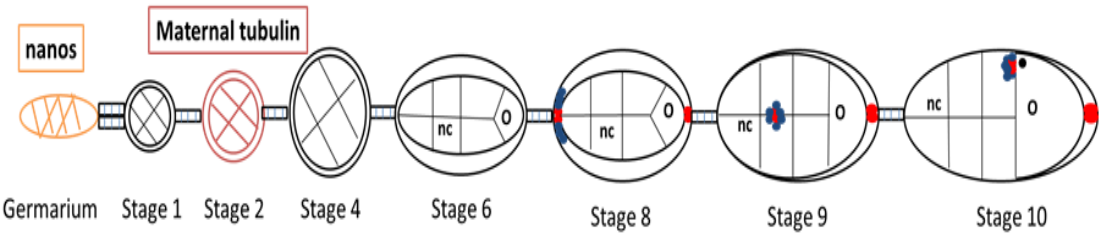

Figure 3- 2: Expression domains of *nanos* and *alpha tubulin 67c* during *Drosophila* oogenesis. The image is a schematic representation of a *Drosophila* ovariole showing the germarium and a linear array of egg chambers at increasing stages of development. The expression domains of *nanos* and *alpha tubulin 67c* are depicted. *nanos* is expressed precociously in the germarium (domain in orange; Forbes and Lehmann 1998) while α-tubulin 67C is expressed starting from stage 2 throughout egg-chamber development (domain in red; Matthews KA et al. 1989). Polar cells are shown in red are, border cells in blue. O: oocye; nc: nurse cells. For details about border cells specification and migration refer to introduction and chapter 5.

This chapter will describe the establishment of a Spindly loss-of-function background in early embryos and will describe the effects of Spindly depletion on embryo survival and syncytial embryonic development.

3.1.1. Generation of loss-of-function phenotype by mRNA knockdown

To unravel the activity of Spindly during the syncytial nuclear divisions, a conditional knockdown approach based on RNAi technology was adopted. Firstly, the expression of the shRNA was driven in the female germline by using the *maternal* alpha-*tubulin>Gal4* driver.

An important requirement to investigate the effects of Spindly depletion on *Drosophila* embryogenesis and score for loss-of-function phenotypes was to test the efficacy of the transgenic RNAi. Western blot analysis was performed to determine variations in Spindly protein levels in lysates from 0-3 hour embryo collections. The analysis revealed a marked reduction in the levels of Spindly protein at any of the temperatures

tested (Figure 3-3, S2), suggesting that the driver used was effective in causing the RNAi-dependent depletion of the protein encoded by the targeted mRNA.

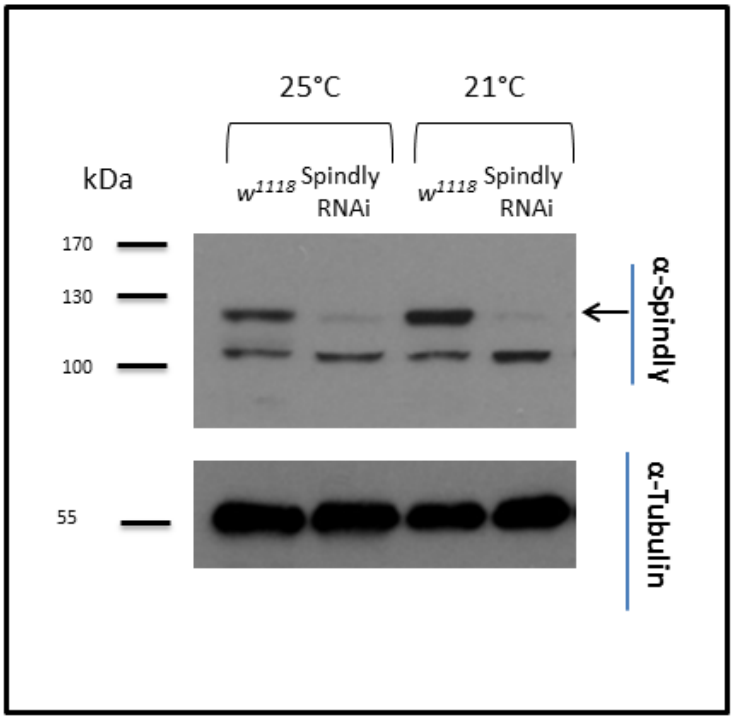

Figure 3- 3: Efficiency of Spindly knockdown. Western blot analysis shows Spindly knockdown in early *Drosophila* embryos. Protein lysates were collected from 0-3 hour wild-type (w^{1118}) and *mat67*>Gal4; *UAS*>$Spindly^{Valium20}$ (Spindly-RNAi) embryos and run on a SDS-PAGE gel. Egg collection was performed at different temperatures: 25°C and 21°C. Membranes were probed for Spindly using an affinity-purified antibody raised against the C-terminal half of the protein. α-Tubulin was included as loading control. For a precise molecular weight determination, a standard protein molecular weight marker was used and numbers in kDa are shown on the left. Images are representative of two biological replicates.

To establish to what extent the depletion of Spindly affects completion of embryogenesis, the survival rate of the embryos upon RNAi treatment was determined by calculating the number of embryos able to hatch into larvae. Development of Spindly-RNAi embryos was strongly compromised and the survival rate ranged between 0% and 7% depending on the temperature tested (Figure 3-4).

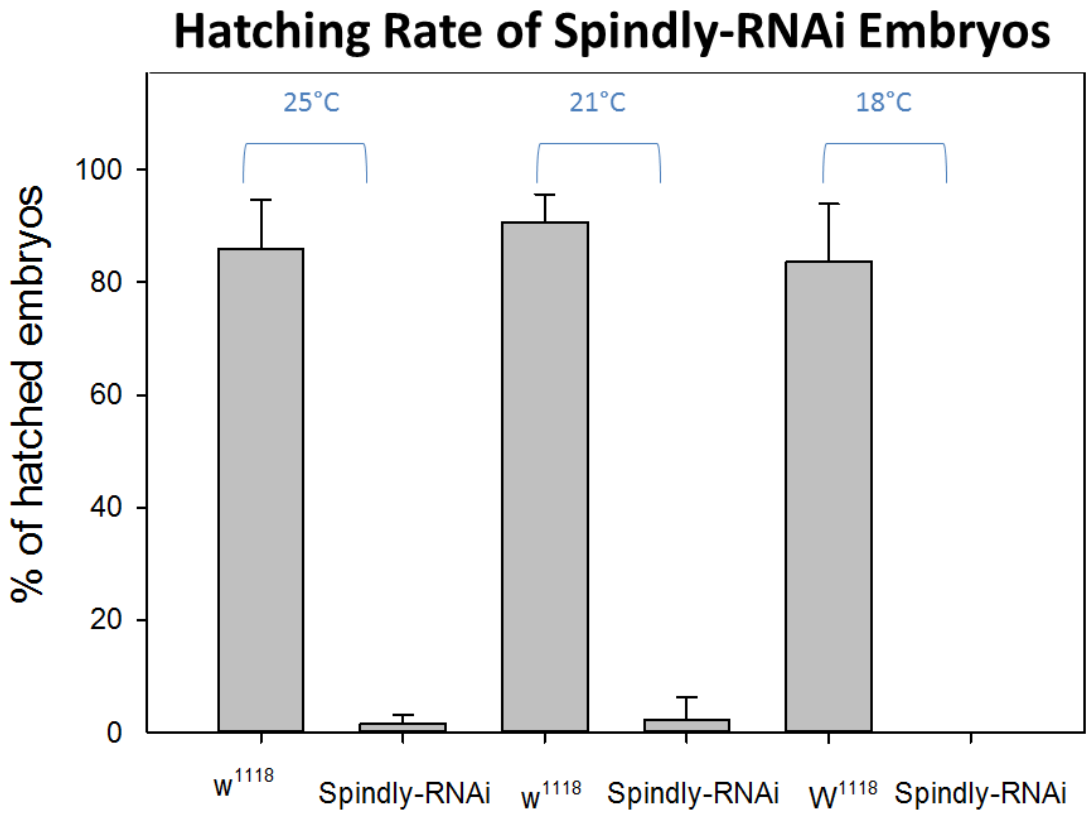

Figure 3- 4: Embryo viability upon maternal *spindly* RNAi. The survival rate of embryos is estimated by monitoring the ability of *mat67*>Gal4; *UAS*>*Spindly*^{Valium20} embryos to hatch as first instar larvae. Knockdown of Spindly causes a high rate of embryonic lethality at any of the three temperatures tested. Results represent the average of three independent technical replicates.

To examine whether the observed embryonic lethality was based upon defects during syncytial mitotic cycles, imaging of fixed preparations of 0-3 hour old embryos was performed and the defects in syncytial divisions were scored by counting the number of embryos that arrest early in embryogenesis before cellularisation. 83% Spindly-RNAi embryos were markedly impared in the completion of syncytial cleavage divisions, suggesting an arrest of development after a few rounds of mitotic divisions (Figure 3-5).

Specifically, the majority of the embryos arrested during metaphase of the first 1–3 mitotic divisions. In 40% of the embryos (n=30), only a single metaphase-arrested nucleus was present within the egg whereas only in 13% of the cases examined

embryos had a variable number of 2 to 4 mitotic spindles. Our ability to find a polar body rosette in 46.6% of these embryos suggested that meiosis was able to resume and complete (Figure 3-6).

Phenotypes observed by RNAi experiments can be subject to so-called “off-target effects” (OTEs) caused by unintended downregulation of genes other than the targed gene that share sequence homology with the target gene. The high frequency of OTEs in *Drosophila* RNAi screens often leads to the identification of false positive hits. To verify the specificity of the phenotypes observed upon depletion of *spindly* mRNA we sought to conduct a rescue experiment. To this end an RNAi-resistent construct was generated that encodes for a GFP-tagged full-length version of Spindly in which the shRNA target site was mutated without changing the primary sequence of the polypeptide. The specificity of the RNAi was confirmed by measuring the survival rate of embryos derived from crosses that would produce 75% of progeny expressing RNAi-resistent GFP-Spindly in a Spindly-depleted background. A selected number of fertilised eggs were collected and allowed to hatch. The overexpression of the GFP-tagged transgene restored viability to wild-type levels (Figure 3-7, rescue). As a control, a GFP-tagged version of the histone protein 3 (H_3) was overexpressed in embryos knocked down for the endogenous Spindly. This GFP-tagged construct did not exhibt any rescueing activity, confirming that the RNAi machinery targeted selectively *spindly* mRNA (Figure 3-7, UAS>H3GFP).

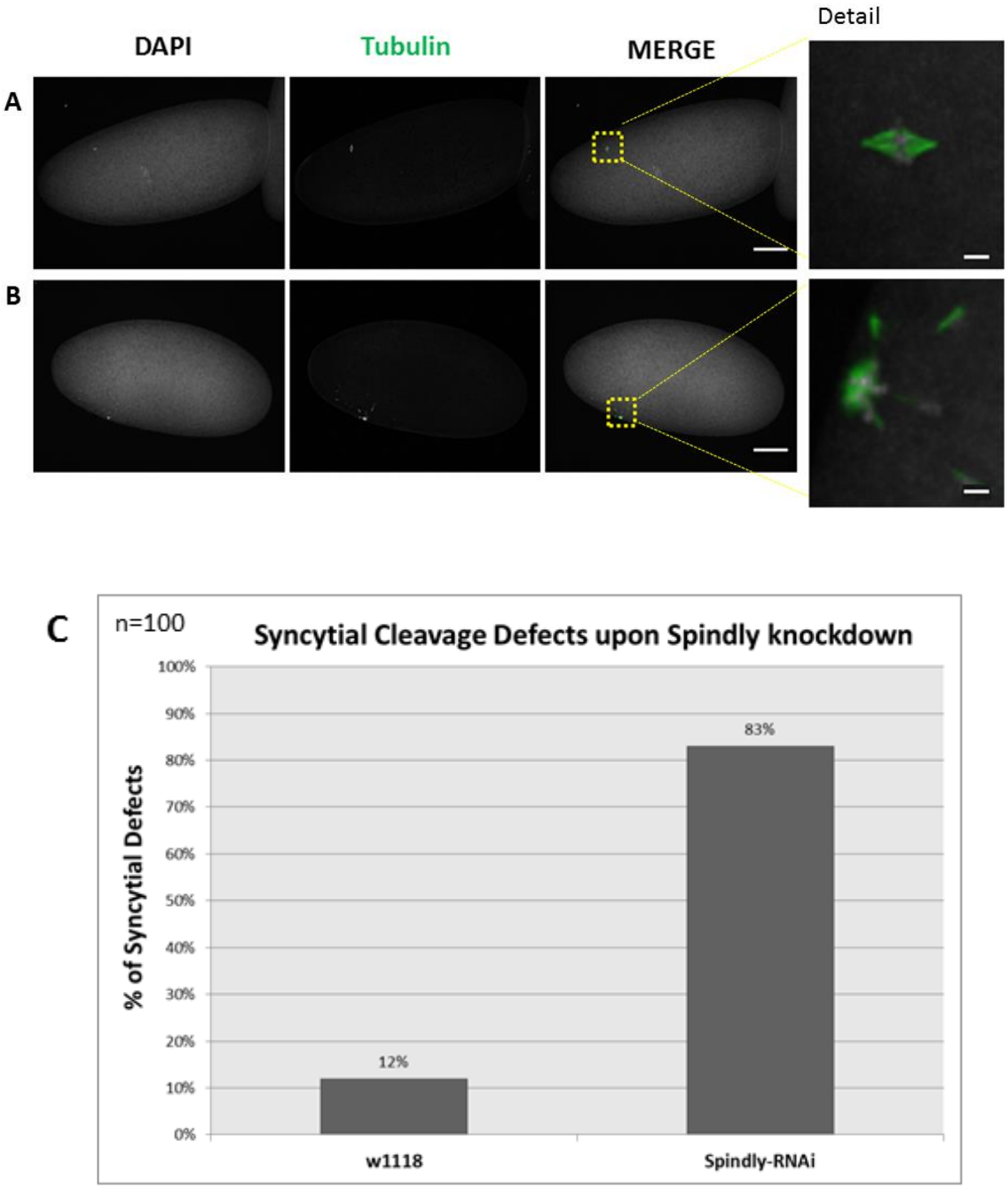

Figure 3- 5: Spindly-RNAi embryos show marked syncytial division defects. A) Representative images of Spindly-RNAi embryos. The images are maximum-intensity projection of a 10 µm stack. Z-stacks were acquired at a spacing of 1 µm. Spindly-RNAi embryos collected at 25°C arrest early in embryogenesis and fail to progress through the first mitotic divisions of the pre-blastoderm stage. Embryos normally arrest with a single metaphase-arrested nucleus (A). In some cases a polar body rosette is visible (B). Nuclei are stained with DAPI (grey), microtubules are in green. Scale bar represent 50 µm; Details: 5 µm C) Quantification of the phenotype described in (A). Spindly-RNAi embryos show severe syncytial defects, arresting early in embryogenesis before cellularisation (n=100).

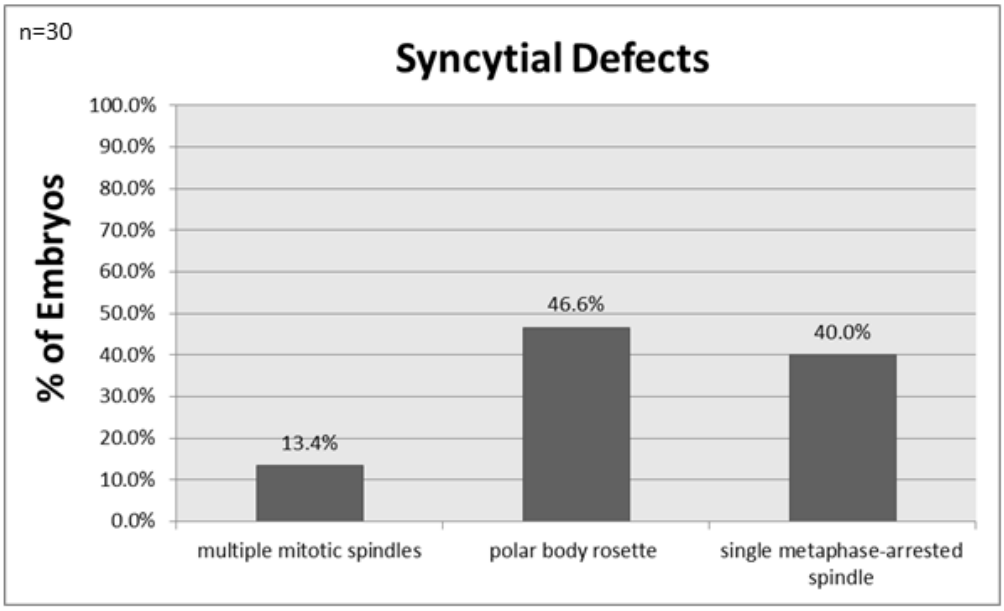

Figure 3- 6: Quantification of syncytial cleavage defects upon Spindly knockdown. Immunostaining of Spindly RNAi embryos allowed the identification of a variety of mitotic abnormalities that fall into distinct phenotypic classes. 0-3-hour-old Spindly-RNAi embryos typically arrested with a single nucleus (40%, n=30). In 46.6% of the cases examined it was possible to identify only the polar body rosette. Finally, a small percentage of the embryos arrested after few rounds of divisions with 2 to 4 mitotic spindles.

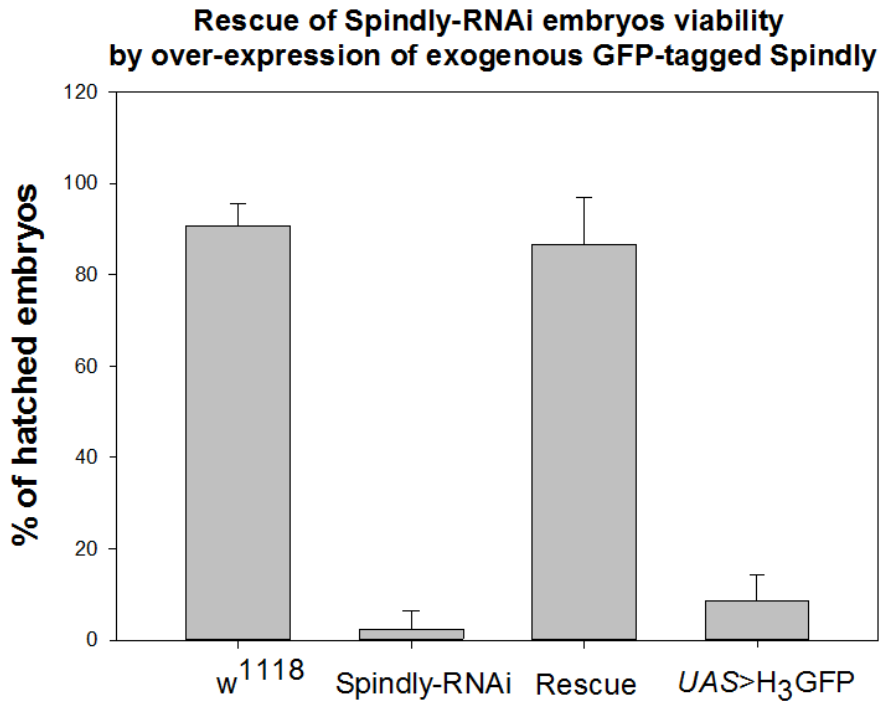

Figure 3- 7: Rescue of the viability of Spindly-RNAi embryos. Exogenous expression of a GFP-tagged version of Spindly in a Spindly-RNAi background restored the viability of *Drosophila* embryos to wild-type levels (86%, n=100). Conversely, Spindly-RNAi embryos overexpressing GFP-tagged histone protein 3 (*UAS*>H_3-GFP) are unable to hatch as first instar larvae (9%, n=100). Results represent the average of three technical replicates.

The RNAi experiments performed demonstrat that maternal downregulation of *spindly* results in embryonic lethality. However, the analysis did not give any insights as to the processes that require Spindly during syncytial cleavages. To address this problem, the same set of experiments was performed inducing the expression of the shRNA transgene with the *nanos*>Gal4 driver. The second driver was equally effective in knocking down Spindly. Despite this, the analysis performed at different temperature showed that the system was remarkably temperature sensitive. The GAL/UAS system had highest activity at 25°/23°C: at these temperatures the most efficient depletion of the target protein was observed despite a small amount being still detectable (Figure 3-8 A and B). At 21°C, the knockdown of Spindly was less severe (Figure 3-8 B) and at 18°C the protein level remained similar to the control (Figure 3-8 C).

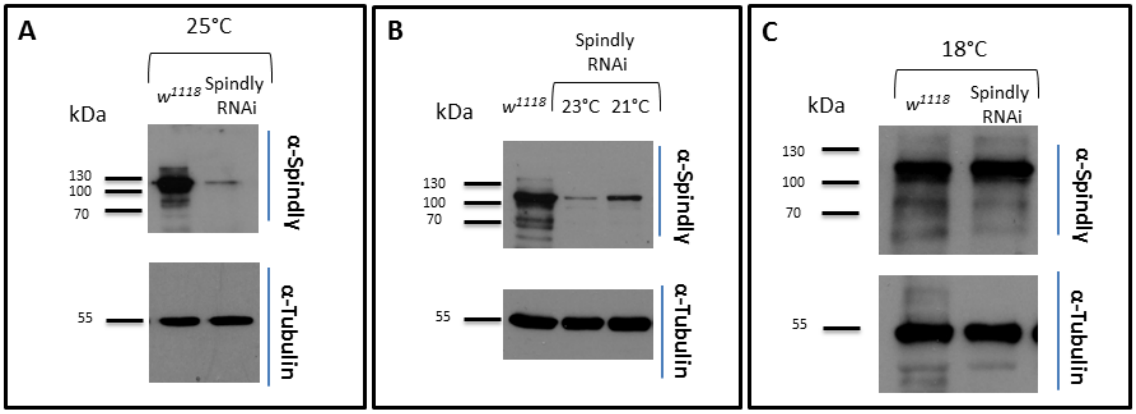

Figure 3- 8: Efficiency of Spindly knockdown. Western blot analysis shows Spindly knockdown in early *Drosophila* embryos. Protein lysates were collected from 0-3 hour wild-type (w^{1118}) and Spindly-depleted embryos, run on a SDS-PAGE gel and blotted onto nitrocellulose membrane. Egg collection was performed at different temperatures: 25°C, 23°C 21°C and 18°C. Membranes were probed for Spindly using an affinity-purified antibody raised against the C-terminal half of the protein. α-Tubulin was included as loading control. For molecular weight determination, a standard protein molecular weight marker was used and numbers in kDa are shown on the left. The images are representative of three independent biological replicates with the exception of the analysis at 21°C that was performed once.

For each condition tested, the survival rate of embryos upon maternal RNAi was determined. In agreement with the previous results, the development of Spindly-depleted embryos was significantly compromised. When the RNAi was performed at

23°C, only 16% of embryos were able to hatch compared to the wild-type. Survival of Spindly-RNAi embryos improved when eggs were raised at 21°C (Figure 3-9). Thus, assessment of embryo viability was consistent with the Western Blot data. Immunostaining of embryos were performed at either 23°C or 21°C to further analyse what caused the severe lethality observed. DAPI staining of Spindly-RNAi embryos and quantification of syncytial cycle defects were consistent with a requirement for Spindly in normal embryonic development (Figure 3-10).

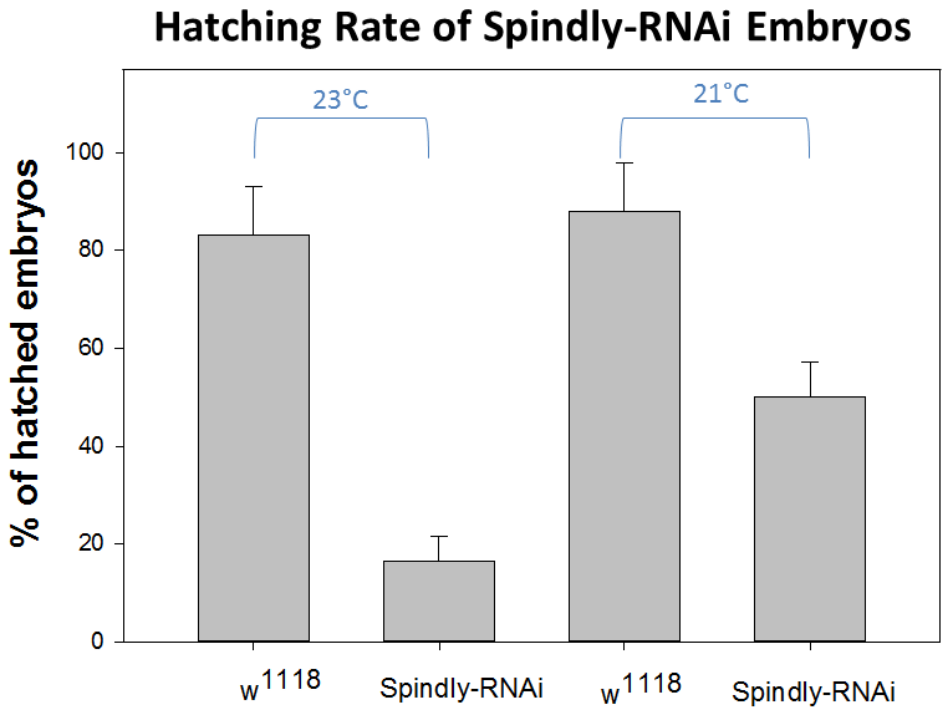

Figure 3- 9: Determination of embryo viability upon maternal *spindly* RNAi. The survival rate of embryos was estimated by monitoring the ability of *nanos*>Gal4; *UAS*>Spindly^{Valium20} embryos to hatch as first instar larvae. Knockdown of Spindly caused marked embryonic lethality at any of the two temperatures tested, 23°C and 21°C respectively. Results represent the average of three independent technical replicates. For each replicate, 100 embryos were used to assess the hatching.

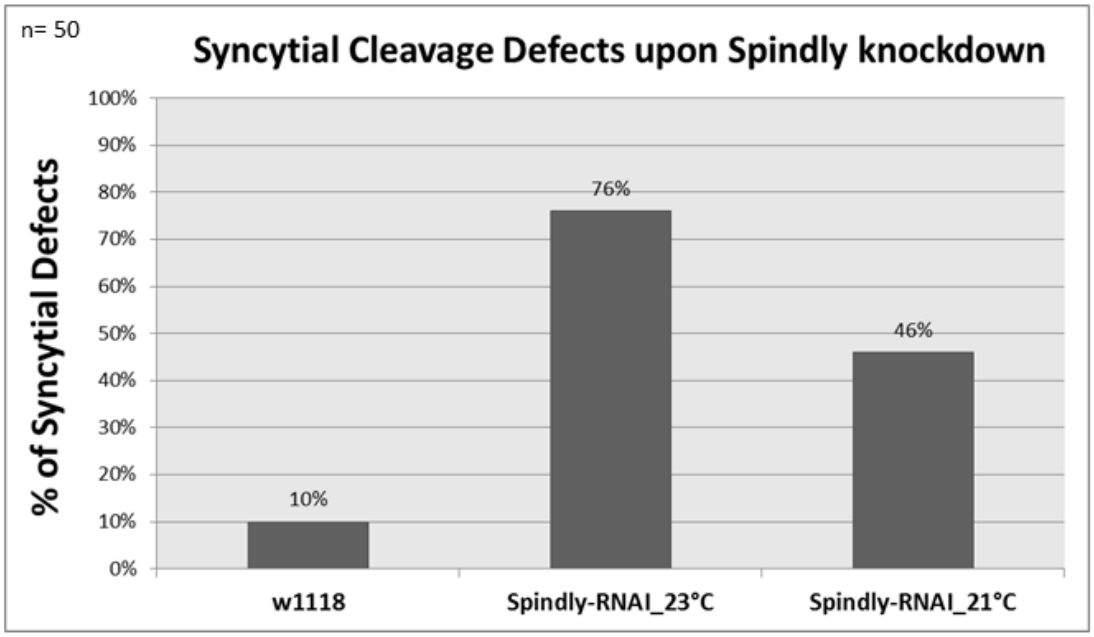

Figure 3- 10: Measurement of syncytial defects after Spindly knockdown. *nanos*>Gal4; *UAS*>Spindly^{Valium20} embryos show remarkable defects in embryonic development, arresting their development early in embryogenesis before cellularisation.

3.1.2. Analysis of mitotic defects caused by severe downregulation of Spindly.

To investigate the function of Spindly in mitosis, fluorescent microscopy of fixed early embryos was performed to study the effects of Spindly loss-of-function in terms of nuclei distribution, centrosome positioning and mitotic spindle morphology. Staining of Spindly-RNAi embryos raised at 23°C unequivocally demonstrated that the knockdown of Spindly impaired normal syncytial development; the majority of the embryos arrested early in embryogenesis before cellularisation (76% n=50), compared to the control (10%) (Figure 3-10). Using this approach it was possible to identify a variety of abnormalities and mitotic defects (Figure 3-11).

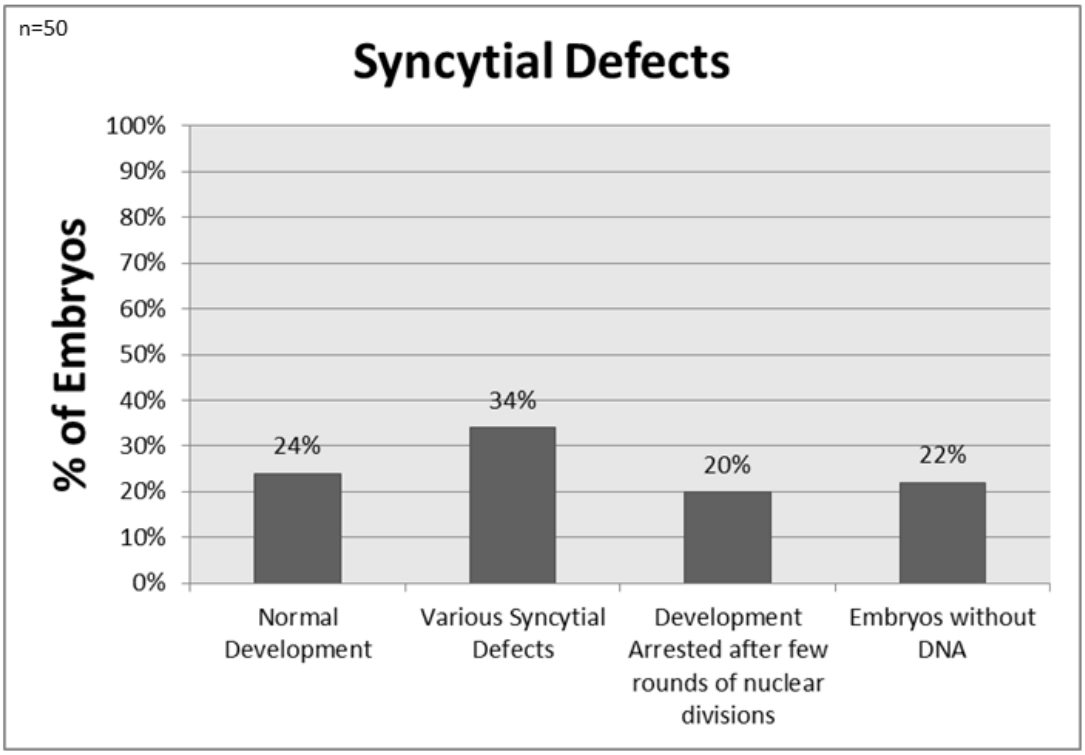

Figure 3- 11: Quantification of syncytial cleavage defects upon Spindly knockdown at 23°C. Immunostaining of *nanos*>Gal4; *UAS*>Spindly^{Valium20} embryos collected at 23°C allowed the identification of a variety of mitotic abnormalities that fall into distinct phenotypic classes. 76% of the embryos failed to complete the early stages of embryonic development (n=50). Of these embryos, 22% did not show any DAPI staining while 20% arrested their development after few rounds of mitotic divisions. Finally, 34% of Spindly-RNAi embryos showed defects in nuclei distribution, spindle assembly and centrosome positioning.

Of all embryos, 22% did not show any DAPI staining while 20% arrested development after a few rounds of mitotic cycles. Of this latter category, 10% of the embryos were characterised by patches of disorganised chromatin associated with multiple centrosomes (Figure 3-12 A and B).

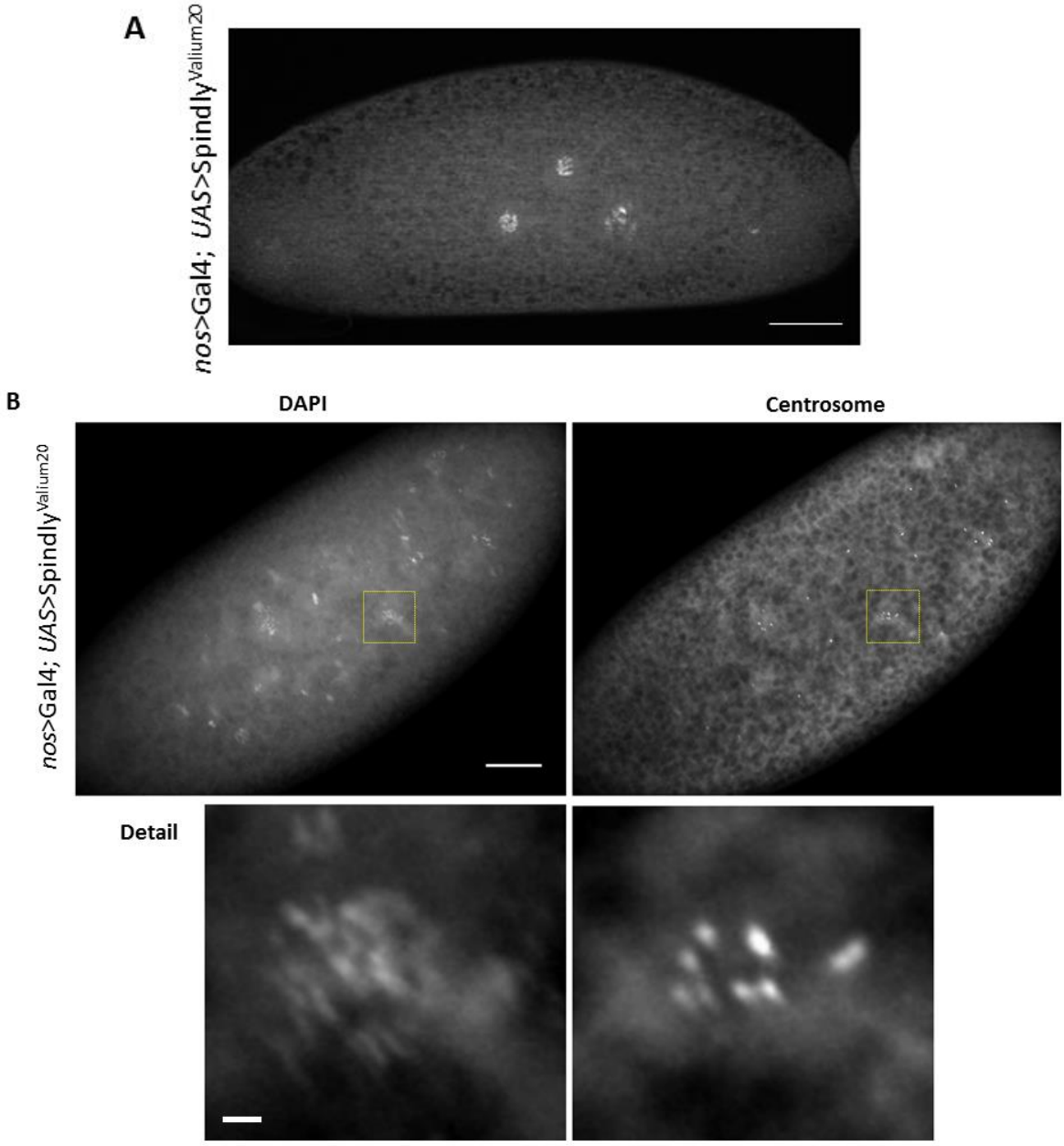

Figure 3- 12: Spindly-depleted embryos arrest their development after few rounds of mitotic divisions. Downregulation of Spindly significantly affects normal progression through the syncytial cycles (A). Embryos are not able to sustain repeated cycles of nuclear divisions and arrest early their development with patches of disorganised chromatin occasionally associated with multiple centrosomes (B). RNAi of Spindly was performend at 23°C and was driven by the *nanos*>Gal4 maternal driver. Nuclei were stained with DAPI. Scale bars represent 50 µm in (A) and (B). Scale bar of the detail represents 10 µm.

Distinct from wild-type embryos, nuclei were unequally distributed throughout the surface of the embryos and the regular spacing of the mitotic domains typical of the wild-type condition was lost (Figure 3-13 A). Frequently, the normal organisation of the mitotic spindle was compromised and condensed chromatin was found associated with patches of tubulin (12%, n=50; Figure 3-13 B).

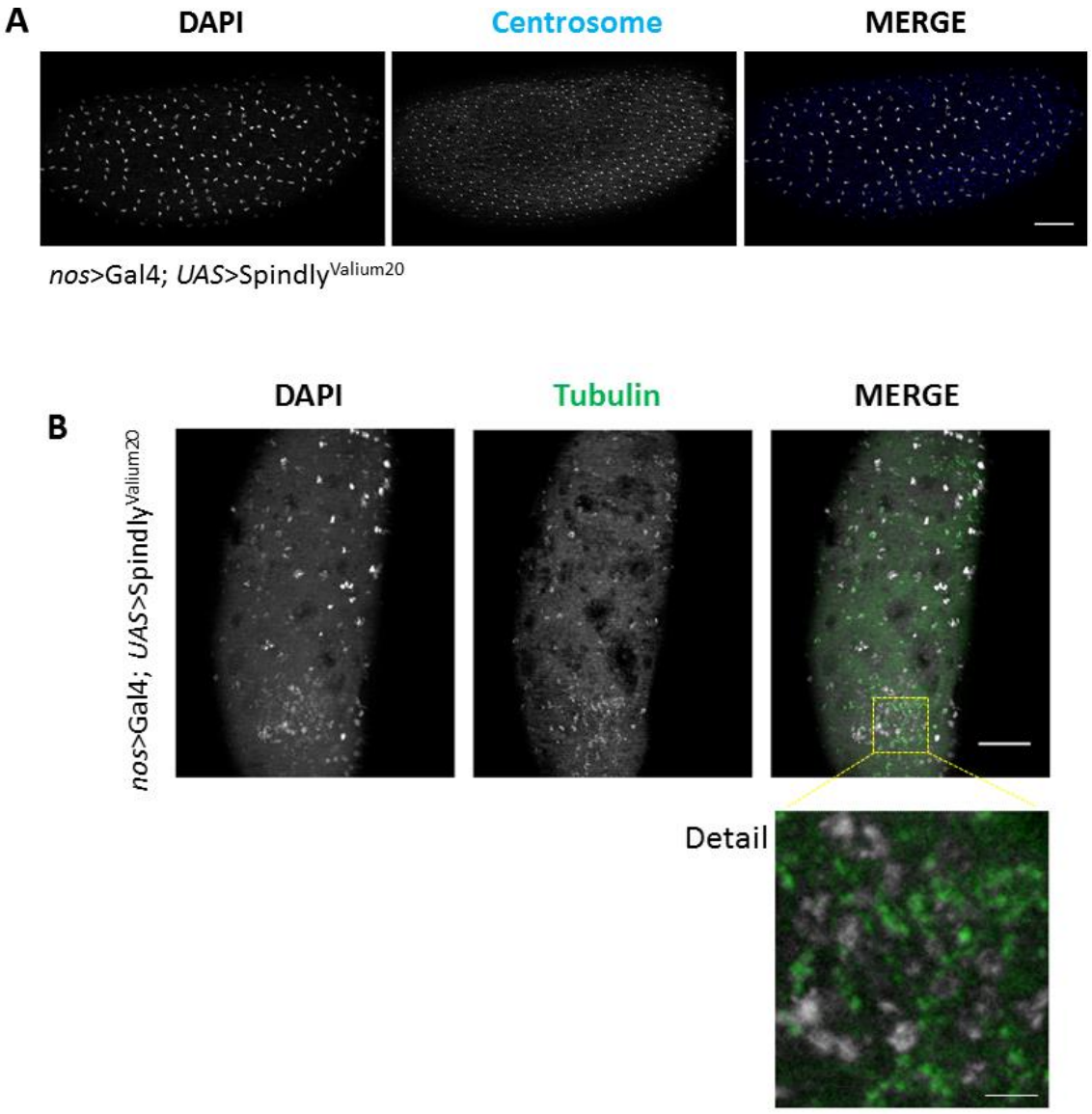

Figure 3- 13: Knockdown of Spindly causes uneven distribution of nuclei and high level of disorganisation of the microtubule cytoskeleton. Representative images of syncytial blastoderm *nanos*>Gal4;*UAS*>Spindly^{Valium20} embryos collected at 23°C. (A) Depletion of Spindly significantly affects the regular distribution of the nuclei along the A/P axis of the embryos. (B) Example of Spindly-depleted embryo in which condensed chromatin was associated with patches of tubulin. A detail from the yellow dashed box in figure (Merge) is shown separately. Nuclei were stained with DAPI (grey), tubulin is in green, centrosomes in blue. Scale bars represent 50 µm in (A) and (B). Scale bar of the detail represents 10 µm.

Furthermore, in 4% of the cases examined, areas characterised by different rates of mitotic activity were observed within the same embryo. Particularly, it was possible to identify regions enriched in interphase nuclei and others in which nuclei were actively dividing (Figure 3-14).

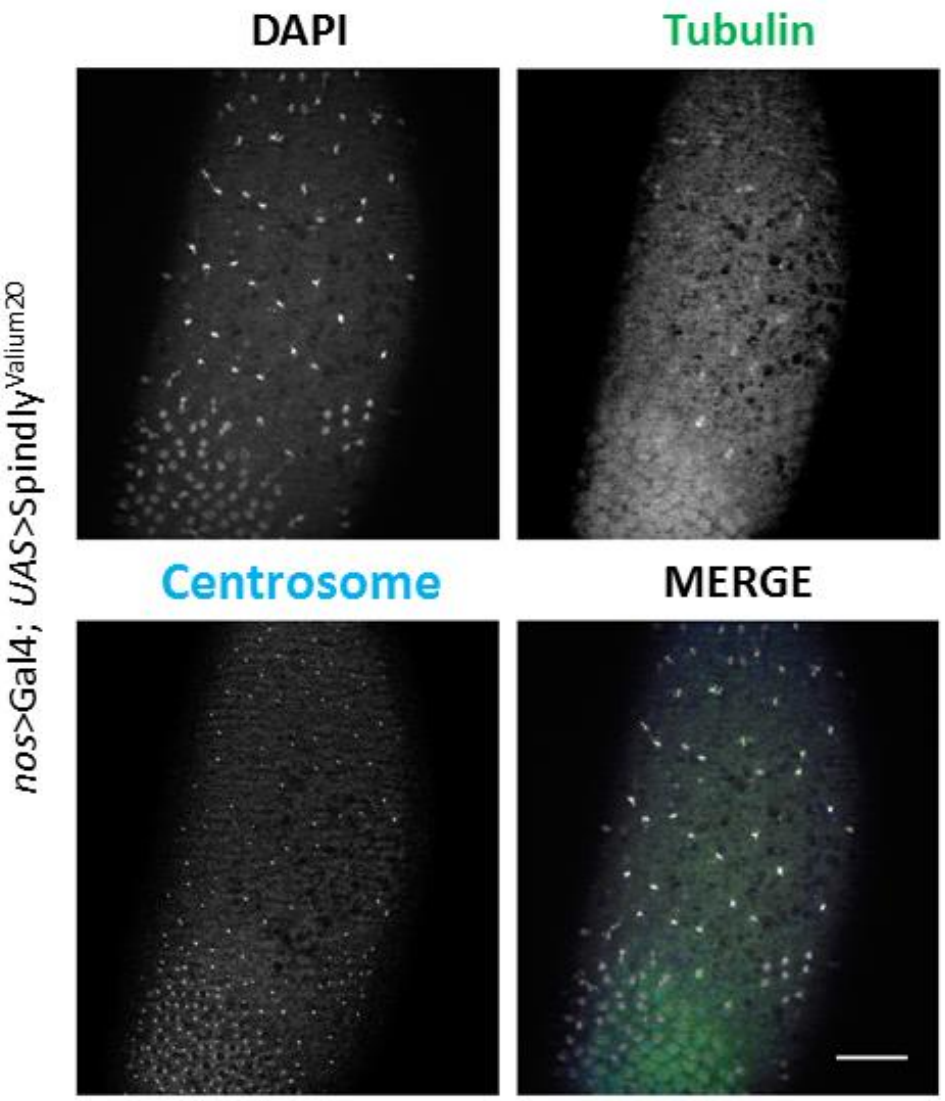

Figure 3- 14: Knockdown of Spindly results in asynchrony in the mitotic divisions. Representative images of syncytial blastoderm *nanos*>Gal4;*UAS*>Spindly^{Valium20} embryos collected at 23°C. Depletion of Spindly disrupts the synchrony of the syncytial cleavages. A gradient of differential mitotic rate is observed along the A/P axis of the embryos. Areas of active mitotic divisions are easily discernible from areas enriched in interphase nuclei (4%, n=50). Nuclei were stained with DAPI (grey), Tubulin is in green, Centrosomes in blue. Scale bar represents 50 µm.

Embryos arrested at slightly later division cycles stages exhibited multiple defects (12%, n=50). Highly disorganised patches of chromatin were unevenly distributed throughout the cortical cytoplasm of the embryos and the microtubule cytoskeleton was only occasionally organised into a bipolar mitotic spindle. In addition, free centrosomes were detected as individual centrosomes randomly dispersed along the A/P axis (Figure 3-15).

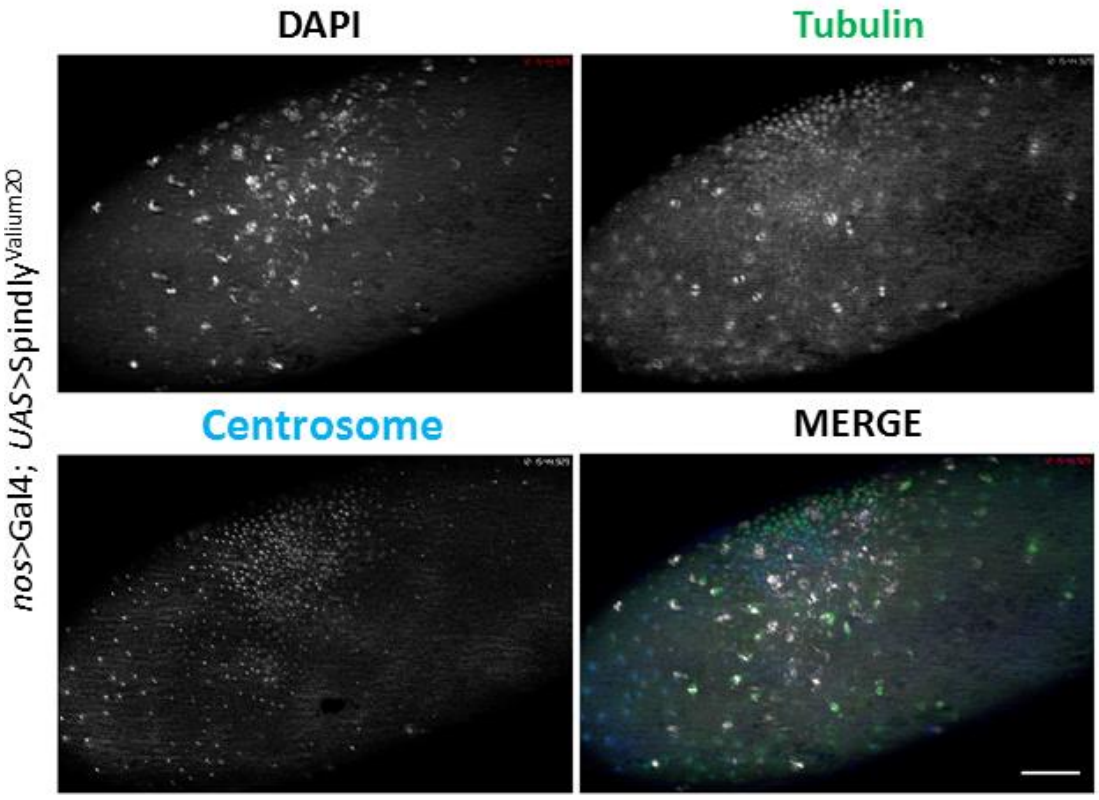

Figure 3- 15: Spindly-RNAi embryos accumulate a variety of mitotic defects at later stages of embryonic development. Representative images of syncytial blastoderm *nanos*>Gal4; *UAS*>Spindly^{Valium20} embryos collected at 23°C. Embryos that reach later stages of development are highly disorganised. The characteristic even distribution of mitotic domains is hardly detectable. Patches of highly condensed chromatin associate with disorganised tubulin and rarely the microtubule cytoskeleton is arranged in a functional bipolar spindle. Free centrosomes are detectable as individual entities throughout the surface. This phenotypic class is observed in 12% of the cases examined (n=50). Nuclei were stained with DAPI (grey), tubulin is in green, centrosomes in blue. Scale bar represents 50 µm.

3.1.3 Moderate levels of Spindly downregulation result in a variety of mitotic defects

Analysis of Spindly protein levels in whole-embryo lysates by Western Blot confirmed the temperature-sensitive nature of the Gal4-UAS system upon which the TRIP technology relies. Indeed, since the system is highly flexible, it was possible to obtain a different level of expression of the shRNA transgene simply by varying the temperature. This is therefore similar to different strengths of loss-of-function mutations ranging from hypomorphic to amorphic mutations. At 21°C, the downregulation of Spindly was less pronounced (Figure 3-8) and this resulted in a significant improvement in the fitness of the embryos with 50% of them able to hatch as larvae (Figure 3-9). Therefore, the effects of milder depletion of Spindly on syncytial nuclear divisions were investigated by imaging Spindly-RNAi embryos stained for microtubules and centrosomes. 46% (n=50) of all embryos displayed syncytial defects (Figure 3-10) that were classified in distinct phenotypic classes (Figure 3-16).

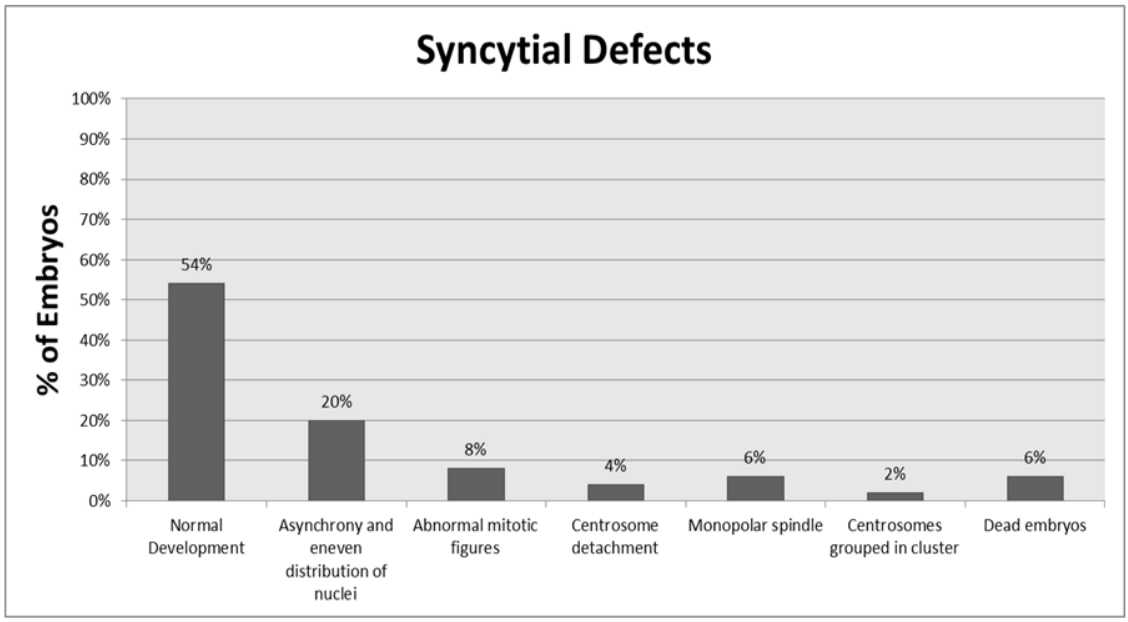

Figure 3- 16: **Quantification of syncytial cleavage defects upon Spindly knockdown at 21°C.** Immunostaining of *nanos*>Gal4; *UAS*>Spindly^{Valium20} embryos collected at 21°C allowed the identification of a variety of mitotic abnormalities that fall into distinct phenotypic classes. 46% of the embryos failed to complete the early stages of embryonic development (n=50). Spindly-RNAi embryos display a variaty of mitotic defects ranking from uneven spacing of the mitotic

domains and asynchrony of the nuclear divisions, to defects in mitotic spindle activities and centrosome attachment.

1) Asynchrony of mitotic divisions and uneven spacing of nuclei. Knockdown of Spindly affected the synchrony of the syncytial divisions. This defect resulted in domains characterised by different rates of mitotic activity within the same embryo. The synchrony of the divisions was impaired and only specific areas of the embryos were enriched in nuclei that were actively dividing. Additionally, nuclei seemed to be unevenly spaced through the surface (Figure 3-17).

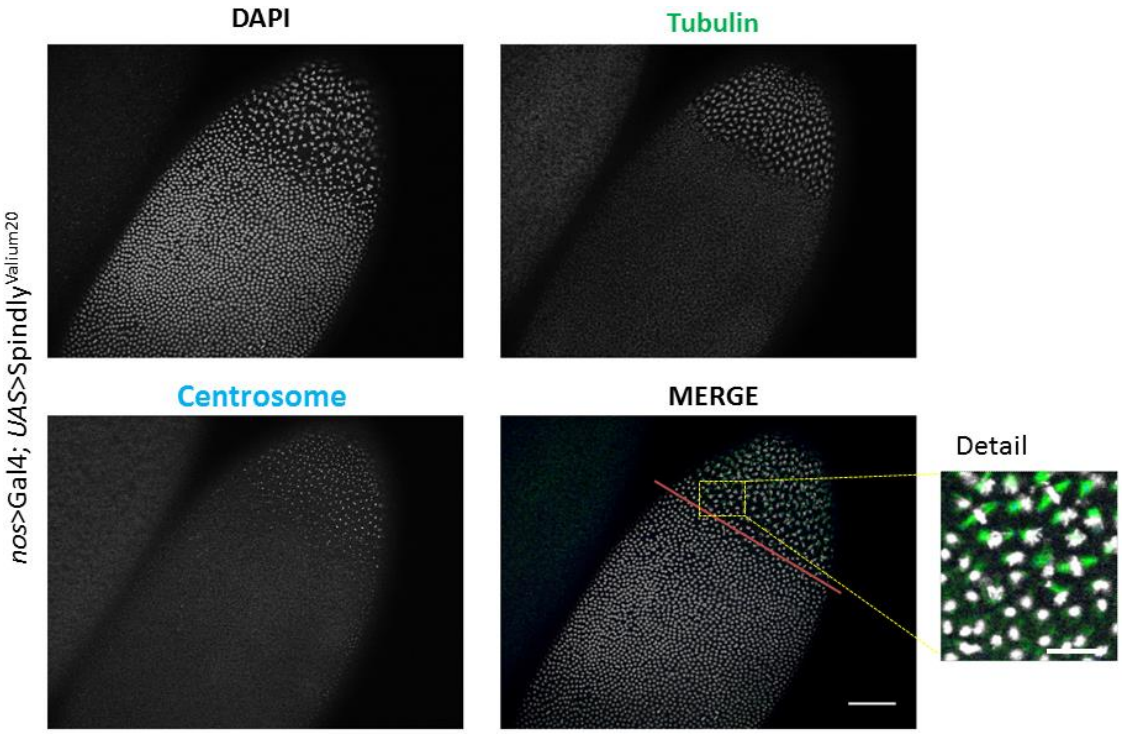

Figure 3- 17: Downregulation of Spindly breaks the synchrony of the mitotic divisions and affects the regular distribution of nuclei along the A/P axis of the embryo. The image is an example of a *nanos*>Gal4;*UAS*>Spindly^{Valium20} syncytial blastoderm embryo in which domains characterised by different mitotic rate are visible. Embryo collection was performed at 21°C. The red line in figure defines the boundary between a region enriched in interphase nuclei and a region in which active mitotic divisions occur. Additionally, the two domains seem to differ in term of nuclear density. A detail from the yellow dash box in figure (Merge) is shown separately. The detail shows a region of the embryos at the boundary between the two domains and contains nuclei in interphase as well as nuclei in metaphase. Nuclei are stained with DAPI (grey), tubulin is in green, centrosomes in blue. Scale bar represent 50 µm. Scale bar of the detail represents 10 µm.

2) Mitotic spindle defects. Microscopic analysis of mitotic spindle organisation in Spindly-RNAi embryos revealed the presence of severe mitotic spindle defects, resulting from the irregular spacing of the mitotic domains. Mitotic spindles stacked together, fusing into abnormal mitotic structures such as tripolar spindles (Figure 3-18).

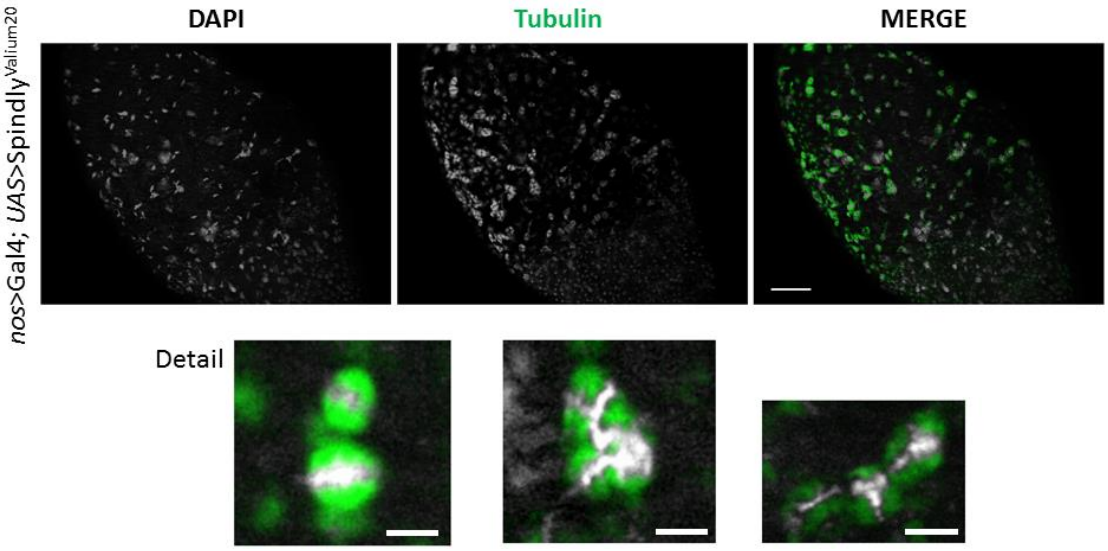

Figure 3- 18: The regular spacing between adjacent mitotic domains is compromised in a Spindly-RNAi background. Representative image of a syncytial blastoderm *nanos*>Gal4;*UAS*>Spindly^{Valium20} embryo at 21°C. Downregulation of Spindly disrupts the homogenous distribution of the mitotic domains through the surface of the embryos and results in mitotic spindles that collapse and fuse (Detail 1) originating abnormal microtubule-based structures associated with chromatin (Detail 2). Tripolar spindles are also observed (Detail 3). Details are from the dashed yellow boxes in figure (Merge). Nuclei are stained with DAPI (grey), tubulin is in green. Scale bar represent 50 µm. Scale bar of the details represent 5 µm.

3) Centrosome detachment and overduplication. An additional phenotype observed in fixed preparations of embryos in which the expression of Spindly was reduced by RNAi was the presence of centrosomes detaching from one or both spindle poles. In some cases, these free centrosomes were able to undergo reduplication, resulting in a pair of centrosomes associated with one or both poles (Figure 3-19). Loss of cohesion

between centrosomes and spindle poles resulted in the presence of free centrosomes dispersed throughout the surface of the embryos. Centrosomes were observed as individual entities or clustered in groups. In few cases, free centrosomes were able to enucleate microtubule fibres and give rise to monopolar spindles.

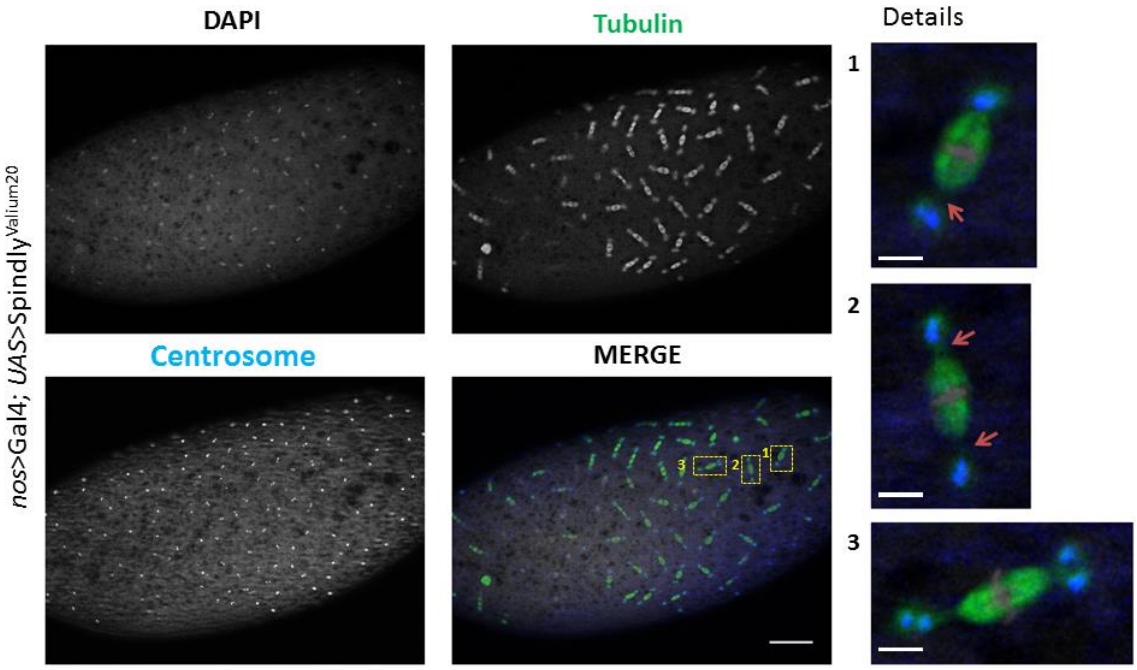

Figure 3- 19: Spindly is required for maintaining cohesion between centrosomes and spindle poles. Representative image of a syncytial blastoderm *nanos*>Gal4;*UAS*>Spindly^{Valium20} embryo at 21°C. Following depletion of Spindly, centrosomes are not tightly associated with the spindle poles and detach from one or both poles (Detail 2 and 3, respectively. Red arrows point to detaching centrosomes). Detached centrosomes initiate an extra cycle of duplication, resulting in a pair of centrosomes associated to a single spindle pole (Detail 1). Details are from a selected area of the figure marked with a dashed yellow box. Nuclei are stained with DAPI (grey), tubulin is in green, centrosomes in blue. Scale bar represent 50 µm. Scale bar of the details represent 5 µm.

3.1.4 Analysis of Spindly requirement in the control of the functional On-Off state of the SAC

Previous work in flies, worms and human cells led to the characterisation of a family of Spindly proteins that function as a dynein receptor at the kinetochore (Griffis, Stuurman et al. 2007, Gassmann, Essex et al. 2008, Chan, Fava et al. 2009). The *Drosophila* homologue of Spindly was the first to be identified and it was shown to be required for the dynein-dependent regulation of the level of SAC components at the kinetochore during the process of SAC silencing in cultured S2 cells (Griffis, Stuurman et al. 2007).

The loss-of-function analysis reported in this PhD thesis showed that Spindly plays a fundamental role in controlling syncytial cleavages during early *Drosophila* embryogenesis suggesting a function in the regulation of cytoskeletal components in mitosis as well as centrosome attachment and duplication. Despite the growing body of information, little is known about the protein structure and the functional roles and protein interactions of each individual protein domain. This limited knowledge clearly restricts our understanding of the function(s) of Spindly during cell division as well as the activity of the protein in other contexts. The characterisation of the different structural domains would therefore be beneficial to clarify how Spindly influences the molecular architecture of the kinetochore and to define the range of dynamic interactions that this protein establishes during mitosis.

Contrary to the other known protein homologues of the family, *Drosophila* Spindly is characterised by a long carboxy-terminal domain that contains a conserved, putative Mad-2 binding site close to its Carboxy-terminus (769-RIVVSSRKP-777). The identification of this consensus raised the question whether Spindly could have an

additional function in the control of the functional On-Off state of the mitotic checkpoint. In this regard, two alternative activities can be hypothesised: Spindly could either help to localise Mad-2 at the kinetochore, triggering the activation of the SAC, or it could contribute to MCC disassembly with similar mechanisms to $p31^{COMET}$. The first possibility suggests a novel function for *Drosophila* Spindly in the generation of the wait-anaphase signal in addition to its well-established role in kinetochore stripping. A similar activity has been reported for the *C. elegans* homologue SPDL-1 that was proved to interact with MDF-1, homologue of Mad-1, inducing the activation of the SAC (Yamamoto, Watanabe et al. 2008). Alternatively, Spindly would still contribute to mitotic checkpoint inactivation but it would participate in the process acting in multiple parallel pathways.

Despite these possibilities, it has not been shown whether the putative consensus for Mad-2 is functional. This section aims to verify biochemically whether a productive interaction between Spindly and Mad-2 occurs and if the motif identified is the binding site used.

3.1.4.1 Biochemical analysis of the interaction between Spindly and Mad-2

To test whether a direct interaction between Spindly and Mad-2 occurs and to verify whether the putative consensus for Mad-2 is functional, we aimed to compare the Mad-2 binding ability of a wild-type Spindly and a mutated version of the protein that lacked the Mad-2 binding site by performing *in vitro* binding assays. For this purpose, a series of constructs encoding Spindly proteins with deletions were expressed as Maltose Binding Protein (MBP)/6X-His-double tagged proteins and purified. The affinity-purified variants were then incubated with a wild-type Glutathione S-transferase (GST)-tagged Mad2 or with GST as control (Figure 3-20).

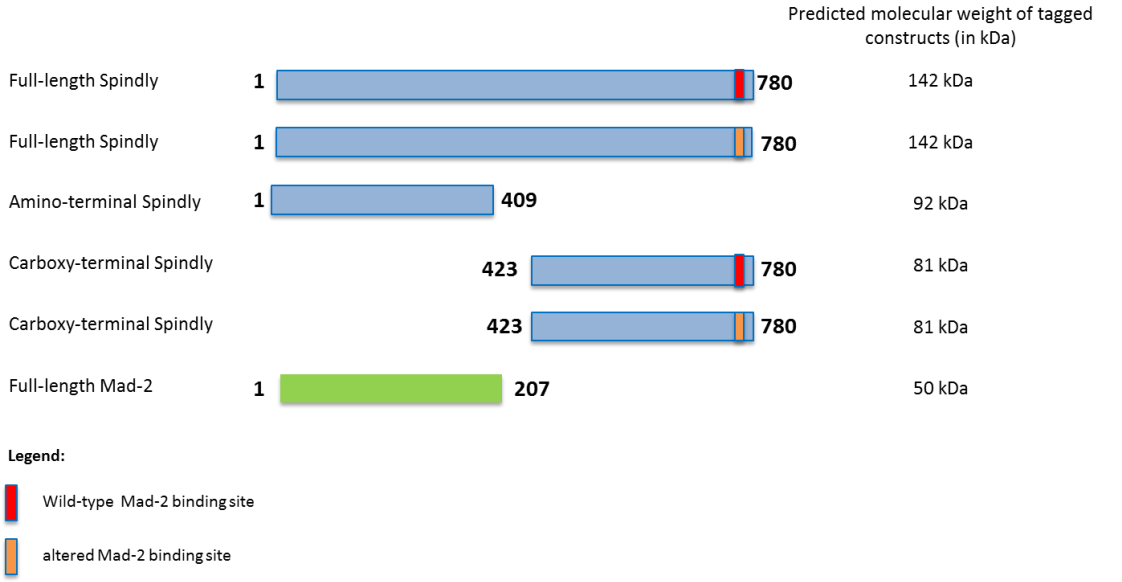

Figure 3- 20: *Drosophila* Spindly constructs to test the interaction with the SAC protein Mad-2. (A) Diagram of the *Drosophila* Spindly protein and a series of Spindly truncations cloned in the pLou3 vector. Two of the five constructs used in this study contain the mutation in the Mad-2 binding site (orange box), at conserved position 769-RIV-771. A wild-type full-lenght Mad-2 construct was cloned in the pGEX6-P1 vector. The predicted molecular weight of each tagged-protein is indicated on the right.

Following a period of incubation, the protein complexes were affinity-purified using a glutathione-covered chromatography matrix and Western blot analysis was performed to detect any resulting interaction. This set of experiments failed to reveal any binding activity of Spindly towards Mad-2, suggesting that the two proteins are unlikely to interact under the conditions tested (Figure 3-21).

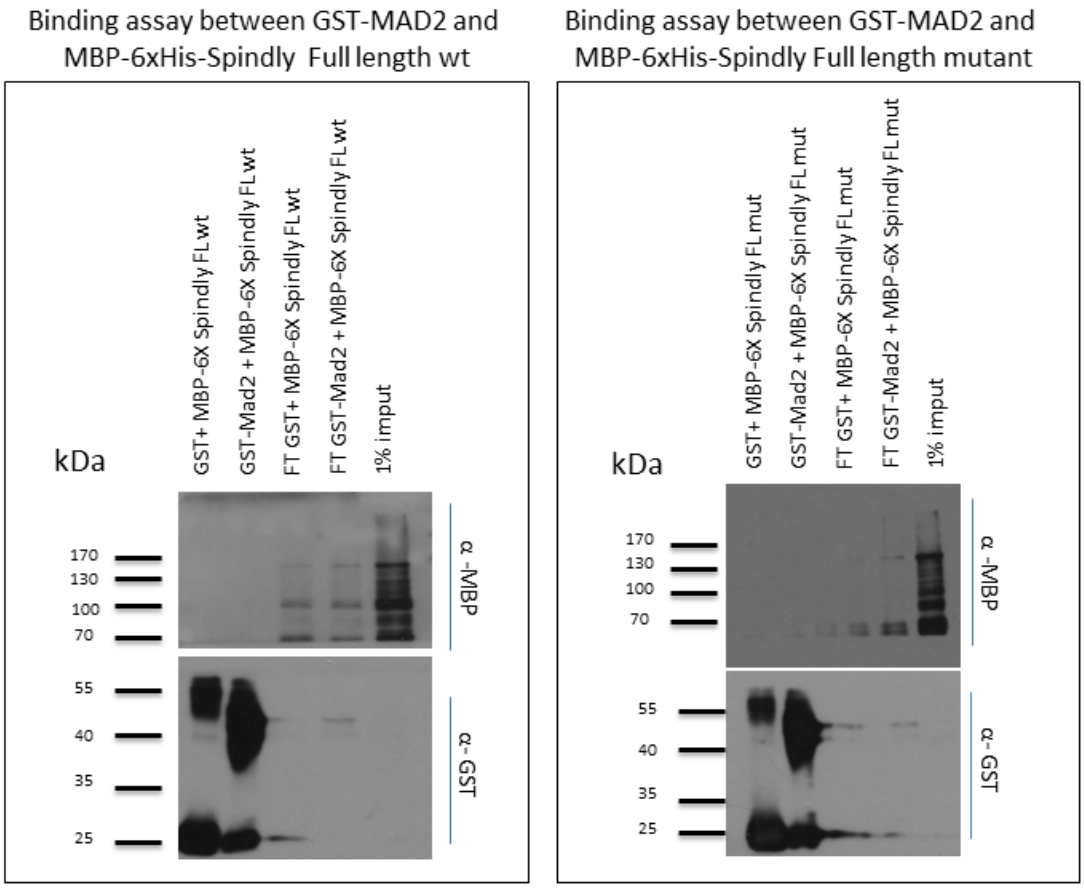

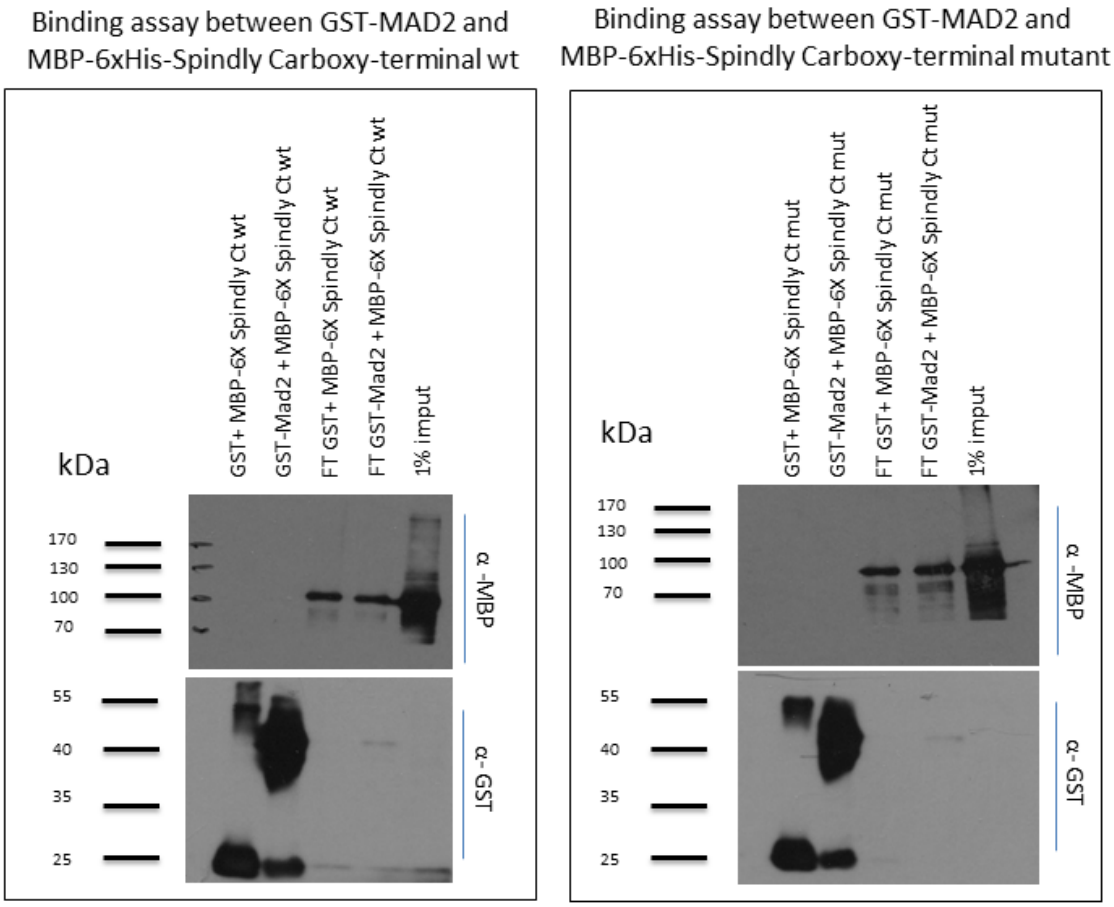

Figure 3- 21: Experiments to demonstrate interaction of Spindly with Mad-2 failed in vitro. The indicated Spindly variants were incubated with GST-Mad-2 or GST as control. After incubation, the putative protein complexes were immobilised on a Glutathione Sepharose matrix. Following extensive washes, bound proteins were resolved by SDS-PAGE. The images are representative of two independent experiments. A standard protein molecular weight marker is included and numbers in kDa are shown on the left.

These *in vitro* approaches do not necessarily exclude the possibility that these proteins interact *in vivo*. Therefore, in an alternative way to test the interaction between Spindly and its putative binding partner, co-immunoprecipitation experiments were performed. Wild-type 0-2-hour-old embryos were collected and lysed to isolate proteins. Since the ability of detecting a productive interaction between candidate proteins relies on the ability of precipitating the proteins of interest from embryo lysate, first the efficiency of the extraction method was tested by Western Blot. Aliquots of each fraction (pellet, input, unbound, immunoprecipitate) were collected

during the procedure and used for SDS-PAGE (Figure 3-22 A). To ensure that during the embryo lysis the proteins of interest were extracted and preserved in a soluble fraction, an aliquot of the pellet and the input samples were run on adjacent lane on a SDS-PAGE. The membrane was probed against Spindly and Mad-2 and the analysis confirmed the successful extraction of both proteins from the embryos (Figure 3-22 A and Figure 3-23 A). In addition, to estimate the efficiency of immunoaffinity isolation of the proteins of interest, we compared the amount of protein detected in the input (soluble fraction) with the amount of unbound protein following immune-precipitation (flow-through) (Figure 3-22 A and Figure 3-23 A).

Endogenous Spindly was isolated from the whole-lysate using an affinity-purified antibody raised against the carboxy-terminal portion of the protein. Western blot analysis was performed to confirm the efficient enrichment of Spindly following IP as well as to visualise the amount of co-precipitated Mad-2. The procedure described failed to identify a positive interaction between these two SAC players in early embryos (Figure 3-22 B). Similarly, reciprocal co-immunoprecipitation experiments also produced negative results (Figure 3-23).

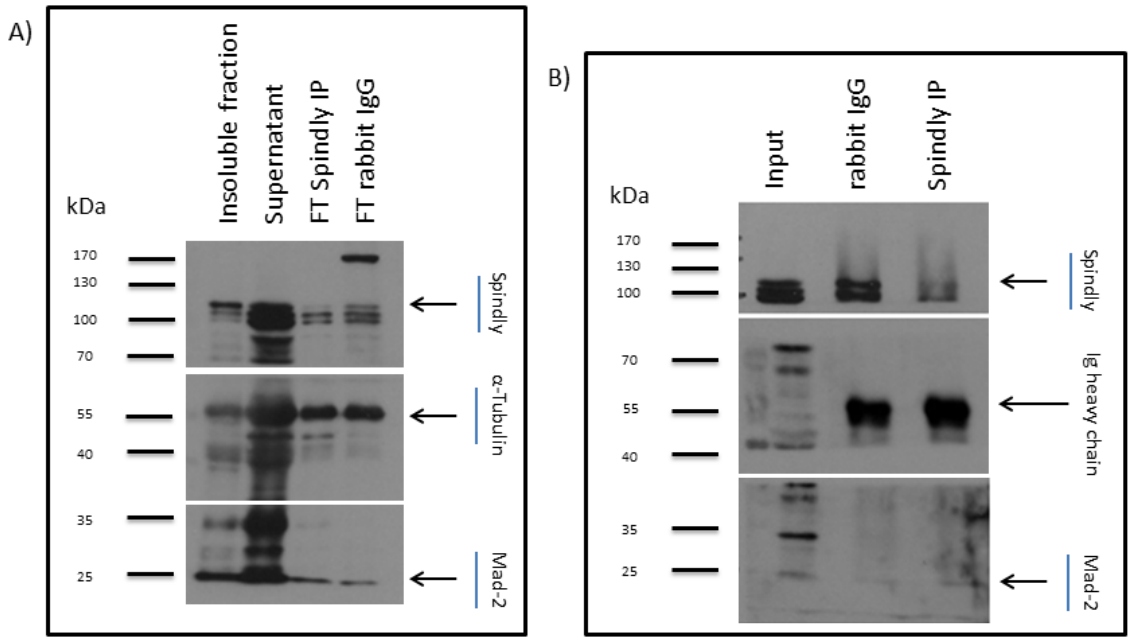

Figure 3- 22: Immunoprecipitation of Spindly. (A) Evaluation of the extraction efficiency of Mad-2 and Spindly from early *Drosophila* embryos. An aliquot of the pellet (insoluble fraction) and the input (supernatant) samples were run on adjacent lane on a SDS-PAGE and the membrane was probed against Spindly and Mad-2. The Western blot analysis confirmed that both proteins were extracted and preserved in a soluble fraction. Additionally, as a measure of the efficiency of immunoaffinity isolation of the proteins of interest, an aliquot of unbound protein following immune-precipitation (flow-through, FT) was run on adjacent lanes. (B) Detection of *Drosophila* Mad-2 and Spindly after immunoprecipitation of Spindly from embryo whole lysate. The images are representative of three independent experiments. A standard protein molecular weight marker is included and numbers in kDa are shown on the left.

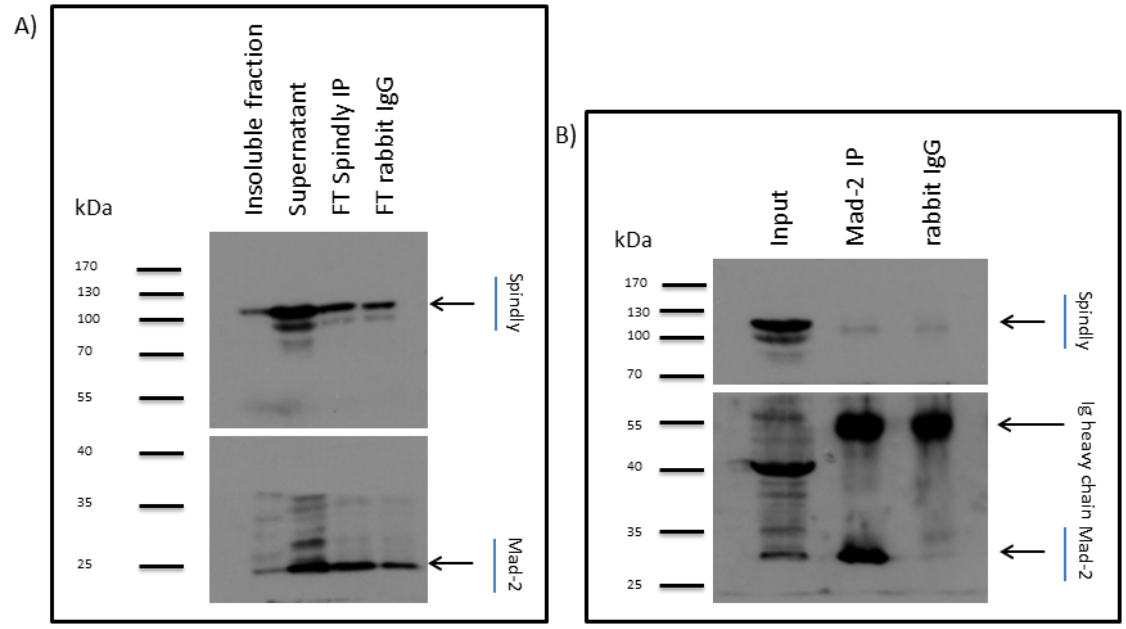

Figure 3- 23: Immunoprecipitation of Mad2. (A) Evaluation of the extraction efficiency of Mad-2 and Spindly from early *Drosophila* embryos. An aliquot of the pellet (insoluble fraction) and the input (supernatant) samples were run on adjacent lane on a SDS-PAGE and the membrane was probed against Spindly and Mad-2. The Western blot analysis confirmed that both proteins were extracted and preserved in a soluble fraction. Additionally, as a measure of the efficiency of immunoaffinity isolation of the proteins of interest, an aliquot of unbound protein following immune-precipitation (flow-through, FT) was run on adjacent lanes. (B)

Detection of *Drosophila* Mad-2 and Spindly after immunoprecipitation of Mad-2 from embryo whole lysate. The images are representative of three independent experiments. A standard protein molecular weight marker is included and numbers in kDa are shown on the left.

We reasoned that the ability of Spindly to bind to Mad-2 could be tightly regulated during mitosis and this could result in a transient and labile interaction. Therefore, *Drosophila* S2 cells were used to test whether a drug-induced mitotic arrest could facilitate the detection of the interaction. Cells were exposed for a period of 12 hours to Colchicine, a compound that inhibits microtubule polymerisation inducing the arrest of the cell cycle in prometaphase. The treatment resulted in an effective enrichment of cells in mitosis as suggested by the higher levels of Cyclin B in the treated sample compared to the control (S2 A). Proteins were extracted from both asynchronous and synchronous populations of S2 cells and co-immunoprecipitation experiments were performed incubating the samples with affinity-purified Spindly antibody. The condition tested failed in detecting a productive interaction between these two SAC proteins despite the induced hyper-activation of the mitotic checkpoint (S2 B).

3.2 Concluding Remarks

In the presented work we utilised the characteristic development of the early *Drosophila* embryo as a model to unravel the *in vivo* activity of Spindly during the fast thirteen syncytial divisions. Since mutant alleles for *spindly* are not available yet, the application of a novel RNAi technology in flies (Max V. Staller and Lizabeth A. Perkins 2013) was utilised to determine how and to what extent the depletion of the maternal protein affects embryo development. By testing two different maternal Gal4 drivers and by varying the temperature we were able to tune the expression levels of Spindly in the germline and study the effects of the differential reduction of this protein on mitotic progression. The study reported in this chapter points to Spindly as a fundamental factor to ensure normal progression through the fast and synchronous mitotic divisions during the early stages of embryonic development that precede cellularisation. A significant reduction of Spindly protein level severely compromised early nuclear divisions and resulted in marked embryonic lethality as demonstrated by determining the hatching ability of Spindly-RNAi embryos and by the high rate of syncytial defects. Moderate downregulation of Spindly combined with microscopy analysis of fixed preparations of early embryos revealed that a broad variety of mitotic defects were generated as a consequence of Spindly depletion. Differently from the wild-type condition, the mitotic divisions did not occur simultaneously and nuclei were irregularly distributed through the surface of the embryos. Additionally, the phenotypic analysis of Spindly-RNAi embryos suggested severe defects in the assembly of a functional mitotic spindle and pointed to a potential activity of Spindly in linking the centrosomes to the spindle poles.

To substantiate our knowledge about the function of Spindly at the kinetochore *in vitro* binding assay and co-immunoprecipitation experiments were perfomed to test the interaction between Spindly and a key player of the mitotic checkpoint, Mad-2. These experiments were carried out with the aim of testing whether Spindly could have additional activities in the control of the Spindle Assembly Checkpoint beyond the control of the kinetochore stripping. Unfortunately, in this study it was not possible to demonstrate by biochemical means that a productive interaction between these two components of the SAC takes place, even though this possibility cannot be completely excluded.

All together, the data reported in this chapter suggest a crucial function for Spindly in regulating normal embryonic development and show that the downregulation of this protein results in multiple mitotic abnormalities. This loss-of-function study suggests that Spindly could regulate cytoskeletal components in mitosis and supports a novel function for this protein as a regulator of dynein in its multiple non-kinetochore functions.

Chapter IV: Results Part I

Effect of Spindly overexpression on Drosophila embryogenesis

Chapter IV: Results Part I

Effect of Spindly overexpression on Drosophila embryogenesis

4 Introduction to chapter IV

Traditionally, genetic screens have been extensively used for identifying gene products based on loss-of-function phenotypes, that is by describing the biological effects of perturbing cellular or developmental processes when the gene product is absent or its function is severely reduced. However, knockout studies are often insufficient to fully describe the functions of a given gene and increasing the gene dosage above the physiological level can be an equally informative genetic tool to uncover novel gene functions that would remain undetected using the traditional loss-of-function methods (R0RTH 1996, Pernille Rørth1 and Katrin Weigmann 1998). Additionally, overexpression of a gene product can be effectively used to study genetic interactions and to connect genes to specific biological pathways. Indeed, in the case that overexpression of a gene can modulate an existing phenotype by suppressing or enhancing the effects of a mutation in another gene, then their protein products are likely to be operating in the same pathway.

From a clinical point of view, overexpression studies greatly impact our understanding of the causes of human diseases and potential therapeutic strategies. Indeed a broad range of human diseases correlates with an increased or ectopic gene expression. It is therefore important to clarify by which mechanism(s) this upregulation causes mutant phenotypes.

Similarly to knockdown experiments, the GAL4-UAS system in *Drosophila* can be used to drive the ectopic overexpression of gene products in a cell and tissue-specific

manner, providing the possibility of identifying biologically relevant phenotypes and genetic interactions. In this chapter, we exploit this versatile genetic system to characterise the effects of Spindly overexpression on the development of the embryo.

4.1. Maternal overexpression of Spindly affects embryos viability

The loss-of-function studies reported in this PhD thesis demonstrated that Spindly is essential for sustaining the early mitotic cell cycles in the syncytial embryo. *Drosophila* embryos lacking maternal Spindly showed a broad spectrum of defects including asynchrony in the mitotic divisions, aberrant morphology of the mitotic spindles and centrosome detachment. We hypothesied that increased expression of Spindly above the wild-type threshold levels could enhance some of the biological activities of the protein, which then may result in phenotypes that could elucidate the developmental pathway(s) in which Spindly operates. To test this hypothesis, we adopted the GFP-tagged Spindly construct impervious to the RNAi machinery and we induced its expression early during oogenesis using either the *maternal tubulin67c*>Gal4 driver or the *nanos*>Gal4 driver.

Levels of expression of the transgene were determined in lysates from 0-3-hour-old embryo collection at 25°C by Western Blot. The analysis showed that a significant amount of GFP-tagged Spindly was maternally expressed by the transgene provided (Figure 4-1).

Having proved by Western blot analysis that we were able to induce the expression of the GFP-tagged transgene using the Gal4-UAS system (Figure 4-1), we performed the rest of the experiments reported in this chapter using the *maternal tubulin67c*>Gal4.

Indeed, we previously demonstrated that this maternal driver is more efficient than the *nanos*>Gal4 driver at any of the experimental condition tested (see Chapter 3).

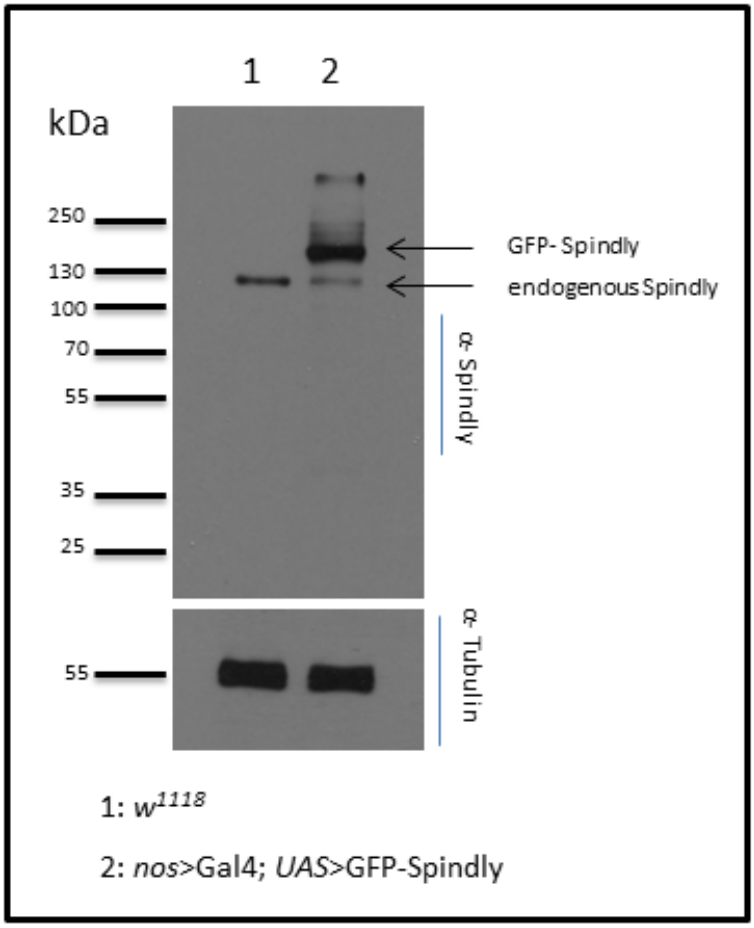

Figure 4- 1: Western Blot analysis on early *Drosophila* embryos overexpressing GFP-Spindly. 10 µg of proteins from wild-type and *nanos*>Gal4;*UAS*>GFP-Spindly embryos were loaded on adjacent lanes of a SDS-polyacrylamide gel (lane 1 and lane 2, respectively). After Western blotting and transfer of the proteins onto a nitrocellulose membrane, the membrane was probed using affinity-purified anti-Spindly antibody, allowing the specific identification of the endogenous and the GFP-tagged transgenic protein (calculated molecular weight: 120 kDa). α-Tubulin was included as loading control. For a precise molecular weight determination, a standard protein molecular weight marker was used and numbers in kDa are shown on the left. The image is representative of two independent experiments.

To quantify the effect of increased Spindly expression on embryo viability, the ability of the embryos to complete embryogenesis and hatch into larvae was evaluated. Eggs from crosses that would produce 100% GFP-Spindly expressing embryos were collected, counted and allowed to hatch. The analysis revealed that embryo viability was greatly reduced compared to the wild-type control, scoring only 30% of embryonic

survival (Figure 4-2 A). Simultaneous knockdown of the endogenous protein in the overexpression background restored embryo viability to wild-type level, suggesting that the decreased viability of the embryos was specifically caused by overexpression of Spindly (Figure 4-2 A, rescue).

To gain an idea of the developmental defects that could cause embryonic lethality, unhatched embryos were collected 48 hours after egg laying (AEL) and the chorion was removed to score the extent of development by examining the differentiation of the larval cuticle. Unhatched embryos were grouped into three classes. The first class was constituted of opaque embryos dead before cuticle deposition (65.8%, n=138). The remaining of the eggs showed clear signs of segmentation defects (Class 3_ 21.7%, n=138) or severe dorsal closure defects (Class 2_ 10.1%, n=138) (Figure 4-2 B).

Analysis of cuticle preparations of larvae derived from embryos overexpressing Spindly revealed a strong defect in egg morphology. A high percentage of the eggs were rounded in shape (48% of the cases examined) (Figure 4-3 A, n=100) and smaller in size compared to the wild type (Figure 4-3 B, n=100), as estimated by measuring the ratio between the length (anterior-posterior (A/P) axis) and the width (dorsal-ventral (D/V) axis) of the embryo. Knockdown of the endogenous protein was able to restore the AP/DV ratio to the wild-type level (Figure 4-3 B, Rescue).

Additionally, the dorsal appendages, that mark the dorsal anterior region of the embryo, appeared to be shorter, closer to the midline and sometimes fused at the base, indicating a moderate ventralisation phenotype (Figure 4-4.

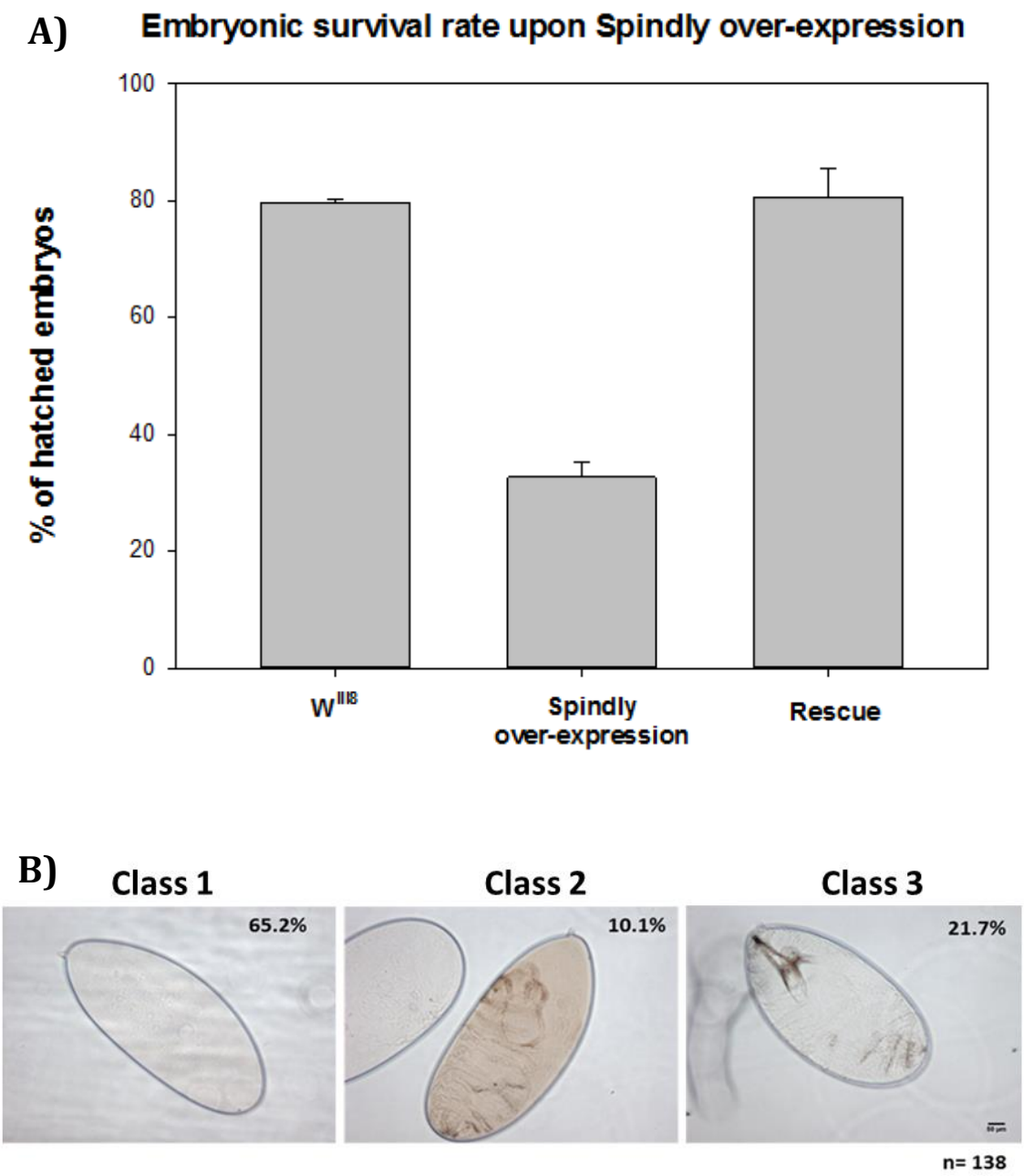

Figure 4- 2: Overexpression of Spindly is embryonic lethal. A) The graph shows the survival rate of *Drosophila* embryos upon Spindly overexpression. Overexpression of Spindly was driven using the *maternal tubulin*>Gal4 driver and the experiment was performed at 25°C. Increased expression of Spindly significantly reduces embryo viability compared to the wild-type control, with only 30% of the embryos being able to hatch as first instar larva (n=100). Viability is restored to wild-type level by knocking down the endogenous protein. Results represent the average of three independent technical replicates. For each replicate, 100 embryos were used to assess the hatching. B) Cuticle preparation of developed *mat tubulin 67*>Gal4; *UAS*>GFP-Spindly embryos at 25°C. The majority of the embryos die before cuticle deposition (65.2%, Class 1). The remaining 31.8% of the embryos examined proceed further in development. However they show either severe dorsal closure defects (Class 2) or segmentation pattern defects (Class 3).

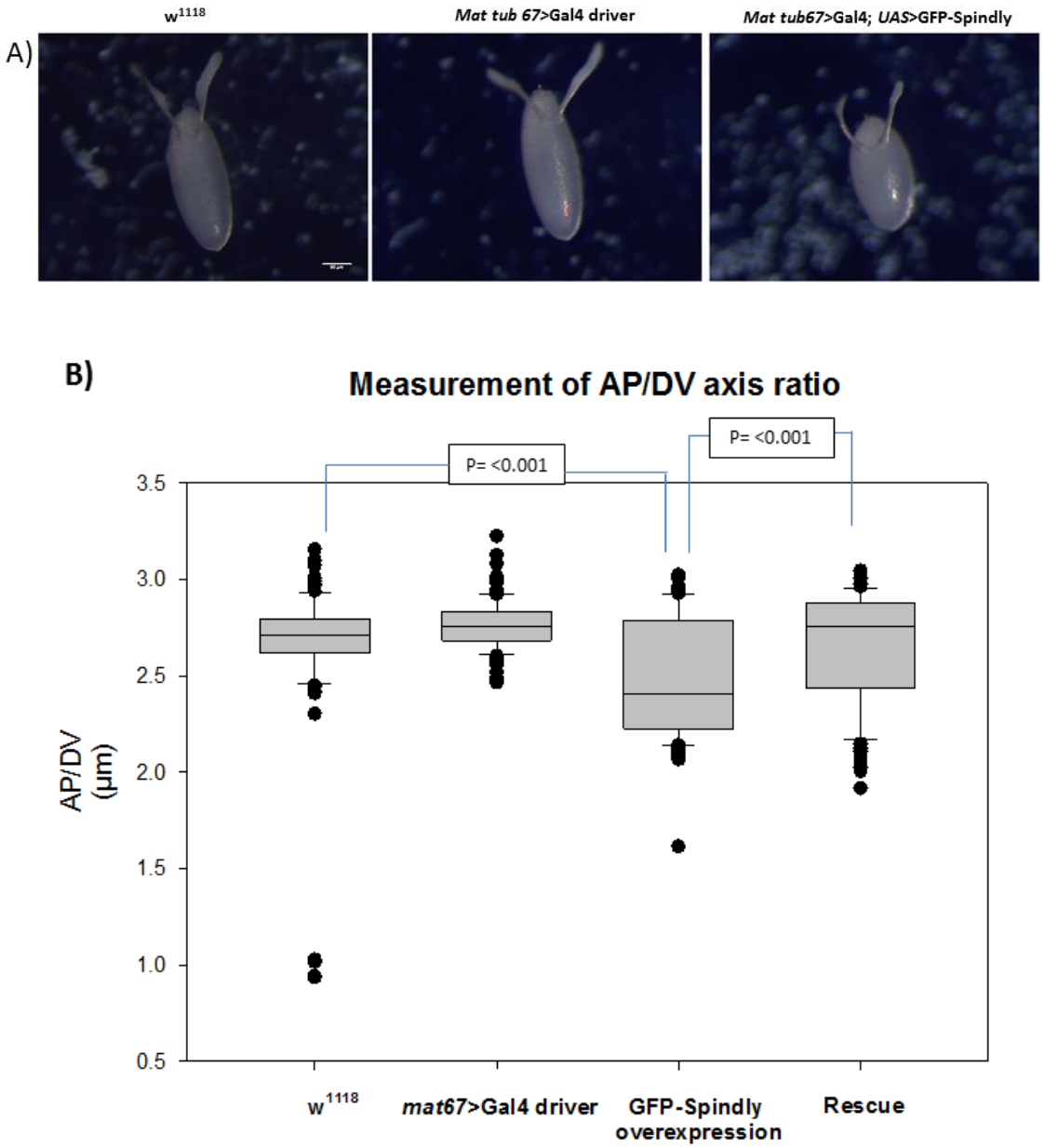

Figure 4- 3: Overexpression of Spindly alters normal egg morphology. (A) Eggs laid at 25°C by female flies overexpressing Spindly remain rounded and fail to elongate compared to the controls (48%, n=100). Scale bar represents 50 µm. (B) The overall size of these eggs is significantly different compared to the control. This phenotype is suppressed by depletion of the endogenous protein. The size of the eggs was evaluated calculating the ratio between the length (A/P axis) and the width (D/V axis) of each embryo, for a total of 100 embryos. The statistical significance of the difference was estimated performing a nonparametric Mann-Whitney U Statistic test (p=<0.001).

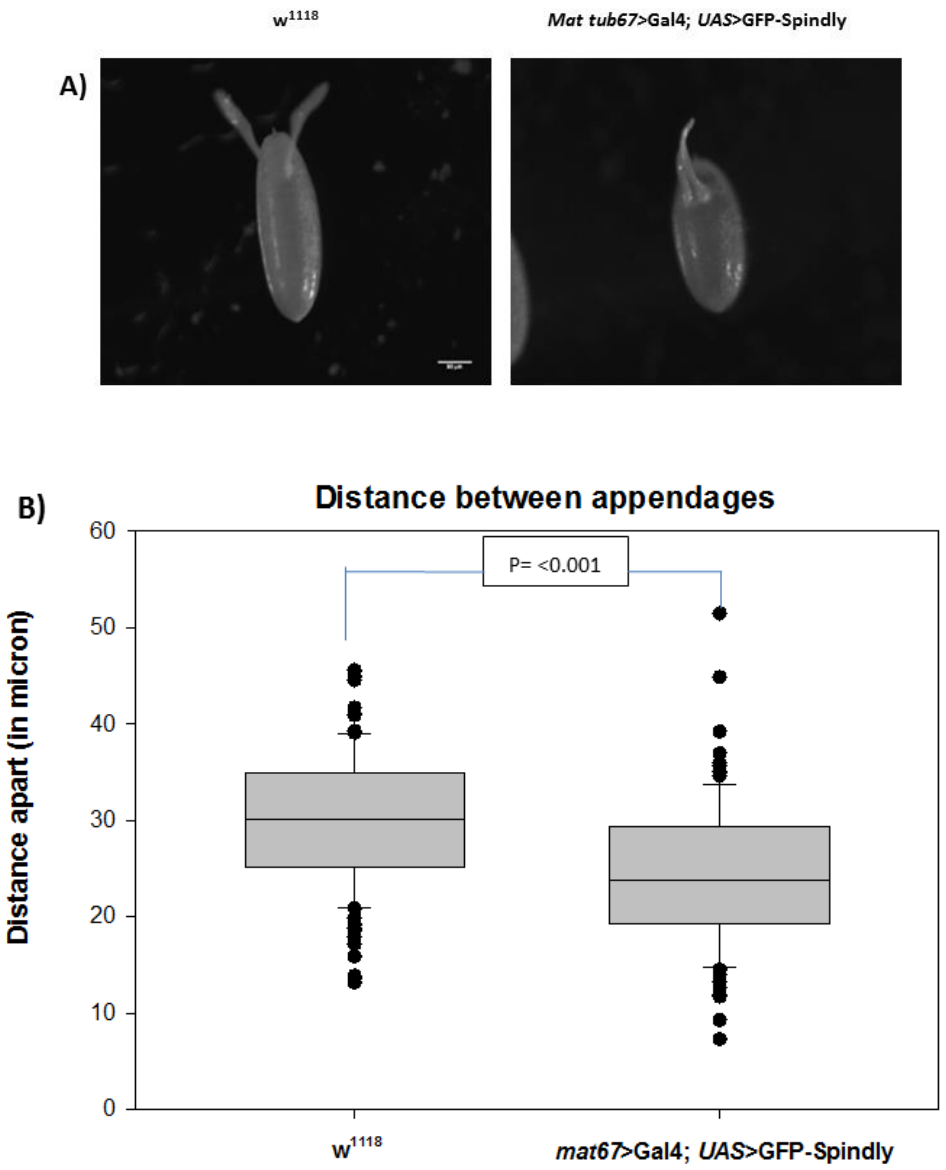

Figure 4- 4: Overexpression of Spindly causes moderate ventralisation of the egg. (A) Representative images of eggs laid at 25°C by flies overexpressing Spindly. The chorion of the eggs indicates moderate defects in the dorsal-ventral polarity of the developing embryos. The dorsal appendages look shorter and are closer apposed to each other along the dorsal midline compared to the wild-type control. Scale bar represents 50 µm. (B) Measurement of the distance between the dorsal appendages in wild-type and Spindly-overexpressing eggs. The distance between the appendages is significantly shorter in the eggs overexpressing Spindly (nonparametric Mann-Whitney U Statistic test, p=<0.001; n=100).

4.2 Concluding remarks

Knockdown and overexpression are useful means to uncover gene functions during development. Knockdown experiments of maternal Spindly showed the fundamental requirement for this protein in sustaining early stages of the development of the *Drosophila* embryo, in particular in controlling the correct progression through the fast and synchronous mitotic cell cycle during syncytial division. In this chapter the Gal4/UAS system was adopted to boost the expression of a GFP-tagged version of Spindly early during oogenesis and increase the amount of maternal protein loaded in the embryos. This approach allowed the further analysis of Spindly activity during *Drosophila* embryos development, pointing to novel, previously uncharacterised functions of the protein.

The data reported in this chapter show that the overexpression of Spindly is embryonic lethal. The majority of the embryos died during early stages of embryonic development, before cuticle deposition, while 32% proceeded further in development and accumulated severe patterning defects.

Additionally, Spindly overexpression caused profound alteration in the morphology of the egg. Embryos were rounded in shape and this phenotype points to impared egg elongation. This phenotype could be either caused by a failure in the polarisation of the follicular epithelium of the egg chamber or defective dumping of the egg during late oogenesis. Both mechanisms are actin-dependent. The data reported here therefore provide a basis for studying the requirement of Spindly in the regulation of the actin cytoskeleton during other well-characterised developmental processes.

All together these data suggest additional functions of Spindly in supporting normal *Drosophila* embryonic developmet and point to more complex actitivities of the protein in addition to control of cell cycle progression.

Chapter V: Results Part II

Requirement of Spindly for Cell Migration

Chapter V: Results Part II
Requirement of Spindly for cell migration

5. Introduction to Chapter V

Cell migration is a fundamental process for normal development of an organism. Cell migration also contributes to important physiological processes in the adult, including immune system activity and wound healing. Therefore, it should not come as a surprise that aberrations in the machinery controlling cell motility are implicated in the physiology of many pathological conditions, such as inflammatory disease and metastatic tumours.

The regulation of cell migration is a complex event that relies on the ability of cells to receive environmental signals and integrate them in a spatially and temporally controlled manner. To become motile and acquire invasive potential, cells activate a complex intracellular programme that results in dramatic changes in gene expression, cell adhesion and cytoskeletal organisation (Steeg 2006).

Over the past decades, *in vitro* models have been extensively used to enable the characterisation of the basic molecular mechanism(s) that regulate the diverse aspects of cell motility. However, the migratory behaviour of cells is influenced by the natural environment. Therefore, genetically tractable organisms have become powerful tools for the identification of genes that regulate cell migration and for the characterisation of their functional relevance *in vivo*.

The fruit fly *Drosophila melanogaster* provides many excellent models of cell migration each of which has contributed to better clarify the genetic control of cell motility and the molecular pathways that guide the migrating cells along their proper route.

Specifically directed movement of haemocytes towards a wound has been used as a system to study inflammatory response and wound healing (Wood 2011) while border cell migration is considered a good model to study collective migration and invasiveness (Jang, Starz-Gaiano et al. 2007).

5.1 Spindly and cell migration

Much like other mitotic checkpoint proteins, Spindly is proposed to have an additional function during interphase. Knockdown of the protein drastically alters S2 cell morphology. Spindly-RNAi cells are defective in the formation of actin lamellae and they organise the microtubule cytoskeleton in long bundles that protrude from the cell surface (Griffis, Stuurman et al. 2007). Furthermore, overexpression of a GFP-tagged version of the protein reveals its accumulation at the (+) ends of microtubules along with other microtubule-plus-end binding factors such as EB-1. This evidence led to the hypothesis that Spindly has a role in regulating the motile behaviour of cells by controlling the dynamics of the actin and tubulin cytoskeleton in post-mitotic cells.

Moreover, in addition to its mitotic activity in connecting dynein to kinetochores, *in vitro* experiments clearly show that Spindly is indispensable for increasing the processivity of the motor protein as well as the directionality of its movement, pointing to a more general requirement for Spindly in assisting dynein activity in its multiple functions, including in cell migration (Richard J. McKenney 2014, Schlager, Hoang et al. 2014).

Taking into account these considerations, it is appealing to speculate that Spindly may have a major impact on cell migration via multiple mechanisms such as cytoskeleton remodelling, regulation of dynein activity or a combination of these two possibilities.

This chapter will focus on this question by studying the requirement of Spindly for cell migration in two alternative models: border cells and embryonic haemocytes.

5.2 Knockdown of Spindly affects border cell migration

Border cells in the *Drosophila* ovary are accepted as a good genetic model for studying epithelial-to-mesenchymal transition and cell motility. The fly ovary is made up of 16 ovarioles each of which is a string of egg chambers at increasing stages of maturation, connected by 5 to 8 stalk cells. Each egg chamber is composed of 16 germline cells, 15 nurse cells and one oocyte, surrounded by a mono-layered follicular epithelium of 650 cells. Border cells originate from the follicular epithelium at stage 8 of development (Figure 5-1). During stage 9 they round up, delaminate from the epithelium and migrate posteriorly as a coherent cluster until they reach the nurse cell-oocyte boundary by stage 10 of egg-chamber development (Montell 2003) (Figure 5-1). In fixed tissue, this small group of cells can be easily visualised staining the nuclei with DAPI and the actin cytoskeleton with conjugated phalloidin.

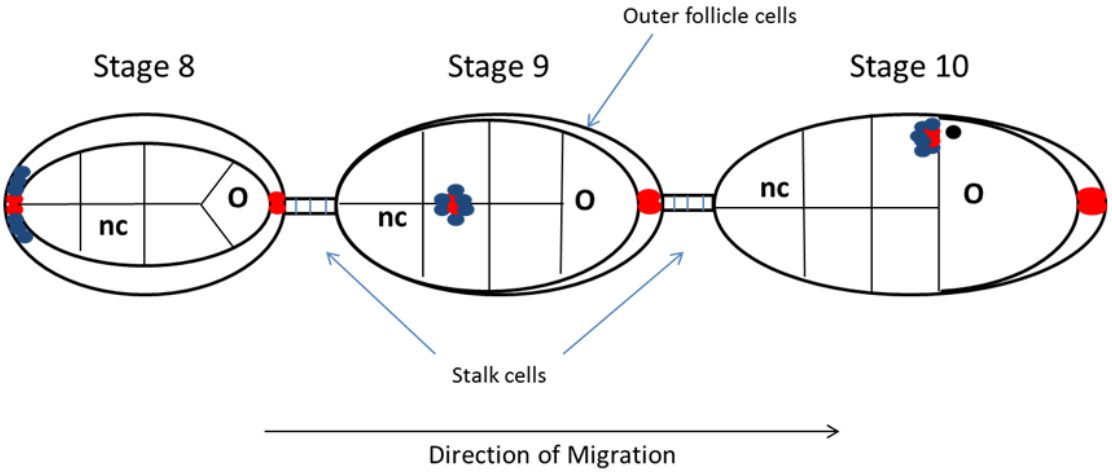

Figure 5- 1: Schematic of border cell migration and outer follicle cells rearrangement. The picture shows egg chambers at stage 8-10 of development connected by stalk cells. Each egg chamber consists of 16 cells: 15 nurse cells (nc) and one oocyte (o). At stage 8, polar cells (in red) at the anterior pole of the follicular epithelium recruit from 4 to 8 neighbouring cells (in blue) forming the migrating border cell cluster. At stage 9 of development, the cluster delaminates from the epithelium and starts migrating posteriorly toward the oocyte. The cluster reaches the nurse-cell-oocyte boundary at stage 10 of oogenesis. Concomitantly, the outer follicle cells migrate posteriorly and they no longer cover the nurse cells.

To determine whether the activity of Spindly influences the migratory ability of cells, we tested the effect of an RNAi construct on border cell migration using fixed tissues. The knockdown of *spindly* was specifically driven by the border cell-specific *slow border cells*-Gal4 (*slbo*>Gal4)-driver. Ovaries were isolated from 4-day-old female flies and stained for DNA and actin cytoskeleton. This procedure allowed easy imaging of the cyst and helped to determine the stage of egg-chamber development as well as to establish the position of the border cell cluster in relation to the nurse cells-oocyte boundary. In the wild-type control the majority of border cell clusters did not show any migration defects (82%, n= 66) while a small percentage (18%) had already completed their migration by late stage 9 of egg-chamber development (Figure 5-2 A and B). However, when the level of Spindly expression was knocked down by RNAi, 40% of the clusters had already completed migration at late stage 9 (n=66) (Figure 5-2 A and B). This observation suggested that Spindly negatively regulates border cell migration by

unknown mechanism(s). Therefore, knockdown of the protein caused the cluster to migrate either earlier or faster along the anterior- posterior axis towards the oocyte.

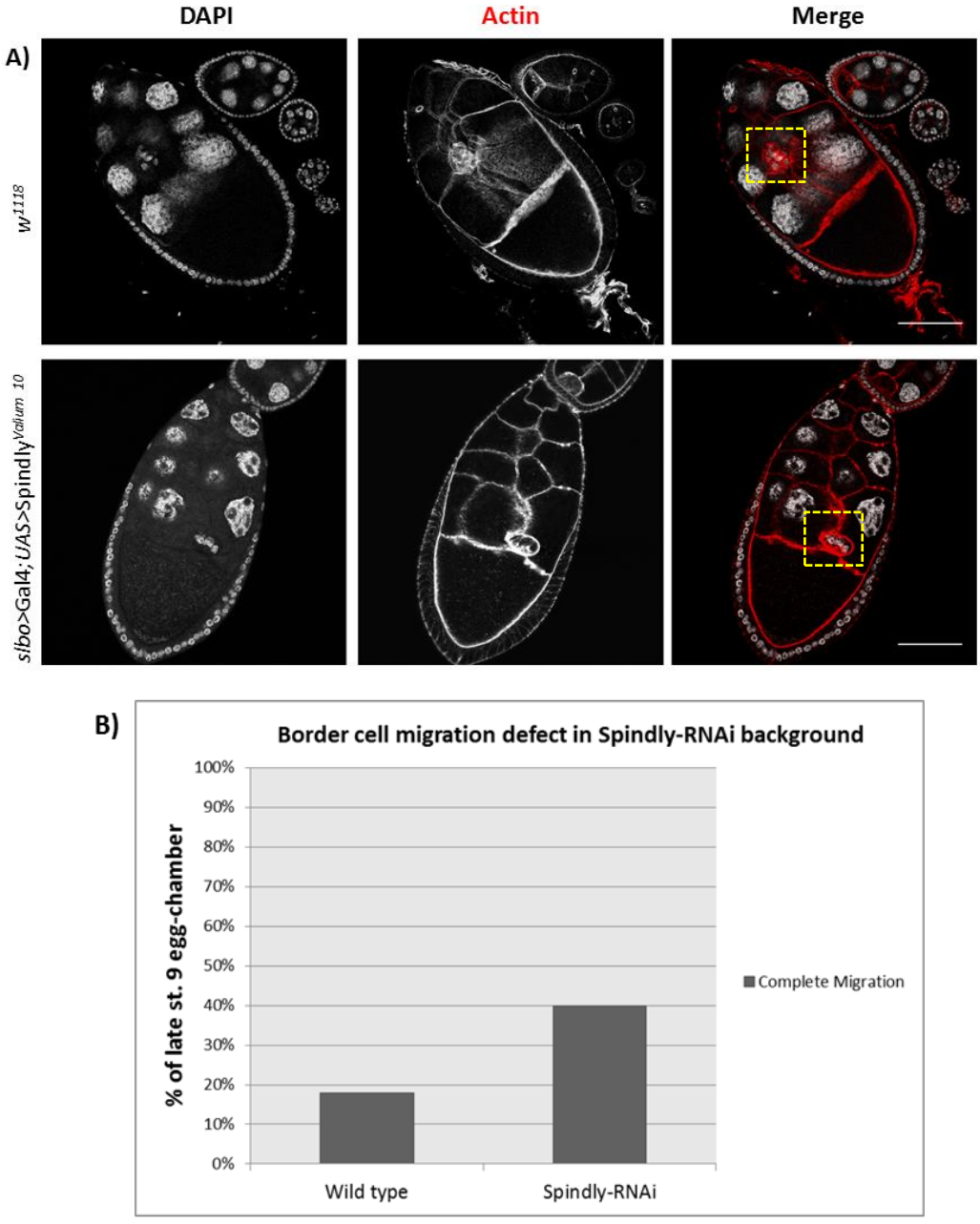

Figure 5- 2: Knockdown of Spindly affects the migration of the border cell cluster. A) Confocal optical section of egg chambers at stage 9 of development from wild-type or *slbo*>Gal4; *UAS*>Spindly^{Valium10} female flies kept at 25°C. In this experiment, the knockdown of Spindly was achieved crossing females from a TRIP line, that brings the sequence of the shRNA specific for *spindly* mRNA under the control of *UAS* promoter, with males of the driver *slbo*>Gal4 line, which directs shRNA expression in border cells. Depletion of Spindly using RNAi alters border cell migration: the cluster reaches its final position, close to the oocyte, earlier during egg-chamber development compared to wild-type control. Cell outlines are labelled with Phalloidin Alexa-594 (red), nuclei with DAPI (gray). The position of the border cell cluster is marked by a yellow dashed box (Merge). Scale bars represent 50 µm. (B) Quantification of the phenotype described in (A). The defect in border cell migration was observed in 40% of mid-stage 9 egg chambers examined (n= 66).

To further prove the requirement of Spindly for border cell migration, we drove the expression of a GFP-tagged version of the protein in the cluster using the *slbo*>Gal4 driver. Staining of egg chambers at stage 10 of development confirmed that the transgene had overlapping expression pattern with the Slbo transcription factor, demonstrating the specificity of the Gal4 system (Figure 5-3).

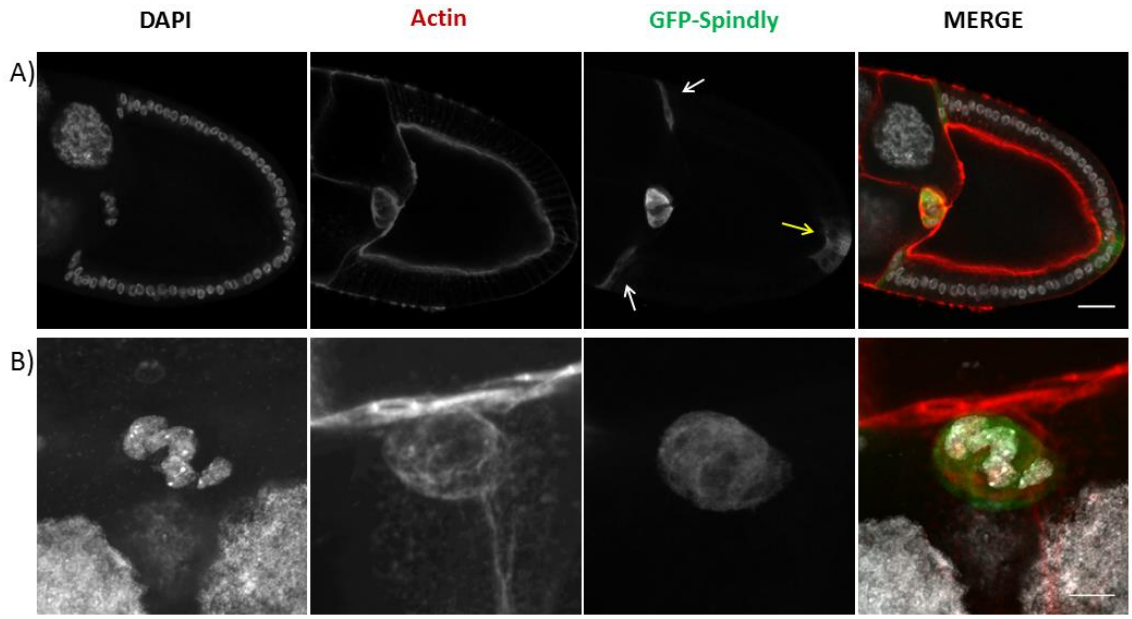

Figure 5- 3: Localisation of GFP-Spindly in border cells. A) Confocal optical section of an egg chambers at stage 10 of development from a *slbo*>Gal4; *UAS*>GFP-Spindly fly kept at 25°C. A GFP-Spindly fusion protein was driven in the border cell cluster using the *slbo*>Gal4 driver line. The image shows the localisation pattern of GFP-Spindly in the egg chamber (green). The GFP signal is detectable in the cluster (yellow dashed box), in the centripetal cells (white arrows) and in the posterior polar cells (yellow arrow). The egg chamber shown in picture (A) is oriented posterior to the right. B) Magnified view of a border cell cluster. The image is a maximum-intensity projection of a 7 µm stack. Z-stacks were acquired at a spacing of 1 µm. GFP-Spindly shows cytoplasmic localisation and enrichment at the plasma membrane as shown by colocalisation with the F-actin. Cell outlines are labelled with Phalloidin Alexa-594 (red), nuclei with DAPI (gray). Ovaries were immune-stained with anti-GFP antibody to visualise GFP-Spindly transgene (green). Scale bar represent 20 µm in (A) and 10 µm in (B).

We then asked whether the overexpression of Spindly could slow down the migration rate of the cluster. The analysis revealed that 34% (n= 74) of the border cell clusters were delayed in their migration towards the oocytes at stage 10 of egg-chamber development. To exclude non-specific genetic background effects due to the driver, we examined stage 10 egg chambers derived from *slbo*>Gal4 female flies. Although we

scored incomplete migration at stage 10 of oogenesis in 19% (n= 80) of the cases examined, the penetrance of the phenotype was significantly lower compared to the GFP-Spindly overexpression background (Figure 5-4 A and B). Additionally, overexpression of a GFP-tagged version of the histone protein H_3 did not alter border cell migration, confirming that the increased level of Spindly expression is responsible for the incomplete migration phenotype observed (Figure 5-4 A and B).

Gain-of-function experiments allowed the identification of an additional phenotype. Overexpression of Spindly caused the cluster to lose its integrity. Cell-cell contacts between border cells appeared to be less strong and individual cells detached from the group and started to migrate as single entities (Figure 5-5 A and B).

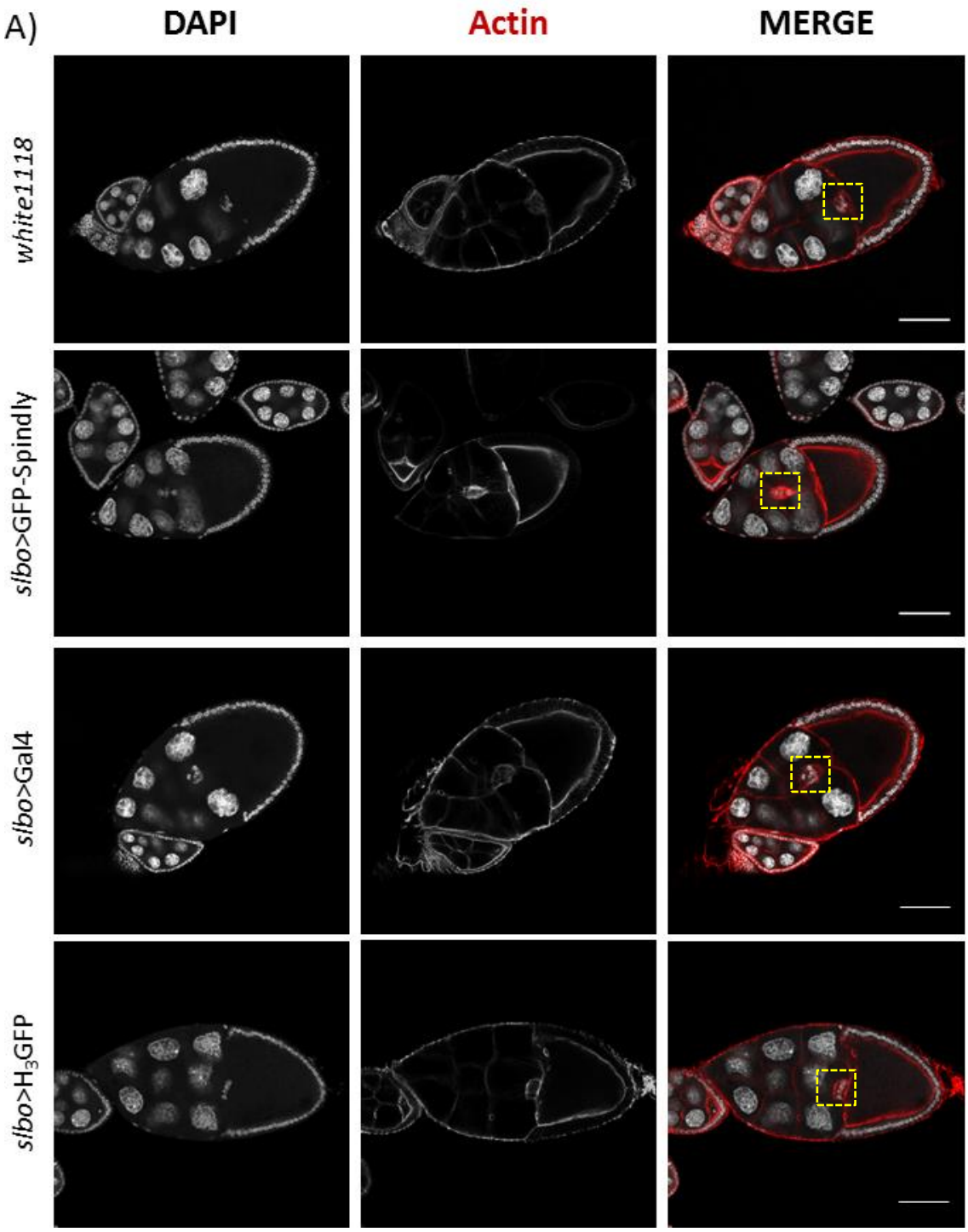
A)
DAPI
Actin
MERGE
white1118
slbo>GFP-Spindly
slbo>Gal4
slbo>H3GFP

B)

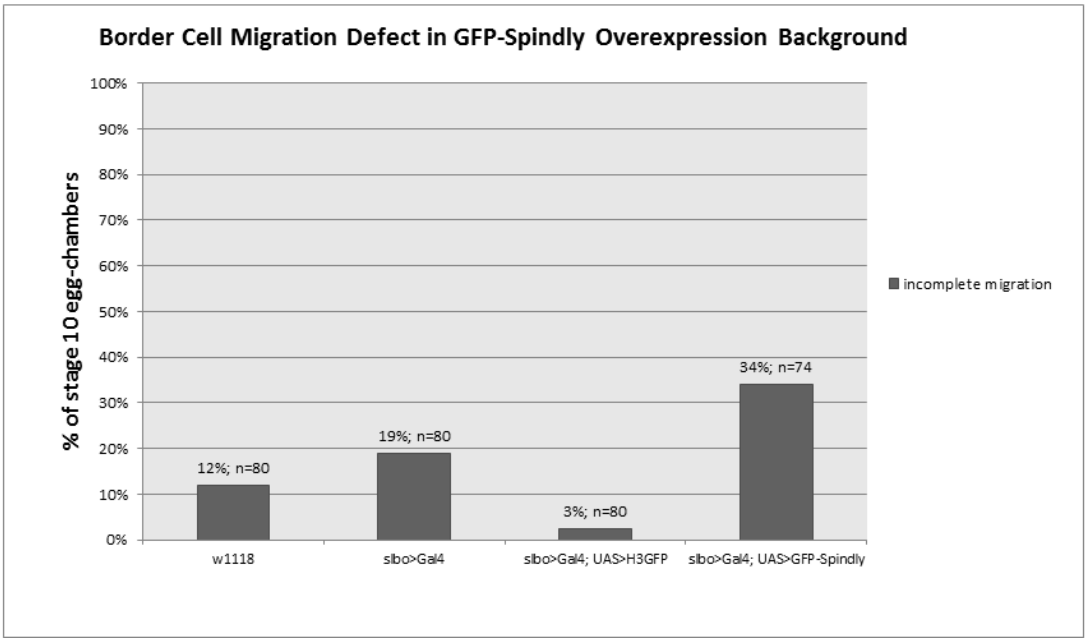

Figure 5- 4: Spindly overexpression delays border cell cluster migration. A) Confocal optical section of egg chambers at stage 10 of development from flies of the indicated genotypes kept at 25°C. Migration of border cells is delayed in the GFP-Spindly overexpression background. Cell outlines are labelled with Phalloidin Alexa-594 (red), nuclei with DAPI (gray). The position of the border cell cluster is marked by a yellow dashed box (Merge). Ll images are oriented posterior to the right. Scale bars represent 50 µm. (B) Quantification of the phenotype described in (A). 34% of clusters overexpressing Spindly have not completed migration by stage 10 of egg-chamber development (n= 74).

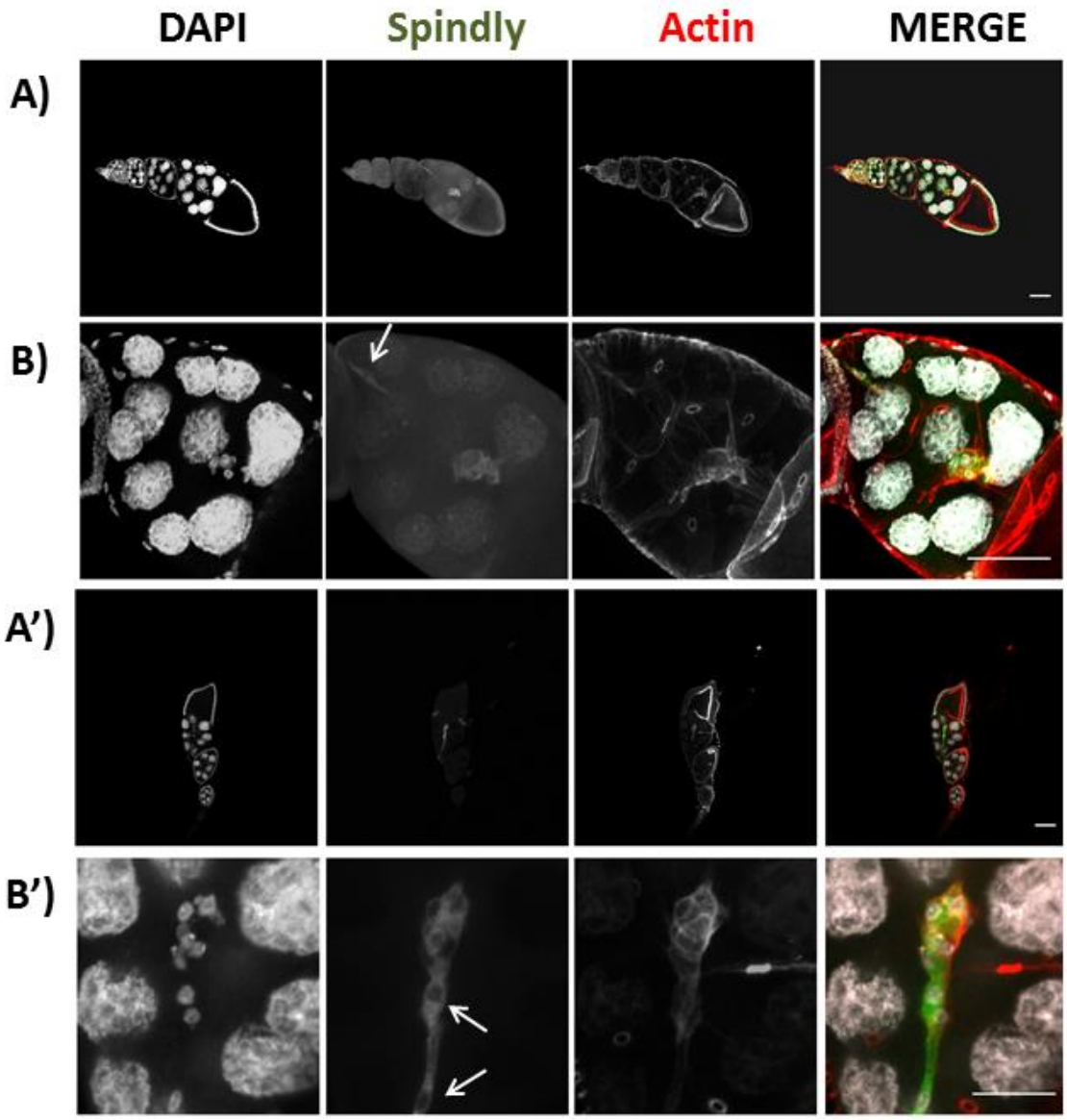

Figure 5- 5: Overexpression of Spindly affects border cell clustering. A; A') Confocal optical sections of egg chambers at stage 10 of development from a *slbo*>Gal4; *UAS*>GFP-Spindly flies kept at 25°C. B, B') Magnification of the pictures in A and A', respectively. The images are maximum-intensity projection of a 10 µm stack. Z-stacks were acquired at a spacing of 1 µm. Overexpression of Spindly negatively regulates contacts between border cells. The cluster loses integrity and individual cells undergoing migration are visible (white arrows). The phenotype was observed in 16% of the cases examined (n= 74). Cell outlines are labelled with Phalloidin Alexa-594 (red), nuclei with DAPI (gray). Ovaries were immune-stained with anti-GFP antibody to visualise GFP-Spindly transgene (green). Scale bars represent 50 µm in A, A',B, 20 µm in B'.

5.3 Haemocyte migration to wounded-hypodermis is insensitive to the knockdown of Spindly

Wound re-epithelialisation is a fundamental process for maintaining tissue homeostasis and integrity. An early step in the wound response pathway is the recruitment of specialised cells to the site of damage, the haemocytes, whose function is to efficiently clear up wound debris. Haemocytes are quickly attracted to the wound by the production of an immune cell attractant and recently the mechanism of recruitment has been described at the molecular level. Shortly after wounding, the epidermis triggers an instantaneous release of calcium that spreads as a wave via gap junctions over a distance of 40 µm from the wound edge (Razzell, Evans et al. 2013). Cytosolic calcium activates DUOX, a NADPH oxidase (NOX) enzyme, leading to the production of hydrogen peroxide (H_2O_2), identified as the earliest wound attractant signal for *Drosophila* macrophages (Moreira, Stramer et al. 2010, Razzell, Evans et al. 2013). Haemocytes then respond to the chemoattractant gradient, polarising their cytoskeleton and migrating directionally towards the wound with an average speed of 2.6 µm/min, completely surrounding the site within 30 min post-wounding. At the site of damage haemocytes ensure the efficient and fast removal of cell debris. Subsequently, cells slowly start to disperse and full re-epithelisation is completed within 3 hours post-wounding (Stramer, Wood et al. 2005).

To address whether Spindly can regulate the motility of *Drosophila* haemocytes, we performed wound-healing assay on embryos at stage 15 of development asking if cells depleted for Spindly were still capable of directing their movement towards the site of a laser-induced wound. Migration of the macrophages to the site of damage was analysed using live time-lapse imaging of cells expressing GFP driven by the

haemocyte-specific *serpent*-Gal4 (*srp*-Gal4) driver. The movies provided information about the morphology of cells and the dynamics of their recruitment to the site of damage, especially in term of timing of recruitment and migration speed.

Wild-type haemocytes respond rapidly to the laser-wounding procedure: cells polarise their movement towards the wound, making extended membrane ruffles in the direction of the damaged zone. Cells moved quickly, surrounding the wound within 30 min. Also, big cytoplasmic vacuoles were visible indicating that these haemocytes actively removed apoptotic cell debris in their attempt to repair the tissue (Figure 5-6 A).

Knockdown of Spindly did not result in severe alteration of cell morphology or in a significant variation in the temporal response to laser-wounding. With few and rare exception of cells showing a cruciform shape (Figure 5-6 B yellow arrow), Spindly-RNAi haemocytes were morphologically indistinguishable from their wild-type counterparts, having the ability of making dynamic and broad lamellipodia and filopodia (Figure 5-6 B). Additionally, similarly to the control, large vacuoles were present in the cytoplasm of Spindly-RNAi haemocytes, meaning that the ability of these cells to engulf cell debris while migrating to the site of damage was not affected by the treatment. The motility of Spindly-RNAi macrophages was not compromised and these cells were still able of polarised and directed movement to the site of damage.

Similarly to the wild-type control, an average number of 6 cells were present at the site of damage by 30 min post-wounding, indicating that Spindly-RNAi haemocytes retained the ability to sense the environmental cues and orient their movement accordingly (Figure 5-7).

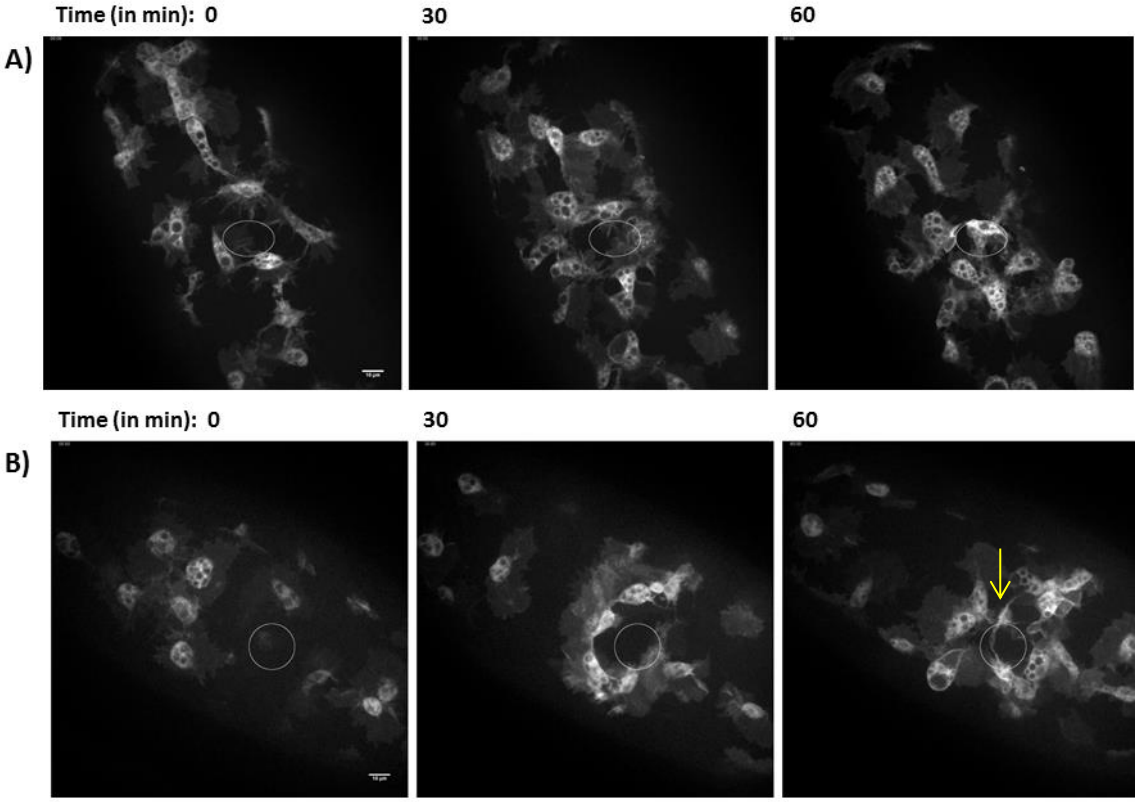

Figure 5- 6: Knockdown of Spindly does not affect the timing of haemocyte migration towards a wound. Stills taken from live imaging of wt (A) or Spindly-RNAi (B) haemocytes expressing GFP undergoing migration to an epithelial wound (white circle) in embryos at stage 15 of development. Migration of haemocytes in which Spindly is depleted by RNAi is largely unaffected. Cells migrate towards the wound with the same timing as the wild-type control, completely surrounding the site of damage within 30 minutes post-wounding. Additionally, down-regulation of Spindly does not profoundly affect cell morphology: membrane ruffling is highly dynamic and haemocytes make wide lamellipodia while moving. Rarely cells with a cruciform shape were observed (panel B, yellow arrow). Time is shown in 30-min intervals. Scale bars represent 10 µm.

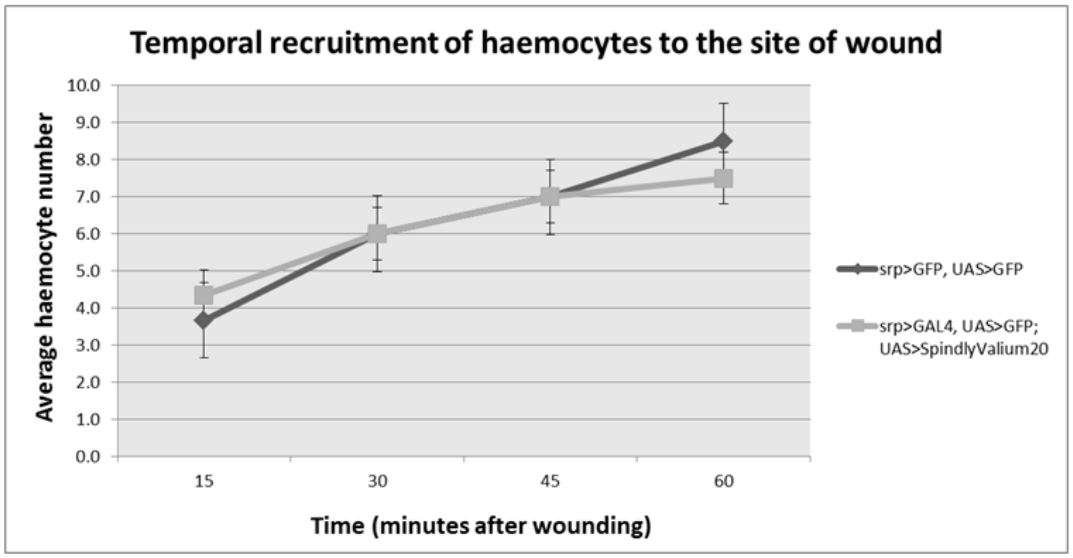

Figure 5- 7: Graph illustrating the temporal recruitment of macrophages to the site of a laser wound. The dynamic recruitment of haemocytes to the site of damage was monitor by live-imaging of cells expressing GFP. The number of cells at the wound zone was counted every 15 min over a period of 1 hour. A comparable number of cells was at the site of damage with an average number of 6 cells in both, control (dark gray line◆) and Spindly knockdown (light gray line ■).

Finally, single-cell tracking analysis revealed no difference in the migration velocity of Spindly-RNAi haemocytes towards a wound compared with the wild-type control (Figure 5-8 A, B and C).

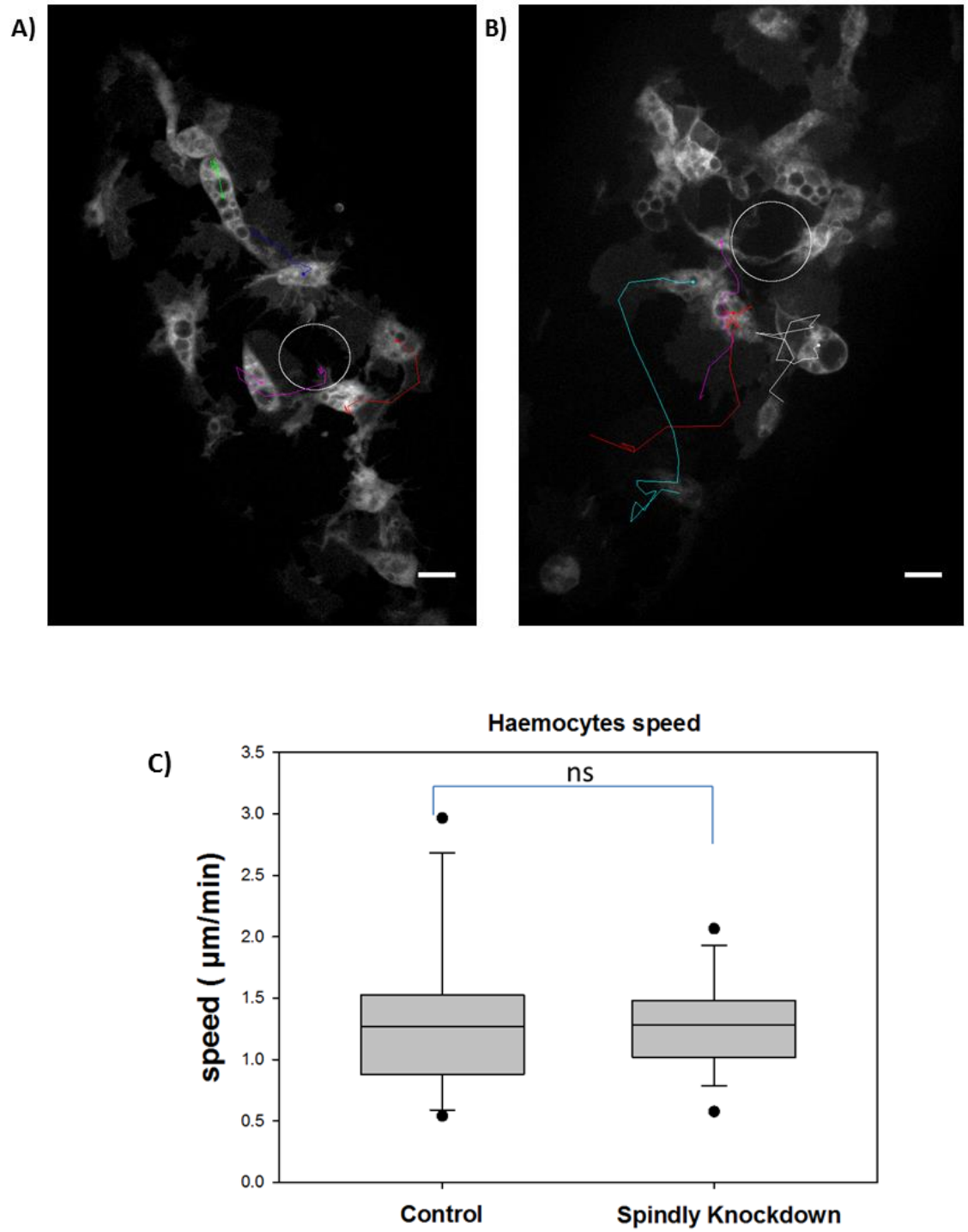

Figure 5- 8: Spindly-RNAi haemocytes migrate with the same speed as the wild-type control in wound-healing assay. Stills taken from movies of wild-type (A) or Spindly-RNAi (B) haemocytes migrating to an epithelial wound (white circle). Haemocyte migration was tracked every 3 minutes post-wounding over a period of 60 minutes. 5 cells for each movie were analysed (total of 3 movies for each genotype). (C) Tracking reveals no difference in the speed of Spindly-RNAi haemocytes compared to the wild-type control when migrating towards a wound cue (average speed= 1.3 µm/min). Scale bars represent 10 µm.

5.4 Concluding remarks

The aim of the experiments described in this chapter was to unravel novel functions for Spindly in interphase cells. Preliminary data in *Drosophila* S2 cells point to a potential activity for Spindly in regulating and coordinating actin and tubulin cytoskeletal components in post-mitotic cells, suggesting that Spindly might regulate cell motility via still unknown mechanism(s).

To test this hypothesis, we looked at two distinct and well-established models in *Drosophila*: border cell migration and embryonic haemocytes.

Loss-of-function experiments and analysis of fixed egg chambers suggested that Spindly negatively regulates the migration of border cells, either modulating their speed or setting up the right timing for delamination and invasion of the migrating cluster. Overexpression of a GFP-tagged version of the protein corroborates this observation. Under this condition, 34% of border cells showed incomplete migration towards the oocyte at stage 10 of egg-chamber development. Moreover, overexpression of Spindly caused the cluster to lose its integrity in 16% of the cases examined, suggesting that the increased expression of the protein above physiological levels alters the morphology of the cluster weakening cell-cell contacts and resulting in individual cells that detach from the main cluster and migrate as single entities towards the oocyte. The experimental observations made by manipulating Spindly expression in the border cell cluster need to be further validated. Specifically, a more precise staging of the stage 9 egg chambers would help in quantifying the complete migration phenotype observed upon downregulation. A carefull staging of the egg chamber can be achieved by taking into account not only the displacement of the

border cell cluster from the anterior follicle epithelium but also the simoultaneous and coordinated migration of the outer follicle cells in relation to the nurse cells-oocyte border. Moreover, additional biological replicates are required to confirm the incomplete migration phenotype scored upon Spindly overexpression and to validate that the differences observed are statistically significant compare to the controls.

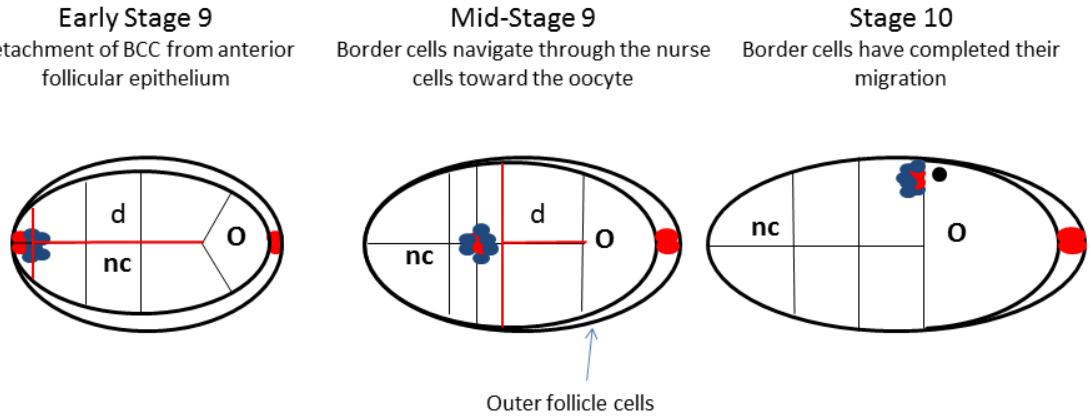

Figure 5- 9: Strategy for a precise staging of stage 9 egg chambers. A stage 9 egg chamber can be easily identified not only by the displacement of the border cell cluster (BCC) from the anterior follicular epithelium but also from the simultaneous migration of the follicle cells toward the oocyte. It is therefore possible to discriminate between early and mid-Stage 9 egg chamber by measuring the degree of migration of the outer follicular epithelium in relation to the nurse cells-oocyte border (distance d in the picture). Polar cells are shown in red are, border cells in blue. O: oocye; nc: nurse cells.

Conversely to what reported for border cell migration, knockdown of Spindly did not perturb significantly the migratory properties of embryonic haemocytes in terms of migratory speed, cell shape and the ability to make protrusions.

These observations suggest that the ability of Spindly to modulate the motile properties of cells varies depending on the biological context. Further experiments are required to investigate how Spindly controls border cell migration and clarify those molecular mechanisms that, if altered, cause the migration phenotypes described in this chapter.

Chapter VI: Results Part III

Identification of potential binding partners of Spindly via Mass Spectrometry

Chapert VI: Results Part III
Identification of potential binding partners of Spindly via Mass Spectrometry

6. Introduction to chapter VI

The study of protein-protein interactions (PPIs) and the identification of new multiprotein complexes provide an important basis for major advances in cell biology. Proteins within a cell rarely function as single entities instead they interact with each other building up intricate interaction networks. These networks define the metabolic and signalling pathways that govern cell viability and their molecular characterisation greatly contribute in understanding how cells integrate and respond to environmental signals.

For a protein of unknown function, the identification of its binding partners has a significant benefit in modelling its cellular activity. In other words, the functionality of a protein can be anticipated on the basis of its interactors and of the biological processes for which their activity is required.

The isolation of proteins by immuno-precipitation followed by Mass Spectrometry analysis (Affinity-purification Mass Spectrometry or AP-MS) has been dominating the field of protein analysis over the past decade, becoming one of the most common methods to perform large-scale studies of protein-protein interactions. Immuno-precipitation is in fact a well-established strategy for the isolation of a bait protein from a protein mixture that combined with the accuracy and sensitivity of mass spectrometry allows the reliable identification of specific and functional PPIs and the characterisation of biological complexes. The development and the optimisation of AP-MS methods were therefore important breakthroughs in the field of proteomics being

beneficial for both, biological and medical research. This method has indeed greatly improved our understanding of the interplay between proteins and of the dynamic assembly of macromolecular complexes in the context of specific cellular and developmental processes. Moreover, the identification of novel, unexpected PPIs has provided an important contribution to our understanding of the molecular mechanisms underlying the development of human diseases that are often caused by the disruption of normal pattern of protein-protein interactions.

The aim of this part of the PhD thesis was to identify novel interaction partners that regulate and modulate the activity of *Drosophila* Spindly *in vivo*. This chapter describes the application of the AP-MS proteomic approach as a tool to design the interaction network of Spindly in the context of *Drosophila* embryo development.

6.1 Identification of binding partners for Spindly

6.2.1 An affinity-purification method to isolate Spindly from *Drosophila* embryos:

One of the limiting steps for a better and comprehensive understanding of Spindly function is the lack of information about its binding partners and their relationship with biological processes. *Drosophila* embryos stand out as a good *in vivo* system for performing AP-MS, providing a powerful and unbiased strategy to build the network of Spindly interactions and get a complete view of the activity of Spindly in the context of *Drosophila* embryo development.

An important precondition to isolate protein complexes containing Spindly is to determine the developmental expression pattern of Spindly protein. *Drosophila* embryos laid by wild-type female flies were collected every two hours over a period of

24 hours and the time-course samples were analysed by Western Blot aiming to detect the embryonic stage(s) at which Spindly is expressed.

Analysis of the expression profile of Spindly during embryogenesis showed that the protein is present up to 10 hours after egg fertilisation (AEF) and its levels declined afterwards (Figure 6-1).

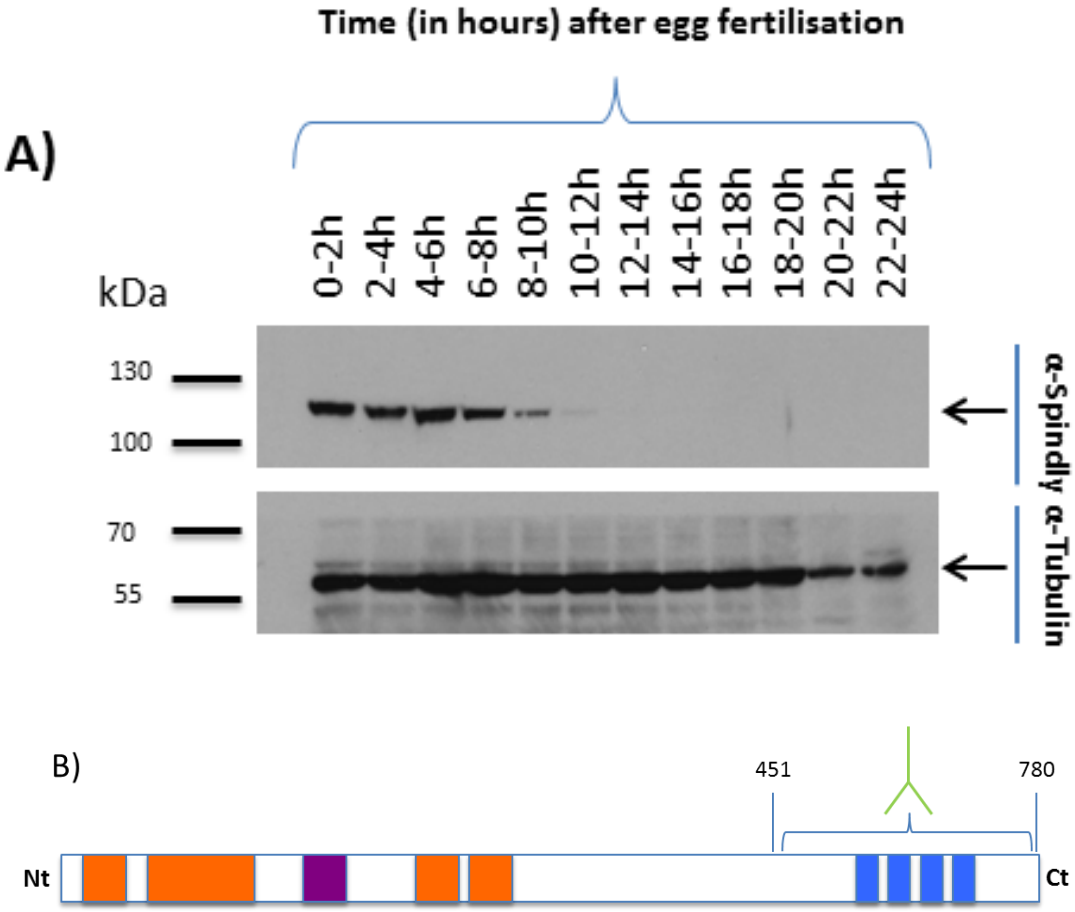

Figure 6- 1: Expression profile of Spindly during embryogenesis. A) Spindly is highly expressed up to 10 hours AEF. Its expression is not detectable during late stages of embryogenesis. Membrane was probed with an affinity-purified antibody raised against the Carboxy-terminal (Ct) half of Spindly (amino acids 451-780). α-Tubulin was included as loading control. For a precise molecular weight determination, a standard protein molecular weight marker in used and numbers in kDa are shown on the left. Dr Z. Lipinszki performed the Western Blot experiment shown in figure. B) Affinity-purified antibody used for Western blot analysis and immunoprecipitation experiments. The antibody was raised against the Ct-terminal epitope of the protein (amino acids 451-780).

Based on this expression pattern, protein lysates for AP-MS were prepared from 0-7 hour old embryos (cleavage and gastrulation stages) and used for immunoprecipitation (IP) experiments. Three independent biological replicates of the IP experiment were performed. For each experiment, embryos were collected at 25°C, washed and lysed in lysis buffer. The protein extracts derived from this procedure were divided into two halves: one half was incubated with either an affinity-purified antibody (Figure 6-1 B) or with serum of an immunised rabbit. Concomitantly, the other half was incubated with either normal rabbit immunoglobulin (IgG) or pre-immune serum as a negative control (Figure 6-3 A).

Since the successful characterisation of protein complexes relies on the ability of isolating the protein of interest along with potential interactors, the efficiency of the extraction method as well as the degree of enrichment of the endogenous Spindly following IP were tested by Western Blot. Aliquots of each fraction (pellet, input, unbound, immunoprecipitate) were collected during the procedure and used for SDS-PAGE. As shown in the representative images of Figure 6-2, the experimental conditions adopted for the IP experiment guaranteed the extraction of the native protein from the embryos. To ensure that during the embryo lysis the protein of interest was extracted and preserved in a soluble fraction, an aliquot of the pellet and the input samples were run on adjacent lane on a SDS-PAGE. The membrane was probed against Spindly. The analysis confirmed the successful extraction of the protein from the embryos (Figure 6-2 A, insoluble fraction, supernatant). In addition, to estimate the efficiency of immunoaffinity isolation of the protein of interest, we compared the amount of Spindly detected in the input (soluble fraction) with the

amount of unbound protein following immune-precipitation (flow-through) (Figure 6-2 A, supernatant, Flow Through).

The efficient isolation of Spindly from the whole-lysate after immunoprecipitation was proved by Western blot analysis (Figure 6-2 B).

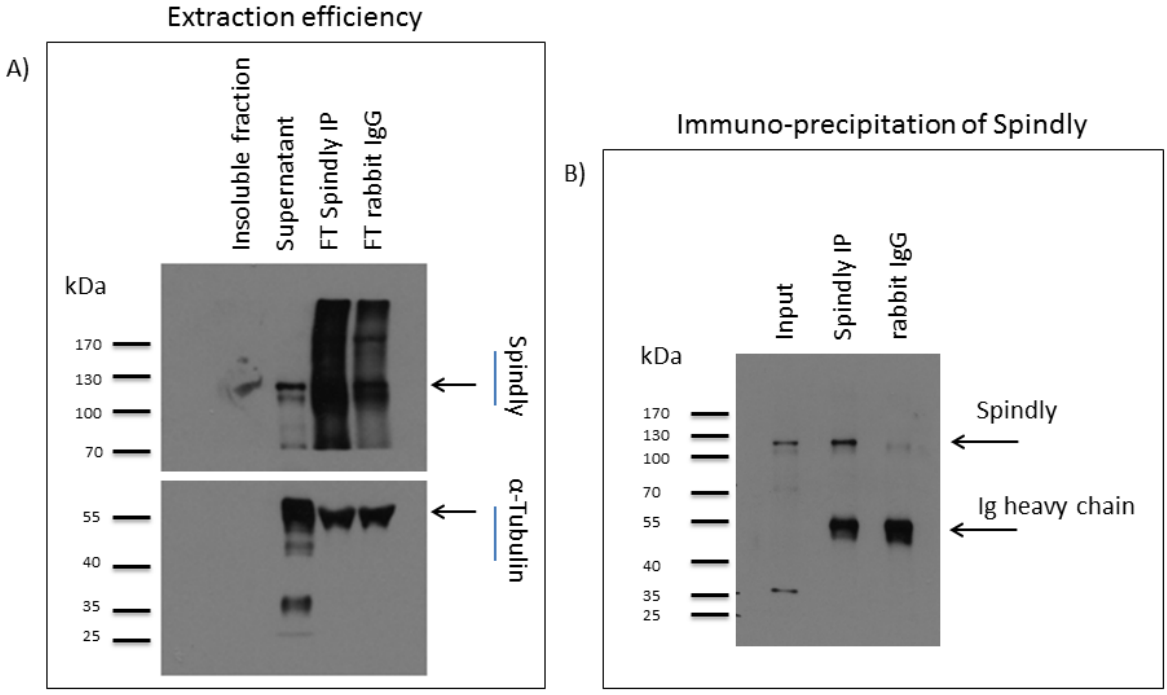

Figure 6- 2: Immunoprecipitation of Spindly. (A) Extraction of *Drosophila* Spindly after immunoprecipitation of the protein from embryos whole-lysate. An aliquot of the pellet (insoluble fraction) and the input (supernatant) samples were run on adjacent lane on a SDS-PAGE and the membrane was probed against Spindly. The Western blot analysis confirmed that both proteins were extracted and preserved in a soluble fraction. Additionally, as a measure of the efficiency of immunoaffinity isolation of the proteins of interest, an aliquot of unbound protein following immune-precipitation (flow-through, FT) was run on adjacent lanes. (B) Detection of *Drosophila* Spindly after immunoprecipitation of the protein from embryos whole-lysate. The images are representative of more than three independent Western blot experiments. A standard protein molecular weight marker is included and numbers in kDa are shown on the left.

In order to identify novel interactors associated in complexes with the endogenous Spindly, the immunoprecipitates were eluted from beads, digested into peptides and processed for Mass Spectrometry (MS) analysis. To determine the level of variability, technical replicates of the MS run were performed for two of the three biological

replicates. The protein lists obtained from each pair of technical replicates were compared to one another and the overlapping hits constituted a unique dataset (Figure 6-3 B).

Hereafter, we will refer to the different datasets as “Spindly IgG dataset”, “Immunoserum dataset 1” and “Immunoserum dataset 2” respectively, indicating the protein lists resulting from the biological replicate number 1 and those lists resulting from the biological replicates number 2 and 3 (Figure 6-3 B).

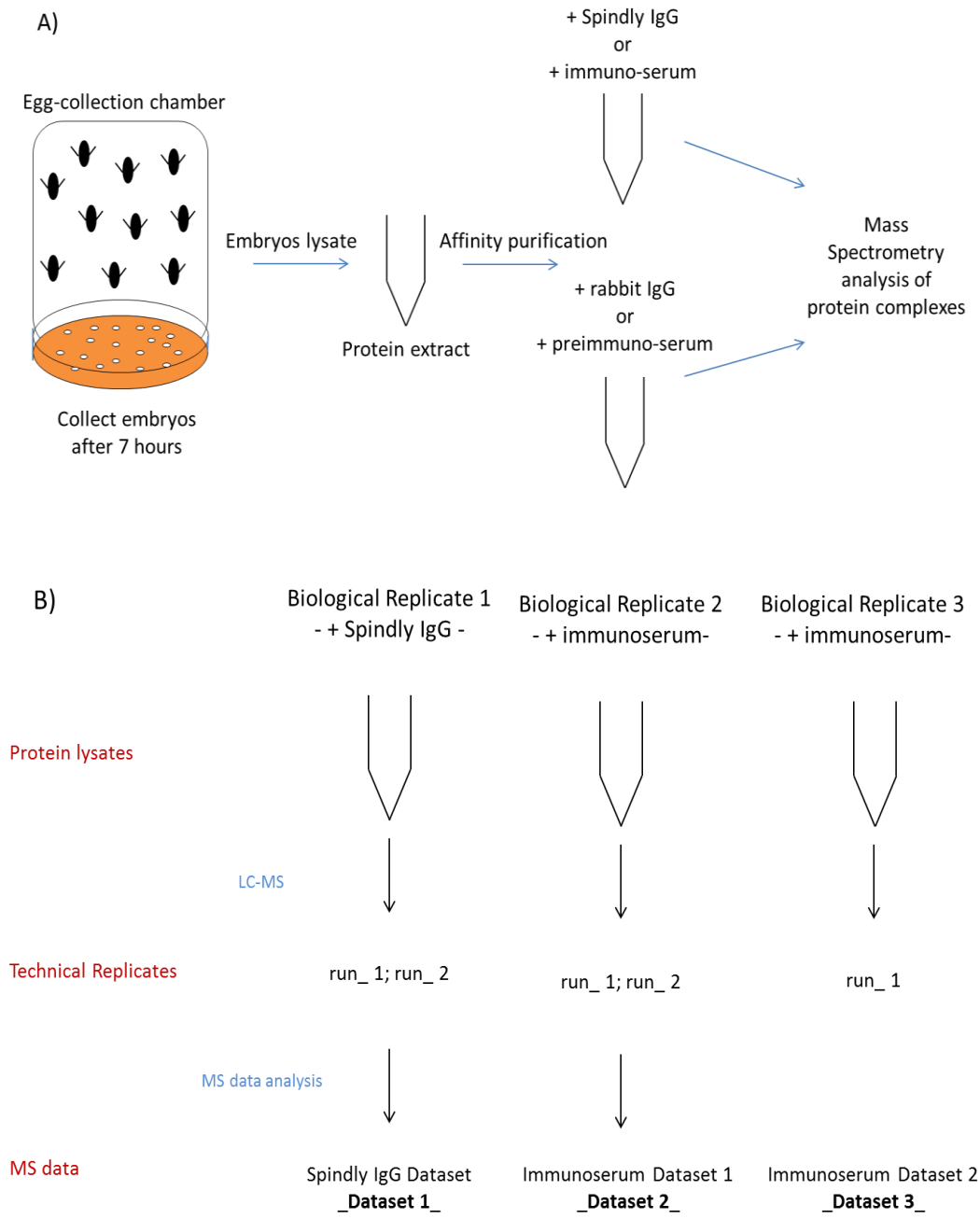

Figure 6- 3: Affinity-purification Mass Spectrometry (AP-MS) procedure to identify binding partners of Spindly. A) Schematic of the AP-MS procedure adopted in this study. Wild-type flies were places in egg-collection chambers and females laid eggs for seven hours. Embryos were collected and processed for protein extraction. The embryos whole-lysate was used for immunoprecipitation experiments. The isolated immune complexes were eluted from beads, lyophilised and processed for MS analysis. B) The picture summarises the number of biological and technical replicates performed. Proteins were enzymatically cleaved, separated by liquid-chromatography and analysed in the mass spectrometer. For the biological replicates number 1 and 2, the MS run was performed in duplicate (Technical Replicates 1 and 2). The analysis of the MS data resulted in three distinct protein lists (Datasets 1, 2, 3).

As for any other analytical technique, sample preparation is an important step in mass spectrometry-based approaches. Sample mishandling introduces bias into the analysis resulting in high background signal and artefacts that will affect the final detection of proteins. In this regard, a standard procedure in proteomics is to evaluate the quality of MS/MS runs by plotting the average intensity values of each identified protein against the protein count to assess the statistics of the entire population of potential interacting partners for a given bait protein. Good quality data are graphically represented by a bell-shaped Gaussian curve (Figure 6-4). In a normal distribution, the majority of proteins are expected to cluster around a centre resulting in a symmetric bell-shape Gaussian curve. The bait protein and its potential binding partners are characterised by the highest intensity value and are therefore expected to populate the right side of the graph. Finally, the remaining proteins (left side of the graph), characterised by lowest mean intensity values, are likely to be contaminants. Skewed data distributions are indicative of bias in the dataset arising from various technical limitations, such as protein degradation or human error in the experimentation. This kind of analysis is therefore informative in proteomics as it provides a readout of data quality and helps to empirically identify proteins with a higher level of enrichment and therefore likely binding partners of the bait (Figure 6-4).

The quality of the MS runs for each single biological replicate was evaluated using several means; starting by studying the population statistics of the entire population of potential interacting partners for Spindly, as described (Figure 6-5).

Secondly, the reproducibility and quality of the AP-MS procedure was estimated by performing correlation studies between technical and biological replicates. For each pair-wise comparison, the Log_2 Intensity values of the samples were plotted against

each other and the degree of correlation was measured calculating the Pearson's Correlation Coefficient (PCC). High correlation between samples was associated with a PCC of 0.7 or higher. The technical replicates of the AP-MS experiments 1 and 2 correlated with a PCC of above 0.8, indicating that these mass spectrometry runs were very good replicates of each other (Figure 6-6). However, the correlation study between the different biological replicates revealed a moderate level of correlation (0.3<PCC<0.5). This difference may reflect variations in the experimental conditions, such as a different efficiency of the IP procedure, as confirmed by the comparison of the intensity values relative to Spindly across multiple MS runs (Table 6-1). The most efficient enrichment of Spindly was achieved by using the affinity-purified antibody (Biological Replicate 1) as deduced by calculating the ratio between the Intensity values of the IP sample (I_{IP}) over the intensity values of the Control (CTRL) sample (I_{CTRL}). Conversely, the use of the rabbit immune-serum was found to be less reliable in isolating endogenous Spindly from the whole embryo-lysate. Moderate levels of the bait protein were enriched in the Biological Replicate 2 while the outcome of the IP procedure was poor for the third Biological replicate, with Spindly being found to be equally enriched in the IP sample and in the control.

Taking into account this analysis, it is reasonable to predict that the comparison between dataset 1 and 2 will allow the identification of a greater number of potential binding partners for Spindly, giving a better overview on the network of Spindly interactions.

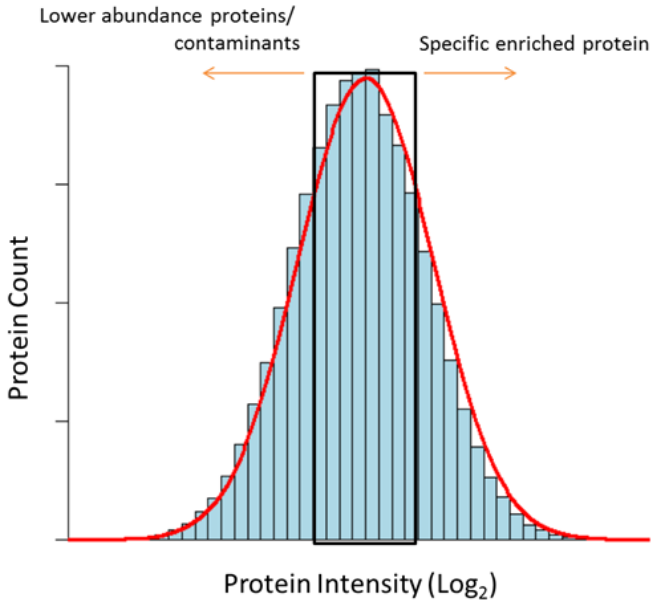

Figure 6- 4: Population Statistics. The figure is a representation of a normal distribution of average protein intensity values (log_2). In a bell-shape distribution, the proteins with the highest protein count are considered to be contaminants (black box). The hits that populate the right side of the graph are the enriched proteins, likely to be specific binding partners for the bait. Finally, the lower abundance proteins constitute the left side of the graph and are either weak interactors or contaminants.

	Protein IDs	Gene name	PEP	Peptides Count	Sequence coverage [%]	I_{CTRL}	I_{IP}	I_{IP}/I_{CTRL}
Biological replicate 1	Q9VQS4	Spindly	0	36	57.5	1042700	247100000	236.980915
Technical Replicate 1	Q4V527	CG15415	0	33	43.4	0	33612000	
Technical Replicate 2	Q9VQS4	Spindly	0	51	65	3401000	1421700000	418.024111
	Q4V527	CG15415	0	39	48.2	0	107130000	
Biological replicate 2								
Technical Replicate 1	Q9VQS4	Spindly	0	8	12.8	1876600	5228600	2.7862091
	Q4V527	CG15415	0	8	11.9	0	863420	
Technical Replicate 2	Q9VQS4	Spindly	0	19	30.7	3956100	65106000	16.4571169
	Q4V527	CG15415	0	18	26.1	0	7972200	
Biological replicate 3								
	Q9VQS4	Spindly	0	8.5	6	4024600	6921100	1.71969885
	Q4V527	CG15415	0	6.2	5	0	0	

Table 6- 1: Summary of the intensity values for Spindly. The Intensity values relate to the abundance of the bait protein in the AP mixture and provide a measurement of the IP efficiency. The comparison of the ratio between the Intensity values of the IP sample (I_{IP}) over the intensity values of the Control (CTRL) sample (I_{CTRL}) across the replicates highlight a reduced enrichment of Spindly in the third biological replicate, pointing at an inefficient affinity-purification of the endogenous Spindly from the whole-lysate.

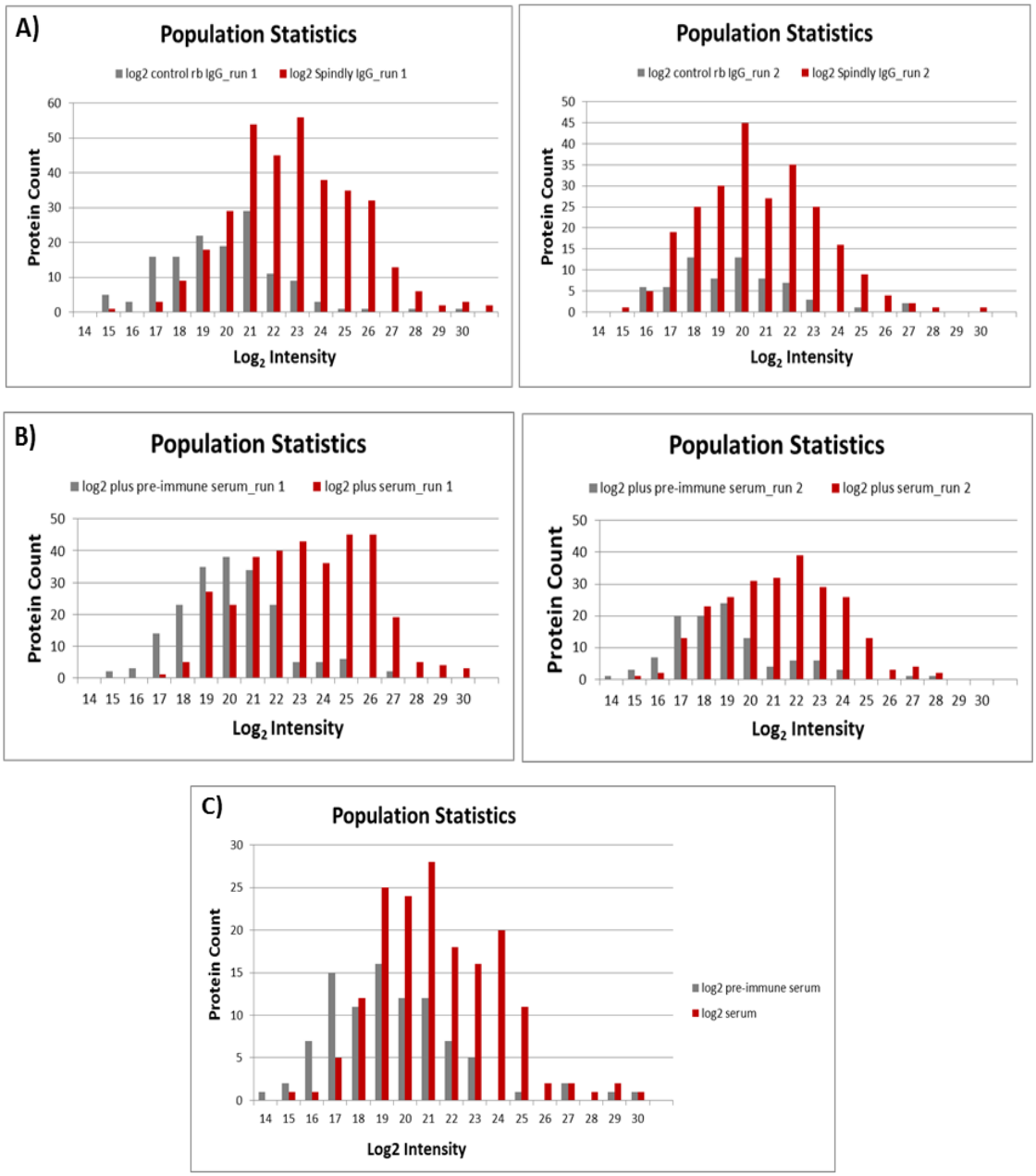

Figure 6- 5: Normal distribution of average protein intensities (log_2). The graphs are realised plotting the mean protein intensity values (log_2) versus the number of proteins and show the normal protein intensity distribution for the MS runs of each biological replicate (A: Biological Replicate 1; B: Biological Replicate 2; C: Biological Replicate 3).

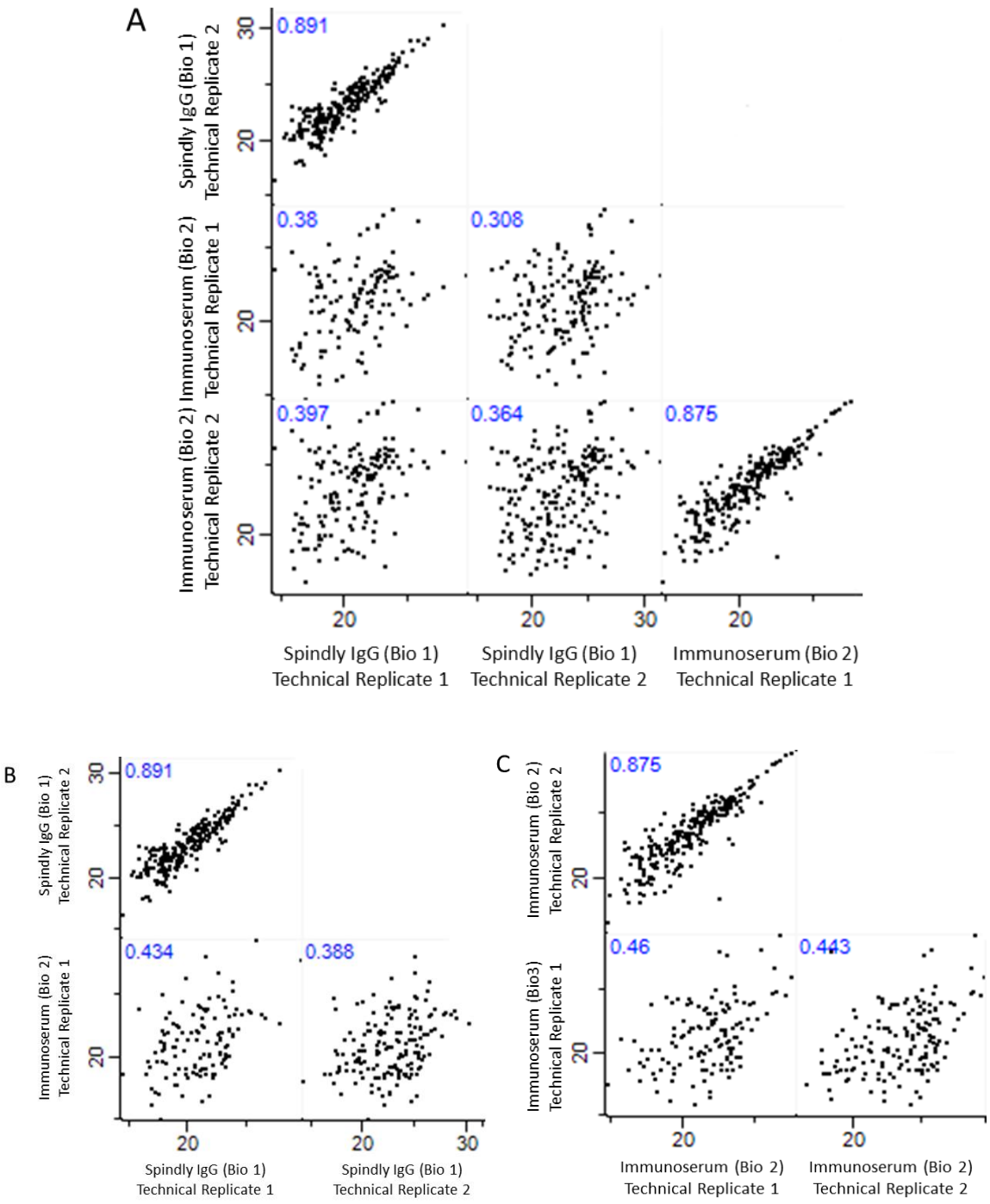

Figure 6- 6: Intensity correlation study of the AP-MS samples. The graphs show the correlation between technical and biological replicates. Graphs in (A) represent the pair-wise comparisons between the Log (2) intensity values of the biological replicates 1 and 2. Graphs in (B) and (C) represent the pair-wise comparison between Log (2) intensity values of the biological replicates 1 and 3 and the biological replicates 2 and 3, respectively. Numbers in light blue represent the Pearson's correlation coefficient. Good correlation is associated to a PCC value of 0.7 or higher. Correlation analysis was performed using the freeware software Perseus (http://141.61.102.17/perseus_doku/doku.php?id=start).

6.2 Analysis and comparison of the protein datasets for the identification of putative binding partners of Spindly

As previously mentioned, little is known about the protein interactions that Spindly establishes during development and this limited knowledge restricts our understanding about the mechanisms of its activity. The AP-MS technique has been adopted in this study as a sensitive and accurate method to isolate protein complexes and solve the complexity of the Spindly interactome. To face this problem, we undertook an unbiased approach to analyse and compare our protein datasets aiming at establishing a reliable selection of putative interactors of Spindly.

The MS/MS datasets were analysed using the MaxQuant software package with the aim of identifying proteins enriched in the affinity-purified complexes (Cox and Mann 2008). One of the limitations of the IP procedure is the isolation of a high amount of non-specific binders along with putative interactors. Therefore, to reliably identify likely interactors of Spindly by analysing the IP datasets, it is necessary to determine the range of non-specific binding. To assess the rate of false identification, the MaxQuant software searches the raw data files against both, a forward *Drosophila* database and a reverse (or decoy) one. Any peptide that aligns with the decoy database is considered as false positive and therefore discarded. The probability of false identification is associated to a specific false-discovery rate (FDR) value. For this specific experiment, the FDR cutoff score was set to 1%, meaning that 1% of the identification in the forward dataset were false hits. Additionally the raw data are run against a contaminants database (CON database) aiming to eliminate all those candidates that are common contaminants, such as keratins. Therefore, using a

combination of three different databases, Max Quant facilitates the elimination of all those false hits that could compromise the analysis.

To enrich for a selection of the most likely candidates, we adopted the following strategy. Firstly, for each potential positive hit we took into account the number of peptides that identified it and the posterior error probability (PEP score), a statistic value that measures the probability of the identification. On the base of these parameters we considered as false hits all those proteins that were identified by a single peptide and associated with PEP value higher than 0.05.

Secondly, the list of proteins of each single biological replicate was normalised to the relative control sample. The correlation between each individual sample and the relative control was determined and all the proteins that were equally enriched in the IP sample and in the relative control were discarded (Figure 6-7, red squares).

For the remaining hits, we took into account the intensity values associated to each peak in the spectrum and we selected for proteins that were either present only in the IP sample and not in the negative control or enriched at least 5-fold more in the IP sample compared to the control.

The procedure here described and the final number of proteins identified for each biological replicate is reported in Table 6-2.

Biological Replicate 1		Technical Replicate 1	Technical Replicate 2
	potential results	330	289
	present in the control	121 (90 of which enriched 5-fold more in the IP sample)	90 (33 of which enriched 5-fold more in the IP sample)
	1 peptide; p value> 0.05	13	60
	short-list	**196**	**139**
Biological Replicate 2			
	potential results	252	247
	present in the control	44 (10 of which enriched 5-fold more in the IP sample)	124 (73 of which enriched 5-fold more in the IP sample)
	1 peptide; p value> 0.05	10	82
	short-list	**260**	**142**
Biological Replicate 3			
	potential results	184	
	present in the control	90 (38 of which enriched 5-fold more in the IP sample)	
	1 peptide; p value> 0.05	61	
	short-list	**70**	

Table 6- 2: The table summarises the elimination process for putative Spindly interacting proteins identified by MS/MS. The final number of identified candidates (short-list) is reported for the three biological replicates of the experiment.

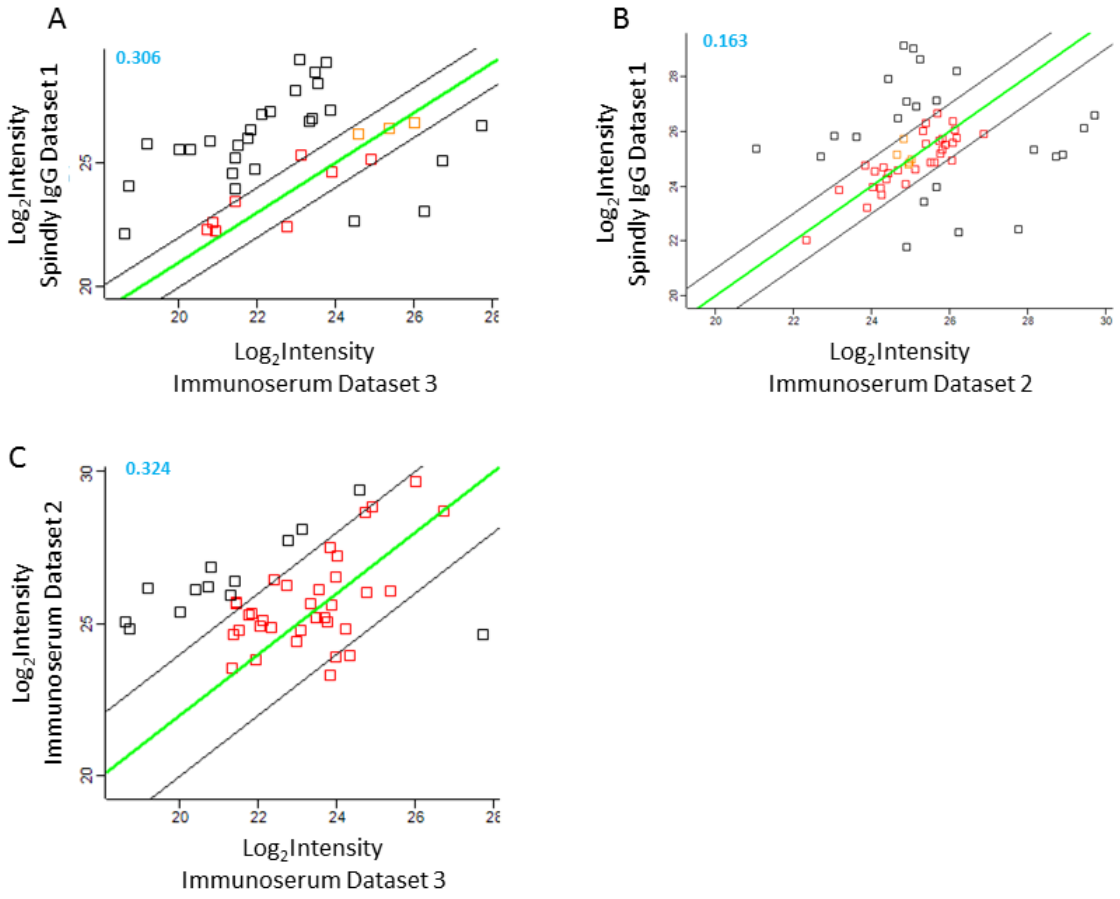

Figure 6- 7: Pair-wise correlation comparison of each MS run to the relative control. The graphs show the correlation between each MS run and the relative control. Graphs in (A), (B) and (C) refer to the technical replicates of the MS runs performed for each biological replicate. Graphs were realised plotting the Log (2) intensity values of the IP versus the relative control. Numbers in light blue represent the Pearson's correlation coefficient. In each dot-plot, the red squares indicate proteins with same intensity value in IP sample and control. Correlation analysis was performed using the freeware software Perseus.

Before proceeding with the final identification of *bona fide* interactors of Spindly, the normalised datasets obtained from each pair of technical replicates were compared to one another and the overlapping hits constituted a unique dataset (Figure 6-8). The final protein lists of each Dataset are reported in Appendix (Supplemental information, CD-ROM).

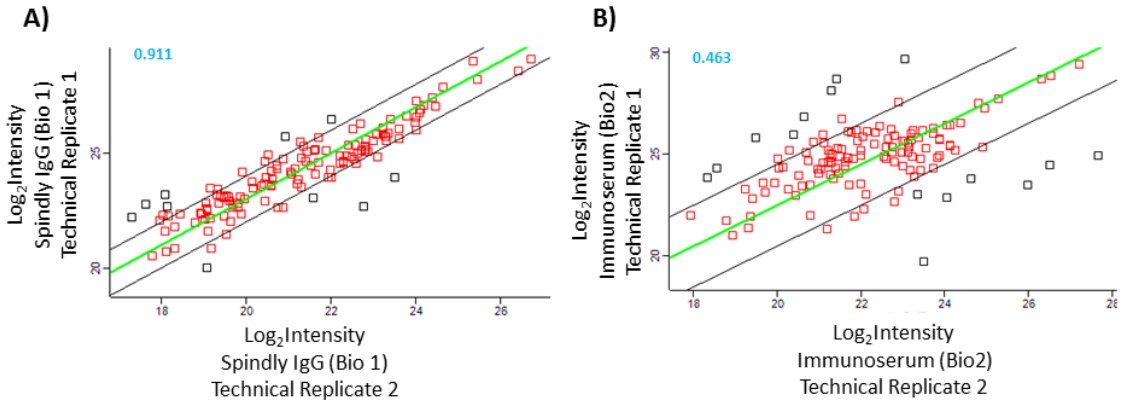

Figure 6- 8: Correlation analysis between the technical replicates of the AP-MS experiment 1 and 2. The normalised datasets resulting from the analysis of technical replicates 1 and 2 of the biological replicate 1 (A) and 2 (B) were compared to each other to obtain the final shortlists (Dataset 1 and Dataset 2). Graphs were realised plotting the Log (2) intensity values of the replicate 1 versus those one of the replicate 2. Numbers in light blue represent the Pearson's correlation coefficient for each dot-plot. In each graph, the red squares indicate proteins with the highest correlation that will constitute a unique shortlist. Correlation analysis was performed using the freeware software Perseus.

To analyse reproducibility between the distinct biological replicates and draw up a reliable network of biologically significant interactions, the three final shortlists were compared to each other (Figure 6-9). In a way of identifying high-confidence interactors for Spindly we scored as positive hits those proteins that were common to all the three independent biological replicates.

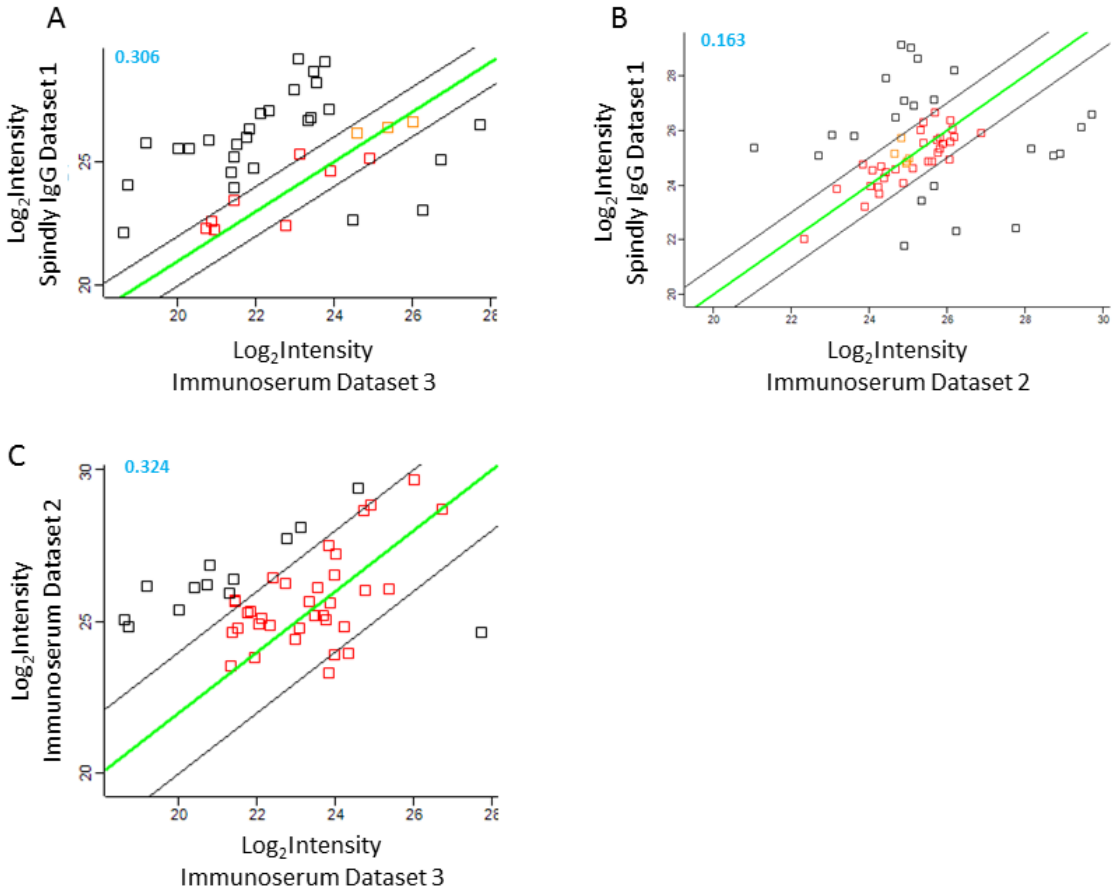

Figure 6- 9: Correlation analysis between the final datasets for the identification of *bona fide* binding partners of Spindly. The normalised datasets 1, 2 and 3 were compared in pairs. Numbers in light blue represent the Pearson's correlation coefficient for each dot-plot. In each graph, the red squares indicate proteins with the highest correlation and therefore likely interactors of Spindly. Correlation analysis was performed using the freeware software Perseus.

This strategy resulted in a final short-list of 29 high confident candidates, of which 17 were ribosomal proteins (Figure 6-10 A and B). The complete list of candidates is reported in Appendix (Supplemental information, CD-ROM).

A)

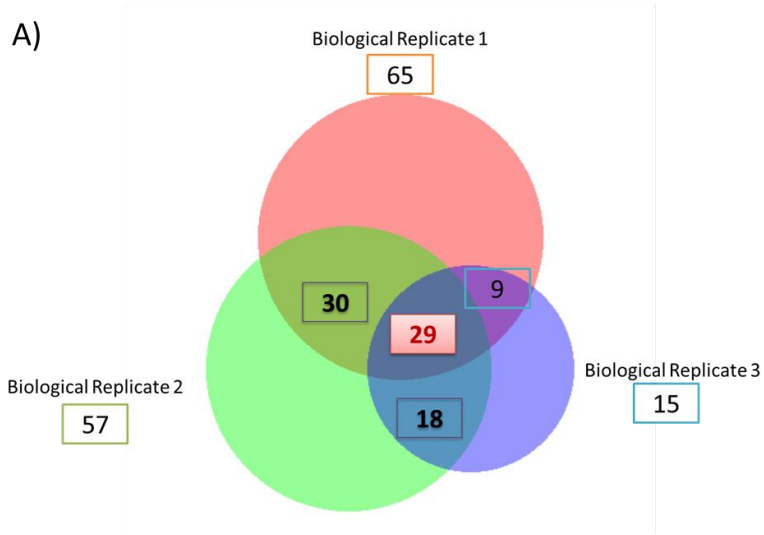

B)

Comparison between Biological Replicates	Number of common hits
Biological Replicate 1-2	30
Biological Replicate 1-3	9
Biological Replicate 2-3	18
Biological Replicate 1-2-3	29

Figure 6- 10: Comparison of the three datasets. A) The Venn diagram shows the number of common proteins identified by comparing the three short-lists. The image was generated using the open sources BioVenn (http://www.cmbi.ru.nl/cdd/biovenn/). B) The table summarises the degree of overlapping between the three distinct datasets. All pairwise comparisons are reported.

To describe the functional interactions between these hits and the biological processes on which their activity impinges, we performed *in silico* analysis. A good variety of software is freely available to question the literature and perform network analysis. Of these software packages, STRING is one of the most widely used (http://string.db.org/;(Jensen, Kuhn et al. 2009)). STRING is a database that collects all the available information about already known physical and functional interactions derived from experimental data, knowledge stored in the literature and computational predictions and it integrates them to reconstruct a network of protein-protein association for any given biological process.

The bioinformatics tool String was therefore used to link the protein hits identified by MS together and predict the biological significance of each individual functional interaction (Figure 6-11). This clustering strategy was combined with Gene Ontology analysis for biological processes in order to provide a systematic description of the biological functions of candidates. The Gene Ontology Analysis was carried out using the DAVID Functional Annotation Tool (http://david.abcc.ncifcrf.gov/). We found that some of these genes are involved in cell division (26%), mitotic spindle organisation and elongation (26%) and microtubule-based processes (37%) (Figure 6-12 A). A list of the genes required for these processes is provided in Figure 6-12 B.

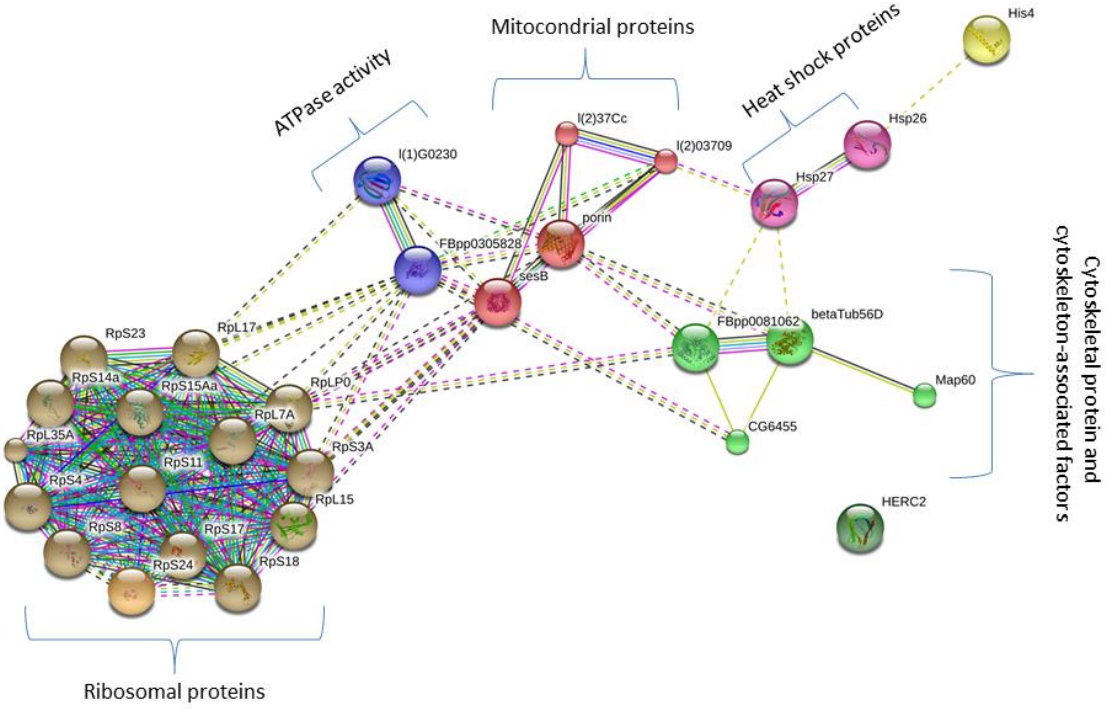

Figure 6- 11: STRING analysis of protein-protein interactions. The figure is a summary of the known and predicted interactions between 29 of the potential binding partners for Spindly. Each protein is represented by a node. Proteins grouped in the same cluster have the same colour code. Protein interactions inside a given cluster are represented by solid lines. Inter-cluster interactions are represented by dashed-lines.

A)

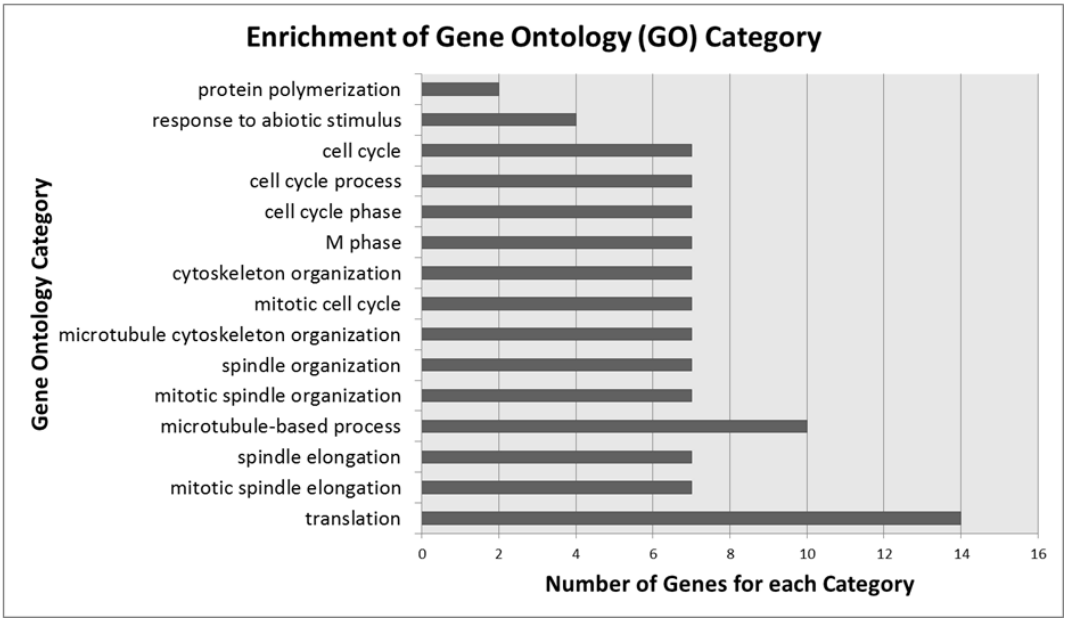

B)

Protein names	Flybase Gene ID	PEP	Peptide BioRep 1	Peptide BioRep 2	Peptide BioRep 3
Tubulin beta-1 chain	FBgn0003887	0	23	5	5
Map60	FBgn0010342	2.30E-194	17	13	12
60S ribosomal protein L15	FBgn0028697	1.05E-111	7	5	2
40S ribosomal protein S18	FBgn0010411	4.31E-64	9	5	4
40S ribosomal protein S4	FBgn0011284	3.14E-63	12	8	6
40S ribosomal protein S3a	FBgn0017545	1.65E-55	10	4	3
60S ribosomal protein L7	FBgn0014026	2.27E-35	9	4	2
60S ribosomal protein L17	FBgn0029897	1.68E-16	4	4	2

Figure 6- 12: Enrichment of Gene Ontology (GO) Category of the genes forming the network. A) GO enrichment of 29 hits identified as potential binding partners for Spindly by comparing the datasets of the three biological replicates. The analysis was performed using the Bioinformatics resource DAVID version 6.7. B) List of proteins that could potentially implement Spindly activity during mitosis. These candidates contribute to microtubule-based processes, cytoskeleton organisation, mitotic spindle organisation and elongation and cytokinesis. Proteins are listed in increasing order of PEP value.

Furthermore, we performed *in silico* analysis of those 57 candidates that were present at least across two independent biological replicates (Figure 6-10). Clustering combined to GO analysis revealed that some of these genes are involved in cell division (10%) and mitotic spindle organisation and elongation (40%) (Figure 6-13 and Figure 6-14).

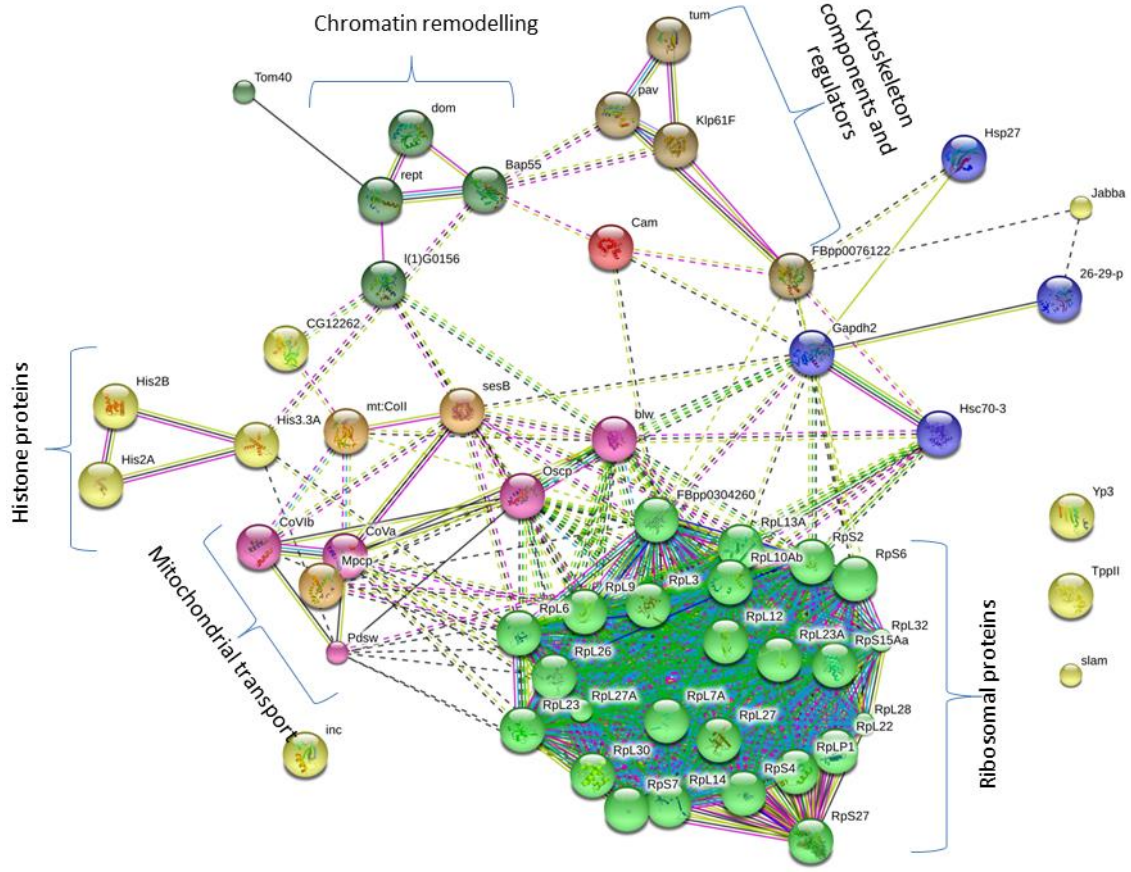

Figure 6- 13: STRING analysis of protein-protein interactions. The figure is a summary of the known and predicted interactions between 57 of the potential binding partners for Spindly. Each protein is represented by a node. Proteins grouped in the same cluster have the same colour code. Protein interactions inside a given cluster are represented by solid lines. Inter-cluster interactions are represented by dashed-lines.

A)

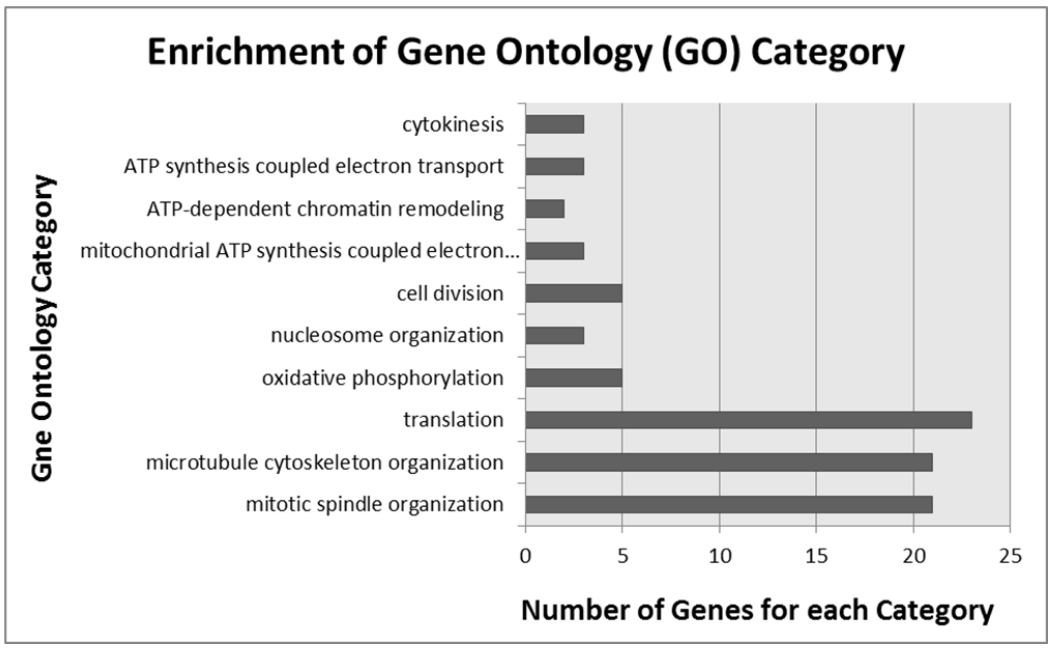

B)

Protein names	Flybase Gene ID	PEP	Peptide BioRep 1	Peptide BioRep 2	Peptide BioRep 3
60S ribosomal protein L10a-2	FBgn0036213	5.64E-98	7	5	-
Bipolar kinesin KRP-130 (Klp61F)	FBgn0004378	3.60E-92	-	2	15
60S ribosomal protein L3	FBgn0020910	3.30E-80	11	4	-
Tubulin alpha-4 chain	FBgn0087040	1.20E-77	12	-	2
60S ribosomal protein L22	FBgn0015288	6.56E-62	9	7	-
Pavarotti	FBgn0011692	3.44E-61	-	4	7
Ribosomal protein L6	FBgn0039857	1.25E-59	8	8	-
Brahma associated protein 55kD	FBgn0025716	7.24E-56	9	-	2
60S ribosomal protein L7a	FBgn0014026	1.77E-44	4	4	-
60S ribosomal protein L23	FBgn0010078	4.84E-44	-	2	2
60S ribosomal protein L9	FBgn0015756	4.18E-42	8	3	-
Ribosomal protein L12	FBgn0034968	5.85E-42	5	5	-
60S ribosomal protein L32	FBgn0002626	1.48E-41	3	2	-
60S ribosomal protein L30	FBgn0086710	2.39E-41	4	4	-
tumbleweed	FBgn0086356	1.8E-33	-	3	7
Ribosomal protein L23 A	FBgn0026372	8.47E-29	7	3	-
Calmodulin	FBgn0000253	2.50E-26	5	2	-
60S ribosomal protein L28	FBgn0035422	1.50E-21	6	3	-
60S ribosomal protein L14	FBgn0017579	1.09E-20	5	4	-
Ribosomal protein L26	FBgn0036825	2.22E-16	2	4	-
60S ribosomal protein L27	FBgn0039359	1.25E-10	7	6	-

Figure 6- 14: Enrichment of Gene Ontology (GO) Category of the genes forming the network. A) GO enrichment of 57 hits identified as potential binding partners for Spindly from the pair-wise comparisons of the three Datasets. The analysis was performed using the Bioinformatics resource DAVID version 6.7. B) List of proteins that could potentially implement Spindly activity during mitosis. These candidates contribute microtubule-based processes, cytoskeleton organisation, mitotic spindle organisation during mitosis. Proteins are listed in increasing order of PEP value.

In addition to the analysis described, we further investigated the remaining 65 protein hits constituting the Spindly IgG Dataset (Figure 6-10). Judging from the efficiency of the affinity purification (Table 6-1) and the high level of correlation between the normalised technical replicates (Figure 6-8 A), the AP-MS experiment performed using the affinity-purified antibody resulted to be the most successful and a deeper analysis of the Spindly IgG Dataset could improve our knowledge about the network of Spindly interactions. As previously described, we performed clustering and GO analysis (Figure 6-15 and Figure 6-16) and we identified additional genes involved in microtubule-based processes (18%) and mitotic spindle organisation (12%), even if additional experiments are required to validate these interactions.

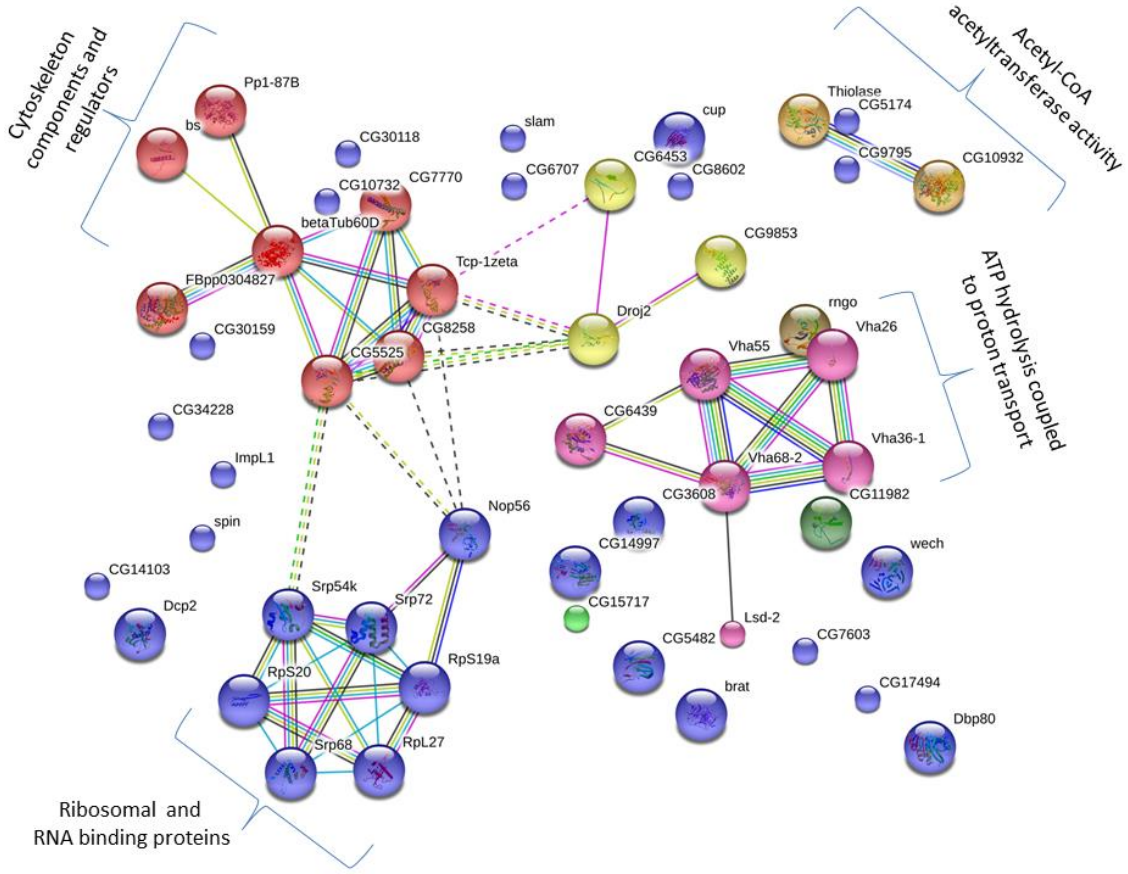

Figure 6- 15: STRING analysis of protein-protein interactions. The figure is a summary of the known and predicted interactions between 65 potential binding partners for Spindly (Spindly IgG Dataset). Each protein is represented by a node. Proteins grouped in the same cluster have the same colour code. Protein interactions inside a given cluster are represented by solid lines. Inter-cluster interactions are represented by dashed-lines.

A)

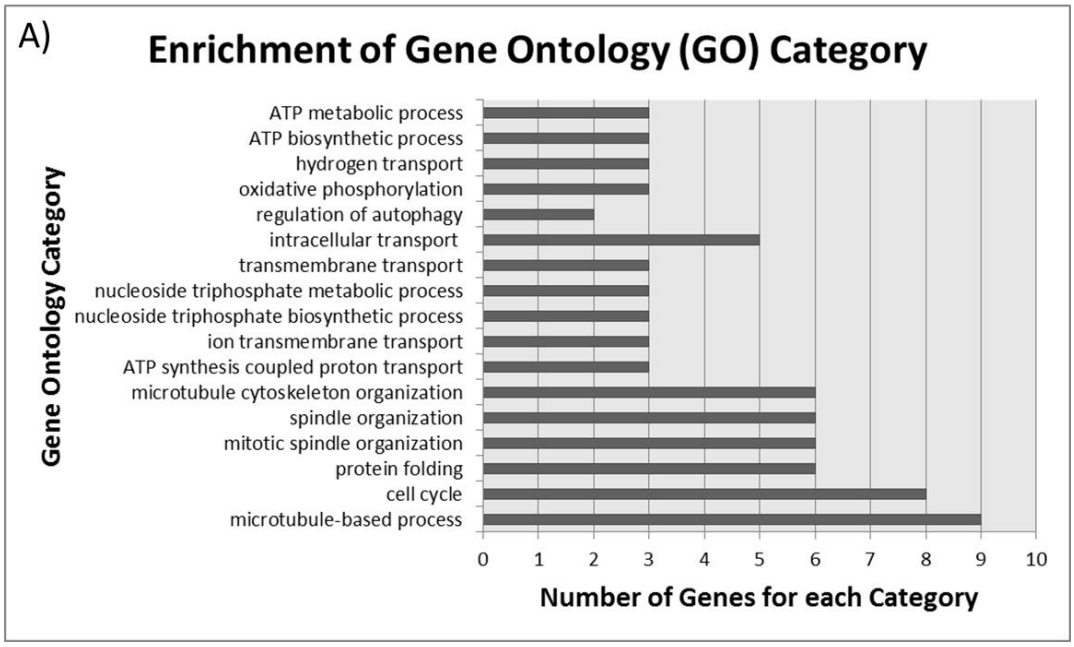

B)

Protein names	Gene names	Flybase Gene ID	PEP	Peptides
	beta-Tub60D	FBgn0003888	2.67E-131	23
Tcp-1zeta	CG8231	FBgn0027329	1.00E-125	4
Serine/threonine-protein phosphatase alpha-2 isoform	CG9156	FBgn0003132	6.53E-107	4
	CG8258	FBgn0033342	2.59E-90	15
	CG10932	FBgn0029969	2.21E-41	5
60S ribosomal protein L27a	RpL27A	FBgn0261606	3.85E-20	7
Tubulin gamma-2 chain	gammaTub37C	FBgn0010097	4.28E-15	8
T-complex protein 1 subunit delta	CG5525	FBgn0032444	2.05E-13	4

Figure 6- 16: Enrichment of Gene Ontology (GO) Category of the genes forming the network. A) GO enrichment of 65hits identified as potential binding partners for Spindly from Dataset 1 (Spindly IgG Dataset). The analysis was performed using the Bioinformatics resource DAVID version 6.7. B) List of proteins that could potentially implement Spindly activity during mitosis. These candidates contribute microtubule-based processes, cytoskeleton organisation, mitotic spindle organisation during mitosis. Proteins are listed in increasing order of PEP value.

6.3 Identification of two potential interactors of Spindly

The experiments described in this chapter sought to identify interacting partners for Spindly, combining the immunoprecipitation procedure to MS analysis.

The analysis of the protein datasets and the comparisons of the final short-lists allowed the identification of two putative interactors that could assist Spindly during mitosis. These proteins are Map-60 and Klp61F.

Identified in 1992, Map-60 is also known as CP-60 and it has been shown to have bi-functional activity, shuttling between centrosome and microtubules depending on the phase of the cell cycle. This protein is part of a multi-protein complex that localises at the centrosome and whose stability is controlled by phosphorylation in a cell-cycle specific manner. Once released from the complex as a consequence of decreased phosphorylation, Map-60 shows increased affinity for microtubules (Jordan W. Raft 1993, Douglas R. Kellogg 1995).

The other putative interactor is Klp61F, a kinesin-like protein. A phosphorylated version of this protein is involved in the formation of the mitotic spindle, in the regulation of spindle poles positioning and in the control of the activity of the mitotic spindle during chromosome segregation. The protein performs its function by cross-linking and sliding apart anti-parallel microtubules, helping the assembly and stabilisation of a bipolar spindle (David J. Sharp, à et al. 1999).

Therefore, these two candidates can be considered for further analysis and functional validation. Clarifying the significance of these interactions will provide further insights into the mechanisms by which Spindly acts during mitosis.

6.4 Concluding remarks

This chapter has described the development of an AP-MS approach to identify potential binding partners of Spindly. Even though this method has provided a list of possible candidates, opening up a variety of scenarios for which the activity of Spindly may be required, it needs to be improved as highlighted by some technical limitations.

The IP experiment was performed independently three times and technical replicates of the MS run were included to limit inconsistency due to experimental variation, such as machine and human errors. For two out of three runs, the number of shortlisted proteins was comparable. For the third biological replicate instead the number of candidates that were identified was two times smaller. Conceivably, this discrepancy is due to technical problems such as inefficient immunoprecipitation of the endogenous Spindly, as suggested by the comparison of the intensity values relative to the Spindly protein across multiple MS runs.

A striking observation that comes from the analysis of all the three short-lists is the absence of proteins for which indirect evidences of an interaction with Spindly have been reported in literature before. Examples of these potential binding partners are the components of the RZZ complex and cytoplasmic dynein, which are known to bind Spindly at the kinetochore during mitosis, and the microtubule-binding protein EB-1, which is thought to interact with Spindly during interphase (Griffis, Stuurman et al. 2007). Two possibilities could explain the lack of previously documented interactors in all the three datasets. The conditions applied might not be suitable enough to ensure the pull-down of all the native protein-protein complexes and to allow the detection of low-affinity and labile interactions, suggesting that the IP protocol needs to be optimised. The second possibility relates to the relative abundance of the proteins in the AP mixture and with the tendency of the AP-MS method of detecting preferentially stable and highly enriched interactors. Therefore the inability of identifying some of the known binding partners for Spindly is possibly justified by the lower abundance of these factors in the protein mixture, by the transient nature of the binding or by the specific developmental stage at which the interaction occurs.

Lastly, a common problem when performing high-throughput screening based on the analysis of AP-MS datasets is the adoption of filtering strategy to eliminate false positives and increase the accuracy of PPIs identification. Indeed the immunoprecipitation is a technique that normally results in the isolation of a variety of contaminants. These contaminants are normally highly abundant proteins such as actin, tubulin, ribosomal proteins and heat-shock proteins. Therefore the identification of *bona fide* binding partners for a given proteins relies on appropriate experimental design and controls, enabling the discrimination between contaminants and true interactors.

Chapter VII: Discussion

Chapter VII: Discussion

7. Introduction to chapter VII

Identified in 2007, *Drosophila* Spindly is the founder of a family of proteins that act as positive regulators of the metaphase-to-anaphase transition, (Griffis, Stuurman et al. 2007, Chan, Fava et al. 2009, Barisic, Sohm et al. 2010, Gassmann, Holland et al. 2010). Further analysis points to Spindly as crucial coordinator between chromosome alignment and cell cycle progression and suggests an important role in coupling achievement of bi-orientation to SAC deregulation (Gassmann, Essex et al. 2008). With the exception of one study that aimed to characterise the mitotic functions of the *C. elegans* homologue (Gassmann, Essex et al. 2008), the biological activity of Spindly has been established using tissue culture cell lines. Therefore, the contribution of Spindly to the correct execution of mitosis in the context of a living organism remains largely obscure. Additionally, experiments performed on *Drosophila* S2 cells suggested a potential post-mitotic activity of Spindly in the control of cytoskeleton remodelling in post-mitotic cells but this suspected activity has remained unexplored (Griffis, Stuurman et al. 2007).

Moreover, thus far nothing is known about the functional relevance of Spindly's protein domains. The homologues of the Spindly family have been identified on the basis of the structural conservation of the amino-terminal coiled-coil domains and the presence of a highly conserved motif, known as Spindly box, in the amino-terminal half of the protein. However, the domains important for these protein function(s) are still waiting to be identified. A structure-function analysis has been performed for the human homologue (Barisic, Sohm et al. 2010). This study has classified the carboxy-

terminal half of the protein as the domain essential for its kinetochore localisation. Later reports showed that the C-terminal half of the protein undergoes farnesylation and that this post-translational modification is essential for hSpindly to bind to the kinetochore (Holland, Reis et al. 2015, Moudgil, Westcott et al. 2015). In addition Barisic et al. also identified those domains required for the displacement of hSpindly from the kinetochore upon microtubule attachment (Barisic, Sohm et al. 2010). However, this kind of information is missing for the other homologues of the family, including *Drosophila* Spindly.

Finally, a better and comprehensive understanding of Spindly function relies on the identification of its binding partners. Co-imunoprecipitation experiments confirmed the binding of Spindly to the RZZ complex for the human and the worm homologues and additional experiments clarified the importance of this interaction for the kinetochore localisation of Spindly (Gassmann, Essex et al. 2008, Barisic, Sohm et al. 2010). Furthermore, hSpindly has been shown to directly interact with the dynein-dynactin motor complex at the kinetochore (Barisic, Sohm et al. 2010) (Griffis, unpublished data). In *Drosophila*, there is indirect evidence for a potential interaction with these proteins, mainly based on immunofluorescence data. RNAi of Rough Deal (Rod), a component of the RZZ complex, impaired the localisation of GFP-Spindly to the kinetochore, suggesting that recruitment of Spindly at the kinetochore specifically relies on binding to the RZZ complex. Similarly, downregulation of Spindly resulted in loss of dynein from metaphase kinetochores (Griffis, Stuurman et al. 2007). However, beside this limited evidence, the network of Spindly interactions in mitotic and post-mitotic cells remains unsolved and this lack of information limits our understanding of its function in multiple contexts.

Since there are no mutant alleles available for *spindly*, in the present study we exploit the UAS/Gal4 system to performed loss- and gain-of-function experiments and explore the activity of the *Drosophila* homologue in a variety of cellular and developmental processes. The experiments reported in this thesis point to a fundamental role of Spindly in supporting the development of early embryos. We found that loss of Spindly disrupts embryonic development and compromises the normal synchrony and progression through the syncytial mitotic divisions. Not only Spindly knockdown, but also increased levels of the protein affected embryo survival and resulted in altered egg morphology and a moderate ventralisation phenotype. Since the molecular basis of Spindly functions are not well investigated and protein interaction partners for Spindly have not been systematically analysed, we performed AP-MS experiments. The analysis led to the identification of multiple factors, such as Kinesin motor proteins, that could cooperate with Spindly during mitosis and suggested a variety of regulatory pathways in which the activity of the protein may be required.

The Gal4-UAS system made it possible to explore the non-mitotic activity of Spindly by performing loss- and gain-of-function experiments in post-mitotic cells. Indeed, an additional goal of this research project was to establish the contribution of Spindly to cell migration. Our data suggest that Spindly influences the migratory behaviour of the border cell cluster and it regulates the cohesion between border cells while migrating.

This chapter discusses the results found in this work and their implications and suggests ways to develop this research project further.

7.1 Biological consequences of a differential expression pattern of *spindly* shRNA during oogenesis

RNAi is a widely used approach to perform reverse genetic screens and unravel the activity of uncharacterised genes by examining loss-of-function phenotypes. It is therefore not surprising that over the years this technique has become a powerful tool to analyse the functions of a gene when mutant alleles are not available (Kuttenkeuler and Boutros 2004). In this study the UAS/GAL4 system was adopted to induce the expression of a shRNA transgene targeting *spindly* mRNA and evaluate the developmental effects of the female germline-RNAi of this poorly characterised gene. Indeed, despite two recent reports suggesting that Spindly dephosphorylation may be required for egg activation (Krauchunas, Horner et al. 2012, Amber R. Krauchunas 2013), the activity of the protein in the regulation of developmental processes remains largely unknown. Two different maternal Gal4 lines have been tested in this study, *nanos*>Gal4 (*nos*>G4) and maternal *alpha tubulin 67c*>Gal4 (*mat-Tub*>G4). Both driver lines caused a significant downregulation of the maternal protein as verified by evaluation of Spindly protein levels in whole-embryo lysates.

These two driver lines are characterised by a differential pattern of expression during oogenesis. The gene *nanos* is expressed early in the germarium, while the *maternal-tubulin 67c* gene is expressed when the egg chamber pinches-off from the germarium, from stage 2 of development onwards.

Given the early temporal expression during oogenesis, the use of the *nos*>G4 driver posed a problem as germline Spindly-RNAi female flies became sterile over time. Indeed, these flies laid few eggs for a period of time that did not exceed a week. Ovaries were abnormally small compared to the wild-type control and

immunofluorescence analysis revealed profound morphological alteration of the egg chambers. In particular, ovaries dissected from 7-day-old female flies were rudimentary, lacked developing egg chambers and did not contain dividing germ cells (See Appendix, Figure S-5 and Figure S-6). These severe defects in ovaries architecture and egg production could depend upon a failure in germ cell division caused by the requirement of Spindly for mitosis. This scenario would suggest a role for Spindly in the maintenance of the pool of dividing stem cells in the germarium and in supporting cystoblast divisions but further experiments are needed to validate this hypothesis.

The other driver used (*mat-Tub*>G4) helped to bypass early oogenesis defects, allowing the production of a higher number of eggs. In this case, the shRNA specific for *spindly* mRNA started to be expressed in the young cysts that leave the germarium. Consequently, we hypothesise that the rounds of asymmetric divisions characteristic of the germline stem cells as well the cystoblast divisions remain uneffected because the levels of Spindly expression are unaltered at these early stages of oogenesis, allowing the cyclic production of new egg chambers and therefore substaining the normal production of eggs.

In terms of efficiency of RNAi, the *mat-Tub*>G4 was the most effective in driving the shRNA transgene despite the downregulation of Spindly started at later stages of oogenesis. This apparent discrepancy can be explained taking into account once again the different temporal expression pattern associated to the two driver lines. *nos*>G4 is expressed precociously but in an extremely restricted temporal window. Additionally, the ability of this driver to downregulate Spindly expression is temperature and time dependent. Knockdown of Spindly was evaluated at three different temperatures, high (H, 25°C), medium (M, 21°C) and low (L, 18°C) to verify the shRNA dose-dependent

effects of the downregulation of Spindly on embryo development. The analysis performed with the *nos*>G4 driver showed a gradual decrease in Spindly protein levels in response to a step-wise increase of the temperature. Moreover, the analysis performed on Spindly-RNAi ovaries showed the temporal dependency of the RNAi phenotype suggesting that the system undergoes a period of adaptation before becoming fully functional. As a consequence of the combinatorial effect of these two features, the analysis of fixed preparations of 0-3-hour-old embryos led to the identification of a variety of phenotypic classes ranging from severe to milder knockdown effects similar to those that would result from the analysis of either amorphic or hypomorphic mutant alleles.

Conversely, the *mat-Tub*>G4 is expressed at later stages of oogenesis but its expression is constant for the entire duration of the oogenesis. Consequently, the use of this driver resulted in a high level of Spindly knockdown at any of the temperature tested as verified by Western blot, challenging the modulation of the level of downregulation.

7.2 Spindly is required during early embryonic development

To establish the requirement of Spindly for *Drosophila* embryogenesis we determined the hatching ability of Spindly-RNAi embryos and the percentage of syncytial defects. The data reported in this thesis point to Spindly as a crucial regulator of the thirteen syncytial mitotic divisions. Strong downregulation of the protein (mat-Tub>G4_H, M, L and nos>G4_H) dramatically compromised embryo development and only a small percentage of embryos was able to hatch. Imaging of fixed embryos showed that the progression through the syncytial mitotic cycles was severely compromised, suggesting

that the high lethality rate observed correlates with a severe impairment in the completion of the early stages of embryogenesis. When the knockdown of Spindly was achieved by using the mat-Tub>G4 driver, 40% of the embryos stopped developing with a single metaphase-arrested nucleus. This could either be an arrested first zygotic division that includes chromosomes from both pronuclei after their migration and fusion or a single male pronucleus. The identification of a polar body rosette in 46.6% of the cases examined suggested that meioisis was completed in these embryos. Previous studies have shown a requirement for Spindly for the meiotic maturation of mouse oocytes (Qing-Hua Zhang 2010), however the presence of the polar body raises doubts that in *Drosophila* Spindly is involved in the control of the completion of meiosis.

Similar analysis performed with the *nos*>G4 driver (*nos*>G4_H) showed that 22% of the embryos did not have visible nuclei while a significant proportion of the embryos arrested their development after few rounds of mitotic divisions with over-duplicated centrosomes. All together, these observations suggest a failure in the fusion of the two pronuclei in the zygote. One possibility to explain this phenotype would be that Spindly may be required to control the assembly of the microtubule network that is nucleated by the male aster and necessary to guide the female pronucleus towards the male pronucleus. This could be a plausible mechanism of action given the severe disruption of the microtubule cytoskeleton observed in early Spindly-RNAi embryos. Alternatively Spindly might control the activity of motor proteins involved in the process. The migration of the female pronucleus relies on the activity of the dynein-dynactin complex in many species (Loppin, Dubruille et al. 2015). However, in *Drosophila* the requirement of dynein in this process has not been demonstrated and other motor

proteins, such as the kinesin Klp3A, promote female pronuclear migration (Byron C. Williams 1997).

In summary, we support the idea that Spindly is required to control the transition from a mature oocyte into developing embryos. The protein might be involved in pronuclear migration either by microtubule cytoskeleton remodelling or by controlling the activity of motor proteins that move the female pronucleus like a cargo along the male aster. In the future it would be interesting to substantiate this hypothesis and establish the molecular details behind the phenotypic alterations observed.

In *nanos*>Gal4; *UAS*>Spindly^{Valium20} embryos raised at less stringent conditions for viability (*nos*>G4_M) the depletion of Spindly was less pronounced and as a consequence, an increased number of embryos was able to hatch in the first larval stage. However, 46% of these embryos still displayed problems in cell cycle progression despite the residual amount of Spindly protein was sufficient to sustain the completion of a higher number of mitotic cycles. Therefore, analysing the developmental effects of a moderate downregulation of the protein was more informative in establishing the mechanism(s) by which Spindly may contribute to the regulation of the early stages of embryogenesis (see 7.3).

Collectively our data clearly point to Spindly as fundamental factor to ensure normal progression through the fast and synchronous mitotic divisions during the early stages of embryonic development that precede cellularisation.

One frequently observed issue with the RNAi technology is the specificity of the phenotypes due to problems with off-target effects. Therefore, to confirm our Spindly-RNAi phenotypes, rescue experiments were performed using a GFP-tagged Spindly

construct impervious to the RNAi machinery and comparing the rescue ability of this construct to that of an unrelated GFP-H_3 transgene. Our data showed that embryo viability was restored to wild-type levels only by overexpressing GFP-Spindly upon depletion of the endogenous protein. This result demonstrated that the RNAi is specific for *spindly* mRNA and thus excludes off-target effects. Furthermore, this analysis has another important implication, pointing to the possibility of performing structure-function experiments in a Spindly-RNAi background and assessing several mutant versions of Spindly for their functional properties. This strategy will test the hypothesis whether certain domain(s) are required for kinetochore localisation and determine those essential to bind partners such as dynein/dynactin and RZZ and those ones important in the binding of cytoskeletal components. In the future this transgenic complementation study will greatly contribute to define domains important for the biological activity of Spindly.

7.3 Spindly controls the initiation of embryo development through multiple processes

The successful downregulation of Spindly in the female germline has made it feasible to start testing the role of Spindly in the initiation of *Drosophila* embryo development. Changes in Spindly protein levels upon RNAi were investigated by performing Western blotting. The analysis revealed that even when the levels of Spindly expression dropped dramatically (*nos*>Gal4_H) a small amount of protein was still detectable. Therefore, the Gal4-UAS system allowed to generate a partial loss-of-function phenotype, comparable to that of hypomorphic mutant alleles. Our immunofluorescence data showed that RNAi of Spindly resulted in a broad range of mitotic abnormalities that have been grouped into distinct phenotypic classes.

Variability in the knockdown efficiency at the single-embryo level could result in embryos in which the depletion of the target protein was stronger than in others explaining the variaty of mitotic defects observed. Another intriguing possibility that would explain the different RNAi phenotypic strength is what we call the “activity threshold model”. For a multifunctional protein as Spindly, a certain biological function would be performed only when the levels of protein expression hits a certain threshold. This model suggests that Spindly could have different localised activity thresholds for distinct functions. Consequently, in a biological background in which the abundance of the protein is reduced, Spindly would not been able to carry out all its biological activities, limiting them to a small subset of cellular functions according to the threshold of protein expression reached. Therefore, the model implies that certain levels of knockdown would correspond to a certain category of defects. This model suggests that the expression levels of Spindly must be under tight control for the protein to properly fulfill its multiple activities.

The different classes of Spindly-RNAi phenotypes are reported below and a potential mechanistic explanation is provided for each of them.

1. Asynchrony in mitotic divisions and uneven distribution of nuclei

During normal syncytial embryo development the nuclei divide synchronously and are evenly distributed throughout the embryo. In Spindly-RNAi embryos instead, nuclear divisions became asynchronous, suggesting that lack of Spindly delays progression in mitosis. Moreover, the distribution of nuclei along the anterior-posterior axis of the embryos was irregular, resulting in areas characterised by a much lower nuclear density. Even though this phenotype needs to be confirmed by carefully comparing it to wild-type embryos, it suggests defects in axial expansion, an actin-dependent

process that guides nuclei distribution along the anterior-posterior axis (Jayne Baker 1993).

Both these phenotypes can be explained by variations in the overall levels of cyclin-B, which was upregulated upon Spindly RNAi compared to the wild-type control (Appendix, Figure S-4). Tight regulation of cyclin-B levels controls exit from mitosis during early syncytial divisions (Tin Tin Su 1998, Raff, Jeffers et al. 2002). In light of this observation, it is tempting to hypothesise that the increased levels of cyclin-B upon Spindly RNAi may be responsible for the asynchrony in the mitotic divisions, preventing nuclei from exit mitosis. However, it is noteworthy to mention that similar asynchrony defect was also found in *Drosophila* embryos injected with dynein inhibitors (David J. Sharp 2000). Since Spindly has been originally suggested to be a co-factor for dynein at the kinetochore, the phenotype observed could reflect a more general inhibition of dynein activity and could therefore further support a role for Spindly as regulator of this major microtubule minus-end motor.

Regarding the uneven distribution of nuclei, it is known that downregulation of the levels of Cyclin-B at the exit from mitosis promotes the myosin-dependent contraction of the actin cytoskeleton responsible for the axial expansion of the syncytial nuclei along the A/P axis (Royou, Sullivan et al. 2002). During synctyal cycles, myosin undergoes cycles of cortical recruitment and dispersion that are regulated in a cell cycle-dependent manner by Cdk 1/Cyclin B activity. The experimental data reported by Royou et al. propose a model in which Cdk1, highly active during mitosis, negatively regulates myosin by inhibiting the phosphorylation of the light regulatory chain (RLC) on Serine-21. During interphase, cyclin B is degraded and Cdk1 is not active. Under this condition, the inhibition of RLC is relifed and myosin can be assembled in active bipolar

filament underneath the cortex, allowing cortical contraction and distribution of the nuclei along the long axis of the embryo (Royou, Sullivan et al. 2002).

In the context of our study, the higher levels of cyclin-B could inhibit the cortical recruitment of myosin and impair the axial expansion process, resulting in the uneven distribution of nuclei that had been observed.

It is northworthy to specify that defects in nuclear migration, cell cycle regulation and abnormalities in the process of axial expansion have been reported in other contexts. An example is offered by embryos lacking maternal and zygotic Pten activity, a phosphatase that in early *Drosophila* embryos has been shown to be involved in the regulation of actin-dependent processes (von Stein, Ramrath et al. 2005). Specifically, in Pten mutant embryos the nuclear density in the posterior region of pre-blastoderm embryos is much lower that the anterior region. Moreover, nuclei are unevenly spaced and divide asynchronously also during the syncytial blastoderm stage (von Stein, Ramrath et al. 2005). Very similar phenotypes have been reported for mutants in other genes required for the organisation of the actin cytoskeleton (Miklós Erdélyi 1995, Sally Wheatley 1995, Michael T.Tetzlaff 1996) and for embryos treated with the actin depolimerising agent cytochalasin D (OKADA 1991). The Asynchrony in mitotic divisions and the uneven distribution of nuclei observed upon Spindly misexpression strongly recall the aforementioned abnormalities observed in other biological contexts and point to a requirement for Spindly in the regulation of actomyosin-dependent processes.

2. Mitotic spindle defects

Spindly-RNAi embryos displayed marked mitotic spindle defects. At the highest levels of knockdown (*nos*>G4_H), the normal organisation of the mitotic spindle was severely compromised and condensed chromatin was found associated with patches of tubulin. Moderate downregulation of Spindly (*nos*>G4_M) caused milder defects: the spindles collapsed and fused into abnormal mitotic figures such as tripolar spindles. These observations suggest that Spindly might regulate the stability of the mitotic spindle apparatus by regulating the repeated cycles of microtubule growth and shrinkage or by crosslinking adjacent microtubules together. Alternatively, Spindly might control the stability of the spindle indirectly, by regulating the activity of proteins that perform this function during mitosis.

Indirect evidence supporting the ability of Spindly to bind to microtubules has been reported in the literature. Specifically, overexpression of GFP-Spindly in *Drosophila* S2 cells showed that the protein is able to decorate the entire lenght of microtubules during interphase and it is specifically enriched at the dynamic microtubules plus-ends (Griffis, Stuurman et al. 2007).

The plus-ends of microtubules are important sites of regulation of microtubule dynamics. The so-called +TIP proteins are indeed implicated in the regulation of the repeated cycles of microtubule growth and shrinkage in many biological models (Akhmanova and Steinmetz 2008, Steinmetz 2010). Of these proteins, EB-1 regulates the dynamic assembly and the structure of the microtubule fibres. RNAi of EB-1 causes a significant reduction in the length of microtubules, greatly affecting spindle stability (Rogers, Rogers et al. 2002, Tirnauer, Grego et al. 2002). Conversely, Lissencephaly-1 (Lis-1) has been reported to have the opposite effect and to act by inhibiting

microtubules depolymerisation (Moon, Youn et al. 2014). In both cases, changes in the stability of the microtubules results in the establishment of improper kinetochore-microtubule interactions and increased rate of chromosome misegregation.

As previously mentioned, in *Drosophila* S2 cells GFP-Spindly has been found to colocalise to the microtubule plus-ends with EB-1. However, there is no evidence supporting the possibility of a direct interaction of Spindly with microtubules. Therefore, it would be beneficial to test *in vitro* the microtubule-binding ability of Spindly and establish whether this protein classifies indeed as a novel MAP able to regulate microtubule dynamics by mechanisms similar to those described for members of the +TIP family of proteins or for other MAP protein.

Alternatively, Spindly could regulate mitotic spindle stability by promoting crosslinking and bundling of microtubules. The stabilisation of the mitotic spindle by direct binding to the microtubule fibres and the fine regulation of their dynamics is a mechanism of action common to many proteins. A good example is provided by the novel *Drosophila* MAP protein, Mars that has been proven to be essential for the development of early *Drosophila* embryos because of its ability to stabilise microtubules *in vivo* (Zhang, Breuer et al. 2009, Zhang, Beati et al. 2013). Specifically, the N-terminal portion of the protein is required to bind microtubules and to promote their crosslinking and bundling. The protein is therefore essential for maintaining the integrity and the stability of the mitotic spindle and the overexpression of the N-terminal half causes adjacent mitotic spindles to fuse together in abnormal mitotic figures, similar to those observed upon Spindly misexpression (Zhang, Beati et al. 2013). In addition, similarly to the phenotypes observed upon Spindly downregulation (see 7.3, point 3), overexpression of the N-terminal half of Mars causes narrowing of the spindle poles

and detachment of the centrosomes from the poles with subsequently generation of monopolar spindles (Zhang, Breuer et al. 2009, Zhang, Beati et al. 2013).

Spindly could promote microtubule crosslinking and bundling either directly, as described for Mars, or regulating other proteins involved in the process, such as members of the kinesin family of motor proteins

Many motor proteins as well as microtubule-associated proteins (MAPs) have been reported to regulate the stability of microtubules during mitosis (Peterman and Scholey 2009). These proteins help in organising microtubules into bundles and they have also the ability of sliding parallel or anti-parallel microtubules on one another. Therefore, these factors have been shown to stabilise the mitotic microtubules and to assist the spindle in coordinating chromosome movement (Peterman and Scholey 2009).

Taking into account these considerations, Spindly could achieve mitotic spindle stabilisation by regulating and coordinating the activity of different motor proteins during mitosis. Several studies have shown that multiple complementary and antagonistic motors contribute to spindle assembly and to the maintenance of the spindle length throughout mitosis (David J. Sharp 2000, Wang H. 2014). Therefore, the architecture of the spindle depends on the balanced activity of dynein and kinesin motors (Figure 7-1). In particular, while dynein slides microtubules poleward and contributes to microtubules clustering at the pole (Figure 7-1, box 1), the plus-end-directed kinesin motors slide antiparallel overlapping microtubules, pushing the pole apart (Figure 7-1, box 2).

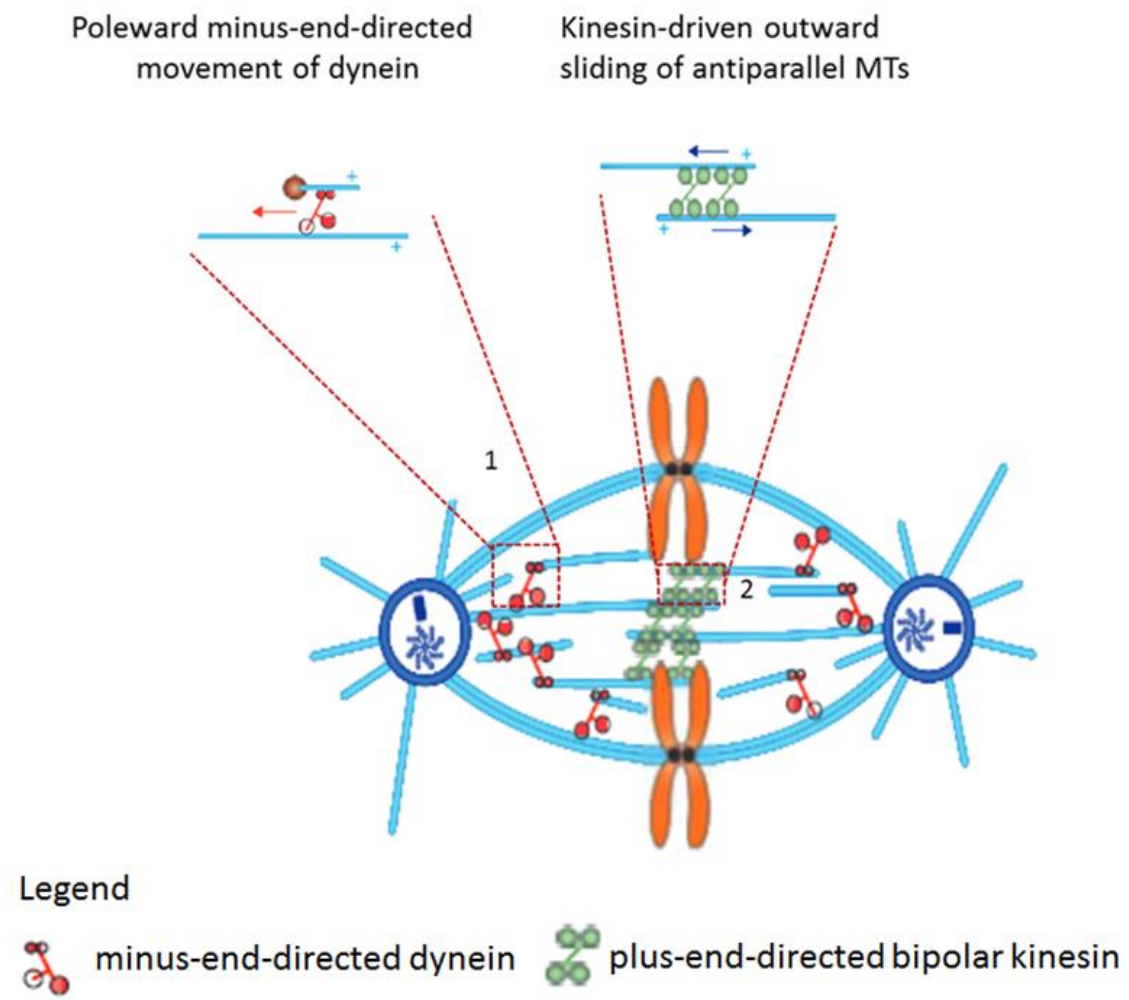

Figure 7- 1: **The architecture of the mitotic spindle depends on microtubules and kinesin and dynein motors.** During mitosis, multiple motors characterised by different polarity and mechanism of action, control the stability of the mitotic spindle. Of these motors, the family of the bipolar kinesins (in green) localises at the spindle midzone where they crosslink and slide antiparallel microtubules. Antiparallel microtubule sliding allows plus-end-directed kinesins to push the spindle poles apart (box 2), allowing the elongation of the mitotic spindle. Conversely, minus-end-directed kinesins, such as C-terminal kinesin (not depicted in the figure, see Figure 7-2 for details), pull the spindle poles together. Motors of the dynein family, slides microtubules poleward and contributes to microtubules clustering at the pole (box 1). In addition, dynein localises at the cortex and with its minus-end-directed activity it helps pulling the spindle poles apart and positioning the entire spindle within the cell (detail not shown in the picture). Image was adopted from (Wang H. 2014).

Accurate analysis of the rate of spindle pole separation in the presence of inhibitors of specific motor proteins has clarified how the activity of these motors contributes to spindle maintenance and elongation (David J. Sharp 2000).

According to these studies, the initial assembly of the mitotic spindle relies on the activity of dynein at the poles and the activity of C-terminal kinesin at the equator zone. Initially, the degree of microtubule overlap at the midzone is minimal and the outward force generated by dynein is greater that the inward force generated by C-terminal kinesin (Figure 7-2 A). However, as the poles separate further and the growing microtubules interdigitate more, the activity of the C-terminal kinesin increases until it balances the forces generated by dynein. As soon as the outward and inward forces are balanced, the spindle reaches a stady-state that lasts until nuclear envelope breakdown. At this stage of mitosis, an additional outward force generated by bipolar kinesis motors (suche as Klp61F) operates on the spindle (Figure 7-2 B). The combined activity of cortical dynein and bipolar kinesin at the equator exceeds the inward forces generated by the C-terminal kinesin resulting in spindle elongation and a metaphase-like structure. Finally, the inactivation of C-terminal kinesin favours bipolar kinesin activity and contributes to the final separation of the spindle poles during anaphase (Figure 7-2 C).

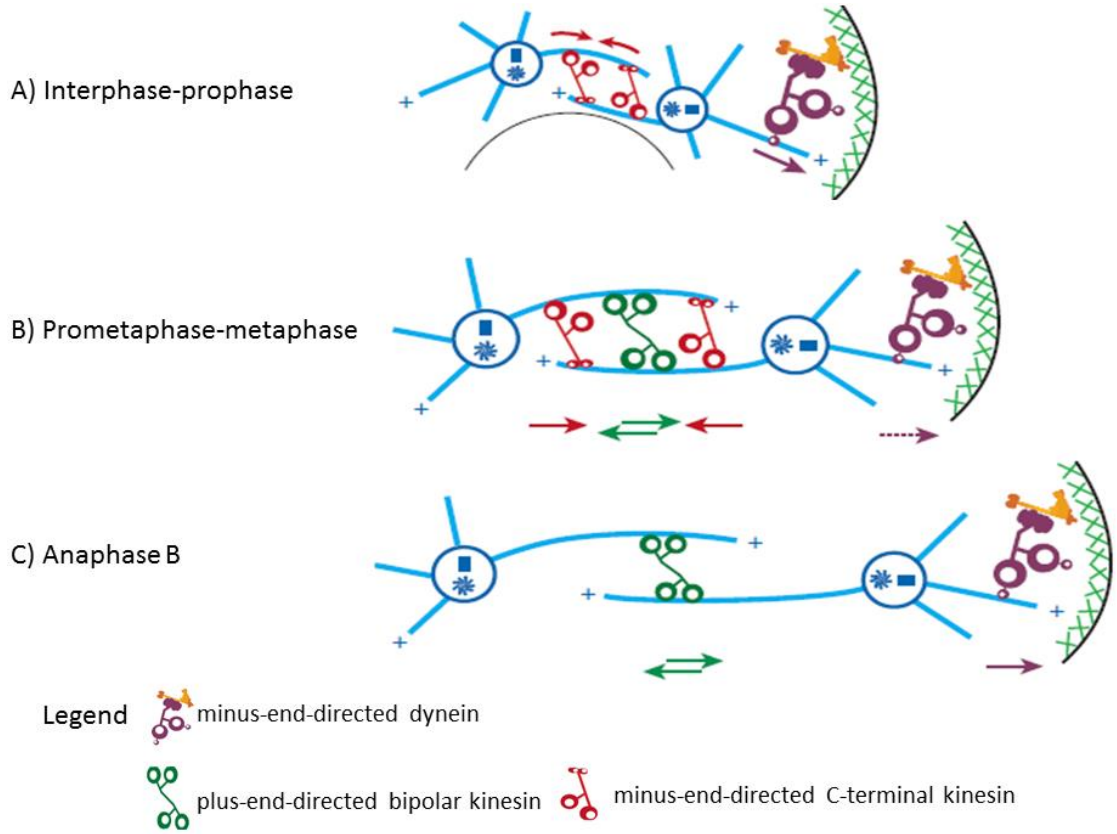

Figure 7- 2: **The activity of multiple motor proteins contributes to spindle assembly, maintenance and elongation.** The coordinated and antagonistic activity of minus-end-directed dynein and minus and plus-end directed kinesins motors orchestrate the multiple and complex rearrangements of the spindle during mitosis. The image was adopted from (David J. Sharp 2000).

To clarify the activity of Spindly during the syncytial mitotic cycles and to clarify whether Spindly can assist the activity of any of the motor proteins aforementioned, AP-MS experiments have been performed to identify potential binding partners that could assist Spindly during its mitotic activity. The AP-MS experiments here reported revealed a potential interaction with two kinesin motors, Klp61F and Klp67A.

Klp61F is a kinesin motor protein that oligomerises into bipolar homotetrameric complexes. This motor crosslinks antiparallel microtubules originating from the opposite poles of the spindle and slide them along another in opposite directions. By operating this mechanism, Klp61F promotes the establishment of a bipolar spindle,

favouring spindle pole separation and spindle dynamics (David J. Sharp, à et al. 1999, van den Wildenberg, Tao et al. 2008).

Klp67A is a member of the Kip3 subfamily of kinesin motors and it is classified as a microtubule destabilising protein. Loss of Klp67A activity results in highly disorganised bipolar spindles characterised by abnormally long and bent kinetochore microtubules and robust astral microtubules (Matthew S. Savoian 2004). Additional studies have focused on the dynamic localisation of this protein during mitosis. At prometaphase and metaphase Klp67A binds to the kinetochore whereas it redistributes to the central spindle later on during anaphase. Klp67A is indeed involved in the formation, localisation and stabilisation of the central spindle complex promoting therefore cytokinesis (Melanie K. Gatt 2005, Matthew S. Savoian 2010).

Even though the physical interaction between Spindly and these two members of the kinesin family needs to be validated by other biochemical approaches and additional experiments are required to clarify how the activity of Spindly as dynein cofactor might correlate with the activity of Spindly as coordinator of kinesin motor proteins, the mass spectrometry data suggest that knockdown of Spindly could result in an unbalanced activity of motor proteins that regulate spindle stability, leading to an altered activity of the mitotic spindle and chromosome segregation defects described in this work.

3. Centrosome detachment and overduplication.

An additional mitotic defect observed in fixed preparation of embryos lacking Spindly was the presence of detached and supernumerary centrosomes. Live imaging of *Drosophila* embryos injected with an anti-Spindly antibody revealed the dissociation of the centrosomes from the spindle poles and their abnormal duplication (Griffis, data

not published). This *in vivo* experiment showed that, despite the mitotic block caused by the inhibition of Spindly activity, centrosomes continue to be duplicated, suggesting that the cycle of centrosome division was uncoupled from the nuclear mitotic cycle. The results we obtained on fixed embryos are in agreement with this observation.

The crucial role of the motor protein dynein in maintaining a tight association between the centrosomes and the spindle poles has been exhaustively described in *Drosophila* early-embryos as well as in S2 cells (John T. Robinson 1999, Morales-Mulia and Scholey 2005). Therefore it will be interesting to determine whether the phenotypes described in this report are similar to those described when dynein function is affected and whether Spindly is involved in the regulation of dynein in multiple processes in mitosis and interphase cells.

The minus-end directed motor dynein is not the only factor involved in the maintenance of the attachment of the centrosome to the spindle poles and many factors have been implicated in the process. For example, the crosslinking activity of kinesin Klp61F has been shown to help the association between centrosomes and spindle poles by linking centrosome and non-centrosome microtubules (Garcia, Stumpff et al. 2009). Goshima *et al.* discovered instead that in *Drosophila* S2 cells Calmodulin (CaM) cooperates with Abnormal Spindle Protein (Asp) in determining the organisation of the spindle poles and RNAi of Asp results in centrosomes detachment and unfocused spindles (Goshima, Wollman et al. 2007). Finally, a recent screen based on immuno-isolation of *Drosophila* embryonic centrosomal components combined to mass spectrometry and RNAi validation of the proteomic data has resulted in the identification of components of the translation machinery, actin- and RNA-binding

proteins that are unexpectedly required for maintaining the integrity of the centrosome structure (Muller, Schmidt et al. 2010).

The Mass Spectrometry analysis on Spindly interacting protein performed in this PhD thesis revealed interactions with the aforementioned factors, including the RNA-binding protein Cup as well as some of the ribosomal proteins identified by Müller 2010. Therefore, to begin to understand the mechanisms behind the activity of Spindly in mitotis, it would be beneficial to test whether downregulation of these factors in *Drosophila* early embryos recapitulates the phenotypes observed upon Spindly-RNAi and study the biological relevance of their interaction with Spindly.

In this context it is noteworthy to stress that a strong correlation exists between centrosomes and cytoskeletal organisation in early *Drosophila* embryos. CP190 and its partner Map60 are proteins that rely upon each other to localise at the centrosome and their binding to this organelle is regulated in a cell-cycle dependent manner. Even though the function(s) of these two factors at the centrosome remains unclear, CP190 has been shown to be an upstream regulator of actin cytoskeleton and CP190 mutants fail in axial expansion (Chodagam, Royou et al. 2005). AP-MS analysis suggested Map60 as likely interactor of Spindly. It would be therefore interesting to establish whether these three proteins operate in the same biological pathway in early *Drosophila* embryos and clarify to what extent this ternary complex contributes to centrosome maintenance and cytoskeleton regulation.

Moreover, mutants for the centrosomal marker centrosomin showed defects in the spatial organisation of nuclei and abnormalities in microfilament as well as microtubule arrays (Schejter 1999). Thus it would be interesting to firmly establish

whether the centrosome abnormalities reported here are primary defects that cause early cytoskeleton-dependent developmental defects.

7.4 Overexpression studies of Spindly shed light on novel non-mitotic activities of the protein

The early stages of *Drosophila* embryogenesis rely on the correct execution of thirteen fast and synchronous mitotic cell cycles without intervening cytokinesis. RNAi of maternal Spindly showed the crucial role for this protein in controlling the faithful progression through the syncytial mitotic divisions. The variable strength of the RNAi phenotypes as well as the results of the rescue experiments suggested that the tight control of the levels of Spindly expression is crucial for its balanced activity. We therefore hypothesise that overexpression studies would test for conditions in which the levels of this protein are increased over its biological threshold limit.

Overexpression of a GFP-tagged full-length variant of the protein allowed to further analyse the activity of Spindly during embryos development, potentially pointing to novel, previously uncharacterised functions of the protein. Similarly to Spindly knockdown, its overexpression led to embryonic lethality for 65% of the individuals and analysis of larval cuticles derived from embryos overexpressing Spindly revealed a strong defects in egg morphology. In 48% of the cases, eggs were rounded in shape and smaller in size. Knockdown of the endogenous protein alleviated the phenotype, confirming the specificity of the approach. Additionally, increased levels of Spindly caused moderate ventralisation of the eggs, as verified by observing mispositioning of the dorsal appendages.

The round-egg phenotype could depend upon impared egg elongation potentially caused by a failure in the polarisation of the follicular epithelium of the egg chamber

or defective dumping of the egg during late oogenesis (Horacio M. Frydman 2001) (Jack Bateman and Vactor 2001, Groen, Spracklen et al. 2012, Sally Horne-Badovinac 2012). These mechanisms are both dependent on the dynamic remodelling of the actin cytoskeleton. The phenotype observed upon Spindly overexpression raises the question whether this protein is required for organising F-actin in bundles or in the regulation of the cycles of acto-myosin contraction during dumping. Analysis of the actin cytoskeleton and careful comparison to the wild-type condition will allow to discriminate between these two possibilities.

The observation that the knockdown of the endogenous protein rescued the round-egg phenotype raises once again the possibility to use the overexpression of Spindly as background to perform structure-function analysis. Overexpression of mutant variants of the protein will help in identifying the domains(s) responsible for the phenotype reported and test the requirement of that/those particular domain(s) involved in actin cytoskeleton regulation and egg elongation.

The establishment of dorsal/ventral polarity occurs during mid-oogenesis and relies on a dorsalising signal generated by the *gurken* gene (Schupbach 1987, Forlani, Ferrandon et al. 1993). The mild dorsal/ventral patterning defects of eggs overexpressing Spindly could be interpreted as a consequence of a reduced expression of Gurken or could be caused by mislocalisation of this determinant from its usual antero-dorsal position around the oocyte nucleus. Staining and immunofluorescence analysis of ovaries isolated from wild-type and GFP-Spindly female flies will help to clarify the molecular basis of the ventralisation phenotype observed by analysis of the chorion. A potential scenario could be that overexpression of Spindly causes a displacement of the oocyte nucleus and consequently of the protein Gurken away from the antero-dorsal cortex.

Since the anchoring of the oocyte nucleus to the antero-dorsal cortex of stage 10 egg chambers is mediated by dynein (Jason E. Duncan 2002) this phenotype could support the idea of Spindly acting as a dynein co-factor during egg patterning.

7.5 Study of Spindly requirement in interphase: regulation of cell migration

RNAi-based screen for genes involved in the control of S2 cell morphology in interphase identified Spindly as novel regulator of actin and tubulin cytoskeletal components, implicating the protein in the control of cell shape. Indeed, Spindly-RNAi S2 cells showed a peculiar phenotype in interphase, displaying severe defects in the lamellae network as well as in the overall organisation of the tubulin cytoskeleton (Griffis, Stuurman et al. 2007). Moreover, Spindly has the ability to localise at the (+) ends of microtubules (Griffis, Stuurman et al. 2007). Overall these experimental data suggested that Spindly could exert direct control on the dynamics of actin and tubulin cytoskeleton during interphase. In addition, Spindly is shown to be a co-factor for the dynein-dynactin motor complex at the kinetochore. Furthermore, *in vitro* experiments demonstrated that Spindly is necessary to increase the processivity and directionality of dynein (Richard J. McKenney 2014, Schlager, Hoang et al. 2014), suggesting a more general function for Spindly in assisting this motor protein in its multiple mitotic and post-mitotic functions. Therefore, in the light of these observations we aimed to test the requirement of Spindly for cell migration, examining the migratory behaviour of border cells and embryonic haemocytes in response to either Spindly downregulation or overexpression.

The experimental observations reported in this study suggest that the ability of Spindly to control cell motility is largely cell-type specific. Downregulation of Spindly in

haemocytes did not cause major variations in the motile properties of these cells towards a wounded-hypodermis. Indeed it was observed that migratory speed, cell shape and the ability to make protrusions were overall unaltered in a Spindly-RNAi background compared to the wild-type control. The wound-healing assays reported in this study were performed on embryos at stage 15 of development (600-800 min AEL, Campos-Ortega, 1985). Western blot performed to analyse variations in the expression levels of Spindly during embryogenesis showed that the protein is undetectable at this late stage of embryo development. This does not exclude however that the protein is expressed at low levels in this small fraction of cells of the embryo. Immunofluorescence to detect Spindly in haemocytes failed because the anti-Spindly antibody used in this study is not suitable for histological staining. In situ hybridisation could therefore be a valid option to verify whether Spindly is expressed in haemocytes.

The results of the wound-healing assay suggested that RNAi of Spindly in haemocytes did not result in any obvious abnormality and occasionally it was possible to detect cells showing a cruciform shape. The imaging was performed visualising GFP as marker. The use of more specific markers to label either microtubules or F-actin (i.e. GFP-CLIP170 or mCherry-moesin, respectively) could help in detecting subtle defects that may have stayed hidden during our analysis and that may be at the basis of these rare morphological alterations.

The loss- and gain-of-function experiments performed on follicular border cells have opened a more fruitful background to test the role of Spindly in the regulation of cell motility. Downregulation of Spindly positively regulates the migration of border cells towards the oocyte. This result has two potential explanations. On one hand, it could suggest that knockdown of the protein causes an increase in the migratory speed of

the cluster. Alternatively, Spindly could be involved in the transduction of the ecdysone-dependent signal that set the right timing of border cells delamination and cluster migration (Michael Buszczak and Segraves 1999, Jianwu Bai 2000). If this were the case, our data suggest that in the absence of Spindly the cluster starts migrating earlier along the anterior-posterior axis of the egg-chamber. Time-lapse imaging of the migrating cluster will provide the time-resolution to discriminate between these two possibilities and establish whether or not Spindly is a factor required to translate the extracellular cues that set the right timing for the detachment of the cluster from the follicular epithelium.

The effect of the RNAi experiment predicted that the upregulation of the protein resulted in the opposite phenotype. Indeed, overexpression of a GFP-tagged version of Spindly in border cells resulted in an incomplete migration phenotype. Additionally, the overexpression of Spindly disrupted the morphological organisation of the cluster. Border cells normally move as a coherent cluster towards the oocyte. Our phenotypic observations suggest that Spindly may regulate cell-cell adhesion keeping the cells together as a collective group. The cluster morphology defects observed upon Spindly upregulation resembled those caused by loss of JNK activity (Llense and Martin-Blanco 2008, Melani, Simpson et al. 2008) or by alteration of the Src-Rack1 pathway (Luo, Zuo et al. 2015). Both these signalling pathways are required for border cell migration and maintenance of cluster cohesion. Specifically, they regulate the motile behaviour of the cluster by controlling the expression levels of key elements of cell polarity, such as Par-3/Bazooka, and of molecules that mediate cell-cell contacts and cell-substrate attachments, such as DE-Cadherin. The inhibition of either JNK or Src-Rack1 pathways results in the loss of multiple cell-cell adhesion complexes and consequently in a

severe dissociation phenotype and reduced invasive potential (Llense and Martin-Blanco 2008, Melani, Simpson et al. 2008, Luo, Zuo et al. 2015). Similar phenotypes have been reported in this thesis upon Spindly overexpression in migrating border cells and are consistent with defects in cell polarity and/or cell-cell adhesion.

Furthermore, a recent publication pointed to a requirement for dynein, Lis-1 and Nuclear distribution-E (Nud-E) in border cell migration. Specifically, it was shown that knockdown of these proteins delayed border cell migration (Yang, Inaki et al. 2012). In addition, RNAi of Lis-1 disturbed the normal organisation of the cluster and resulted in abnormal localisation of adhesion molecules (Yang, Inaki et al. 2012). Dynein has been shown to contribute to epithelial cell polarity (Sally Horne-Badovinac 2008). These data suggest that altering the activity of dynein might cause defects in border cell cluster morphology. In the context of our study, we can hypothesis that overexpression of Spindly might have similar consequences to the overexpression of dynamitin (N.J. Quintyne 1999, Schroer 2000), resulting in the inhibition of dynein activity and altered distribution of polarity markers and/or adhesion molecules.

Therefore, it would be crucial to establish whether alterations in the levels or localization of E-cadherin, Integrins and polarity proteins, such as Par-3/Bazooka, are detectable upon Spindly overexpression.

The approach undertaken in this study was effective in detecting additional function of Spindly in post-mitotic cells, specifically in the regulation of border cell migration. However, further analysis is needed to establish the molecular details behind the loss- and gain-of-function phenotypes here reported, and in the future they may be further validated using loss-of-function mutations in mosaic analysis.

7.6 Conclusions

The aim of this PhD project was to define the contribution of *Drosophila* Spindly to multiple developmental processes by investigating the defects caused by variations in its expression levels. Previous publications clarified the importance of this protein for the regulation of cell division in tissue culture cells. To establish the contribution of Spindly to the development of living organisms, the present research project was modelled around three main goals: to establish whether and to what extent Spindly controls early-embryo development, to unravel novel function(s) in post-mitotic cells and to define the network of Spindly interaction. Our study showed Spindly to be essential for the regulation of the fast and synchronous mitotic cycles that take place during the early stages of *Drosophila* embryo development. Our analysis confirmed that Spindly is involved in the control of mitotic progression by several mechanism(s), including the fine regulation of cytoskeleton components as well as of centrosome biology. Additionally, loss- and gain-of-function experiments support a role for this protein in other important developmental processes including egg elongation and cell migration, pointing to more complex, non-mitotic functions of Spindly.

The poorly defined network of Spindly interactions poses the problem of identifying the signalling and developmental pathways that require the activity of Spindly. In this study, we adopted a global and unbiased method based on affinity-purification experiments combined to mass spectrometry aiming to the faithful identification of potential binding partners. The method helped in the identification of binding partners, such as members of the kinesin family of motor proteins that could assist Spindly in mitosis.

An important question that still needs to be answered is the identification of the protein domains that are important for Spindly function and establish their individual contribution for the diverse activities of the protein. Therefore, a main goal is to perform an *in vivo* structure/function analysis to define domains important for the biological activity of Spindly. The rescue experiment pointed to the possibility of using both the loss- and gain-of-function backgrounds to this purpose. However, null-allele for the *spindly* locus would provide a useful background to perform a transgenic complementation study and assay several mutant versions of Spindly for their functional properties. In addition, mutant alleles will provide with a powerful tool to generate genetic mosaics in a variety of cell and tissue-specific context, giving the possibility to study in more details whether loss of Spindly exhibits cytoskeletal defects and abnormalities in cell migration and cell polarity. Overall, the different approaches will reveal insight into the molecular details of Spindly function by clarifying the roles of Spindly protein domains for its localisation and mitotic and post-mitotic activities.

Acknowledgements

Many people helped me during these four years and I want to express my appreciation to all of them.

First and foremost I would like to thank my supervisor Dr. Arno Müller for the great opportunity to develop my research project in his lab. Dear Arno, you have supported and encouraged me from the very beginning and at every stage of my PhD. Beside the secrets of “fly pushing”, you taught me to have the courage and the determination to achieve my goals and most importantly to “smile to science”. Thank you.

I want to thank Dr. Eric Griffis and all the members of his lab: Sara Carvalhal, Claudia Conte and Taciana Kasciukovic, for the help with my project and for hosting me in their lab every time I needed.

A big thanks to the members of my thesis committee, Prof. Inke Näthke and Prof. Tom Owen-Hughes for their support and precious advice.

I am extremely grateful to Dr. Jens Januschke for his expert advice and the exciting and stimulating conversations during lab meetings. It was a pleasure to meet and work with such a great scientist and person.

A big thanks goes to Prof. Inke Näthke and Prof. Andreas Wodarz for accepting to read and comment on my thesis and for agreeing to be the examiners for my viva.

I want to thank the experts whose help greatly improved this work. Dr. Sara ten Have and Kelly Hodge adviced me for the proteomic analysis and this section of my thesis would have not been possible without their help and constant support. A huge thanks to all the staff of the Microscopy Facility of the University of Dundee and all the members of the Central Technical Services.

During my PhD I had the possibility to visit and work in other *Drosophila* research groups in Europe. I want to thank Prof. David Glover and Prof. Will Wood for hosting my visits to their labs and their lab members for helping me during my stay in Cambridge and Bristol. A special thank goes to Dr. Marcin Przewloka and Dr. Zoltan Lipinszki and to Dr. Kate Comber for their help and warm welcome.

My staying in Dundee would have not been the same without all the special friends and people I met. Dear HAM Lab members thank you all for making my time in the lab so enjoyable. Ryan, thank you for the invaluable help, endless friendship and most importantly for not locking yourself in the office every time I came along for a “little” chat! I can’t image a new lab without you. Thanks to Hannah for sharing the office with me for such a long time, for the constant support and patience. A big thank you to one of my favourite ceilidh dancer: dear Hamze, thank you for all the help, the time and the ideas we shared while injecting embryos or sorting flies. Thank you for all the food,

fun and good movies/TV series, you are great! Lastly, I would like to thank Martina. I am thankful to my friend Alistair Langlands and to Villo Muha: it was a great pleasure to meet you and work with you.

I want to acknowledge other three special people that belong to the small family of Dundonian Drosophilists: Matthew, Anne and Nicolas. Thank you, guys for making the lab an even better place to be.

Also, thanks to everyone working in the flyroom, especially Dr. Daniel Mariyappa, for all the laughter and fun during the long hours sorting flies.

Thanks to all the members of the CDB division and all the friends from GRE, especially Sharon Mudie and all the present and past members of the Rocha lab.

All my gratitude goes to my little dundonian family. Dear Laura, you were the first person to welcome me in Dundee. Your smile and kindness helped me in feeling our beautiful Sicily less far away. Tuzza, thank you for providing with food during these four years and for taking care of all of us. Thank you for listening to all the complaints, for the support and the endless friendship. Dear Claudia, thank you for all the Saturday evenings spent together and for spotting the best places to dance in Dundee. Most importantly, thank you for all the time spent together planning our future in front of a good pint. Dear Kasia, the only polish in the world that will leave Scotland with an Italian accent. Thank you for all the time spent chatting away on your sofa and for being the best personal trainer ever! Step classes will not be the same without you...but you taught me the art of cheating! Guys, it is such a blessing to have you in my life. You make it brighter.

Last but not least, I would like to thank my family: my beloved parents that are and always will be an inspiration to me, my grandmother and my brothers for providing me with the confidence in my abilities.

Cancer Research UK funded my PhD project.

Reference List

Akhmanova, A. and M. O. Steinmetz (2008). "Tracking the ends: a dynamic protein network controls the fate of microtubule tips." Nat Rev Mol Cell Biol **9**(4): 309-322.

Amber R. Krauchunas, K. L. S., and Mariana F. Wolfner (2013). "Phospho-Regulation Pathways During Egg Activation in Drosophila melanogaster." Genetics, **195**: 171–180.

Amy C. Groth, M. F., Roel Nusse and Michele P. Calos (2004). "Construction of Transgenic Drosophila by Using the Site-Specific Integrase From Phage ϕC31." Genetics **166**: 1775–1782.

Andrea H. Brand, a. N. P. (1993). "Targeted gene expression as a means of altering cell fates and generating dominant phenotypes." Development **118**: 401415.

Bader, J. R., J. M. Kasuboski, M. Winding, P. S. Vaughan, E. H. Hinchcliffe and K. T. Vaughan (2011). "Polo-like kinase1 is required for recruitment of dynein to kinetochores during mitosis." J Biol Chem **286**(23): 20769-20777.

Barisic, M., B. Sohm, P. Mikolcevic, C. Wandke, V. Rauch, T. Ringer, M. Hess, G. Bonn and S. Geley (2010). "Spindly/CCDC99 is required for efficient chromosome congression and mitotic checkpoint regulation." Mol Biol Cell **21**(12): 1968-1981.

Bataille, L., B. Auge, G. Ferjoux, M. Haenlin and L. Waltzer (2005). "Resolving embryonic blood cell fate choice in Drosophila: interplay of GCM and RUNX factors." Development **132**(20): 4635-4644.

Belles X, P. (2014). " Ecdysone signalling and ovarian development in insects_ from stem cells to ovarian follicle formation ".

Bischof, J., R. K. Maeda, M. Hediger, F. Karch and K. Basler (2007). "An optimized transgenesis system for Drosophila using germ-line-specific phiC31 integrases." Proc Natl Acad Sci U S A **104**(9): 3312-3317.

Bonnie L. Hall, C. S. T. (1998). "The RXR homolog Ultraspiracle is an essential component of the Drosophila

ecdysone receptor." Development **125**: 4709-4717.

Borghese, L., G. Fletcher, J. Mathieu, A. Atzberger, W. C. Eades, R. L. Cagan and P. Rorth (2006). "Systematic analysis of the transcriptional switch inducing migration of border cells." Dev Cell **10**(4): 497-508.

Bruckner, K., L. Kockel, P. Duchek, C. M. Luque, P. Rorth and N. Perrimon (2004). "The PDGF/VEGF receptor controls blood cell survival in Drosophila." Dev Cell **7**(1): 73-84.

Buffin, E., D. Emre and R. E. Karess (2007). "Flies without a spindle checkpoint." Nat Cell Biol **9**(5): 565-572.

Byron C. Williams, A. F. D., Jaakko Puro, Seppo Nokkala, Michael L. Goldberg (1997). "The Drosophila kinesin-like protein KLP3A is required for proper behavior of male and female pronuclei at fertilization." Development **124**: 2365-2376.

Chan, Y. W., L. L. Fava, A. Uldschmid, M. H. Schmitz, D. W. Gerlich, E. A. Nigg and A. Santamaria (2009). "Mitotic control of kinetochore-associated dynein and spindle orientation by human Spindly." J Cell Biol **185**(5): 859-874.

Cheeseman, I. M. and A. Desai (2008). "Molecular architecture of the kinetochore-microtubule interface." Nat Rev Mol Cell Biol **9**(1): 33-46.

Chodagam, S., A. Royou, W. Whitfield, R. Karess and J. W. Raff (2005). "The centrosomal protein CP190 regulates myosin function during early Drosophila development." Curr Biol **15**(14): 1308-1313.

Ciferri, C., S. Pasqualato, E. Screpanti, G. Varetti, S. Santaguida, G. Dos Reis, A. Maiolica, J. Polka, J. G. De Luca, P. De Wulf, M. Salek, J. Rappsilber, C. A. Moores, E. D.

Salmon and A. Musacchio (2008). "Implications for kinetochore-microtubule attachment from the structure of an engineered Ndc80 complex." Cell **133**(3): 427-439.
Clemens, J. C., C. A. Worby, N. Simonson-Leff, M. Muda, T. Maehama, B. A. Hemmings and J. E. Dixon (2000). "Use of double-stranded RNA interference in Drosophila cell lines to dissect signal transduction pathways." Proc Natl Acad Sci U S A **97**(12): 6499-6503.
Cox, J. and M. Mann (2008). "MaxQuant enables high peptide identification rates, individualized p.p.b.-range mass accuracies and proteome-wide protein quantification." Nat Biotechnol **26**(12): 1367-1372.
Crozatier, J.-M. U., Alain Vincent, Marie Meister (2004

). "Cellular Immune Response to Parasitization in Drosophila Requires the EBF Orthologue Collier." Plos Biology **2**(8): 1107-1113

Daniel A. Starr, B. C. W., Thomas S. Hays and M. L. Goldberg (1998). "ZW10 Helps Recruit Dynactin and Dynein to the Kinetochore." The Journal of Cell Biology **142**(3): 763–774.
David J. Sharp, G. C. R., Jonathan M. Scholey (2000). "Microtubule motors in mitosis." Nature **407**.
David J. Sharp, G. C. R. a. J. M. S. (2000). "Cytoplasmic dynein is required for poleward chromosome movement during mitosis in Drosophila embryos." Nature Cell Biology **2**: 922-930.
David J. Sharp, H. M. B., Mijung Kwon, Gregory C. Rogers, Gina Holland, and Jonathan M. Scholey (2000). "Functional Coordination of Three Mitotic Motors in Drosophila Embryos." Molecular Biology of the Cell

11: 241–253.
David J. Sharp, K. L. M., à, H. J. M. Heather M. Brown, Claire Walczak,, Ron D. Vale, Timothy J. Mitchison and J. M. Scholey (1999). "The Bipolar Kinesin, KLP61F, Cross-links Microtubules within Interpolar Microtubule Bundles of Drosophila Embryonic Mitotic Spindles." Journal of Cell Biology: 125-138.
De Antoni, A., C. G. Pearson, D. Cimini, J. C. Canman, V. Sala, L. Nezi, M. Mapelli, L. Sironi, M. Faretta, E. D. Salmon and A. Musacchio (2005). "The Mad1/Mad2 complex as a template for Mad2 activation in the spindle assembly checkpoint." Curr Biol **15**(3): 214-225.
Denise J. Montell, P. R., and Allan C. Spradling (1992). "slow border cells, a Locus Required for a Developmentally Regulated Cell Migration during Oogenesis, Encodes Drosophila C/EBP." **71**: 51-62.
Douglas R. Kellogg, K. O., Jordan Raff, Ken Schneider, Bruce M. Alberts (1995). "CP60: A Microtubule-associated Protein that Is Localized to the Centrosome in a Cell Cycle-specific Manner." Molecular Biology of the Cell

6: 1673-1684.
Edward Wojcik, R. B., Madeline Serr, Frédéric Scaërou, Roger Karess and Thomas Hays (2001). "Kinetochore dynein: its dynamics and role in the transport of the Rough deal checkpoint protein " NATURE CELL BIOLOGY **3**: 1001-1007.
Espert, A., P. Uluocak, R. N. Bastos, D. Mangat, P. Graab and U. Gruneberg (2014). "PP2A-B56 opposes Mps1 phosphorylation of Knl1 and thereby promotes spindle assembly checkpoint silencing." J Cell Biol **206**(7): 833-842.

Evans, I. R. and W. Wood (2014). "Drosophila blood cell chemotaxis." Curr Opin Cell Biol **30**: 1-8.
Fire, A., S. Xu, M. K. Montgomery, S. A. Kostas, S. E. Driver and C. C. Mello (1998). "Potent and specific genetic interference by double-stranded RNA in Caenorhabditis elegans." Nature **391**(6669): 806-811.
Forlani, S., D. Ferrandon, O. Saget and E. Mohier (1993). "A regulatory function for K10 in the establishment of dorsoventral polarity in the Drosophila egg and embryo." Mech Dev **41**(2-3): 109-120.
Foster, S. A. and D. O. Morgan (2012). "The APC/C subunit Mnd2/Apc15 promotes Cdc20 autoubiquitination and spindle assembly checkpoint inactivation." Mol Cell **47**(6): 921-932.
Garcia, K., J. Stumpff, T. Duncan and T. T. Su (2009). "Tyrosines in the kinesin-5 head domain are necessary for phosphorylation by Wee1 and for mitotic spindle integrity." Curr Biol **19**(19): 1670-1676.
Gassmann, R., A. Essex, J. S. Hu, P. S. Maddox, F. Motegi, A. Sugimoto, S. M. O'Rourke, B. Bowerman, I. McLeod, J. R. Yates, 3rd, K. Oegema, I. M. Cheeseman and A. Desai (2008). "A new mechanism controlling kinetochore-microtubule interactions revealed by comparison of two dynein-targeting components: SPDL-1 and the Rod/Zwilch/Zw10 complex." Genes Dev **22**(17): 2385-2399.
Gassmann, R., A. J. Holland, D. Varma, X. Wan, F. Civril, D. W. Cleveland, K. Oegema, E. D. Salmon and A. Desai (2010). "Removal of Spindly from microtubule-attached kinetochores controls spindle checkpoint silencing in human cells." Genes Dev **24**(9): 957-971.
Geisbrecht, E. R. and D. J. Montell (2002). "Myosin VI is required for E-cadherin-mediated border cell migration." Nat Cell Biol **4**(8): 616-620.
Ghongane, P., M. Kapanidou, A. Asghar, S. Elowe and V. M. Bolanos-Garcia (2014). "The dynamic protein Knl1 - a kinetochore rendezvous." J Cell Sci **127**(Pt 16): 3415-3423.
Goshima, G., R. Wollman, S. S. Goodwin, N. Zhang, J. M. Scholey, R. D. Vale and N. Stuurman (2007). "Genes required for mitotic spindle assembly in Drosophila S2 cells." Science **316**(5823): 417-421.
Griffis, E. R., N. Stuurman and R. D. Vale (2007). "Spindly, a novel protein essential for silencing the spindle assembly checkpoint, recruits dynein to the kinetochore." J Cell Biol **177**(6): 1005-1015.
Groen, C. M., A. J. Spracklen, T. N. Fagan and T. L. Tootle (2012). "Drosophila Fascin is a novel downstream target of prostaglandin signaling during actin remodeling." Mol Biol Cell **23**(23): 4567-4578.
Han, J. S., A. J. Holland, D. Fachinetti, A. Kulukian, B. Cetin and D. W. Cleveland (2013). "Catalytic assembly of the mitotic checkpoint inhibitor BubR1-Cdc20 by a Mad2-induced functional switch in Cdc20." Mol Cell **51**(1): 92-104.
Holland, A. J. and D. W. Cleveland (2009). "Boveri revisited: chromosomal instability, aneuploidy and tumorigenesis." Nat Rev Mol Cell Biol **10**(7): 478-487.
Holland, A. J., R. M. Reis, S. Niessen, C. Pereira, D. A. Andres, H. P. Spielmann, D. W. Cleveland, A. Desai and R. Gassmann (2015). "Preventing farnesylation of the dynein adaptor Spindly contributes to the mitotic defects caused by farnesyltransferase inhibitors." Mol Biol Cell **26**(10): 1845-1856.
Holz, A., B. Bossinger, T. Strasser, W. Janning and R. Klapper (2003). "The two origins of hemocytes in Drosophila." Development **130**(20): 4955-4962.

Horacio M. Frydman, A. C. S. (2001). "The receptor-like tyrosine phosphatase Lar is required for epithelial planar polarity and for axis determination within Drosophila ovarian follicles." Development **128**: 3209-3220.
Horne-Badovinac, S. and D. Bilder (2005). "Mass transit: epithelial morphogenesis in the Drosophila egg chamber." Dev Dyn **232**(3): 559-574.
Horner, V. L. and M. F. Wolfner (2008). "Transitioning from egg to embryo: triggers and mechanisms of egg activation." Dev Dyn **237**(3): 527-544.
Howell, B. J., B. F. McEwen, J. C. Canman, D. B. Hoffman, E. M. Farrar, C. L. Rieder and E. D. Salmon (2001). "Cytoplasmic dynein/dynactin drives kinetochore protein transport to the spindle poles and has a role in mitotic spindle checkpoint inactivation." J Cell Biol **155**(7): 1159-1172.
Huynh, J. R. and D. St Johnston (2004). "The origin of asymmetry: early polarisation of the Drosophila germline cyst and oocyte." Curr Biol **14**(11): R438-449.
Jack Bateman, R. S. R., Haruo Saito and a. D. V. Vactor (2001). "The receptor tyrosine phosphatase Dlar and integrins organize actin filaments in the Drosophila follicular epithelium." Current Biology **11**: 1317–1327.
Jang, A. C., Y. C. Chang, J. Bai and D. Montell (2009). "Border-cell migration requires integration of spatial and temporal signals by the BTB protein Abrupt." Nat Cell Biol **11**(5): 569-579.
Jang, A. C., M. Starz-Gaiano and D. J. Montell (2007). "Modeling migration and metastasis in Drosophila." J Mammary Gland Biol Neoplasia **12**(2-3): 103-114.
Jason E. Duncan, R. W. (2002). "The Cytoplasmic Dynein and Kinesin Motors Have Interdependent Roles in Patterning the Drosophila Oocyte." Current Biology **12**: 1982–1991.
Jayne Baker, W. E. T., Gerold Sehubiger (1993). "Dynamic Changes in Microtubule Configuration Correlate with Nuclear Migration in the Preblastoderm Drosophila Embryo." J Cell Biol: 113-121.
Jennifer R. McGregor, R. X. a. D. A. H. (2002). "JAK signaling is somatically required for follicle cell differentiation in

Drosophila." Development **129**: 705-717.
Jens Januschke, L. G., Sajith Dass,, H. L.-S. Julia A. Kaltschmidt, A. H. B. Daniel St. Johnston and a. A. G. Siegfried Roth (2002). "Polar Transport in the Drosophila Oocyte requires Dynein and Kinesin I Cooperation." Curr Biol **12**: 1971-1981.
Jensen, L. J., M. Kuhn, M. Stark, S. Chaffron, C. Creevey, J. Muller, T. Doerks, P. Julien, A. Roth, M. Simonovic, P. Bork and C. von Mering (2009). "STRING 8--a global view on proteins and their functional interactions in 630 organisms." Nucleic Acids Res **37**(Database issue): D412-416.
Jianwu Bai, Y. U., and Denise J. Montell (2000). "Regulation of Invasive Cell Behavior by Taiman, a Drosophila Protein Related to AIB1, a Steroid Receptor Coactivator Amplified in Breast Cancer." Cell **103**: 1047–1058.
Jocelyn A. McDonald, E. M. P., Denise J. Montell (2003). "PVF1, a PDGF/VEGF homolog, is sufficient to guide border cells and interacts genetically with Taiman." Development **130**(15): 3469-3478.
John T. Robinson, E. J. W., Mark A. Sanders, Maura McGrail, and Thomas S. Hays (1999). "Cytoplasmic dynein is required for the nuclear attachment and migration of centrosomes during mitosis in Drosophila." Journal of Cell Biology **146**(3): 597-608.

Jordan W. Raft, D. R. K., Bruce M. Alberts (1993). "Drosophila y-Tubulin Is Part of a Complex Containing Two Previously Identified Centrosomal MAPs." The Journal of Cell Biology **121**(4): 823-835.
Jung, S. H., C. J. Evans, C. Uemura and U. Banerjee (2005). "The Drosophila lymph gland as a developmental model of hematopoiesis." Development **132**(11): 2521-2533.
Kasuboski, J. M., J. R. Bader, P. S. Vaughan, S. B. Tauhata, M. Winding, M. A. Morrissey, M. V. Joyce, W. Boggess, L. Vos, G. K. Chan, E. H. Hinchcliffe and K. T. Vaughan (2011). "Zwint-1 is a novel Aurora B substrate required for the assembly of a dynein-binding platform on kinetochores." Mol Biol Cell **22**(18): 3318-3330.
Kavanagh, K. and E. P. Reeves (2004). "Exploiting the potential of insects for in vivo pathogenicity testing of microbial pathogens." FEMS Microbiol Rev **28**(1): 101-112.
Kenneth W. Wood, R. S., Lawrence S. B. Goldstein, and Don W. Cleveland (1997). "CENP-E Is a Plus End–Directed Kinetochore Motor Required for Metaphase Chromosome Alignment." Cell **91**: 357–366.
Kops, G. J., Y. Kim, B. A. Weaver, Y. Mao, I. McLeod, J. R. Yates, 3rd, M. Tagaya and D. W. Cleveland (2005). "ZW10 links mitotic checkpoint signaling to the structural kinetochore." J Cell Biol **169**(1): 49-60.
Kotak, S., C. Busso and P. Gonczy (2012). "Cortical dynein is critical for proper spindle positioning in human cells." J Cell Biol **199**(1): 97-110.
Krauchunas, A. R., V. L. Horner and M. F. Wolfner (2012). "Protein phosphorylation changes reveal new candidates in the regulation of egg activation and early embryogenesis in D. melanogaster." Dev Biol **370**(1): 125-134.
Kurucz, E., C. J. Zettervall, R. Sinka, P. Vilmos, A. Pivarcsi, S. Ekengren, Z. Hegedus, I. Ando and D. Hultmark (2003). "Hemese, a hemocyte-specific transmembrane protein, affects the cellular immune response in Drosophila." Proc Natl Acad Sci U S A **100**(5): 2622-2627.
Kuttenkeuler, D. and M. Boutros (2004). "Genome-wide RNAi as a route to gene function in Drosophila." Brief Funct Genomic Proteomic **3**(2): 168-176.
Lehmann, A. F. a. R. (1998). "Nanos and Pumilio have critical roles in the development and function of Drosophila germline stem cells." Development **125**: 679-690.
Liu, D., M. Vleugel, C. B. Backer, T. Hori, T. Fukagawa, I. M. Cheeseman and M. A. Lampson (2010). "Regulated targeting of protein phosphatase 1 to the outer kinetochore by KNL1 opposes Aurora B kinase." J Cell Biol **188**(6): 809-820.
Llense, F. and E. Martin-Blanco (2008). "JNK signaling controls border cell cluster integrity and collective cell migration." Curr Biol **18**(7): 538-544.
London, N. and S. Biggins (2014). "Mad1 kinetochore recruitment by Mps1-mediated phosphorylation of Bub1 signals the spindle checkpoint." Genes Dev **28**(2): 140-152.
London, N., S. Ceto, J. A. Ranish and S. Biggins (2012). "Phosphoregulation of Spc105 by Mps1 and PP1 regulates Bub1 localization to kinetochores." Curr Biol **22**(10): 900-906.
Loppin, B., R. Dubruille and B. Horard (2015). "The intimate genetics of Drosophila fertilization." Open Biol **5**(8).
Luo, J., J. Zuo, J. Wu, P. Wan, D. Kang, C. Xiang, H. Zhu and J. Chen (2015). "In vivo RNAi screen identifies candidate signaling genes required for collective cell migration in Drosophila ovary." Sci China Life Sci **58**(4): 379-389.
M. Andrew Hoyt, L. T., B. Tibor Roberts (1991). "S. cerevisiae Genes Required for Cell Cycle Arrest in Response to Loss of Microtubule Function." Cell **66**: 507-517.
Maldonado, M. and T. M. Kapoor (2011). "Constitutive Mad1 targeting to kinetochores uncouples checkpoint signalling from chromosome biorientation." Nat Cell Biol **13**(4): 475-482.

Matthew S. Savoian, D. M. G. (2010). "Drosophila Klp67A binds prophase kinetochores to subsequently regulate congression and spindle length." Journal of Cell Science **123**: 767-776.
Matthew S. Savoian, M. K. G., Maria G. Riparbelli, Giuliano Callaini and David M. Glover (2004). "Drosophila Klp67A is required for proper chromosome congression and segregation during meiosis I." Journal of Cell Science **117**: 3669-3677.
Matthews, K. A., D. F. Miller and T. C. Kaufman (1989). "Developmental distribution of RNA and protein products of the Drosophila alpha-tubulin gene family." Dev Biol **132**(1): 45-61.
Max V. Staller, D. Y., Sakara Randklev, Meghan D. Bragdon, Zeba B. Wunderlich, Rong Tao, and A. H. D. Lizabeth A. Perkins, and Norbert Perrimon (2013). "Depleting Gene Activities in Early Drosophila Embryos with the "Maternal-Gal4–shRNA" System." Genetics **193**: 51–61.
McDonald, J. A., E. M. Pinheiro, L. Kadlec, T. Schupbach and D. J. Montell (2006). "Multiple EGFR ligands participate in guiding migrating border cells." Dev Biol **296**(1): 94-103.
Melani, M., K. J. Simpson, J. S. Brugge and D. Montell (2008). "Regulation of cell adhesion and collective cell migration by hindsight and its human homolog RREB1." Curr Biol **18**(7): 532-537.
Melanie K. Gatt, M. S. S., Maria G. Riparbelli, Chiara Massarelli, Giuliano Callaini and David M. Glover (2005). "Klp67A destabilises pre-anaphase microtubules but subsequently is required to stabilise the central spindle." Journal of Cell Science **118**: 2671-2682.
Michael Buszczak, M. R. F., John R. Carlson, Michael Bender, Lynn Cooley and a. W. A. Segraves (1999). "Ecdysone response genes govern egg chamber development during midoogenesis in Drosophila." Development **126**: 4581-4589.
Michael T.Tetzlaff, H. J. a. M. J. P. (1996). "Lack of Drosophila cytoskeletal tropomyosin affects head morphogenesis and the accumulation of oskar mRNA required for germ cell formation." The EMBO Journal **15**(06): 1247-1254.
Michele Markstein, C. P., Christians Villalta, Susan E Celniker, and Norbert Perrimon (2008). "Exploiting position effects and the gypsy retrovirus insulator to engineer precisely expressed transgenes." Nat Genet. **40**(4): 476–483.
Miklós Erdélyi, A.-M. M., Antoine Guichet, Jolanta Bogucka Glotzer & Anne Ephrussi (1995). "Requirement for Drosophila cytoplasmic tropomyosin in oskar mRNA localisation." Nature **377**: 524 - 527.
Mische, S., Y. He, L. Ma, M. Li, M. Serr and T. S. Hays (2008). "Dynein light intermediate chain: an essential subunit that contributes to spindle checkpoint inactivation." Mol Biol Cell **19**(11): 4918-4929.
Montell, D. J. (2003). "Border-cell migration: the race is on." Nat Rev Mol Cell Biol **4**(1): 13-24.
Moon, H. M., Y. H. Youn, H. Pemble, J. Yingling, T. Wittmann and A. Wynshaw-Boris (2014). "LIS1 controls mitosis and mitotic spindle organization via the LIS1-NDEL1-dynein complex." Hum Mol Genet **23**(2): 449-466.
Morales-Mulia, S. and J. M. Scholey (2005). "Spindle pole organization in Drosophila S2 cells by dynein, abnormal spindle protein (Asp), and KLP10A." Mol Biol Cell **16**(7): 3176-3186.
Moreira, S., B. Stramer, I. Evans, W. Wood and P. Martin (2010). "Prioritization of competing damage and developmental signals by migrating macrophages in the Drosophila embryo." Curr Biol **20**(5): 464-470.

Moudgil, D. K., N. Westcott, J. K. Famulski, K. Patel, D. Macdonald, H. Hang and G. K. Chan (2015). "A novel role of farnesylation in targeting a mitotic checkpoint protein, human Spindly, to kinetochores." J Cell Biol **208**(7): 881-896.
Moyle, M. W., T. Kim, N. Hattersley, J. Espeut, D. K. Cheerambathur, K. Oegema and A. Desai (2014). "A Bub1-Mad1 interaction targets the Mad1-Mad2 complex to unattached kinetochores to initiate the spindle checkpoint." J Cell Biol **204**(5): 647-657.
Muller, H., D. Schmidt, S. Steinbrink, E. Mirgorodskaya, V. Lehmann, K. Habermann, F. Dreher, N. Gustavsson, T. Kessler, H. Lehrach, R. Herwig, J. Gobom, A. Ploubidou, M. Boutros and B. M. Lange (2010). "Proteomic and functional analysis of the mitotic Drosophila centrosome." EMBO J **29**(19): 3344-3357.
N.J. Quintyne, S. R. G., D.M. Eckley, C.L. Crego, D.A. Compton, T.A. Schroer (1999). "Dynactin Is Required for Microtubule Anchoring at Centrosomes." J Cell Biol **147**(2): 321-334.
Nam K. Cho, L. K., Eric Johnson, Jonathan Heller, Lisa Ryner, Felix Karim (2002). "Developmental Control of Blood Cell Migration by the Drosophila VEGF Pathway." Cell **108**: 865-876.
Nezi, L., G. Rancati, A. De Antoni, S. Pasqualato, S. Piatti and A. Musacchio (2006). "Accumulation of Mad2-Cdc20 complex during spindle checkpoint activation requires binding of open and closed conformers of Mad2 in Saccharomyces cerevisiae." J Cell Biol **174**(1): 39-51.
Ni, J. Q., L. P. Liu, R. Binari, R. Hardy, H. S. Shim, A. Cavallaro, M. Booker, B. D. Pfeiffer, M. Markstein, H. Wang, C. Villalta, T. R. Laverty, L. A. Perkins and N. Perrimon (2009). "A Drosophila resource of transgenic RNAi lines for neurogenetics." Genetics **182**(4): 1089-1100.
Ni, J. Q., M. Markstein, R. Binari, B. Pfeiffer, L. P. Liu, C. Villalta, M. Booker, L. Perkins and N. Perrimon (2008). "Vector and parameters for targeted transgenic RNA interference in Drosophila melanogaster." Nat Methods **5**(1): 49-51.
Ogienko, A. A., S. A. Fedorova and E. M. Baricheva (2007). "Basic aspects of ovarian development in Drosophila melanogaster." Russian Journal of Genetics **43**(10): 1120-1134.
OKADA, K. H. a. M. (1991). "Retarded nuclear migration in Drosophila embryos with aberrant F-actin reorganization caused by maternal mutations and by cytochalasin treatment." Development **111**: 909-920.
Paulina Niewiadomska, D. G., and Ulrich Tepass (1999). "DE-Cadherin Is Required for Intercellular Motility during Drosophila Oogenesis." The Journal of Cell Biology **144**(3): 533-547.
Pernille Rørth1, K. S., Adina Bailey, Todd Laverty, Jay Rehm, Gerald M. Rubin, and M. M. Katrin Weigmann, Vladimir Benes, Wilhelm Ansorge and Stephen M. Cohen (1998). "Systematic gain-of-function genetics in Drosophila." Development **125**: 1049-1057.
Peter Duchek, K. l. n. S., Ga´ spa´r Je´ kely, Simone Beccari, and Pernille Rørth (2001). "Guidance of Cell Migration by the Drosophila PDGF/VEGF Receptor." Cell **107**: 17–26.
Peter Duchek, K. l. n. S., Ga´ spa´r Je´ kely, Simone Beccari, and Pernille Rørth (2001). "Guidance of Cell Migration by the Drosophila PDGF/VEGF Receptor." Cell **107**: 17-26.
Peterman, E. J. and J. M. Scholey (2009). "Mitotic microtubule crosslinkers: insights from mechanistic studies." Curr Biol **19**(23): R1089-1094.
Pinheiro, E. M. and D. J. Montell (2004). "Requirement for Par-6 and Bazooka in Drosophila border cell migration." Development **131**(21): 5243-5251.
Prasad, M. and D. J. Montell (2007). "Cellular and molecular mechanisms of border cell migration analyzed using time-lapse live-cell imaging." Dev Cell **12**(6): 997-1005.

Qing-Hua Zhang, L. W., Jing-Shan Tong, Shu-Tao Qi, Sen Li, Xiang-Hong Ou, Ying-Chun Ouyang, Yi Hou, Li-Guo An, Heide Schatten and Qing-Yuan Sun (2010). "Localization and function of mSpindly during mouse oocyte meiotic maturation." Cell Cycle **9**(11): 2230-2236.
R0RTH, P. (1996). "A modular misexpression screen in Drosophila detecting tissue-specific phenotypes." Proc. Natl. Acad. Sci. USA

93: 12418-12422.
Raaijmakers, J. A. and R. H. Medema (2014). "Function and regulation of dynein in mitotic chromosome segregation." Chromosoma **123**(5): 407-422.
Raff, J. W., K. Jeffers and J. Y. Huang (2002). "The roles of Fzy/Cdc20 and Fzr/Cdh1 in regulating the destruction of cyclin B in space and time." J Cell Biol **157**(7): 1139-1149.
Razzell, W., I. R. Evans, P. Martin and W. Wood (2013). "Calcium flashes orchestrate the wound inflammatory response through DUOX activation and hydrogen peroxide release." Curr Biol **23**(5): 424-429.
Richard J. McKenney, W. H., Marvin E. Tanenbaum, Gira Bhabha, Ronald D. Vale (2014). "Activation of cytoplasmic dynein motility by dynactin-cargo adapter complexes." Science **345**(6194): 337-341.
Rogers, S. L., G. C. Rogers, D. J. Sharp and R. D. Vale (2002). "Drosophila EB1 is important for proper assembly, dynamics, and positioning of the mitotic spindle." J Cell Biol **158**(5): 873-884.
Rong Li, A. W. M. (1991). "Feedback Control of Mitosis in Budding Yeast." Cell **66**: 519-531.
Roth, S. (2003). "The origin of dorsoventral polarity in Drosophila." Philos Trans R Soc Lond B Biol Sci **358**(1436): 1317-1329; discussion 1329.
Roth, S. and J. A. Lynch (2009). "Symmetry breaking during Drosophila oogenesis." Cold Spring Harb Perspect Biol **1**(2): a001891.
Royou, A., W. Sullivan and R. Karess (2002). "Cortical recruitment of nonmuscle myosin II in early syncytial Drosophila embryos: its role in nuclear axial expansion and its regulation by Cdc2 activity." J Cell Biol **158**(1): 127-137.
Sally Horne-Badovinac, D. B. (2008). "Dynein Regulates Epithelial Polarity and the Apical Localization of stardust A mRNA." PLoS Genet **4**(1): 40-51.
Sally Horne-Badovinac, J. H., Gary Gerlach II, William Menegas, David Bilder (2012). "A Screen for Round Egg Mutants in Drosophila

Identifies Tricornered, Furry, and Misshapen

as Regulators of Egg Chamber Elongation." Genes, Genomes, Genetics **2**.
Sally Wheatley, S. K. a. R. K. (1995). "Drosophila nonmuscle myosin II is required for rapid cytoplasmic transport during oogenesis and for axial nuclear migration in early embryos." Development **121**: 1937-1946.
Saurin, A. T., M. S. van der Waal, R. H. Medema, S. M. Lens and G. J. Kops (2011). "Aurora B potentiates Mps1 activation to ensure rapid checkpoint establishment at the onset of mitosis." Nat Commun **2**: 316.
Schejter, D. V.-O. a. E. D. (1999). "Mutations in centrosomin reveal requirements for centrosomal function during early Drosophila embryogenesis." Current Biology **9**(16): 889-898.
Schlager, M. A., H. T. Hoang, L. Urnavicius, S. L. Bullock and A. P. Carter (2014). "In vitro reconstitution of a highly processive recombinant human dynein complex." EMBO J **33**(17): 1855-1868.

SCHNEIDER, I. (1972). "Cell lines derived from late embryonic stages of Drosophila melanogaster." Embryol. exp. Morph. **27**(2): 353-365.
Schroer, S. J. K. a. T. A. (2000). "Dynactin increases the processivity of the cytoplasmic dynein motor." Nature Cell Biology **2**: 20-24.
Schupbach, T. (1987). "Germ line and soma cooperate during oogenesis to establish the dorsoventral pattern of egg shell and embryo in Drosophila melanogaster." Cell **49**(5): 699-707.
Sears, H. C. (2003). "Macrophage-mediated corpse engulfment is required for normal Drosophila CNS morphogenesis." Development **130**(15): 3557-3565.
Shepperd, L. A., J. C. Meadows, A. M. Sochaj, T. C. Lancaster, J. Zou, G. J. Buttrick, J. Rappsilber, K. G. Hardwick and J. B. Millar (2012). "Phosphodependent recruitment of Bub1 and Bub3 to Spc7/KNL1 by Mph1 kinase maintains the spindle checkpoint." Curr Biol **22**(10): 891-899.
Silver D. L., D. J. M. (2001). "Paracrine Signaling through the JAK/STAT Pathway Activates Invasive Behavior of Ovarian Epithelial Cells in Drosophila." Cell **107**: 831–841.
Silver, D. L., E. R. Geisbrecht and D. J. Montell (2005). "Requirement for JAK/STAT signaling throughout border cell migration in Drosophila." Development **132**(15): 3483-3492.
Simone Beccari, L. s. T., Pernille Rørth (2002). "The JAK/STAT pathway is required for border cell migration during Drosophila oogenesis." Mechanisms of Development **111**: 115-123.
Sinenko, S. A., E. K. Kim, R. Wynn, P. Manfruelli, I. Ando, K. A. Wharton, N. Perrimon and B. Mathey-Prevot (2004). "Yantar, a conserved arginine-rich protein is involved in Drosophila hemocyte development." Dev Biol **273**(1): 48-62.
Steeg, P. S. (2006). "Tumor metastasis: mechanistic insights and clinical challenges." Nat Med **12**(8): 895-904.
Steinmetz, A. A. a. M. O. (2010). "Microtubule +TIPs at a glance." Journal of Cell Science **123**: 3415-3419.
Stramer, B., S. Moreira, T. Millard, I. Evans, C. Y. Huang, O. Sabet, M. Milner, G. Dunn, P. Martin and W. Wood (2010). "Clasp-mediated microtubule bundling regulates persistent motility and contact repulsion in Drosophila macrophages in vivo." J Cell Biol **189**(4): 681-689.
Stramer, B., W. Wood, M. J. Galko, M. J. Redd, A. Jacinto, S. M. Parkhurst and P. Martin (2005). "Live imaging of wound inflammation in Drosophila embryos reveals key roles for small GTPases during in vivo cell migration." J Cell Biol **168**(4): 567-573.
Sun, S. C. and N. H. Kim (2012). "Spindle assembly checkpoint and its regulators in meiosis." Hum Reprod Update **18**(1): 60-72.
Tanenbaum, M. E. and R. H. Medema (2010). "Mechanisms of centrosome separation and bipolar spindle assembly." Dev Cell **19**(6): 797-806.
Teichner, A., E. Eytan, D. Sitry-Shevah, S. Miniowitz-Shemtov, E. Dumin, J. Gromis and A. Hershko (2011). "p31comet Promotes disassembly of the mitotic checkpoint complex in an ATP-dependent process." Proc Natl Acad Sci U S A **108**(8): 3187-3192.
Thomas Lecuit, E. W. (2000). "Polarized Insertion of New Membrane from a Cytoplasmic Reservoir during Cleavage of the Drosophila Embryo." The Journal of Cell Biology **150**(4): 849–860

Tim Lebestky, T. C., Volker Hartenstein, Utpal Banerjee (2003). "SpeciÞcation of Drosophila Hematopoietic Lineage by Conserved Transcription Factors." Reports.
Timothy L. Karr, B. M. A. (1986). "Organization of the Cytoskeleton in Early Drosophila Embryos." The Journal of Cell Biology **102**: 1494-1509.
Tin Tin Su, F. S., Paul J. DiGregorio, Shelagh D. Campbell, and Patrick H. O'Farrell (1998). "Exit from mitosis in Drosophila syncytial embryos requires proteolysis and cyclin degradation, and is associated with localized dephosphorylation." GENES & DEVELOPMENT **12**: 1495–1503.
Tipton, A. R., W. Ji, B. Sturt-Gillespie, M. E. Bekier, 2nd, K. Wang, W. R. Taylor and S. T. Liu (2013). "Monopolar spindle 1 (MPS1) kinase promotes production of closed MAD2 (C-MAD2) conformer and assembly of the mitotic checkpoint complex." J Biol Chem **288**(49): 35149-35158.
Tirnauer, J. S., S. Grego, E. D. Salmon and T. J. Mitchison (2002). "EB1-microtubule interactions in Xenopus egg extracts: role of EB1 in microtubule stabilization and mechanisms of targeting to microtubules." Mol Biol Cell **13**(10): 3614-3626.
Todd Maney, A. W. H., Mike Wagenbach, Linda Wordeman (1998). "Mitotic Centromere–associated Kinesin Is Important for Anaphase Chromosome Segregation." The Journal of Cell Biology **142**(3): 787–801

Torsten Wittmann, A. H. a. A. D. (2001). "The spindle: a dynamic assembly of microtubules and motors." NATURE CELL BIOLOGY **3**: 28-34.
Toshiyuki Habu, S. H. K., Jasminder Weinstein and Tomohiro Matsumoto (2002). "Identication of a MAD2-binding protein, CMT2, and its role in mitosis." The EMBO Journal **21**(23): 6419-6428.
Ulrich Tepass, L. I. F., Amina Aziz and Volker Hartenstein (1994). "Embryonic origin of hemocytes and their relationship to cell death in Drosophila." Development **120**: 1829-1837.
Uyen Tram, B. R., William Sullivan (2002). "Cleavage and Gastrulation in Drosophila Embryos." ENCYCLOPEDIA OF LIFE SCIENCES.
Uzunova, K., B. T. Dye, H. Schutz, R. Ladurner, G. Petzold, Y. Toyoda, M. A. Jarvis, N. G. Brown, I. Poser, M. Novatchkova, K. Mechtler, A. A. Hyman, H. Stark, B. A. Schulman and J. M. Peters (2012). "APC15 mediates CDC20 autoubiquitylation by APC/C(MCC) and disassembly of the mitotic checkpoint complex." Nat Struct Mol Biol **19**(11): 1116-1123.
Vader, G., A. F. Maia and S. M. Lens (2008). "The chromosomal passenger complex and the spindle assembly checkpoint: kinetochore-microtubule error correction and beyond." Cell Div **3**: 10.
van den Wildenberg, S. M., L. Tao, L. C. Kapitein, C. F. Schmidt, J. M. Scholey and E. J. Peterman (2008). "The homotetrameric kinesin-5 KLP61F preferentially crosslinks microtubules into antiparallel orientations." Curr Biol **18**(23): 1860-1864.
van Heesbeen, R. G., M. E. Tanenbaum and R. H. Medema (2014). "Balanced activity of three mitotic motors is required for bipolar spindle assembly and chromosome segregation." Cell Rep **8**(4): 948-956.
Varma, D., X. Wan, D. Cheerambathur, R. Gassmann, A. Suzuki, J. Lawrimore, A. Desai and E. D. Salmon (2013). "Spindle assembly checkpoint proteins are positioned close to core microtubule attachment sites at kinetochores." J Cell Biol **202**(5): 735-746.
Vivian A. Lombillo, C. N., Tim J. Yen, Vladimir I. Gelfand, J. Richard McIntosh (1995). "Antibodies to the Kinesin Motor Domain and CENP-E Inhibit Microtubule

Depolymerization-dependent Motion of Chromosomes In Vitro." The Journal of Cell Biology **128**: 107-115.
von Stein, W., A. Ramrath, A. Grimm, M. Muller-Borg and A. Wodarz (2005). "Direct association of Bazooka/PAR-3 with the lipid phosphatase PTEN reveals a link between the PAR/aPKC complex and phosphoinositide signaling." Development **132**(7): 1675-1686.
Wang H., B.-M. I., Scholey J. (2014). "Sliding filaments and mitotic spindle organization." Nature Cell Biology **16**(8): 737-739.
Welburn, J. P., M. Vleugel, D. Liu, J. R. Yates, 3rd, M. A. Lampson, T. Fukagawa and I. M. Cheeseman (2010). "Aurora B phosphorylates spatially distinct targets to differentially regulate the kinetochore-microtubule interface." Mol Cell **38**(3): 383-392.
Westhorpe, F. G., A. Tighe, P. Lara-Gonzalez and S. S. Taylor (2011). "p31comet-mediated extraction of Mad2 from the MCC promotes efficient mitotic exit." J Cell Sci **124**(Pt 22): 3905-3916.
Whyte, J., J. R. Bader, S. B. Tauhata, M. Raycroft, J. Hornick, K. K. Pfister, W. S. Lane, G. K. Chan, E. H. Hinchcliffe, P. S. Vaughan and K. T. Vaughan (2008). "Phosphorylation regulates targeting of cytoplasmic dynein to kinetochores during mitosis." J Cell Biol **183**(5): 819-834.
Wood, I. R. E. a. W. (2011). "Understanding in vivo blood cell migration_Drosophila Haemocytes lead the way." Landes Bioscience **5**(2).
Wood, W., C. Faria and A. Jacinto (2006). "Distinct mechanisms regulate hemocyte chemotaxis during development and wound healing in Drosophila melanogaster." J Cell Biol **173**(3): 405-416.
Wood, W. and A. Jacinto (2007). "Drosophila melanogaster embryonic haemocytes: masters of multitasking." Nat Rev Mol Cell Biol **8**(7): 542-551.
Yamamoto, T. G., S. Watanabe, A. Essex and R. Kitagawa (2008). "SPDL-1 functions as a kinetochore receptor for MDF-1 in Caenorhabditis elegans." J Cell Biol **183**(2): 187-194.
Yang, N., M. Inaki, A. Cliffe and P. Rorth (2012). "Microtubules and Lis-1/NudE/dynein regulate invasive cell-on-cell migration in Drosophila." PLoS One **7**(7): e40632.
Yang, Z., U. S. Tulu, P. Wadsworth and C. L. Rieder (2007). "Kinetochore dynein is required for chromosome motion and congression independent of the spindle checkpoint." Curr Biol **17**(11): 973-980.
Yuru Liu, D. J. M. (2001). "jing: a downstream target of slbo required for developmental control of border cell migration." Development **128**: 321-330.
Zhang, G., H. Beati, J. Nilsson and A. Wodarz (2013). "The Drosophila microtubule-associated protein mars stabilizes mitotic spindles by crosslinking microtubules through its N-terminal region." PLoS One **8**(4): e60596.
Zhang, G., M. Breuer, A. Forster, D. Egger-Adam and A. Wodarz (2009). "Mars, a Drosophila protein related to vertebrate HURP, is required for the attachment of centrosomes to the mitotic spindle during syncytial nuclear divisions." J Cell Sci **122**(Pt 4): 535-545.
Zhang, G., T. Lischetti, D. G. Hayward and J. Nilsson (2015). "Distinct domains in Bub1 localize RZZ and BubR1 to kinetochores to regulate the checkpoint." Nat Commun **6**: 7162.

Chapter IX: Appendix

Supplemental Information

Appendix

Figure S-1: Detailed pLou3 vector information. The vector was derived from the pMal-c2x vector (New England Biolab). Compared to the original vector, the pLou3 contains a N-terminal 6x_His tag and a Tev protease cleavage site between the MBP tag and the polylinker.

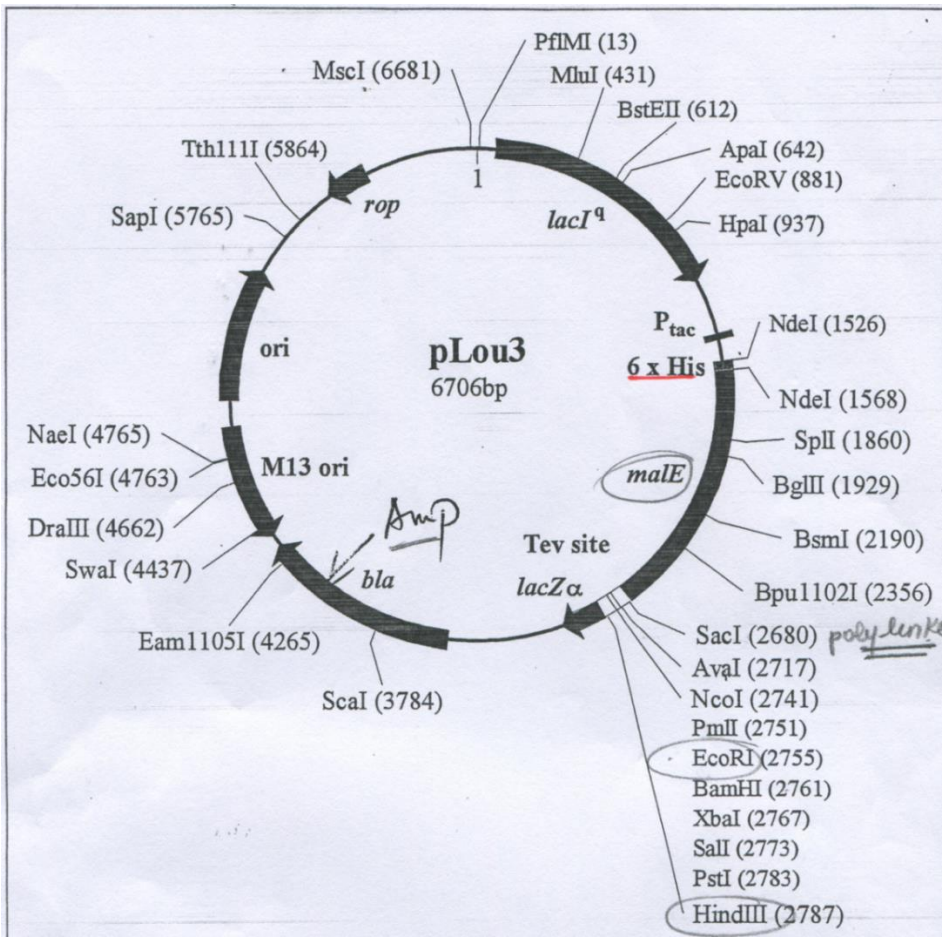

Figure S-2: Efficiency of Spindly knockdown. Western blot analysis shows Spindly knockdown in early *Drosophila* embryos. Protein lysates were collected from 0-3-hour wild-type (w^{1118}) and Spindly-depleted embryos and run on a SDS-PAGE gel. Egg collection was performed at 18°C. Proteins were transferred to a nitrocellulose membrane that was probed for Spindly. Actin was included as loading control. For a precise molecular weight determination, a standard protein molecular weight marker was used and numbers in kDa are shown on the left. The experiment was performed once.

Compare to the Western blot result showed in Figure 3-3, the banding pattern obtained probing the membrane with the anti-Spindly antibody was unusual. Even though we are not able to explain this variation, we observed a significant reduction in the total amount of Spindly protein upon Spindly-RNAi (lane 2) compared to the wild-type control (lane 1). This result suggested that the target protein was efficiently knocked down under the conditions tested but additional biological replicates of the experiment are needed.

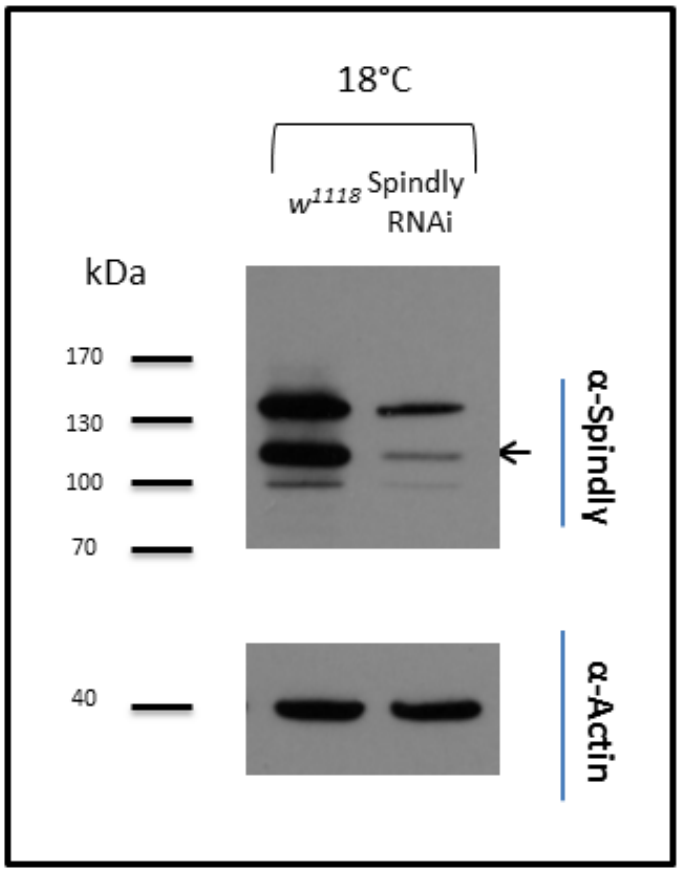

Figure S- 3: Spindly and Mad-2 fail to interact in prometaphase arrested S2 cells. (A) Western Blot analysis was performed to test the efficiency of the treatment with Colchicine. 10 µg of protein lysate from colchicine-treated sample (+colchicine) or control (CTRL) were loaded on adjacent lanes. Membrane was probed for Cyclin-B. Actin was included as loading control. A standard protein molecular weight marker is included and numbers in kDa are shown on the left. (B) Immunoprecipitation from asynchronous (Asynch) and prometaphase-arrested S2 cells was performed using an anti-Spindly antibody. The fractions indicated in picture were analysed by Western blot for detection of Spindly and Mad-2. A standard protein molecular weight marker was included and numbers in kDa are shown on the left. The experiment was performed once.

The aim of this experiment was to test whether a drug-induced mitotic arrest could stimulate the interaction between Spindly and Mad-2. Protein lysate from asynchronous and mitosis-arrested S2 cells were incubated with anti-Spindly antibody to isolate the endogenous protein from the whole-lysate. Co-IP experiments were run in parallel and the potential interaction between the two SAC components was tested by Western blot. A specific band of the right molecular weight was detected for Spindly. However, the potential binding partner Mad-2 was detected in both, the IP sample (Figure S- 3 B, lane 2) and the rabbit IgG control (Figure S- 3 B, lane 3), making difficult to argue in favor of a positive result (red box). In addition, it was not detected any Mad-2 signal in the imput lane (Figure S- 3 B, lane 1) making even more uncertain the interpretation of the data. This inconsistency may depend upon the specificity of the Mad-2 antibody used. Indeed, the antibody was tested in other experimental procedures and it did not always allow to obtain reliable and reproducible Westen blot and Immunofluorescence results.

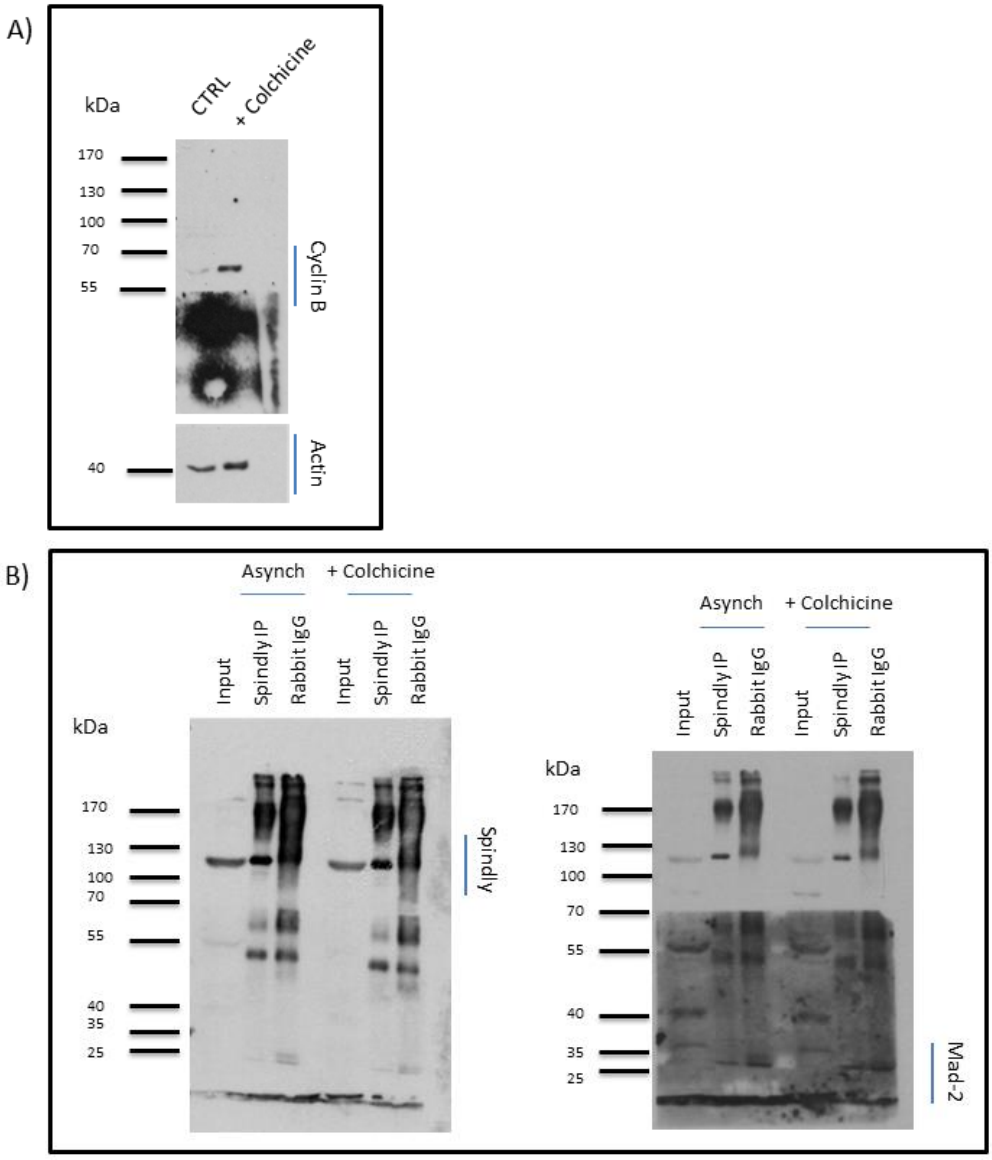

Figure S-4: The expression levels of Cyclin-B increase upon Spindly-RNAi. Western blot analysis shows variations in the expression levels of Cyclin-B upon knockdown of Spindly in early *Drosophila* embryos. Protein lysates were collected from 0-3-hour wild-type (w^{1118}) and Spindly-depleted (*maternal tubulin*>Gal4; *UAS*>$Spindly^{Valium20}$) embryos and run on a SDS-PAGE gel. Knockdown of Spindly was performed at 25°C and 21°C. Membranes were probed for Spindly to verify the efficiency of the knockdown and for Cyclin-B. Actin was included as loading control. For a precise molecular weight determination, a standard protein molecular weight marker was used and numbers in kDa are shown on the left. Images are representative of two biological replicate.

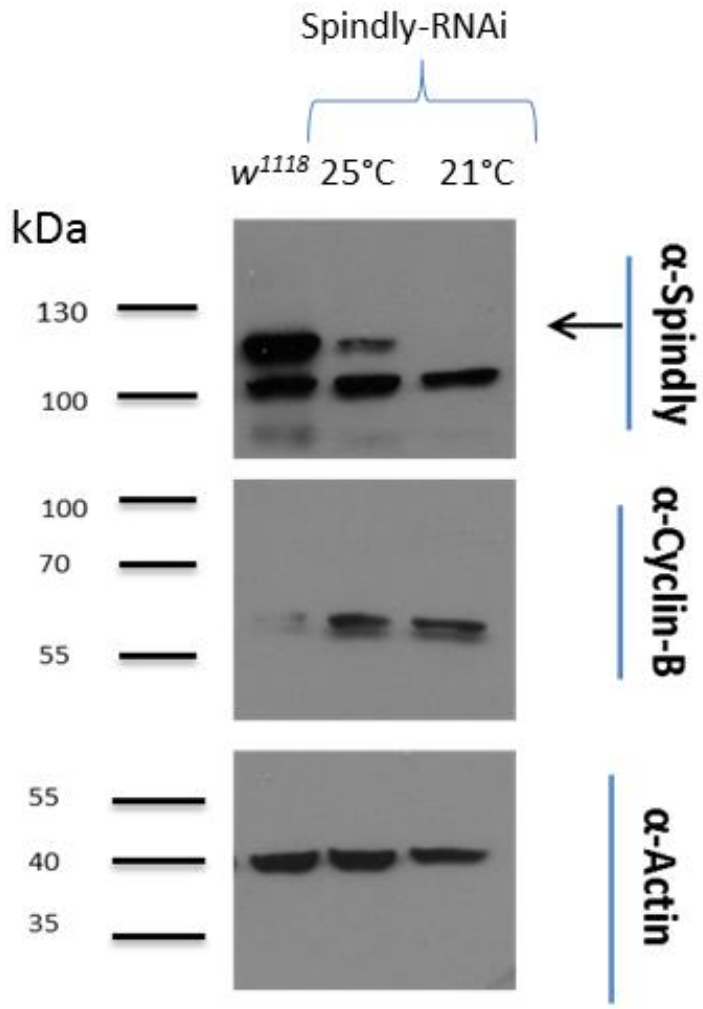

Requirement for Spindly in Drosophila oogenesis:

nanos>Gal4; *UAS*>Spindly^{Valium20} females laid fewer eggs for a shorter period of time than the wild-type strain, suggesting that these flies became sterile over time. To establish whether the egg-laying defects of Spindly-RNAi mothers was caused by a failure in the process of oogenesis, ovaries from 7 day-old flies were dissected and processed for immunofluorescence analysis.

Ovaries isolated from Spindly-depleted germline flies were abnormally small compared to the wild-type and lacked fully-grown eggs at the innermost tip of each ovariole (Figure S5).

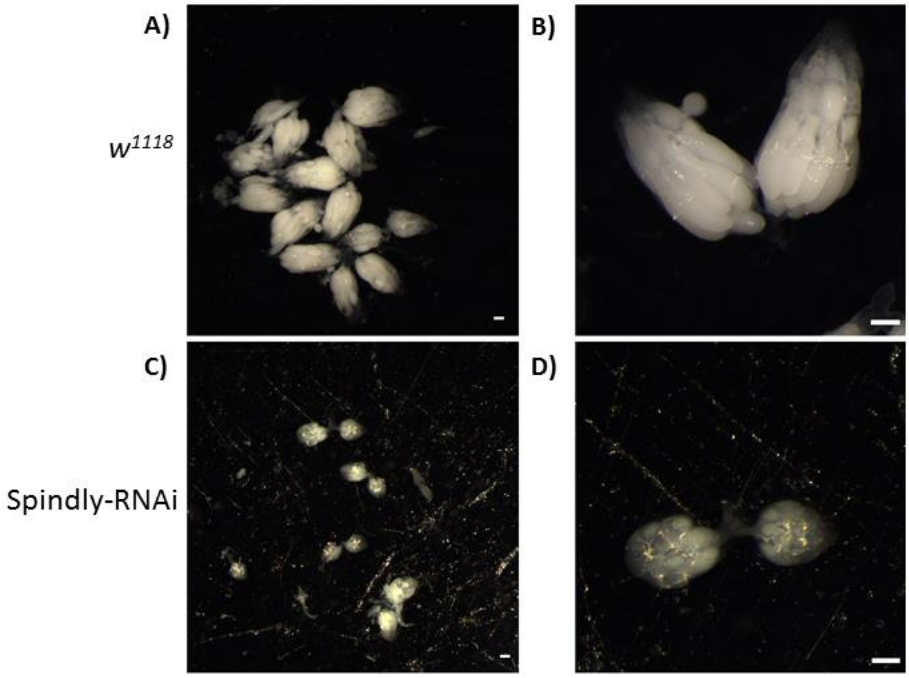

Figure S5: Spindly-RNAi ovaries are abnormally underdeveloped. Micrographs show ovaries isolated from adult flies of the indicated genotypes, 7 days after eclosion. B and D show representative pair of ovaries from a single fly. Ovaries were dissected from wild-type and Spindly-RNAi flies, respectively. The empty ovary of a Spindly-RNAi fruit fly and the marked difference in the ovarian size suggest severe defects in oogenesis. Ovaries were photographed under 8x magnification (A, C) or under 25x magnification (B, D). Scale bars represent 200 µm.

The dissected ovaries were visualised by DAPI and F-actin staining. Immunofluorescence analysis of ovaries isolated from Spindly-RNAi flies raised and mated at 25°C revealed an irregular differentiation and morphology of the egg chamber and suggested a role for Spindly in cystoblast division and stem cell maintenance (Figure S6 A). The failure in cell division cuased by downregulation of Spindly resulted in a dramatic alteration of the architecture of the egg chamber: the regular morphology of the cyst was difficult to identify and few large nuclei were visible (Figure S6 A).

To determine the temperature and temporal dependency of the phenotypes described, ovaries were dissected every day over a period of a week from Spindly-RNAi flies mated at 21°C and the immunofluorescence analysis was repeated (Figure S6 B). Ovaries of 4-day-old mutant females displayed similar morphology compared to the wild-type ovaries. Subsequently, ovaries deteriorated over time and the morphology of the egg chamber was severely altered. Ovaries of seven-day-old females were rudimentary and lacked of developing egg chambers and of dividing germ cells (Figure S6 B). Overall, these pieces of evidence suggested a role for Spindly in the maintenance of the pool of dividing stem cells in the germarium and in supporting cystoblast divisions.

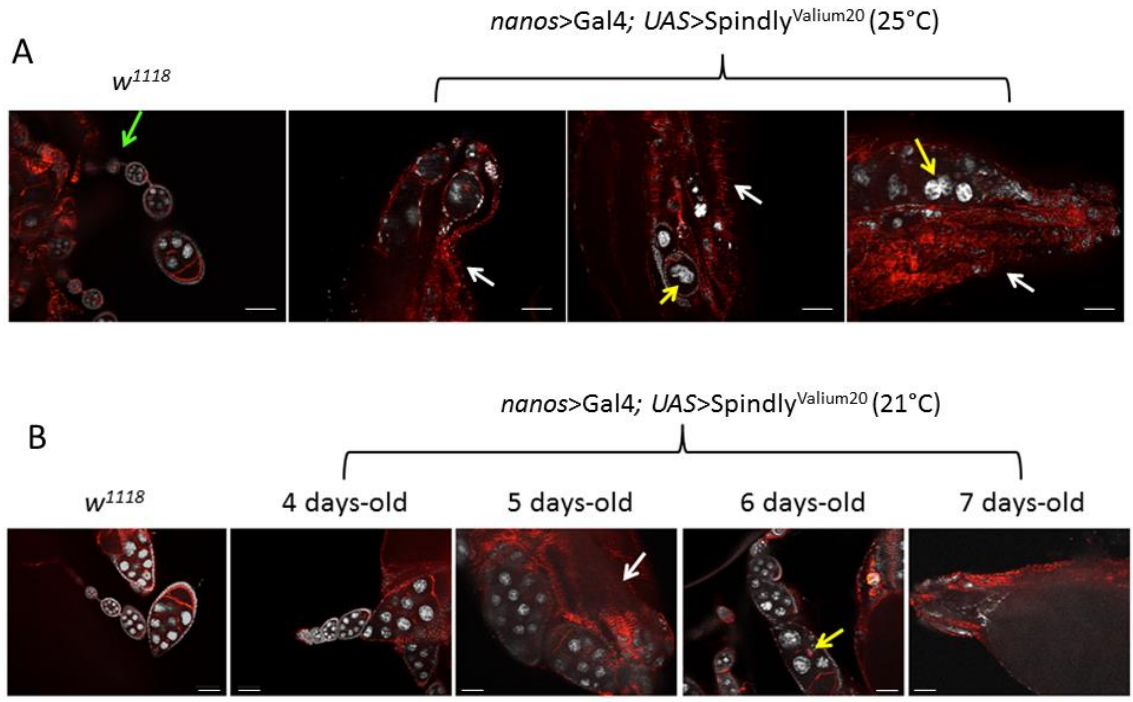

Figure S6: Stainings of Spindly-RNAi ovaries reveal an altered differentiation of the egg chamber.

A) Images show ovarioles isolated from wild-type and *nanos*>Gal4;*UAS*>Spindly^{Valium20} females raised at 25°C. Wild-type ovarioles show progressively developing early-stage egg chambers, each containing nurse cells surrounded by a follicular epithelium. The germarium, anteriormost structure of the ovariole, is visible (green arrow). Maternal RNAi of Spindly disrupts the morphology of the ovaries. Ovaries from Spindly-RNAi flies contain dead ovarioles lacking of any dividing cells, suggesting that the ovarioles had progressively lost the initial pool of germline cells (white arrows). Compared to the wild-type control, egg-chambers are rudimentary with few big nuclei showing an altered morphology, mainly bilobed (yellow arrows). Cell outlines were labelled with Phalloidin-Alexa594 (red), nuclei with DAPI (grey). Scale bars represent 50 µm.

B) Images show ovarioles isolated from wild-type and *nanos*>Gal4;*UAS*>Spindly^{Valium20} flies kept at 21°C. Ovarioles dissected from 4-day-old Spindly-RNAi female flies showed a wild type-like morphology. Over time, empty ovarioles, without any dividing cell, can be detected (5-day-old flies, white arrow) and some egg-chambers in a more advanced stage of differentiation had a reduced number of nurse cells (6-day-old flies, yellow arrow). Eventually, the reproductive apparatus deteriorated (last row, 7-day-old female). Cell outlines are labelled with Phalloidin-Alexa594 (red), nuclei with DAPI (grey). Scale bars represent 50 µm.